

**Natural and synthetic
phase relations
of
cooperite, braggite and vysotskite**

by

SABINE MARIE CHARLOTTE VERRYIN

Submitted in partial fulfilment of the requirements for the degree

PhD(Geology)

in the Faculty of Natural, Agricultural, and Information Sciences

University of Pretoria

Pretoria

August 2000



“My soul magnifies the Lord,
and my spirit rejoices in God, my
saviour”

(Luke 1:47)

ABSTRACT

Natural and synthetic phase relations of cooperite, braggite and vysotskite

by

SABINE MARIE CHARLOTTE VERRYIN

Supervisor: Professor Roland K. W. Merkle

Department of Earth Sciences

PhD (Geology)

In this thesis, results of experimental investigations in the dry system PtS-PdS-NiS at 1200°C, 1100°C, 1000°C, 900°C, 800°C, and 700°C are presented. Experimental results are compared with analyses of naturally occurring cooperite (ideally PtS), braggite ((Pt,Pd)S), and vysotskite (ideally PdS) of this study and with analyses reported in the literature.

Synthetic cooperite is stable at temperatures above 1200°C, whereas synthetic braggite at temperatures below 1100°C, and synthetic vysotskite below 1000°C. Below 900°C in the system PtS-PdS-NiS, Ni-saturated synthetic cooperite, -braggite, and -vysotskite coexist with Ni_{1-x}S. At 900°C only Ni-saturated, Pd-free synthetic cooperite coexists with Ni_{1-x}S, and synthetic braggite and Pd-containing synthetic cooperite coexist with a Pd-Ni-Pt - sulphide melt. At temperatures ≥1000°C all Ni-saturated synthetic cooperite and -braggite coexists with a Pd-Ni-Pt - sulphide melt. There is a clearly defined miscibility gap between cooperite and braggite, but no gap was observed between braggite and vysotskite.

There are well defined, positive, relationships between the Pd-contents of synthetic cooperite, -braggite, and -vysotskite and the Pd-content of the coexisting melt or that of the coexisting Ni_{1-x}S.

The Ni-content of synthetic braggite and -vysotskite with varying Pt/Pd ratios in a Ni-saturated environment is a function of temperature; a higher Ni-content resulting from a lower equilibration temperature. In synthetic cooperite, a similar relationship between the Ni-content and the temperature of formation or equilibration is applicable between 1200° and 900°C. At 800°C, the Ni-content is higher than that at 700°C. The variation in the Ni-content in synthetic cooperite is more restricted than that for synthetic braggite and -vysotskite.

Sulphur fugacity has an effect on the system Pt-Pd-Ni-S. If formed under higher S-pressure, synthetic braggite synthesized at 1000°C contains higher amounts of Ni than formed at lower S-pressure at given Pt/Pd ratios in the initial charge. At constant bulk Pt/Pd ratio, the Pt/Pd ratio of the synthetic braggite decreases with increasing sulphur fugacity. The inter-element relationships for synthetic braggite are not as pronounced for cooperite synthesized at 1000°C.

Compositions of cooperite, braggite, and vysotskite have the potential to indicate at which stage of the development of an ore deposit these phases were exsolved or equilibrated. Comparison of the experimental results with analyses of natural cooperite, braggite, and vysotskite of this study and from the literature, indicate that:

- (i) Cooperite and braggite from the Merensky Reef have equilibrated below 900°C.
- (ii) Analyses of cooperite, braggite, and vysotskite from the UG-2, coexisting with pentlandite follow the trend similar to that experimentally established for temperatures $\leq 700^\circ\text{C}$ and where coexisting with millerite, the trend established for temperatures between 800°C and 700°C.
- (iii) Temperatures of formation or equilibration of cooperite, braggite, and vysotskite from the Sompujävi Reef of the Penikat Intrusion and of Placer Deposits, as well as cooperite from the Stillwater Complex cannot be estimated with certainty.
- (iv) Braggite and vysotskite from the Stillwater Complex may have formed at temperatures below 700°C.
- (v) Cooperite-, braggite-, and vysotskite analyses from Noril'sk indicate formation temperatures of $\leq 700^\circ\text{C}$.

SAMEVATTING

Natural and synthetic phase relations of cooperite, braggite and vysotskite

deur

SABINE MARIE CHARLOTTE VERRYIN

Studieleier: Professor Roland K. W. Merkle

Departement Aardwetenskappe

PhD (Geologie)

In hierdie verhandeling word die eksperimentele resultate van die droë sisteem PtS-PdS-NiS by temperature van 1200°C, 1100°C, 1000°C, 900°C, 800°C en 700°C vergelyk met die samestelling van van natuurlike cooperiet (ideale formule PtS), braggiet ((Pt,Pd)S) en vysotskite (ideale formule PdS) wat hier en uit die literatuur verkry is.

Sintetiese cooperiet is stabiel by temperature bo 1200°C, terwyl sintetiese braggiet stabiel is onder 1100°C en sintetiese vysotskiet stabiel is onder 1000°C. Benede 900°C kom Ni-versadigde sintetiese cooperiet, - braggiet en - vysotskiet voor saam met Ni_{1-x}S in die sisteem PtS-PdS-NiS. By 900°C kom Ni-versadigde, Pd-vrye, sintetiese cooperiet saam met Ni_{1-x}S voor en sintetiese braggiet en Pd-houdende sintetiese cooperiet kom saam met 'n Pd-Ni-Pt - sulfied gesmolte fase voor. By temperature hoër as, of gelyk aan 1000°C kom al die Ni-versadigde sintetiese cooperiet, - braggiet en - vysotskiet voor saam met 'n Pd-Ni-Pt - sulfied gesmolte fase. Terwyl 'n duidelike ontmengingsgaping waargeneem is tussen cooperiet en braggiet kan 'n soortgelyke gaping nie bevestig word tussen braggiet en vysotskiet nie.

'n Goed gedefinieerde, positiewe verhouding bestaan tussen die Pd-inhoud van sintetiese cooperiet, - braggiet en - vysotskiet en die Pd-inhoud van die gesmolte fase wat saam voorkom of met die Ni_{1-x}S fase.

In 'n Ni-versadigde omgewing is die Ni-inhoud van sintetiese braggiet en - vysotskiet met varieerende Pt/Pd verhouding, 'n funksie van temperatuur en kom 'n hoër Ni-inhoud ooreen met 'n laer ewilbreerings temperatuur. Tussen die temperature van 1200°C en 900°C is 'n soorgelyke tendens teenwoordig in sintetiese cooperiet. By 800°C is die Ni-inhoud van sintetiese cooperiet hoër as by 700°C, maar die variasie in die Ni-inhoud van sintetiese cooperiet is minder as die van sintetiese braggiet en - vysotskiet.

Die sisteem Pt-Pd-Ni-S word beïnvloed deur S-fugasiteit. Sintetiese braggiet wat gevorm het by 1000°C onder 'n hoër S-druk, bevat meer Ni as dit wat vorm by laer S-druk met 'n soortgelyke Pt/Pd verhouding in die aanvangs samestelling. By 'n konstante Pt/Pd in die aanvangs samestelling, verlaag die Pt/Pd verhouding van sintetiese braggiet by hoër S-fugasiteite. Die verandering in die inter-element verhouding van sintetiese cooperiet is nie so duidelik as die van sintetiese braggiet wat gevorm is by 1000°C nie.

Die samestellings van natuurlike cooperiet, braggiet en vysotskiet, in 'n erts afsetting, kan potensieël aandui wanneer hierdie fases gevorm het of in ewilibrium was. Die vergelyking van die samestelling van eksperimenteel bereide cooperiet, braggiet en vysotskiet met die van natuurlike minerale, geraporteer hier en in die literatuur, dui die volgende aan:

- (i) Cooperiet en braggiet wat in die Merensky Rif voorkom het ewilibrium bereik benede 900°C.
- (ii) Die samestellings van cooperiet, braggiet en vysotskiet wat in die UG-2 laag saam met pentlandiet voorkom volg die neiging wat eksperimenteel vasgestel is vir temperature minder of gelyk aan 700°C. Waar hierdie minerale voorkom saam met milleriet, volg hul samestellings die neigings wat vasgestel is vir temperature tussen 800°C en 700°C.
- (iii) Die vormings- of ewilibrasie temperature van cooperiet, braggiet en vysotskiet van die Sompujävi Rif van die Penikat Indringing, die van spoelafsettings en die van cooperiet van die Stillwater Kompleks, kon nie met sekerheid afgelei word nie.
- (iv) Braggiet en vysotskiet van die Stillwater Kompleks het moontlik gevorm by temperature benede 700°C.
- (v) Die samestellings van cooperiet, braggiet en vysotskiet afkomstig van Noril'sk dui op vormingstemperature van minder of gelyk aan 700°C.

TABLE OF CONTENTS

SAMEVATTING

ABSTRACT

LIST OF TABLES	1
LIST OF FIGURES	3
LIST OF PHOTOMICROGRAPHS	10
LIST OF ABBREVIATIONS	11
1 INTRODUCTION	12
2 PREVIOUS INVESTIGATIONS OF PHASE RELATIONS	16
2.1 EXPERIMENTAL	17
2.1.1 The system Pd-S	17
2.1.2 The system Pt-S	18
2.1.3 The system Ni-S	19
2.1.4 The system Pt-Pd-S	20
2.1.5 The system Pd-Ni-S	21
2.1.1 Related system Pd-Fe-Ni-S	22
2.2 COMPOSITIONAL VARIATION OF NATURAL COOPERITE, BRAGGITE, AND VYSOTSKITE	24
3 MINERAL PHASES	25
4 EXPERIMENTAL TECHNIQUES	29
4.1 METHOD	30
4.2 REACTANTS AND PLANNING OF EXPERIMENTS	33
4.3 REDUCTION OF METALS	34
4.4 POLISHED SECTIONS	35
5 ANALYTICAL TECHNIQUES	36
6 ISOTHERMAL SECTIONS	
6.1 INTRODUCTION	46
6.2 THE 1200°C ISOTHERMAL SECTION	46
6.2.1 "Cooperite" at 1200°C	50
6.2.2 Melt at 1200°C	52
6.2.3 Relationships at 1200°C	55
6.3 THE 1100°C ISOTHERMAL SECTION	56
6.3.1 "Cooperite" at 1100°C	60
6.3.2 Melt at 1100°C	63
6.3.3 Relationships at 1100°C	64



6.4	THE 1000°C ISOTHERMAL SECTION.....	65
6.4.1	“Cooperite” at 1000°C.....	70
6.4.2	“Braggite” at 1000°C.....	73
6.4.3	Melt at 1000°C.....	76
6.4.4	Relationships at 1000°C.....	77
6.5	THE 900°C ISOTHERMAL SECTION.....	78
6.5.1	“Cooperite” at 900°C.....	85
6.5.2	“Braggite” at 900°C.....	87
6.5.3	Melt at 900°C.....	90
6.6	THE 800°C ISOTHERMAL SECTION.....	91
6.6.1	“Cooperite” at 800°C.....	96
6.6.2	“Braggite” and “vysotskite at 800°C.....	98
6.6.3	Ni _{1-x} S at 800°C.....	100
6.6.4	Relationships at 800°C.....	103
6.7	THE 700°C ISOTHERMAL SECTION.....	104
6.7.1	“Cooperite” at 700°C.....	109
6.7.2	“Braggite” and “vysotskite at 700°C.....	111
6.7.3	Ni _{1-x} S at 700°C.....	113
6.7.4	Relationships at 700°C.....	115
7	VARIABLE INITIAL SULPHUR CONTENT AT 1000°C.....	116
7.1	“BRAGGITE”.....	124
7.2	“COOPERITE”.....	126
8	DISCUSSION: PART I TEMPERATURE DEPENDENT TRENDS.....	127
8.1	TRENDS IN “COOPERITE” COMPOSITIONS.....	131
8.2	TRENDS IN “BRAGGITE-VYSOTSKITE” COMPOSITIONS.....	133
8.3	APPLICABILITY TO COOPERITE, BRAGGITE, AND VYSOTSKITE OCCURRING IN NATURE.....	139
9	DISCUSSION: PART II APPLICATION TO NATURAL COOPERITE, BRAGGITE, AND VYSOTSKITE.....	141
9.1	BUSHVELD COMPLEX	
9.1.1	Merensky Reef.....	142
9.1.2	UG-2.....	148
9.2	SOMPUJÄRVI REEF OF THE PENIKAT INTRUSION IN NORTHERN FINLAND.....	150
9.3	SELECTED ANALYSES FROM THE LITERATURE	
9.3.1	Placer Deposits.....	153
9.3.2	The J-M Reef - Stillwater Complex, Montana.....	154
9.3.3	Noril’sk.....	156
9.3.4	Bushveld Complex.....	158
9.3.5	“Problem” Cases.....	159



10	CONCLUSIONS.....	161
11	ACKNOWLEDGEMENTS.....	168
12	REFERENCES.....	170
	APPENDIX I EXPERIMENTAL CHARGES.....	178
	APPENDIX II REFEREED PUBLICATIONS RESULTING FROM THIS STUDY.....	184

LIST OF TABLES

- Table 1:** Optical properties of the minerals in the system PtS-PdS-NiS (cooperite, braggite, and vysotskite after Criddle & Stanley (1985); millerite after Uytendogaart & Burke (1971)).
- Table 2:** Analytical conditions, detection limits (3 sigma level in per cent by mass) and reproducibilities (1 sigma, determined according to Kaiser and Specker (1956) in mass per cent; N=60 (n.d. = not determined).
- Table 3:** Comparison of mean analytical results using a de-focussed beam as well as various scan area magnifications with the actual composition of the standard analysed (in wt%). Values in parenthesis show the standard deviation at the 1 σ level (N=20).
- Table 4:** Indication of distributions of data points, their best fits, and relevant general equations.
- Table 5:** Mean (arithmetic) compositions of phases in the system PtS-PdS-NiS at 1200°C in weight per cent (wt%) and atomic per cent (at%). Values in parenthesis show the standard deviation at the 1 σ level. N = number of analyses per experiment.
- Table 6:** Type of best fit, equation for best fit at the 95% confidence level, equation number (No), and R²-values of best fits of elements analysed in "cooperite" formed at 1200°C.
- Table 7:** Mean (arithmetic) compositions of phases in the system PtS-PdS-NiS at 1100°C in weight per cent (wt%) and atomic per cent (at%). Values in parenthesis show the standard deviation at the 1 σ level. N = number of analyses per experiment.
- Table 8:** Type of best fit, equation for best fit at the 95% confidence level, equation number (No), and R²-values of best fits of elements analysed in "cooperite" formed at 1100°C.
- Table 9:** Mean (arithmetic) compositions of phases in the system PtS-PdS-NiS at 1000°C in weight per cent (wt%) and atomic per cent (at%). Values in parenthesis show the standard deviation at the 1 σ level. N = number of analyses per experiment.
- Table 10:** Type of best fit, equation for best fit at the 95% confidence level, equation number (No), and R²-values of best fits of elements analysed in "cooperite" formed at 1000°C.
- Table 11:** Type of best fit, equation for best fit at the 95% confidence level, equation number (No) and R²-values of best fits of between elements analysed in "braggite" formed at 1000°C.
- Table 12:** Mean (arithmetic) compositions of phases in the system PtS-PdS-NiS at 900°C in weight per cent (wt%) and atomic per cent (at%). Values in parenthesis show the standard deviation at the 1 σ level. N = number of analyses per experiment.
- Table 13:** Type of best fit, equation for best fit at the 95% confidence level, equation number (No), and R²-values of best fits of elements analysed in "cooperite" formed at 900°C.
- Table 14:** Type of best fit, equation for best fit at the 95% confidence level, equation number (No), and R²-values of best fits of elements analysed in "braggite-vysotskite" formed at 900°C.
- Table 15:** Mean (arithmetic) compositions of phases in the system PtS-PdS-NiS at 800°C in weight per cent (wt%) and atomic per cent (at%). Values in parenthesis show the standard deviation at the 1 σ level. N = number of analyses per experiment.
- Table 16:** Type of best fit, equation for best fit at the 95% confidence level, equation number (No), and R²-values of best fits of elements analysed in "cooperite" formed at 800°C.

- Table 17:** Type of best fit, equation for best fit at the 95% confidence level, equation number (No), and R^2 -values of best fits of elements analysed in “braggite-vysotskite” formed at 800°C.
- Table 18:** Mean (arithmetic) compositions of phases in the system PtS-PdS-NiS at 700°C in weight per cent (wt%) and atomic per cent (at%). Values in parenthesis show the standard deviation at the 1σ level. N = number of analyses per experiment.
- Table 19:** Type of best fit, equation for best fit at the 95% confidence level, equation number (No), and R^2 -values of best fits of elements analysed in “cooperite” formed at 700°C.
- Table 20:** Type of best fit, equation for best fit at the 95% confidence level, equation number (No), and R^2 -values of best fits of elements analysed in “braggite-vysotskite” formed at 700°C.
- Table 21:** Mean (arithmetic) compositions of phases in the system PtS-PdS-NiS at 1000°C with variable initial S-content in weight per cent (wt%) and atomic per cent (at%). Values in parenthesis show the standard deviation at the 1σ level. N = number of analyses per experiment.
- Table 22:** Spearman correlation coefficients between temperature of synthesis and composition (at-%) for compositions of “braggite-vysotskite” not coexisting with “cooperite” and formed in a Ni-saturated environment between 1000°C and 700°C. The highlighted correlation coefficients are significant at a p-level of ≤ 0.05 .
- Table 23:** Coefficient of determination (R^2) depending on variables used in a forward stepwise multiple linear regression analysis with temperature of synthesis as the dependant variable.
- Table 24:** Coefficient of determination (R^2) depending on quadratic variables used in a forward stepwise multiple linear regression analysis with temperature of synthesis as the dependant variable.
- Table 25:** Selected cooperite (co), braggite (br), and vysotskite (vy) analysis from the Merensky Reef (MR) and the UG-2 in association with pentlandite (pent) or millerite (mill).
- Table 26:** Selected braggite (br) and vysotskite (vy) analysis from the Sompujärvi Reef of the Penikat Intrusion, Northern Finland.
- Table 27:** Composition of charges, their pre-reaction-, tempering-, and quenching histories for the investigation of the 1200°C, 1100°C, 1000°C, 900°C, 800°C and 700°C isothermal sections.

LIST OF FIGURES

- Figure 1:** The Pd-S phase diagram in atomic proportions (Taylor, 1985).
- Figure 2:** The Pt-S phase diagram in atomic proportions (from Massalski, 1986).
- Figure 3:** The Ni-S phase diagram in atomic proportions (from Massalski, 1986).
- Figure 4:** The Pt-Pd-S phase diagram in atomic proportions at 1000 °C (Skinner et al., 1976) and 800 °C (Cabri et al., 1978).
- Figure 5:** The system Pd-Ni-S at 900 °C (Karup-Møller & Makovicky, 1993).
- Figure 6:** The system Pd-Ni-S at 725 °C (Karup-Møller & Makovicky, 1993).
- Figure 7:** Phase relations in the system Pd-Ni-Fe-S in atomic proportions at 900 °C (Makovicky & Karup-Møller, 1995).
- Figure 8:** Phase relations in the system Pd-Ni-Fe-S atomic proportions at 725 °C (Makovicky & Karup-Møller, 1995).
- Figure 9:** Compositional variation of cooperite, braggite, and vysotskite analyses from various localities in cation proportions. This Figure excludes the data from Merkle & Verryn, 1991 and Verryn & Merkle, 1994). Data taken from: **B:** Bannister & Hey, 1932; **C:** Cabri et al., 1978; **CA:** Cabri et al., 1996; **CR:** Criddle & Stanley, 1985; **G:** Genkin & Evstigneeva, 1986; **H:** Halkoaho, 1989; **K:** Kingston & El-Dosuky, 1982; **L:** Laputina & Genkin, 1975; **M:** Mostert et al., 1982; **S:** Schweltnus et al., 1976; **T:** Tarkian, 1987; **TO:** Todd et al., 1982; and **V:** Volborth et al., 1986 The black stippled line indicates the border between braggite and vysotskite.
- Figure 10:** X-ray diffractogram ($\text{Cu}_{\text{K}\alpha}$ radiation) of experiment SV701. The peaks corresponding to Ni_{1-x}S (ICDD-PDF number 2-1373) are marked, the remaining peaks belong to “braggite”. The background has been subtracted and the analytical conditions are presented in the text.
- Figure 11:** Modified chamber furnace with horizontal tubes.
- Figure 12:** Setup of reduction furnace.
- Figure 13:** Bulk composition of experimental charges (■), “cooperite” (•) and melt composition (•) connected by tie-lines at 1100 °C in molecular proportions.
- Figure 14:** Phase relations in the system PtS-PdS-NiS in cation proportions at 1200 °C.
- Figure 15:** Ni-content versus Pt-content (in at-%) in “cooperite” formed at 1200 °C. The solid line indicates the best linear fit and the stippled lines the 95% confidence interval according to the equation shown (N=7).
- Figure 16:** Ni-content versus Pd-content (in at-%) in “cooperite” formed at 1200 °C. The solid line indicates the best linear fit and the stippled lines the 95% confidence interval according to the equation shown (N=7).
- Figure 17:** Pt-content versus Pd-content (in at-%) in “cooperite” formed at 1200 °C. The solid line indicates the best linear fit and the stippled lines the 95% confidence interval according to the equation shown (N=7).
- Figure 18:** Ni-content versus Pt/Pd ratio (in atomic proportions) in “cooperite” formed at 1200 °C. The solid line indicates the best fit according to the equation shown (N=6).

- Figure 19:** 3D scatterplot of Pd-, Ni-, and S-content (in at-%) in melt coexisting with “cooperite” at 1200°C (N=7).
- Figure 20:** Pd-content in melt versus Pd-content in “cooperite” at 1200°C (in at-%). The solid line indicates the best linear fit and the stippled lines the 95% confidence interval of that fit (N=7).
- Figure 21:** Phase relations in the system PtS-PdS-NiS in cation proportions at 1100°C.
- Figure 22:** Ni-content versus Pt-content (in at-%) in “cooperite” formed in a Ni-saturated environment at 1100°C. The solid line indicates the best linear fit and the stippled lines the 95% confidence interval according to the equation shown (N=8).
- Figure 23:** Ni-content versus Pd-content (in at-%) in “cooperite” formed in a Ni-saturated environment at 1100°C. The solid line indicates the best linear fit and the stippled lines the 95% confidence interval according to the equation shown (N=8).
- Figure 24:** Pt-content versus Pd-content (in at-%) in “cooperite” formed in a Ni-saturated environment at 1100°C. The solid line indicates the best linear fit and the stippled lines the 95% confidence interval according to the equation shown (N=8).
- Figure 25:** Ni-content versus Pt/Pd ratio (in atomic proportions) in “cooperite” formed in a Ni-saturated environment at 1100°C. The solid line indicates the best fit according to the equation shown (N=7).
- Figure 26:** 3D scatterplot of Pd-, Ni-, and S-content in at-% in melt coexisting with “cooperite” at 1100°C (N=8).
- Figure 27:** Pd-content in melt versus Pd-content in “cooperite” at 1100°C (in at-%). The solid line indicates the best linear fit and the stippled line the 95-% confidence interval of the linear fit (N=8).
- Figure 28:** Phase relations in the system PtS-PdS-NiS in cation proportions at 1000°C.
- Figure 29:** Ni-content versus Pd-content (in at-%) in “cooperite” and “braggite” formed at 1000°C.
- Figure 30:** Ni-content versus Pt-content (in at-%) in “cooperite” formed in a Ni-saturated environment at 1000°C. The solid line indicates the best fit according to the equation shown (N=6).
- Figure 31:** Ni-content versus Pd-content (in at-%) in “cooperite” formed in a Ni-saturated environment at 1000°C. The solid line indicates the best 2nd order polynomial fit and the stippled line the 95% confidence interval according to the equation shown (N=6).
- Figure 32:** Pt-content versus Pd-content (in at-%) in “cooperite” formed in a Ni-saturated environment at 1000°C. The solid line indicates the best linear fit and the stippled lines the 95% confidence interval according to the equation shown (N=6).
- Figure 33:** Ni-content versus Pt/Pd ratio (in atomic proportions) in “cooperite” formed in a Ni-saturated environment at 1000°C. The solid line indicates the fit according to the equation shown (N=5).
- Figure 34:** Ni-content versus Pt-content (in at-%) in “braggite” formed in a Ni-saturated environment at 1000°C. The solid line indicates the best linear fit and the stippled lines the 95% confidence interval according to the equation shown (N=7).
- Figure 35:** Ni-content versus Pd-content (in at-%) in “braggite” formed in a Ni-saturated environment at 1000°C. The solid line indicates the best linear fit and the stippled lines the 95% confidence interval according to the equation shown (N=7).

- Figure 36:** Pt-content versus Pd-content (in at-%) in “braggite” formed in a Ni-saturated environment at 1000°C. The solid line indicates the best linear fit and the stippled lines the 95% confidence interval according to the equation shown (N=7).
- Figure 37:** Ni-content versus Pt/Pd ratio (in atomic proportions) in “braggite” formed in a Ni-saturated environment at 1000°C. The solid line indicates the best logarithmic fit according to the equation shown (N=7).
- Figure 38:** 3D scatterplot of Pd-, Ni- and S-content in at-% in melt at 1000°C coexisting with “cooperite” and/or “braggite”.
- Figure 39:** Pd-content in melt versus Pd-content in “cooperite” and “braggite” in a Ni-saturated environment at 1000°C (in at-%). The solid lines indicate the best linear fits and the stippled line the confidence intervals at the 95% level for the 2 populations individually.
- Figure 40:** Phase relations in the system PtS-PdS-NiS in cation proportions cent at 900°C (the stippled line indicates the border between “braggite” and “vysotskite”).
- Figure 41:** Ni-content versus Pd-content (in at-%) in “cooperite” and “braggite-vysotskite” formed at 900°C.
- Figure 42:** Ni-content versus Pt-content (in at-%) in “cooperite” formed in a Ni-saturated environment at 900°C. The solid line indicates the best linear fit and the stippled lines the 95% confidence interval according to the equation shown (N=6).
- Figure 43:** Ni-content versus Pd-content (in at-%) in “cooperite” formed in a Ni-saturated environment at 900°C. The solid line indicates the best linear fit and the stippled lines the 95% confidence interval according to the equation shown (N=6).
- Figure 44:** Pt-content versus Pd-content (in at-%) in “cooperite” formed in a Ni-saturated environment at 900°C. The solid line indicates the best linear fit and the stippled lines the 95% confidence interval according to the equation shown (N=6).
- Figure 45:** Ni-content versus Pt/Pd ratio (in atomic proportions) in “cooperite” formed in a Ni-saturated environment at 900°C. The solid line indicates the best linear fit and the stippled lines the 95% confidence interval according to the equation shown (N=6).
- Figure 46:** Ni-content versus Pt-content (in at-%) in “braggite-vysotskite” formed in a Ni-saturated environment at 900°C. The solid line indicates the best linear fit and the stippled lines the 95% confidence interval according to the equation shown (N=8).
- Figure 47:** Ni-content versus Pd-content (in at-%) in “braggite-vysotskite” formed in a Ni-saturated environment at 900°C. The solid line indicates the best linear fit and the stippled lines the 95% confidence interval according to the equation shown (N=8).
- Figure 48:** Pt-content versus Pd-content (in at-%) in “braggite-vysotskite” formed in a Ni-saturated environment at 900°C. The solid line indicates the best linear fit and the stippled lines the 95% confidence interval according to the equation shown (N=8).
- Figure 49:** Ni-content versus Pt/Pd ratio (in atomic proportions) in “braggite-vysotskite” formed in a Ni-saturated environment at 900°C. The solid line indicates the best square root fit according to the equation shown (N=8).
- Figure 50:** 3D scatterplot of Pd-, Ni-, and S-content in at-% in melt at 900°C coexisting with “cooperite” and/or “braggite” or “vysotskite”.
- Figure 51:** Phase relations in the system PtS-PdS-NiS in cation proportions at 800°C (the stippled line indicates the border between “braggite” and “vysotskite”).

- Figure 52:** Ni-content versus Pd-content (in at-%) in “cooperite”, “braggite”, and “vysotskite” formed in a Ni-saturated environment at 800°C. The solid lines connect the data points of “cooperite” and “braggite-vysotskite” individually.
- Figure 53:** Ni-content versus Pt-content (in at-%) in “cooperite” formed in a Ni-saturated environment at 800°C. The solid line indicates the best linear fit and the stippled lines the 95% confidence interval according to the equation shown (N=4).
- Figure 54:** Ni-content versus Pd-content (in at-%) in “cooperite” formed in a Ni-saturated environment at 800°C. The solid line indicates the best linear fit and the stippled lines the 95% confidence interval according to the equation shown (N=4).
- Figure 55:** Pt-content versus Pd-content (in at-%) in “cooperite” formed in a Ni-saturated environment at 800°C. The solid line indicates the best linear fit and the stippled lines the 95% confidence interval according to the equation shown (N=4).
- Figure 56:** Ni-content versus Pt-content (in at-%) in “braggite-vysotskite” formed in a Ni-saturated environment at 800°C. The solid line indicates the best linear fit and the stippled lines the 95% confidence interval according to the equation shown (N=4).
- Figure 57:** Ni-content versus Pd-content (in at-%) in “braggite-vysotskite” formed in a Ni-saturated environment at 800°C. The solid line indicates the best linear fit and the stippled lines the 95% confidence interval according to the equation shown (N=4).
- Figure 58:** Pt-content versus Pd-content (in at-%) in “braggite-vysotskite” formed in a Ni-saturated environment at 800°C. The solid line indicates the best linear fit and the stippled lines the 95% confidence interval according to the equation shown (N=4).
- Figure 59:** Compositional variation of $Ni_{1-x}S$ (in cation proportions) coexisting with “cooperite”, “braggite”, or “vysotskite” at 800°C..
- Figure 60:** Pt-content versus Ni-content in $Ni_{1-x}S$ (in at-%) coexisting with “cooperite” or “braggite-vysotskite” at 800°C. The solid lines indicate the best linear fits for the 2 populations individually.
- Figure 61:** Pd-content versus Ni-content in $Ni_{1-x}S$ (in at-%) coexisting with “cooperite” or “braggite-vysotskite” at 800°C. The solid lines indicate the best linear fits for the 2 populations individually.
- Figure 62:** Pt-content versus Pd-content in $Ni_{1-x}S$ (in at-%) coexisting with “cooperite” or “braggite-vysotskite” at 800°C. The solid lines indicate the best linear fits for the 2 populations individually.
- Figure 63:** Pd-content in $Ni_{1-x}S$ versus Pd-content (in at-%) in “cooperite”, “braggite”, and “vysotskite” at 800°C.
- Figure 64:** Phase relations in the system PtS-PdS-NiS in cation proportions at 700°C (the stippled line indicates the border between “braggite” and “vysotskite”).
- Figure 65:** Ni-content versus Pt-content (in at-%) in “cooperite” formed in a Ni-saturated environment at 700°C. The solid line indicates the best linear fit and the stippled lines the 95% confidence interval according to the equation shown (N=6).
- Figure 66:** Ni-content versus Pd-content (in at-%) in “cooperite” formed in a Ni-saturated environment at 700°C. The solid line indicates the best linear fit and the stippled lines the 95% confidence interval according to the equation shown ((N=6).
- Figure 67:** Pd-content versus Pt-content (in at-%) in “cooperite” formed in a Ni-saturated environment at 700°C. The solid line indicates the best linear fit and the stippled lines the 95% confidence interval according to the equation shown (N=6).

- Figure 68:** Pt-content versus Ni-content (in at-%) in "braggite-vysotskite" formed in a Ni-saturated environment at 700°C. The solid line indicates the best linear fit and the stippled lines the 95% confidence interval according to the equation shown (N=6).
- Figure 69:** Pd-content versus Ni-content (in at-%) in "braggite-vysotskite" formed in a Ni-saturated environment at 700°C. The solid line indicates the best linear fit and the stippled lines the 95% confidence interval according to the equation shown (N=6).
- Figure 70:** Pt-content versus Pd-content (in at-%) in "braggite-vysotskite" formed in a Ni-saturated environment at 700°C. The solid line indicates the best linear fit and the stippled lines the 95% confidence interval according to the equation shown (N=6).
- Figure 71:** Ni-content (at-%) versus Pt/Pd ratio (in atomic proportions) in "braggite-vysotskite" formed in a Ni-saturated environment at 700°C. The solid line indicates the best fit according to the equation shown (N=6).
- Figure 72:** Compositional variation of $Ni_{1-x}S$ in cation proportions coexisting with "cooperite", "braggite", or "vysotskite" at 700°C.
- Figure 73:** Pd-content versus Ni-content in $Ni_{1-x}S$ (in at-%) coexisting only with "braggite-vysotskite" at 700°C. The solid lines indicate the best linear fit and the stippled lines the 95% confidence interval of that fit.
- Figure 74:** Pd-content in "cooperite", "braggite", or "vysotskite" versus Pd-content in $Ni_{1-x}S$ in at-% at 700°. The solid lines indicate the best linear fits and the stippled lines the 95% confidence intervals for the 2 populations individually.
- Figure 75:** Phase relations in the system PtS-PdS-NiS in cation proportions at 1000°C. The red tie-lines and sample points represent experiments where the initial S-content in the charge was below 50 at-% and the blue tie-lines and sample points where the initial S-content in the charge was above 50 at-%.
- Figure 76:** Phase relations in the system PtS-PdS-NiS in cation proportions at 1000°C of experiments where the initial S-content in the charge was below 50 at-%.
- Figure 77:** Phase relations in the system PtS-PdS-NiS in cation proportions at 1000°C of experiments where the initial S-content in the charge was above 50 at-%.
- Figure 78:** Pt/Pd ratio versus Ni-content in atomic proportions in "braggite" at 1000°C. Numbers above the symbols indicate the S-content in the initial charge. Tie-lines connect experiments of the same bulk Pt/Pd ratio.
- Figure 79:** Sulphur pressures versus temperature for the equilibria $Pd + S \leftrightarrow PdS$, $Pt + S \leftrightarrow PtS$, and $Ni + S \leftrightarrow NiS$ (data from Barin et al., 1973).
- Figure 80:** Pt/Pd ratio versus Ni-content in atomic proportions in "cooperite" at 1000°C. Numbers above the symbols indicate the S-content in the initial charge. Tie-lines connect experiments of the same initial Pt/Pd ratio.
- Figure 81:** Sketch of phase relations in the system PtS-PdS-NiS in cation proportions from 1200°C to 700°C. Compositional fields of melts at the various temperatures stretch down to the Pd-Ni join and compositional fields of "cooperite", "braggite", and "vysotskite" extend to the Pt-Pd join for the various temperatures. At 800°C and 700°C $Ni_{1-x}S$ is stable. The tie lines combine coexisting "cooperite" and "braggite" formed in Ni-saturated environments at their respective temperatures. The stippled line indicates the border between "braggite" and "vysotskite".
- Figure 82:** Stability ranges of "cooperite", "braggite", and "vysotskite" in mol-% formed in a Ni-free environment between 1200°C and 700°C.

- Figure 83:** Ni-free projected stability ranges of "cooperite", "braggite", and "vysotskite" in mol-% formed in a Ni-saturated environment between 1200°C and 700°C. The horizontal stippled line indicates the stability range in a slightly Ni-undersaturated environment at 700°C.
- Figure 84:** Ni-content (in at-%) in coexisting "cooperite" and "braggite" formed between 1000°C and 700°C in a Ni-saturated environment.
- Figure 85:** Ni-content versus Pt-content in "cooperite" in at-% formed between 1200°C and 700°C in a Ni-saturated environment. The solid lines show the best linear fits of the data for the various temperatures (°C) indicated in the legend.
- Figure 86:** Ni-content versus Pt-content in "braggite-vysotskite" in at-% formed between 1000°C and 700°C in a Ni-saturated environment. The solid lines show the best linear fits of the data for the various temperatures (°C) indicated in the legend.
- Figure 87:** Predicted versus observed temperature of synthesis [°C] for "braggite" and "vysotskite" not coexisting with "cooperite", formed in a Ni-saturated environment between 1000°C and 700°C, according to the linear equation shown. The solid line indicates the best linear fit and the stippled lines the 95% confidence interval of the line.
- Figure 88:** Predicted versus observed temperature of synthesis [°C] for "braggite" and "vysotskite" not coexisting with "cooperite", formed in a Ni-saturated environment between 1000°C and 700°C, according to the quadratic equation shown. The solid line indicates the best fit and the stippled lines the 95% confidence interval of the line.
- Figure 89:** Compositional variation of cooperite and braggite from the Merensky Reef in cation proportions based on 766 analysis. The solid line indicates the compositional trend established for 700°C and the black stippled lines represent tie lines between coexisting "cooperite" and "braggite" synthesized at 700°C.
- Figure 90:** Pd-content (at-%) in braggite from the Merensky Reef versus temperature of formation or equilibration calculated according to Equation 42 ($\text{Temp [}^\circ\text{C]} = 998.07 (\pm 7.88) + 0.05 (\pm 0.02) \times \text{Pt}^2 - 4.24 (\pm 0.16) \times \text{Ni}^2$).
- Figure 91:** Pd-content in at-% of coexisting cooperite and braggite from the Merensky Reef. The solid black lines indicate the upper Pd-content limit for "cooperite" and the lower limit for "braggite" experimentally established at 800°C.
- Figure 92:** Compositional variation in cation proportions of cooperite, braggite, and vysotskite from the UG-2 (full circles are associated with pentlandite and open circles with millerite as the main Ni-bearing phase). The solid lines indicate the compositional trends established for 800°C and 700°C.
- Figure 93:** Compositional variation in cation proportions of braggite and vysotskite from the Sompujärvi Reef (this study = empty circles) and analysis from the AP 1 mineralization (from Halkoaho (1989) = solid circles). The solid lines indicate the compositional trends established for 1000°C and 900°C.
- Figure 94:** Compositional variation in cation proportions of cooperite and braggite from Placer deposits (from Cabri et al., 1996). The solid lines indicate the compositional trends established for 1000°C and 900°C.
- Figure 95:** Compositional variation in cation proportions of cooperite, braggite, and vysotskite from layered intrusions taken from the literature. The solid circles are analyses from the Stillwater Layered Intrusion (Todd et al., 1982; Criddle & Stanley, 1985; Volboth et al., 1986) and the solid lines indicate the compositional trends established for the temperatures indicated.

- Figure 96:** Compositional variation in cation proportions of cooperite, braggite, and vysotskite from layered intrusions taken from the literature. The solid circles are analyses from Noril'sk (Laputina & Genkin, 1975; Genkin & Evstigneeva, 1986; and unpublished data) and the solid lines indicate the compositional trends established for the temperatures indicated.
- Figure 97:** Compositional variation in cation proportions of cooperite, braggite, and vysotskite from layered intrusions taken from the literature. The solid circles are analyses from the Bushveld Complex (Bannister & Hey, 1932; Cabri et al., 1978; Criddle & Stanley, 1985; Kingston & El-Dosuky, 1982; Mostert et al., 1982; Schwelinus et al., 1976; Tarkian, 1987) and the solid lines indicate the compositional trends established for the temperatures indicated. Analyses falling into the field surrounded by the thick stippled line to be referred to in the text.
- Figure 98:** Compositional variation in cation proportions of cooperite, braggite, and vysotskite from layered intrusions taken from the literature. The solid circles are "problem" analyses and are discussed in the text. The solid lines indicate the compositional trends established for the temperatures indicated.

LIST OF PHOTOMICROGRAPHS

- Photomicrograph 1** "Cooperite" (co) and coexisting melt at 1200°C of experiment SV1204 (long side of the photomicrograph is 1.1 mm).
- Photomicrograph 2** "Cooperite" (co) and coexisting melt at 1200°C of experiment SV1206 (long side of the photomicrograph is 0.35 mm).
- Photomicrograph 3** "Cooperite" (co) and coexisting melt at 1100°C of experiment SV337 (long side of the photomicrograph is 0.35 mm).
- Photomicrograph 4** "Cooperite" (co) and coexisting "braggite" (br) at 1000°C of experiment SV316 (digitally enhanced, long side of the photomicrograph is 0.35 mm).
- Photomicrograph 5** "Braggite" (br) and coexisting melt at 1000°C of experiment SV314 (long side of the photomicrograph is 1.1 mm).
- Photomicrograph 6** "Cooperite" (co) and coexisting melt at 900°C of experiment SV322 (long side of the photomicrograph is 0.35 mm).
- Photomicrograph 7** "Braggite" (br) and coexisting melt at 900°C of experiment SV326 (long side of the photomicrograph is 0.35 mm).
- Photomicrograph 8** "Braggite" (br) and coexisting melt at 900°C of experiment SV328 (long side of the photomicrograph is 0.35 mm).
- Photomicrograph 9** "Braggite" (br) and coexisting melt at 900°C of experiment SV330 (long side of the photomicrograph is 0.35 mm).
- Photomicrograph 10** "Cooperite" (co) and coexisting Ni_{1-x}S at 800°C of experiment SV805 (long side of the photomicrograph is 0.35 mm).
- Photomicrograph 11** "Vysotskite" (vy) and coexisting Ni_{1-x}S at 800°C of experiment SV815 (long side of the photomicrograph is 0.35 mm).
- Photomicrograph 12** Coexisting "cooperite" (co), "braggite" (br) and Ni_{1-x}S at 700°C of experiment SV703 (digitally enhanced, long side of the photomicrograph is 0.185 mm).
- Photomicrograph 13** "Cooperite" (co), "Braggite" (br) and coexisting melt at 1000°C of experiment SV289 (digitally enhanced, long side of the photomicrograph is 1.10 mm).
- Photomicrograph 14** Coexisting cooperite (co) and braggite (br) with chalcopyrite (cp) from the Merensky Reef under reflected light (digitally enhanced, the long side of the photomicrograph is 200µm long).
- Photomicrograph 15** Coexisting cooperite (co) and braggite (br) with chalcopyrite (cp) from the Merensky Reef under crossed nicols in reflected light (the long side of the photomicrograph is 200µm long).

LIST OF ABBREVIATIONS

PGM(s)	Platinum-group mineral(s)
PGE(s)	Platinum-group element(s)
BMS	Base metal sulfides
°C	degrees Celsius
µm	micrometre
mm	millimetre
at-%	atomic per cent
at-prop.	atomic proportion
wt-%	weight per cent
mol-%	molecular per cent
kV	kilo Volt
A	Ampere
r	correlation coefficient (Ott, 1988)
R ²	coefficient of determination (Ott, 1988)
3D	3-dimensional
Fig.	Figure
N	Number of observations
mss	monosulfide solid solution



CHAPTER 1

INTRODUCTION

1 INTRODUCTION

Natural cooperite (ideally PtS), braggite ((Pt,Pd)S), and vysotskite (ideally PdS) have been described from various localities throughout the world, including the Merensky Reef and the UG-2 chromitite layer of the Bushveld Complex (e.g. Brynard et al., 1976; Schweltnus et al., 1976; Kingston and El-Dosuky, 1982; Kinloch, 1982; McLaren & De Villiers, 1982; Mostert et al., 1982; Peyerl, 1982; Verryn & Merkle, 1994), the Stillwater Complex (e.g. Todd et al., 1982; Volborth et al., 1986), Noril'sk (e.g. Genkin & Evstigneeva, 1986), the Lukkulaivaara and Imandrosky layered intrusions (Barkov et al., 1995), and the Sompujärvi Reef of the Penikat Intrusion in northern Finland (Alapieti & Lahtinen, 1986; Halkoaho et al., 1990; Huhtelin et al., 1990). Amongst the platinum-group minerals (PGMs) in the UG-2 and the Merensky Reef, these three minerals are the dominant ore minerals (Kinloch, 1982). From an economic point of view, cooperite, braggite, and vysotskite are therefore probably the most important minerals in ores of the platinum-group elements (PGEs). They are also the most common minerals in the system Pt-Pd-S.

In the natural examples mentioned above, cooperite, braggite, and vysotskite do contain profound amounts of Ni and display a distinct compositional variation in which the Pt/Pd ratio and the Ni-content can vary significantly. Accordingly, the minerals cooperite, braggite, and vysotskite should be considered to belong to the system Pt-Pd-Ni-S or, for the purpose of this investigation, to the pseudo-ternary system PtS-PdS-NiS. Likewise, previous studies by Cabri et al. (1978) and Verryn & Merkle (1994) showed that the mineral chemistry of the system PtS-PdS-NiS is not sufficiently understood and should be comprehensively investigated.

Looking at the mineral compositions of braggite and cooperite from the Bushveld Complex (Verryn & Merkle, 1994), the Ni-content within braggite and vysotskite remains fairly constant with varying Pt/Pd ratios when these minerals are associated with specific base metal sulfides (BMS), but appeared to vary depending on the BMS assemblage. The Ni-content seems to be a function of temperature, rather than the activity of NiS. In cooperite, however, the chemical variations are rather small, limiting the confidence in any implied substitution trends. It became apparent during the analytical investigation of braggite from the Sompujärvi Reef (Penikat intrusion, Finland) that the relationships established from the Bushveld Complex are not the only possible

systematic relationship of cation contents in braggite. Here it was found that braggite displays a much lower, approximately constant, Ni proportion (Merkle et al., in preparation).

It stands to reason that this compositional diversity is caused by the intrinsic conditions under which these minerals formed. However, in ores which have cooled slowly from magmatic temperatures, and where exsolution of these minerals from “magmatic” sulphide assemblages on cooling is indicated, the temperature of formation (or of hydrothermal overprinting) is probably the single most important parameter to quantify (Makovicky et al. 1990).

The system Pd-Ni-S was investigated by Karup-Møller & Makovicky (1993) up to 900°C, and the system Ni-NiS-PtS-Pt by Gulyaniitskaya et al. (1979). Experimental investigations by Skinner et al. (1976) at 1000°C and Cabri et al. (1978) at 800°C concentrated on the PtS-PdS join and were not exploring the possible influence of Ni on thermal stabilities and miscibility ranges of minerals in the system.

The system Pd-Fe-Ni-S is believed to be responsible for the bulk of the PGE mineralogy, as well as for its large scale ore geology and PGE distribution (ignoring late stage processes) (Makovicky & Karup-Møller, 1995). In spite of the fact that solidus and subsolidus behaviour in the system Pd-Fe-Ni-S was investigated by Makovicky et al. (1990) and Makovicky & Karup-Møller (1995), the influence of Pt had not been assessed.

The objective of this study is to experimentally investigate the system PtS-PdS-NiS at 700°C, 800°C, 900°C, 1000°C, 1100°C, and 1200°C, in order to:

- (i) Establish the temperature dependance of stability fields and phase relations of the mineral phases, as well as miscibility gaps between synthetic cooperite and braggite.
- (ii) Investigate the influence of temperature on maximum Ni-solubility in cooperite, braggite, and vysotskite (most of the experiments were therefore carried out under Ni-saturated conditions).

- (iii) Determine trends in Ni-content of synthetic cooperite, braggite, and vysotskite related to their Pt- and Pd-content and temperature of synthesis in order to estimate temperatures of formation or equilibration of naturally occurring cooperite, braggite, and vysotskite.
- (iv) Compare the results of the experimental investigation with compositions of naturally occurring phases determined in this study and compositions from the literature, in order to give indications of their temperature of formation or equilibration.

This investigation represents the first step towards the understanding of some of the ore-forming processes for cooperite, braggite, and vysotskite and especially to better understand the interaction of PtS-PdS with nickel saturated sulphide. Although there are effects of variable S-content (Verryn & Merkle, 1996), in this study only initial sulphur contents of 50 at-% are reported on (except for the 1000°C isothermal section, where the sulphur content was varied slightly), as variation of sulphur went beyond the scope of this study.

The mineral chemistry of cooperite, braggite, and vysotskite occurring in nature was taken into account in the planning of experimental investigations of the system PtS-PdS-NiS.

In order to avoid confusion with naturally occurring cooperite, braggite and vysotskite, synthetic cooperite, braggite, and vysotskite are indicated as “cooperite”, “braggite”, and “vysotskite”, respectively in all the following Chapters. This is according to the convention on mineral nomenclature (Nickel, 1995) stating that synthetic phases should be distinguishable from naturally occurring phases.

CHAPTER 2

PREVIOUS INVESTIGATIONS OF PHASE RELATIONS

2 PREVIOUS INVESTIGATIONS OF PHASE RELATIONS

2.1 EXPERIMENTAL

Phase relations in the binary systems Pd-S, Pt-S, and Ni-S and the ternary systems Pd-Ni-S and Pt-Pd-S, have been studied by various authors. The relevant phase diagrams published in the literature for temperatures between 1200°C and 700°C are presented below.

2.1.1 The system Pd-S

Taylor (1985) re-investigated the phase relationships in the binary system Pd-S over the range of 0 to 50 at-% sulphur. This system had previously been researched by Wiebke & Laar (1935). Taylor's investigation shows the maximum stability temperature for PdS in equilibrium with Pd-S liquid to be close to 1000°C (Fig. 1), whereas Zviadadze et al. (1982), who investigated the phase relations in the system Ni-Pd-S, showed that temperature to be 975°C.

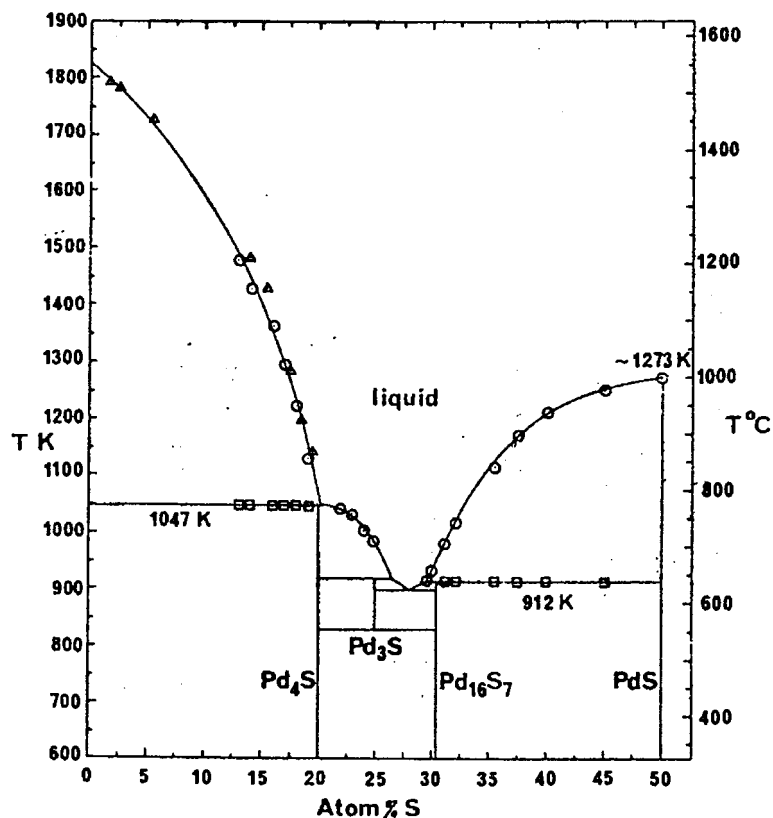


Figure 1 The Pd-S phase diagram in atomic proportions (Taylor, 1985)

2.1.2 The system Pt-S

Phase relationships in the binary system Pt-S over the range of 0 to 60 at-% sulphur are presented by Massalski (1986) (Fig. 2). Reference to this system also appears in Hansen & Anderko (1958) and in Moffat (1984). The maximum stability temperature for PtS in equilibrium with Pt-S liquid and/or vapour is close to 1330°C.

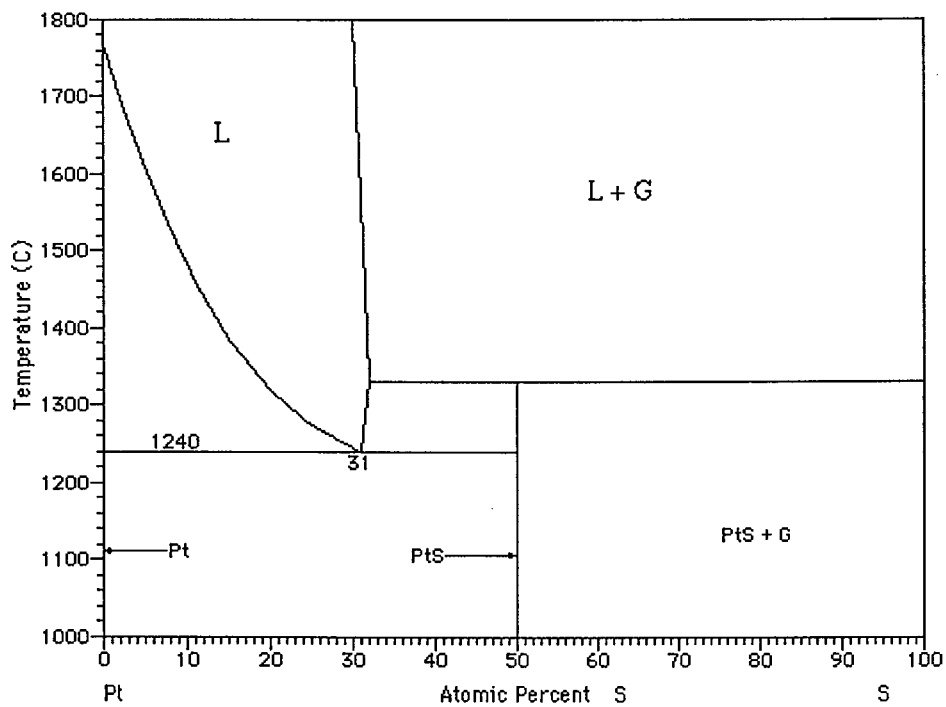


Figure 2 The Pt-S phase diagram in atomic proportions (from Massalski, 1986).

2.1.3 The system Ni-S

Kullerud & Yund (1962), Craig & Scott (1974), Lin et al. (1978), and Massalski (1986) reported, amongst others, on the phase relations in the Ni-S system. Arnold & Malik (1975) looked at the phase relations in the high sulphur (>50 at-%) region. The diagram published by Massalski (1986) is shown here for reference (Fig. 3). It is important to note that “low temperature millerite” (NiS) is only stable below 379°C, between 282°C to 995°C the “high temperature Ni_{1-x}S (δ-NiS in Figure 3) is the stable form.

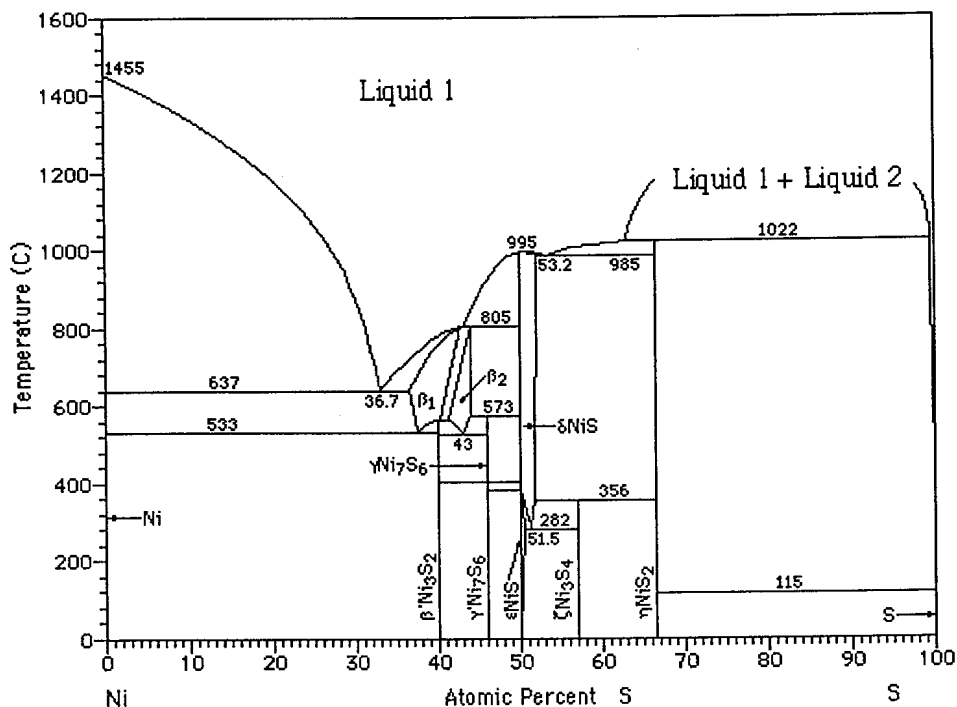


Figure 3 The Ni-S phase diagram in atomic proportions (from Massalski, 1986).

2.1.4 The system Pt-Pd-S

The system Pt-Pd-S was investigated by Skinner et al. (1976) at 1000°C. All experimental charges presented in that investigation contained less than 50 at-% sulphur. Phase relations are dominated by a liquid field lying close to the Pd-S join with a metal : sulphur ratio larger than 1. A complete solid solution series between Pt and Pd as well as “braggite” and “cooperite” are the stable solid phases. At 1000°C, “braggite” displays a compositional range from $(\text{Pd}_{0.40}\text{Pt}_{0.60})\text{S}$ to $(\text{Pd}_{0.84}\text{Pt}_{0.16})\text{S}$ and “cooperite” from PtS to $(\text{Pt}_{0.70}\text{Pd}_{0.30})\text{S}$.

Cabri et al. (1978) studied phase relations in the system Pt-Pd-S at 800°C. No solid phases more sulphur-rich than PtS or PdS were found to appear at this temperature. At 800°C, the same phases as at 1000°C (Skinner et al., 1976) are stable. The stability field of the liquid, however, is smaller. According to Cabri et al. (1978), the composition of “braggite” ranges from $(\text{Pt}_{0.24}\text{Pd}_{0.76})\text{S}$ to PdS and that of “cooperite” ranges from PtS to $(\text{Pt}_{0.54}\text{Pd}_{0.46})\text{S}$. These findings at 800°C do not correspond to the results of this investigation (see Chapter 6.6).

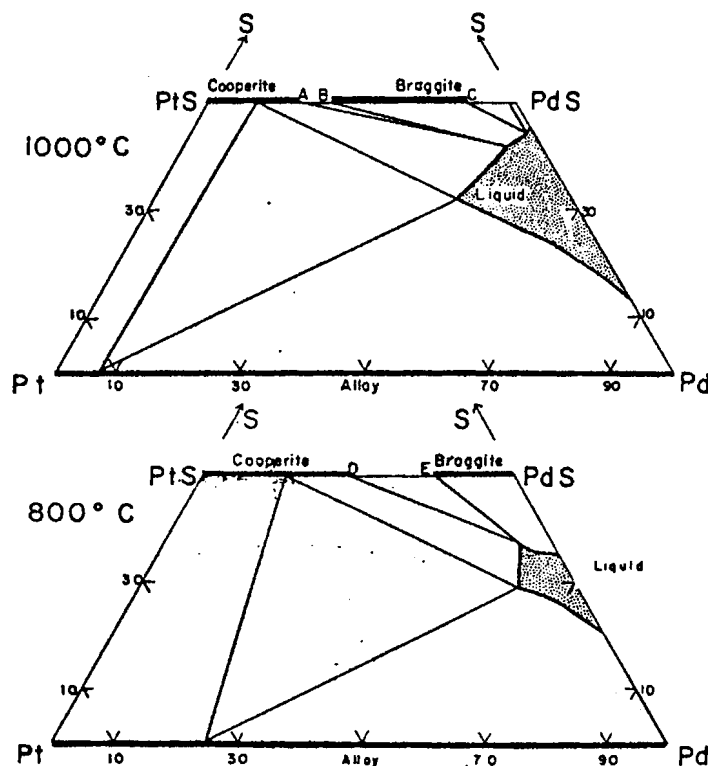


Figure 4 The Pt-Pd-S phase diagram in atomic proportions at 1000°C (Skinner et al., 1976) and 800°C (Cabri et al., 1978).

2.1.5 The system Pd-Ni-S

The system Pd-Ni-S was investigated by Zviadadze et al. (1982), Makovicky et al. (1990), and Karup-Møller & Makovicky (1993).

The paper by Makovicky et al. (1990) is a preliminary synopsis containing data on the system Pd-Ni-S, whereas Karup-Møller & Makovicky (1993) describe the final results of that system at 900°C, 725°C, 550°C, and 400°C in detail. At 900°C (Fig. 5), the central portion of the Pd-Ni-S system is dominated by a sulphide melt. The sulphur-poor boundary of the melt coexists with a continuous solid solution series between Pd and Ni. On the S-rich side, the sulphide melt takes part in the assemblages sulphide-melt - Ni_{1-x}S - NiS_2 , NiS_2 - sulphide-melt \pm liquid sulphur, and PdS - sulphide-melt \pm liquid sulphur. Therefore Ni_{1-x}S and PdS do not coexist at 900°C. At 900°C the maximum solubility of Ni in "vysotskite" coexisting with sulphide-melt is 3.9 at-% and the maximum solubility of Pd in Ni_{1-x}S coexisting with sulphide-melt is 2.1 at-%. At 725°C (Fig. 6), the compositional field of the sulphide melt is reduced, compared to that at 900°C, especially for the associations PdS - melt and PdS - Ni_{1-x}S . At 725°C there is a three-phase assemblage Ni_{1-x}S - PdS - sulphide-melt. In that assemblage PdS contains 8.2 at-% Ni and Ni_{1-x}S contains 0.94 at-% Pd.

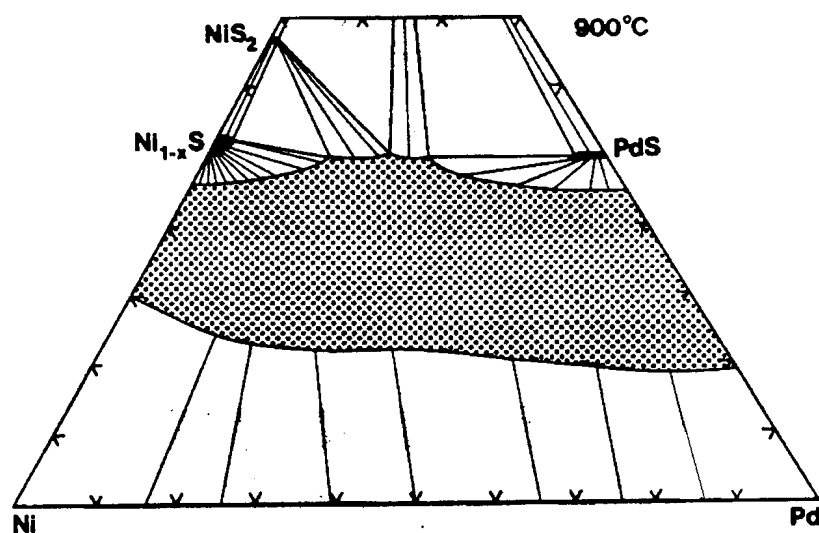


Figure 5 The system Pd-Ni-S at 900°C (Karup-Møller & Makovicky, 1993).

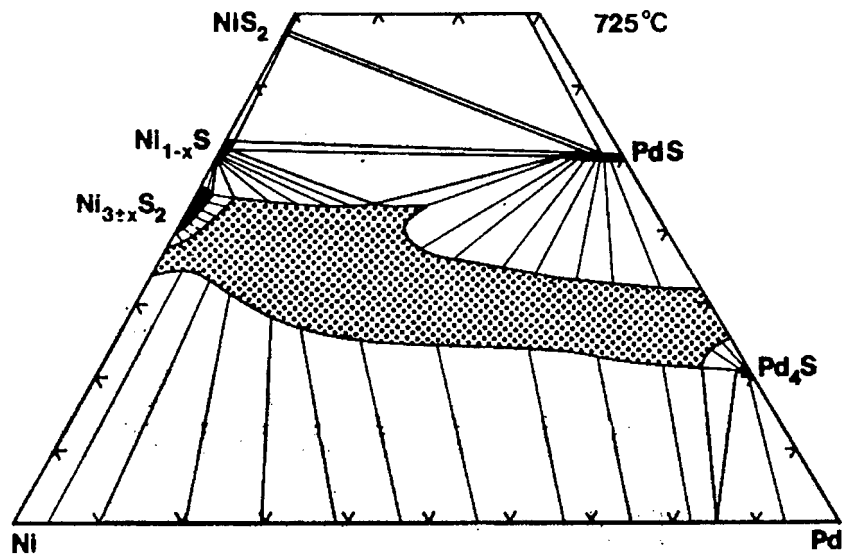


Figure 6 The system Pd-Ni-S at 725°C (Karup-Møller & Makovicky, 1993).

2.1.6 Related system Pd-Fe-Ni-S

As natural cooperite, braggite, and vysotskite can, apart from Ni, contain some Fe (see Chapter 8) the system Pd-Fe-Ni-S as described in the literature is presented here.

Makovicky et al. (1990) published preliminary results at 900°C, 725°C, 550°C, and 400°C and Makovicky & Karup-Møller (1995) present the latest phase study on this system at 900°C and 725°C. Phase relations at 900°C and 725°C in this quaternary system according to Makovicky & Karup-Møller (1995) are shown in Figures 7 and 8 respectively. High solubility of Ni (3.9 at-% at 900°C and 8.2 at-% at 725°C) in Fe-free PdS is contrasted by low solubility of Fe (0.4 at-% at 900°C and at 725°C) in Ni-free PdS (Makovicky & Karup-Møller, 1995). It is also important to note that the maximum Ni-solubility in PdS may be reduced with increasing Fe/Ni ratio in the assemblage at a given temperature.

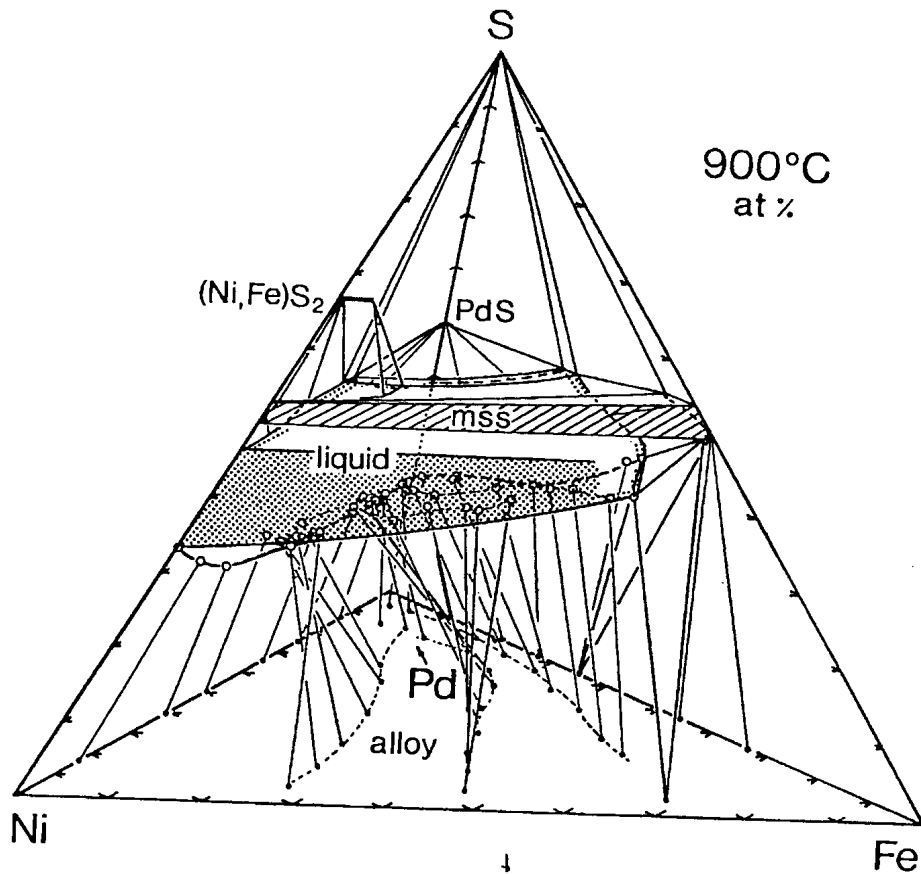


Figure 7 Phase relations in the system Pd-Ni-Fe-S in atomic proportions at 900°C (Makovicky & Karup-Møller, 1995).

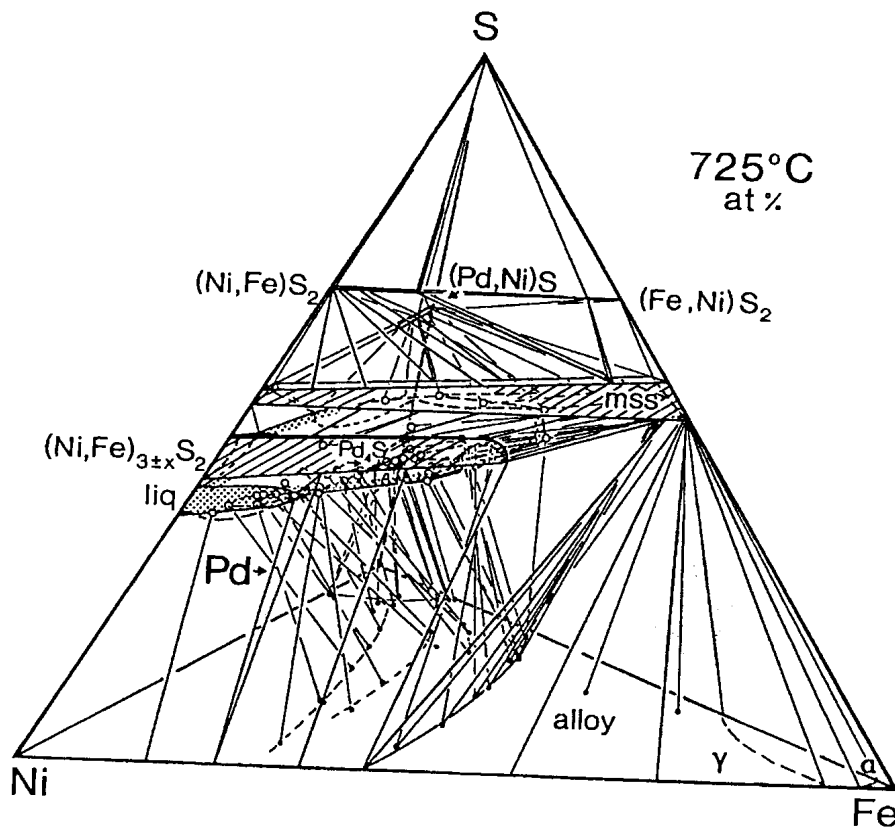


Figure 8 Phase relations in the system Pd-Ni-Fe-S atomic proportions at 725°C (Makovicky & Karup-Møller, 1995).

2.2 COMPOSITIONAL VARIATION OF NATURAL COOPERITE, BRAGGITE, AND VYSOTSKITE

As indicated in the introduction (Chapter 1), cooperite, braggite, and vysotskite have been described from many localities throughout the world. Figure 9 summarizes the compositional variation of the three minerals in the system PtS-PdS-NiS taken from the literature. Cooperite and braggite seem to be separated by a miscibility gap and there is an extensive solid solution between braggite and vysotskite. An arbitrary content of 10 mole per cent PtS is taken as the upper limit for vysotskite compositions (Cabri et al., 1978). Despite their wide distribution, cooperite and braggite are rarely observed in physical contact with each other.

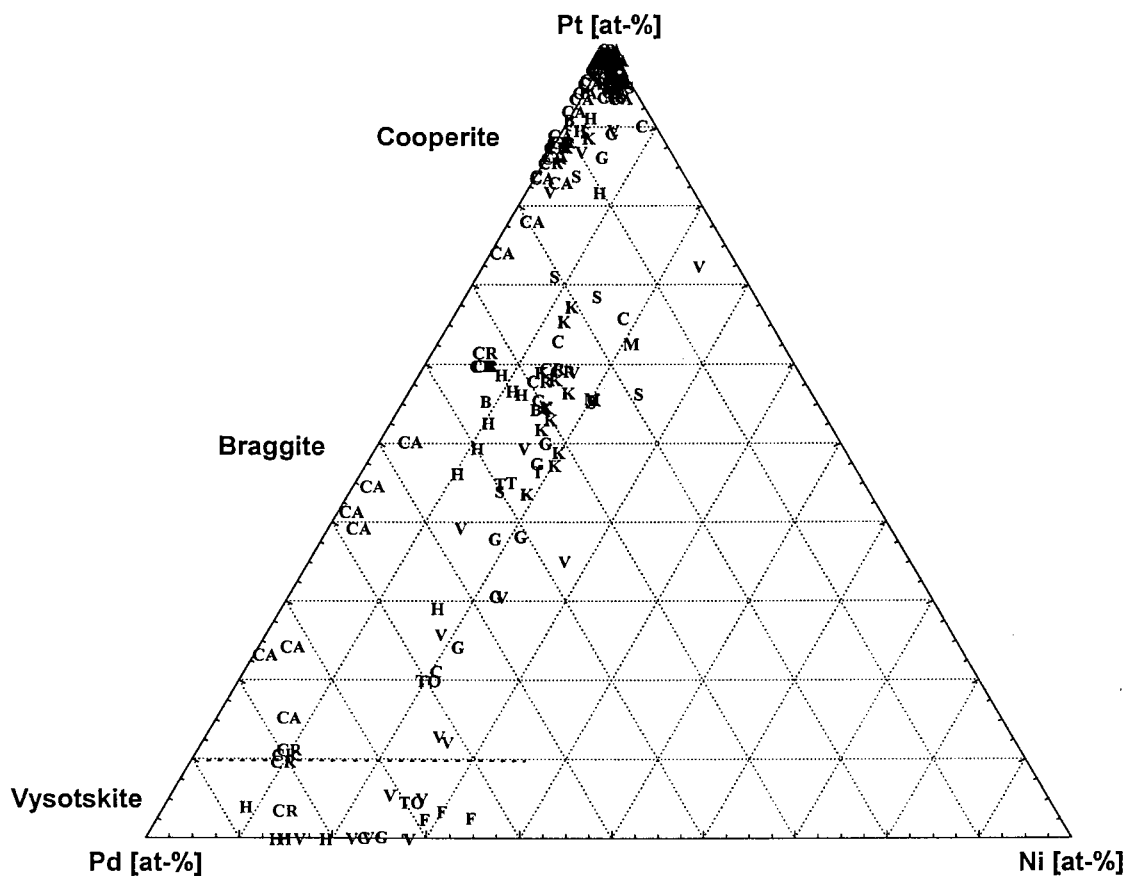


Figure 9 Compositional variation of cooperite, braggite, and vysotskite analyses from various localities in cation proportions. This Figure excludes the data from Merkle & Verryn, 1991 and Verryn & Merkle, 1994). Data taken from: **B**:Bannister & Hey, 1932; **C**: Cabri et al., 1978; **CA**: Cabri et al.,1996; **CR**: Criddle & Stanley, 1985; **G**: Genkin & Evstigneeva, 1986; **H**: Halkoaho, 1989; **K**: Kingston & El-Dosuky, 1982; **L**: Laputina & Genkin, 1975; **M**: Mostert et al., 1982; **S**: Schwellnus et al., 1976; **T**: Tarkian, 1987; **TO**: Todd et al., 1982; and **V**: Volborth et al., 1986. The black stippled line indicates the border between braggite and vysotskite.

CHAPTER 3

MINERAL PHASES

3 MINERAL PHASES

The mineral phases which were encountered in the polished sections of the experimental runs are “cooperite” ((Pt, Pd, Ni)S), “braggite” ((Pt, Pd, Ni)S), “vysotskite” ((Pt, Pd, Ni)S), quenched sulphide liquid, and $Ni_{1-x}S$. From natural samples cooperite, braggite, and vysotskite were analysed. Cooperite and braggite are separated by a miscibility gap, most likely due to the different crystallography of the two minerals. Cooperite belongs to space group $P4_2/mmc$, braggite and vysotskite to $P4_2/m$ (Bannister & Hey, 1932).

As braggite and vysotskite, belonging to the same space group, form a solid solution, these two minerals are discussed together in the following Chapters and are generally referred to as “braggite-vysotskite” or braggite-vysotskite. Vysotskites can be defined as all members of the braggite solid solution series containing less than 10 mole per cent PtS (Cabri et al., 1978).

The description of the optical properties of cooperite and braggite has caused a considerable amount of confusion in the past. Quantitative and descriptive data given for braggite often correspond to the properties of cooperite, whereas several descriptions of cooperite do not correspond to either of the two minerals. Therefore Criddle & Stanley (1985) re-investigated the three minerals with the aid of reflectivity measurements of analysed grains. Cabri et al. (1978) summarized existing compositional data, and Tarkian (1987) also presented compositional data as well as reflectance data. In this investigation it was observed that the frequency of twinning in large grains of natural cooperite and braggite may aid distinction of braggite and cooperite minerals. Looking at the cooperite and braggite grains from the Merensky Reef, only 3 out of 185 cooperite grains, but 40 out of 161 braggite grains were found to be twinned (Verryn & Merkle, 1996). Vysotskite cannot be distinguished optically from braggite, especially when it occurs as small grains. It is also possible to distinguish between cooperite and braggite-vysotskite using the Laser-Raman microprobe technique. Spectra of synthetic “cooperite” are sufficiently different from synthetic “braggite-vysotskite” in order to make a distinction between the two minerals. Raman spectra of synthetic “braggite” vary systematically with changes in Pt/Pd ratio, but this change is less pronounced than that found in “cooperite” (Merkle et al., 1997; 1999; Piki et al., 1998; 1999).

As this investigation concentrates on temperatures between 700°C and 1200°C, the Ni-sulphide encountered in the isothermal sections presented in the subsequent Chapters, is Ni_{1-x}S, which is stable between 282°C and 999°C (Lin et al., 1978). This was confirmed by X-ray powder diffractometry of Charge SV701, tempered at 700°C. In that sample the Ni-sulphide is, in fact, not a millerite, but corresponds well to the hexagonal high temperature NiS_{1.03} (see Fig. 10). The powder diffractogram was obtained on an automated Siemens D501 diffractometer. Monochromated Cu_{Kα} radiation at 40mA and 40 kV and a scanning speed of 1° 2θ/minute (stepsize = 0.04° 2θ, measuring time = 3 seconds) was used.

The optical properties of Ni_{1-x}S seem very close to those of millerite and are quoted as such in Table 1.

The optical properties of the various mineral phases are summarized in Table 1.

Table 1: Optical properties of the minerals in the system PtS-PdS-NiS (cooperite, braggite, and vysotskite after Criddle & Stanley (1985), millerite after Uytendogaart & Burke (1971)).

Phase	Colour	Bireflectance	Anisotropism
Cooperite ((Pt,Pd,Ni)S)	bluish white	in oil: white to bluish white	in oil: strong greenish grey to bright whitish yellow to brown-grey to bright and pale brown
Braggite-Vysotskite ((Pt,Pd,Ni)S)	pinkish white	extremely low	in oil: weak to distinct subdued purplish grey to pinkish brown
Millerite representing Ni _{1-x} S	yellow	in oil: distinct, bright yellow to greyish yellow	lemon-yellow to blue and violet, no complete extinction, basal sections appear isotropic

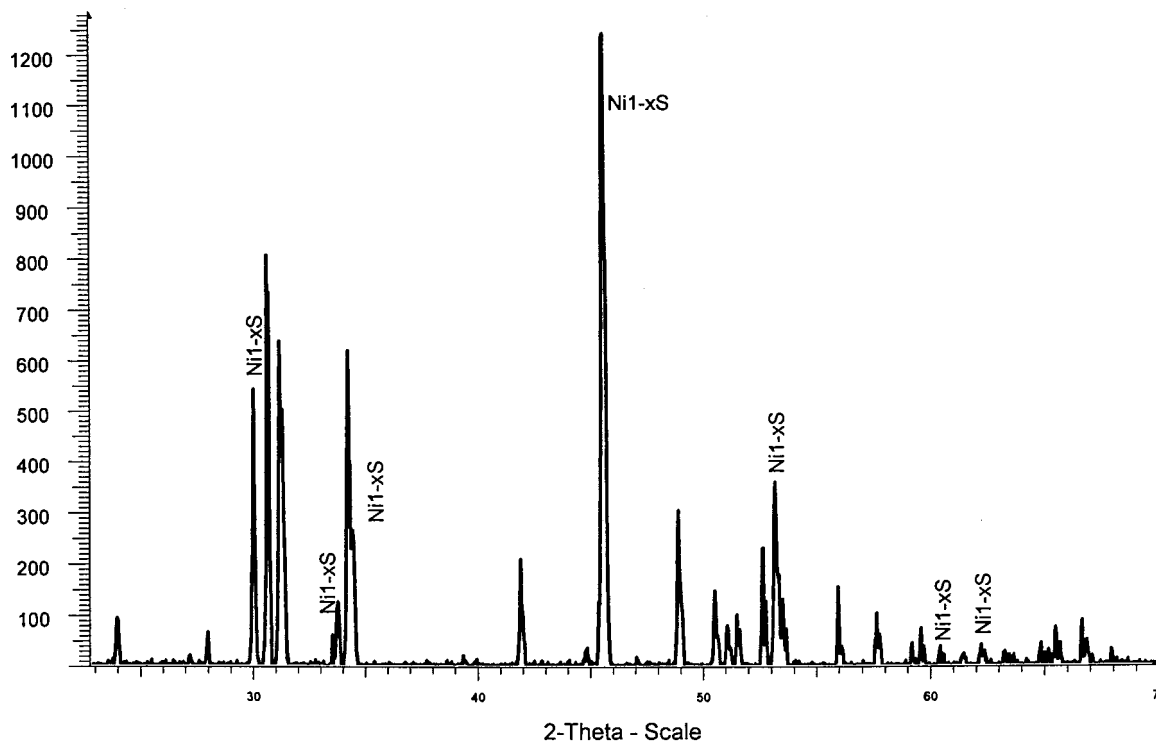


Figure 10 X-ray diffractogram ($\text{Cu}_{K\alpha}$ radiation) of experiment SV701. The peaks corresponding to Ni_{1-x}S (ICDD-PDF number 2-1373) are marked, the remaining peaks belong to “braggite”. The background has been subtracted and the analytical conditions are presented in the text.

CHAPTER 4

EXPERIMENTAL* *TECHNIQUES

4 EXPERIMENTAL TECHNIQUES

4.1 METHOD

All experiments were conducted under dry conditions following standard procedures in evacuated quartz-glass capsules (Kullerud, 1971; Moh & Taylor, 1971). Clear quartz-glass rods and tubes with an inner diameter of 4mm and an outer diameter of 6mm were used in all the experiments.

140 charges of 200-300mg each (only 200mg for charges containing high amounts of Pt in order to save costs) were prepared (see Appendix I).

The quantities of the various elements intended for the various experiments were weighed out to an accuracy of 4 decimal places. Sheets of weighing paper were cut into small pieces of about 5cm x 5cm in size and labelled for the respective elements. The chemicals were transferred onto the weighing paper, positioned on the scale, until the required quantity was reached. After all the elements for a particular experiment were weighed out, the chemicals were placed into a quartz glass tube, which had been sealed by melting one end. Frequently some of the chemicals stuck to the weighing paper, therefore the scale was zeroed after insertion of each element and the quantity corrected by addition of minute quantities of material at a time, until the correct weight was reached. Following that, the top of the tube was closed using the index finger pressed against a small piece of weighing paper placed at the open end of the tube, which was then shaken to achieve some degree of mixing of the chemicals. A glass rod was then added to reduce the volume within the tube. The tube was then sealed under a vacuum of $\sim 2 \times 10^{-2}$ millibar.

The Pt-, Pd-, and Ni- contents in the experimental charges were varied in such a manner, that Ni-saturation was achieved in most experiments, whereas the sulphur content was held constant at 50 at-%. In one batch of charges for experiments at 1000°C, the metal/sulphur ratios were varied in order to obtain an indication of the effects of sulphur pressure. These charges initially contained 47-52 at-% sulphur.

An excess of sulphur can cause experimental difficulties in dry sulphide research. Sulphur-vapour pressures are not known very accurately (Nell, 1987), but to avoid failure of the glass containers due to high sulphur vapour-pressures, the charges were

pre-reacted at at 700 - 850°C for 3-6 weeks. This pre-reaction gives the sulphur enough time to react with metals at a temperature where the sulphur pressure is low enough not to cause failure of the glass tubes (see Appendix I). After pre-reaction, the samples were quenched in air to avoid unnecessary strain on the quartz glass. The charges were then visually examined to ascertain that all the sulphur had reacted with the metals. In cases where sulphur was still observed, the charges were placed back into the pre-reaction furnace and examined again at a later stage.

After pre-reaction, two different heating procedures were employed:

- (i) The charge was placed into the furnace directly at the required temperature.
- (ii) The charge was heated up to a higher temperature than required and melted in order to achieve quick homogenization in the melt stage and then slowly cooled down to the required temperature and tempered. Validity of this method can be assumed as homogeneity between the phases was achieved in the experiments.

The experimental method employed for individual experiments, as well as tempering times of the various charges, can be deduced from Appendix I.

Reaction of the experimental charges took place in a chamber furnace, which had been modified to 6 tube furnaces with ± 40 cm long, horizontal corundum tubes (Fig. 11). The tubes are closed off in front with a refractive material, cut to the diameter of the tube. The laboratory has two such modified chamber furnaces. Advantages of this modified chamber furnace are:

- (i) The large volume heated within the furnace as a whole ensures a more stable temperature than in a furnace of smaller volume.
- (ii) In this furnace the temperature can be monitored more accurately than in an unmodified chamber furnace and charges can be moved to the exact position of the temperature required.
- (iii) Should a charge break or explode during melting or tempering, due to high sulphur pressures (as discussed above), only other charges positioned in that particular tube are affected.
- (iv) Should the tube be damaged after a charge has exploded, only that tube has to be replaced.

The temperature variations throughout the tubes were measured using a calibrated external thermocouple. Temperature differences of up to 25°C were observed between the highest temperature and the temperature at the front end of the individual tubes. Therefore, the temperature of the chamber furnace was set at higher temperatures than required for tempering so that the required temperature was reached somewhere in each of the six tubes (e.g. for a required temperature of 1000°C the furnace was set at 1020°C). The exact position, where the required temperature is reached was then determined with an accuracy of $\pm 2^\circ\text{C}$ for each tube and the charges were placed at that position. The temperature within the tubes was routinely monitored and adjustments were made, when necessary.

After tempering the experimental charges were quenched in a long cylindrical container filled with water placed next to the opening of the tubes of the modified chamber furnace. Using a long cylinder for quenching ensures that the hot charge cannot develop a steam envelope. A long metal rod with a small flat sheet welded to its tip, was used to scrape the charges out of the tubes into the water filled cylinder, where the temperature dropped to room temperature within seconds.

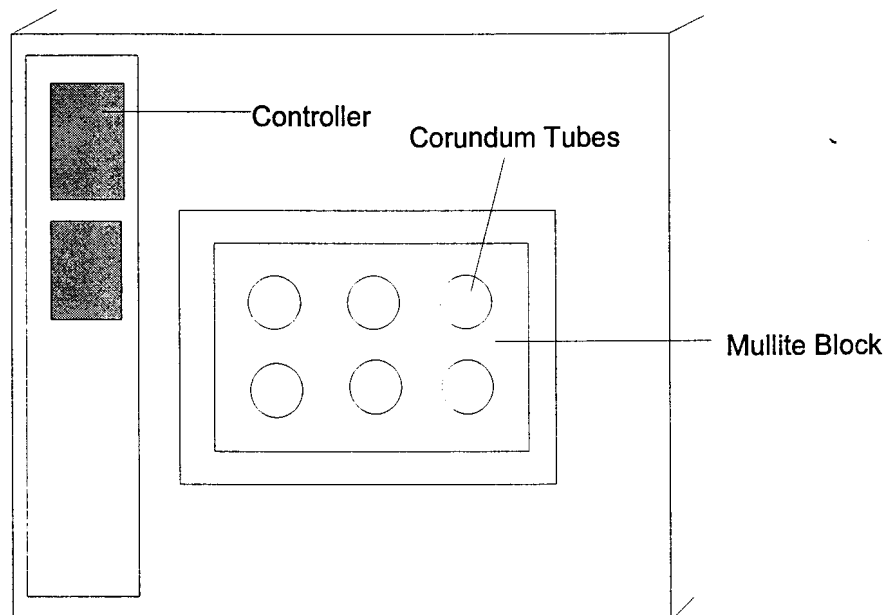


Figure 11 Modified chamber furnace with horizontal tubes

4.2 REACTANTS AND PLANNING OF EXPERIMENTS

Chemically pure (purity of $\geq 99.99\%$) fine powders of the elements platinum, palladium, nickel and sulphur were used for the experiments from 1200°C to 700°C carried out in 100°C intervals.

Phase diagrams of the system Pt-Pd-S published by Skinner et al. (1976) and Cabri et al. (1978) give an indication of the position of the miscibility gap between “cooperite” and “braggite” and were used to plan the experiments (i.e. the relative amounts of Pt, Pd, Ni, and S used in the experimental charges) aimed to determine the compositional variation of coexisting “cooperite” and “braggite” at the temperatures under investigation. Phase diagrams of the system Pt-Pd-S (Skinner et al., 1976; Cabri et al., 1978) and of the system Pd-Ni-S published by Makovicky et al. (1990) and Karup-Møller & Makovicky (1993), as well as analyses of natural cooperite, braggite, and vysotskite from the literature (see Chapter 2.2) and from this study (see Chapters 9.1 & 9.2) were used to plan experiments.

The reaction times of the experimental charges at 1000°C are relatively short (~6 weeks). Therefore, the 1000°C isothermal section was the first to be investigated. The experimental results obtained from the 1000°C isothermal section aided in the planning of the experiments for the 900°C and 1100°C isothermal sections, which were investigated next. The experimental results of the 900°C and 1100°C isothermal sections were then used in the planning of the experiments for the 800°C and 1200°C isothermal sections, respectively and, after the experiments at 800°C had been completed, the experiments for the 700°C isothermal section were planned and carried out.

If, after examination of investigated isothermal sections, it was found that more experiments should be carried out in order to obtain a meaningful result at a particular temperature, the phase diagram completed in part for that temperature was used to plan more experiments. Failed experiments were repeated, if these experiments were necessary to obtain worthwhile results for the construction of the particular isothermal section.

4.3 REDUCTION OF METALS

In order to avoid introduction of oxygen into the charges due to surface oxidation from exposure to the atmosphere, Ni was reduced before use. This was achieved using a modified muffle furnace (Fig. 12) and the following method:

Fine Ni-powder is placed into an open quartz-glass boat, which is placed into a quartz-glass tube of about 44 mm in diameter, fitted into a horizontal tube furnace (Fig.12). The furnace is set to 700°C and flushed with argon, leaving a continuous flow of ~1 bubble per second, which is monitored in the beaker shown in Figure 11. When the furnace reaches a temperature of approximately 350°C on heating, hydrogen is introduced at ~1 bubble per second. After remaining at 700°C for 2 hours, the furnace is turned off and left to cool to ~200°C, at which temperature the hydrogen is switched off and the argon flow continues to complete cooling, after which the sample is removed and stored in a desiccator.

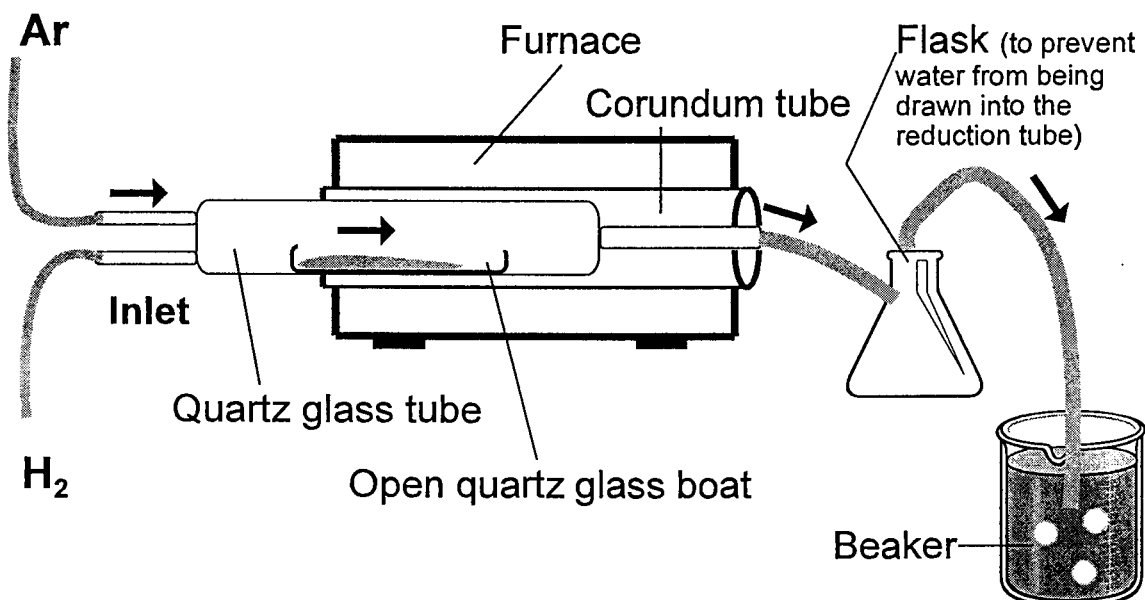


Figure 12 Setup of reduction furnace.

It was not found necessary to reduce Pt and Pd, because oxidation of natural PGE alloys is extremely slow (Westland, 1981).

The sulphur was dried for approximately 18 hours at a temperature of 97-99°C and then stored in a desiccator.

4.4 POLISHED SECTIONS

After quenching, the quartz-glass capsules were opened and each sample was divided into several parts using a stainless steel knife. In addition to the knife, a hammer was used in samples, which were difficult to break up. These samples, however, were wrapped up in a small piece of masking tape in order to avoid loss of material when hit by the hammer. The material was then scraped off the masking tape using a knife and some alcohol.

Approximately one third of the material was mounted in epoxy and polished for microscopic and electron microprobe investigation. The remaining sample is kept as a reference. In some cases, parts were used for X-ray diffraction investigations. As the individual samples are small (0.5 - 2 mm in diameter), samples of 4 different experiments were mounted in one polished section, using a small piece of copper wire as a reference point.

In order to avoid problems during polishing due to the brittleness of the phases present (especially "cooperite"), the samples were impregnated with epoxy under a light vacuum to fill possible voids in samples.

CHAPTER 5

ANALYTICAL TECHNIQUES

5 ANALYTICAL TECHNIQUES

Polished sections of quenched products of each completed experiment were studied by reflected light microscopy (in air). The compositional variation of the products was determined by electron microprobe analysis on a JEOL 733 microprobe in wavelength-dispersive mode. The accelerating potential was 20kV and the beam current 5×10^{-8} A. Standards used as well as X-ray lines, detection limits, and reproducibilities are listed in Table 2.

Table 2: Analytical conditions, detection limits (3 sigma level in per cent by mass) and reproducibilities (1 sigma, determined according to Kaiser and Specker (1956) in mass per cent; N=60 (n.d. = not determined).

Element	Standard	Anal. Crystal	X-Ray Line	Detection Limit		Reproducibility		
				Natural	Synthetic	Braggite	Cooperite	Ni _{1-x} S
Pt	Pt _{0.7} Pd _{0.3} S	LIF	L _α	0.172	0.093	0.256	0.284	0.033
Pd	Pt _{0.7} Pd _{0.3} S	PET	L _α	0.150	0.086	0.253	0.154	0.083
Ni	Ni	LIF	K _α	0.022	0.015	0.096	0.052	0.280
S	Pt _{0.7} Pd _{0.3} S	PET	K _α	n.d.	n.d.	0.218	0.218	0.732
Cu	CuFeS ₂	LIF	K _α	0.030	n.d.	0.063	0.008	n.d
Fe	FeS	LIF	K _α	0.022	n.d.	0.016	0.005	n.d
Co	CoS ₂	LIF	K _α	0.023	n.d.	n.d.	0.009	n.d
Rh	Rh	PET	L _α	0.112	n.d.	n.d.	0.043	n.d
As	PtAs ₂	TAP	L _α	0.055	n.d.	n.d.	n.d.	n.d

50 to 100 spot analyses were taken on each of the different phases (i.e. “cooperite”, “braggite”, “vysotskite”, and Ni_{1-x}S,) observed in the polished section of each experiment. Counting times were 50 seconds at the peak positions and 25 seconds at symmetrical background positions. Totals between 98.5 and 101.5 wt-% were accepted for further calculations.

The composition of solidified melt was analysed using a de-focussed beam (about 50µm in diameter) or scanning multiple preselected areas at low magnifications (depending on the size of the area occupied by melt), using the same standards as for the solid phases. Counting times were 50 seconds at the peak positions and 25 seconds at symmetrical background positions.

This procedure was validated as follows:

- (i) The standards used in the standardization were analysed as the unknown phase at various magnifications. The results of the analyses were in good agreement with the true composition of the standard (see Table 3).
- (ii) In a binary phase assemblage (i.e. only two phases are in equilibrium with each other) within a ternary phase diagram, the bulk composition of a sample (i.e. the amount of chemicals weighed into the initial charge) should plot on the straight line connecting the two phases in equilibrium (i.e. “cooperite”, “braggite”, or “vysotskite” and melt). In this investigation the composition of either “cooperite”, “braggite”, or “vysotskite”, the bulk composition of that experiment, and the composition of the solidified melt, plotted in the ternary diagram PtS-PdS-NiS, can generally be connected by a straight line. This is illustrated using the experimental results obtained for the 1100°C isothermal section (Figure 13).

Table 3: Comparison of mean analytical results using a de-focussed beam as well as various scan area magnifications with the actual composition of the standard analysed (in wt-%). Values in parenthesis show the standard deviation at the 1 σ level (N=20).

	De-focussed beam (~50 μ m)	Scan (600x magnification)	Scan (1000x magnification)	Scan (1600x magnification)	Actual composition
Pt	68.40 (0.32)	68.42 (0.40)	68.22 (0.33)	68.00 (0.43)	68.09
Pd	15.81 (0.32)	15.63 (0.27)	15.73 (0.29)	15.86 (0.25)	15.92
Ni	16.23 (0.38)	15.65 (0.39)	15.68 (0.43)	15.47 (0.49)	15.99
Total	100.44 (0.93)	99.80 (0.79)	99.68 (0.84)	99.32 (0.58)	100.00

Between 10 and 30 analyses of the melt were taken per experiment in polished sections where a melt phase was observed. Except where stated otherwise, totals between 97.0 and 101.5 wt-% were accepted for further calculations. The acceptance of lower totals than that for the analysis of “cooperite”, “braggite”, and “vysotskite”, is due to the presence of voids on the polished sections and within the area of the solidified melt analysed, which may lower the totals of the analyses.

For the analysis of natural cooperite, braggite, and vysotskite counting times were 20 seconds at the peak positions and 10 seconds for symmetrical backgrounds. The elements analysed were Pt, Pd, Ni, S, Cu, Fe, Co, Rh, and As. Arsenic was never present in quantities above the detection limit (0.055 wt-%) and is therefore omitted from the Tables.

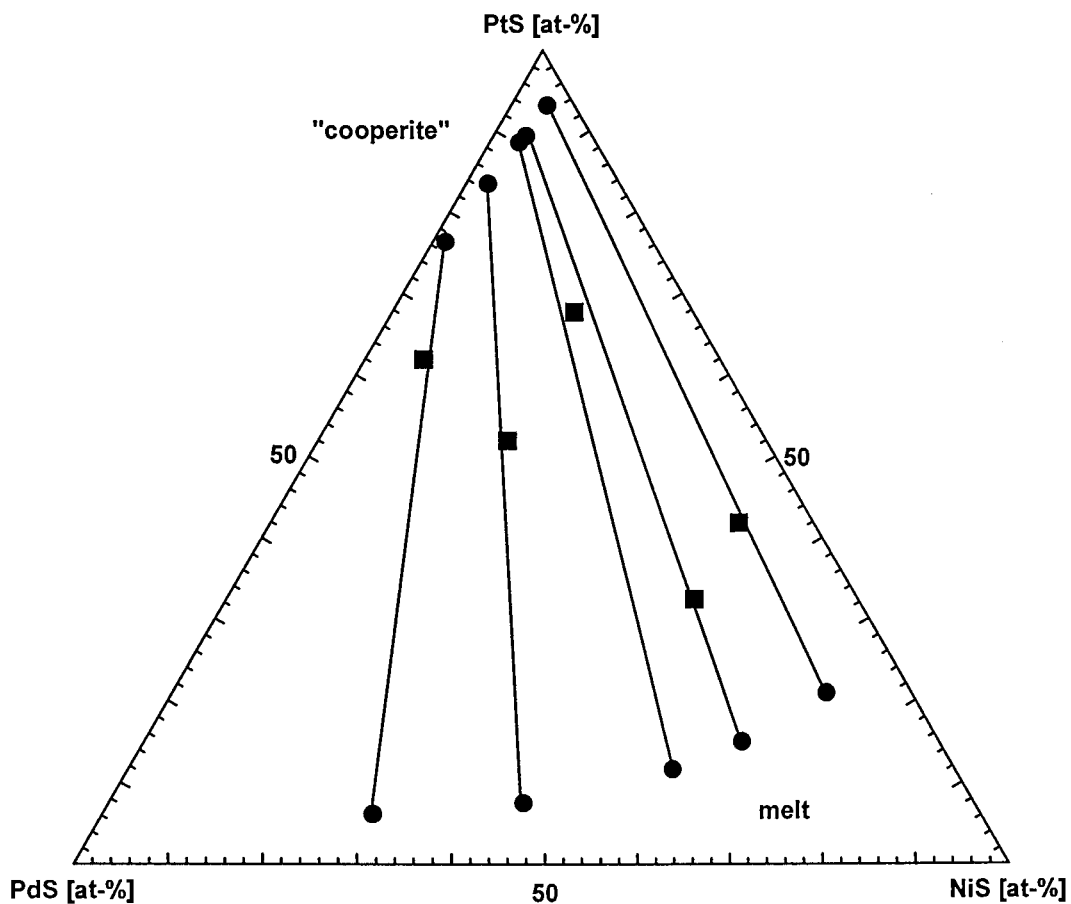


Figure 13 Bulk composition (in molecular proportions) of experimental charges (■), "cooperite" (●) and melt composition (●) connected by tie-lines at 1100°C.

Reproducibilities, based on randomly selected pairs of analyses taken on the same spot, were calculated according to Kaiser & Specker (1956) using the following formula:

$$s = \sqrt{\frac{\sum_{i=1}^{N/2} (x'_i - x''_i)^2}{N}}$$

where s = standard deviation
 x'_i and x''_i = the two values for the i -th sample
 N = number of analyses

The detection limit of an element is a function of counting time, accelerating potential, and beam current; longer counting times resulting in lower detection limits. As longer counting times were used in the analysis of synthetic phases than in the analysis of natural phases, the detection limits are lower for the synthetic phases (see Table 1).

The calculation of ZAF correction factors of the JEOL software used during the analysis of the naturally occurring phases lead to errors in the determination of Pd. Whenever PdS was used as a standard, Pd in an analysis of stoichiometric (Pt, Pd)S (S: 15.99 wt-%, Pt: 68.09 wt-%, Pd 15.92 wt-%) was approximately 2 wt-% too low. When the same (Pt, Pd)S was used as a standard, analyses of pure PdS were found to be approximately 6 wt-% too high. It is suspected that this problem is similar to that discussed by Reid et al. (1988) for Au-Ag alloys and it was also encountered for Cu-Ni alloys by Bruwer (1996). It was decided to use the (Pt,Pd)S standard as a reference and to recalculate all analyses with Pd > 16 wt-% according to the following equation:

$$\text{corrected Pd} = 0.8844 \times \text{measured Pd} + 1.8404 \quad (\text{Equation 1})$$

This problem was not encountered when analysing the synthetic phases as new computer software with better correction procedures was available then.

After correction for Pd (where necessary) analyses with totals between 98.5 and 101.5 wt-% were used for further calculations. Traverse analyses close to the grain boundary of coexisting braggite and cooperite were discarded for calculation of the means if

cooperite showed abnormally high Pd-contents, or if the Pd-contents in braggite were abnormally low compared with the rest of that particular grain. In such cases interference from the neighbouring grain was assumed, because of the large excitation area of about $2.5\mu\text{m}$ (primary and fluorescent radiation) at 20 kV.

CHAPTER 6

ISOTHERMAL SECTIONS

6 ISOTHERMAL SECTIONS

6.1 INTRODUCTION

In this Chapter the experimental results obtained for the temperatures 1200°C, 1100°C, 1000°C, 900°C, 800°C, and 700°C are presented.

After analyses with totals falling outside the acceptable intervals (as discussed in Chapter 5) were eliminated, outliers were discarded through visual inspection of histograms of each element analysed for every phase in each experiment. From the remaining analysis, arithmetic means, including standard deviations at the 1σ level, of the spot analysis (wt-%), were calculated for each phase in each experiment. Totals were calculated in the same manner. Atomic proportions were calculated from these means and their standard deviations are taken from the calculations of the mean of all the analyses recalculated to atomic proportions.

Experiments, where the standard deviations of the means of the elements analysed, lie within 3σ of the reproducibility for all the elements present (see Table 2, Chapter 5), were regarded as homogeneous. All experiments not complying with that criterion were discarded and not used in the discussions in the following Chapters.

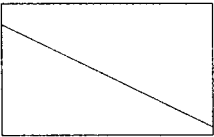
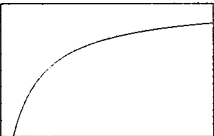
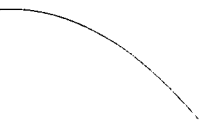
For all calculations and diagrams the atomic proportions calculated from the means are used. Ternary diagrams are presented in cation proportions rather than as PtS-PdS-NiS (implying 50 at-% S), as the solidified melt does sometimes contain less than 50 at-% sulphur (see Chapters 6.2, 6.3, 6.4 and Chapter 7). In the text, however, the Pt-Pd-Ni joins are often referred to as PtS-PdS-NiS joins in order to emphasize the presence of sulphur. Tie lines, as well as boundaries of the stability fields, presented in the ternary diagrams of the following Chapters, represent the exact compositions of the experimental runs as indicated in the relevant Tables.

Preliminary results for 1100°C, 1000°C, and 900°C are published in Verryn & Merkle (2000).

Scatterplots of various combinations of elements were examined visually in order to establish whether relationships between elements are linear, or show a logarithmic-, square root-, an inverse-, or a polynomial relationship (an exponential relationship was never observed). The aim was to use the “simplest” fit describing the relationship between the elements (e.g. a linear fit rather than a logarithmic-/square root-/inverse fit and the latter rather than a polynomial fit) depending on the coefficient of determination (R^2 -value). The coefficient of determination for a model $y = a_0 + a_1x_1 + a_2x_2 + \dots + a_kx_k + b$ is defined as the proportion of the variability in the dependant variable, y , that is accounted for by the independent variables, x_1, x_2, \dots, x_k , of the model (Ott, 1988).

Table 4 lists examples of the equations of fits tested on the various distributions of data points described in the following Chapters.

Table 4: Indication of distributions of data points, their best fits, and relevant general equations.

Examples of distribution of data points	Fit	General Equation
	Linear	$y = a + bx$
	Logarithmic	$y = a + b \log_{10} x$
	Inverse	$y = a + b/x$
	square root	$y = a + b\sqrt{x}$
	2 nd order polynomial function	$y = a + bx + cx^2$

In the subsequent Chapters, the equations of the best fits between various combinations of elements at the 95% per cent confidence level, as well as the R^2 values are presented in Tables. Where relationships between two variables fall into the logarithmic - inverse - square root - group, all the R^2 values are presented and the relevant equation for the best fit is given.

Best linear fits between the Pt- and Ni-content in “cooperite” are calculated for the range of 36 to 50 at-% Pt, the compositional variation of “cooperite” observed in this investigation.

Unfortunately, the statistical software used (Statistica version 5 (StatSoft, Inc., 1995)), does not show the 95% confidence bands for all types of fits and they are omitted in such cases (e.g. the inverse function, the square root function, and the logarithmic function).

Photomicrographs presented in each sub-chapter on the individual isothermal sections, were selected in such a way, that, as a whole, they represent a cross-section of the various possible phase associations encountered in the experimental runs.

6.2 THE 1200°C ISOTHERMAL SECTION

At 1200°C, the two phases recognized are “cooperite” and a melt. The compositional relationship between the “cooperite” and the melt is shown in Figure 14. Sample SV1205 contained only a melt phase and is not used in the following discussion. The average compositions at 1200°C are summarized in Table 5. Photomicrographs 1 and 2 show the typical texture of “cooperite” and the coexisting melt at 1200°C.

The PdS-NiS join is occupied by a melt with a maximum solubility of 19.0 at-% Pt along the PtS-NiS join and of 16.5 at-% Pt along the PtS-PdS join. Towards the central portion of the melt field, along the PdS-NiS join, the Pt-content increases to a maximum of 22.4 at-% Pt. The maximum solubility of Ni in ideal, Pd-free “cooperite” coexisting with a Pd-free melt along the PtS-NiS join is 1.5 at-%. The Pd-content limit in Ni-free “cooperite”, coexisting with a Ni-free melt at 1200°C is 6.3 at-%.

Table 5: Mean (arithmetic) compositions of phases in the system PtS-PdS-NiS at 1200°C in weight per cent (wt%) and atomic per cent (at%). Values in parenthesis show the standard deviation at the 1 σ level. N = number of analyses per experiment.

Sample	Phases		Pt	Pd	Ni	S	TOTAL
SV1201	"Cooperite"	wt%	79.08 (0.33)	6.15 (0.39)	0	14.63 (0.38)	99.86
		at%	44.08 (0.65)	6.29 (0.36)	0	49.63 (0.59)	(N=70)
	Melt	wt%	33.05 (3.51)	56.41 (3.75)	0	10.85 (0.28)	100.76
		at%	16.51 (1.89)	50.96 (2.73)	0	32.53 (0.99)	(N=10)
SV1202	"Cooperite"	wt%	80.56 (0.28)	4.52 (0.30)	0.13 (0.01)	14.34 (0.26)	99.55
		at%	45.63 (0.62)	4.69 (0.31)	0.24 (0.02)	49.44 (0.60)	(N=53)
	Melt	wt%	44.58 (4.26)	39.61 (4.43)	2.66 (0.41)	11.95 (0.44)	98.80
		at%	22.43 (2.49)	36.54 (3.56)	4.45 (0.64)	36.58 (1.74)	(N=10)
SV1203	"Cooperite"	wt%	81.15 (0.17)	3.89 (0.21)	0.26 (0.01)	13.91 (0.17)	99.22
		at%	46.69 (0.33)	4.10 (0.21)	0.50 (0.02)	48.71 (0.24)	(N=15)
	Melt	wt%	45.60 (4.05)	33.12 (3.17)	5.83 (0.68)	13.93 (0.40)	98.48
		at%	21.67 (2.45)	28.85 (2.00)	9.21 (0.84)	40.27 (0.69)	(N=8)
SV1204	"Cooperite"	wt%	82.12 (0.30)	3.13 (0.31)	0.40 (0.05)	13.87 (0.27)	99.52
		at%	47.31 (0.44)	3.31 (0.32)	0.77 (0.09)	48.61 (0.51)	(N=33)
	Melt	wt%	50.58 (5.93)	25.66 (3.23)	9.09 (2.36)	16.62 (0.78)	101.94
		at%	22.09 (3.48)	20.55 (1.90)	13.19 (2.82)	44.17 (1.38)	(N=6)
SV1206	"Cooperite"	wt%	83.16 (0.26)	1.28 (0.40)	0.62 (0.06)	14.07 (0.44)	99.13
		at%	48.02 (0.64)	1.36 (0.43)	1.19 (0.11)	49.43 (0.87)	(N=40)
	Melt	wt%	49.70 (4.03)	13.49 (0.90)	17.07 (2.43)	18.54 (0.52)	98.81
		at%	20.37 (2.14)	10.14 (0.53)	23.25 (2.51)	46.24 (0.80)	(N=6)
SV1207	"Cooperite"	wt%	83.75 (0.26)	0.89 (0.40)	0.71 (0.06)	13.99 (0.44)	99.34
		at%	48.45 (0.72)	0.94 (0.43)	1.36 (0.12)	49.25 (0.84)	(N=50)
	Melt	wt%	47.44 (3.23)	6.28 (1.34)	18.88 (2.51)	20.81 (0.71)	99.41
		at%	19.10 (1.96)	4.64 (0.85)	25.27 (2.29)	50.99 (1.36)	(N=13)
SV1208	"Cooperite"	wt%	84.52 (0.19)	0	0.75 (0.17)	13.80 (0.33)	99.17
		at%	49.43 (0.62)	0	1.46 (0.32)	49.11 (0.54)	(N=34)
	Melt	wt%	47.52 (5.54)	0	23.12 (4.77)	21.04 (1.42)	98.96
		at%	19.03 (3.34)	0	30.44 (4.06)	50.73 (1.13)	(N=21)

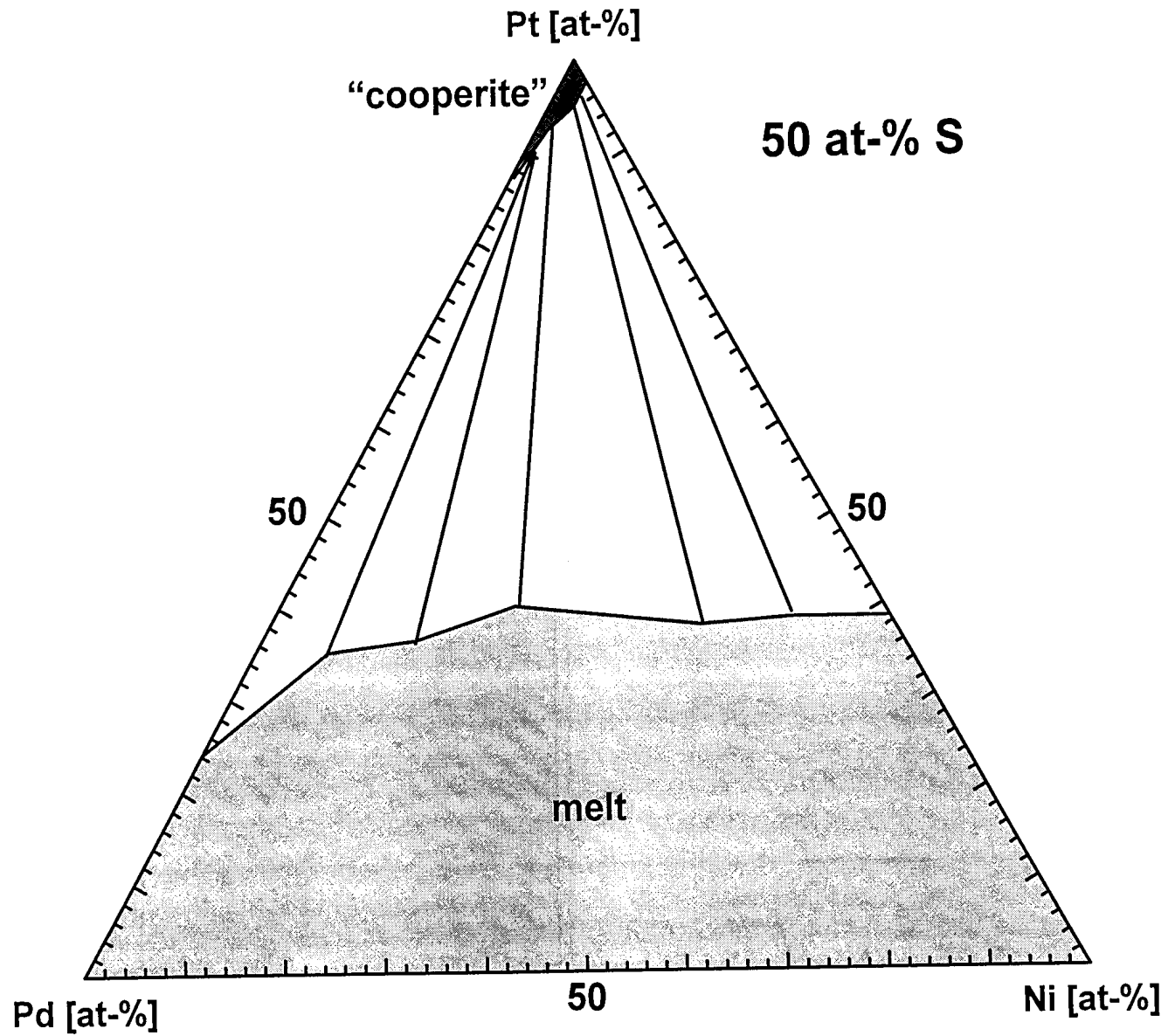
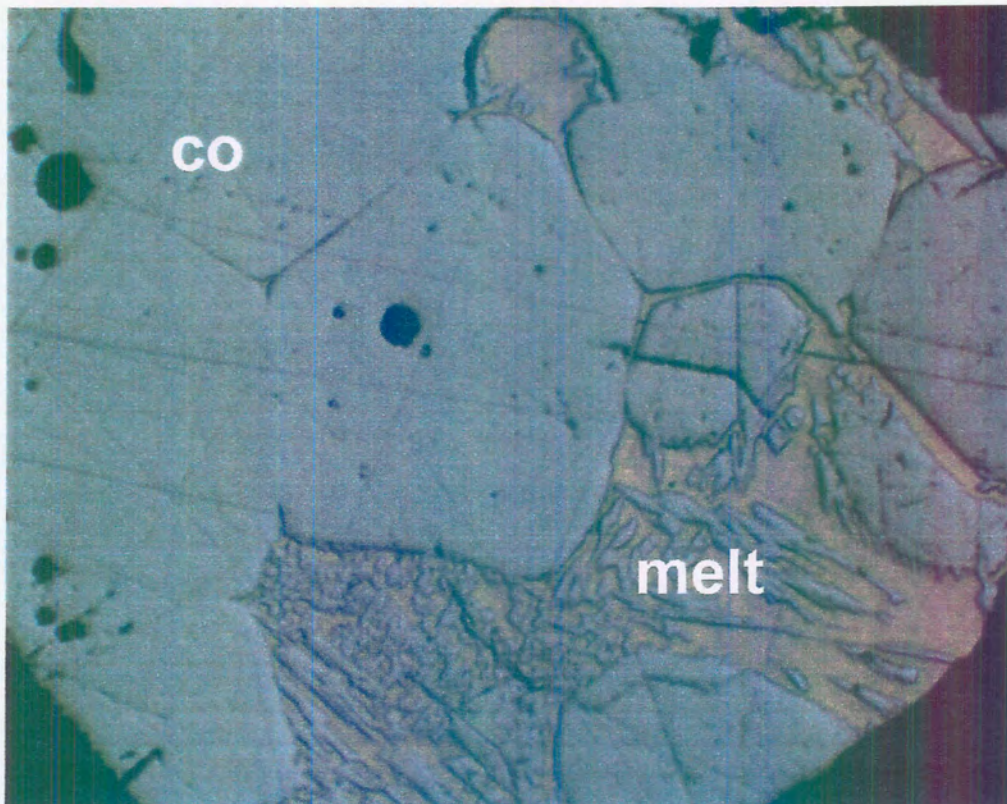
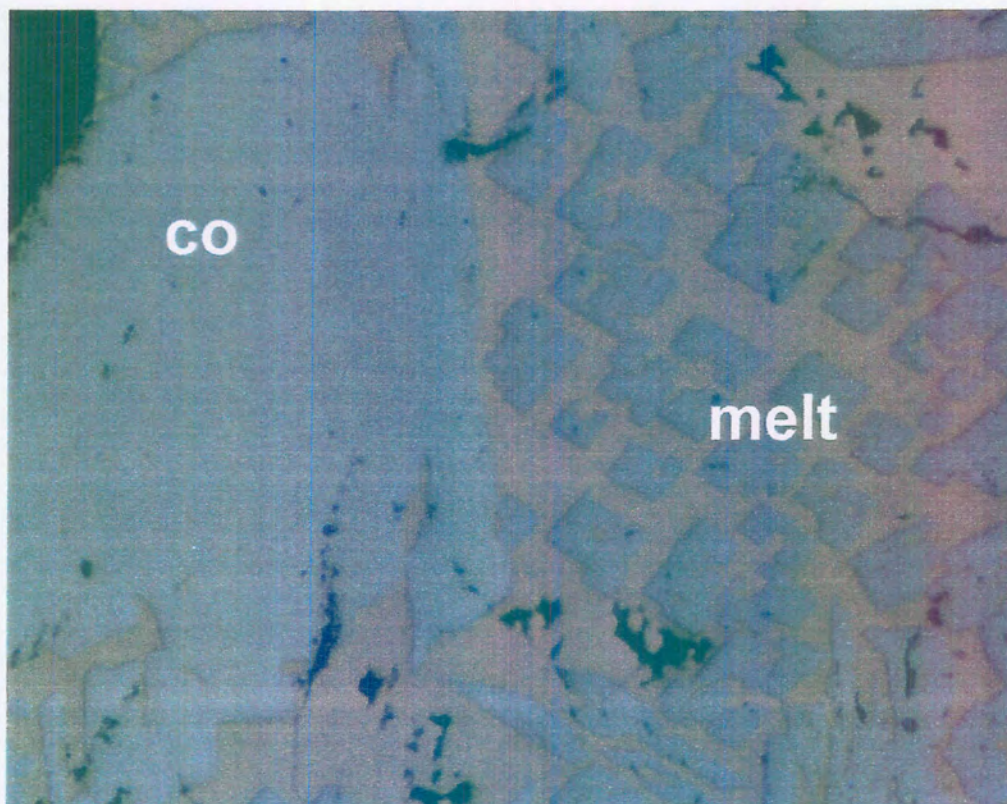


Figure 14 Phase relations in the system PtS-PdS-NiS in cation proportions at 1200°C.



Photomicrograph 1 "Cooperite" (co) and coexisting melt at 1200°C of experiment SV1204 (long side of the photomicrograph is 1.1 mm).



Photomicrograph 2 "Cooperite" (co) and coexisting melt at 1200°C of experiment SV1206 (long side of the photomicrograph is 0.35 mm).

6.2.1 “Cooperite” at 1200°C

The Ni-content in “cooperite” at 1200°C decreases slightly with increasing Pd-content. Least square fittings of the data for “cooperite” (in cation per cent) lead to the equations presented in Table 6.

Table 6: Type of best fit, equation for best fit at the 95% confidence level, equation number (No), and R²-values of best fits of elements analysed in “cooperite” formed at 1200°C.

Variables	Fit	Equation	No	R ²
Ni, Pt	Linear	$Ni = -2.612 (\pm 0.367) + 0.307 (\pm 0.033) \times Pt$	2	0.9456
Ni, Pd	Linear	$Ni = 1.523 (\pm 0.049) - 0.249 (\pm 0.014) \times Pd$	3	0.9854
Pt, Pd	Linear	$Pt = 49.388 (\pm 0.263) - 0.778 (\pm 0.073) \times Pd$	4	0.9582
Ni, Pt/Pd	Logarithmic			0.9516
	Inverse	$Ni = 1.596 (\pm 0.497) - 12.702 (\pm 0.713) / (Pt/Pd)$	5	0.9906
	Square root			0.9181

Equations 2-5 are represented graphically in Figures 15 to 18:

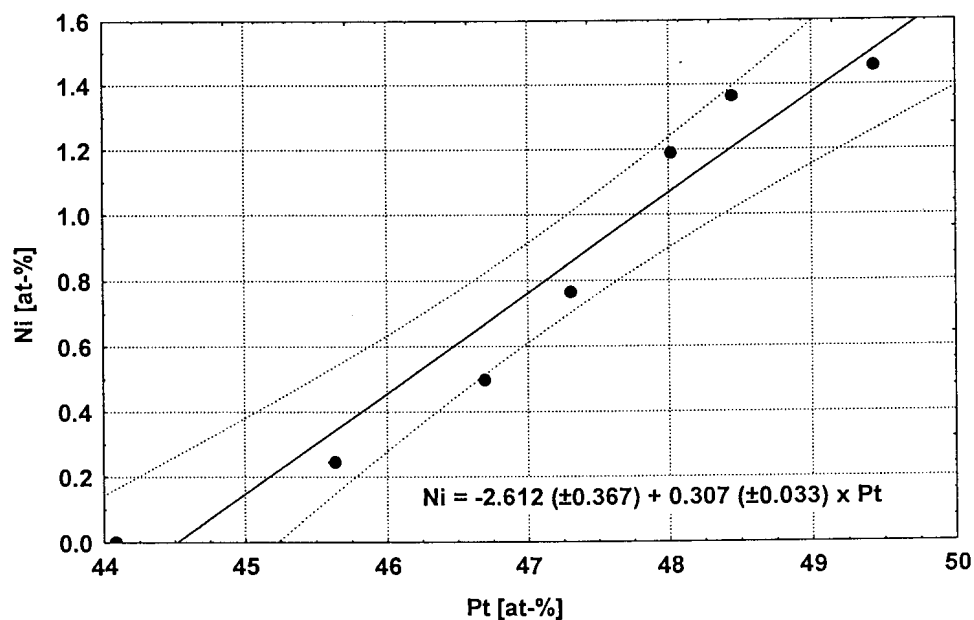


Figure 15 Ni-content versus Pt-content (in at-%) in “cooperite” formed at 1200°C. The solid line indicates the best linear fit and the stippled lines the 95% confidence interval according to the equation shown (N=7).

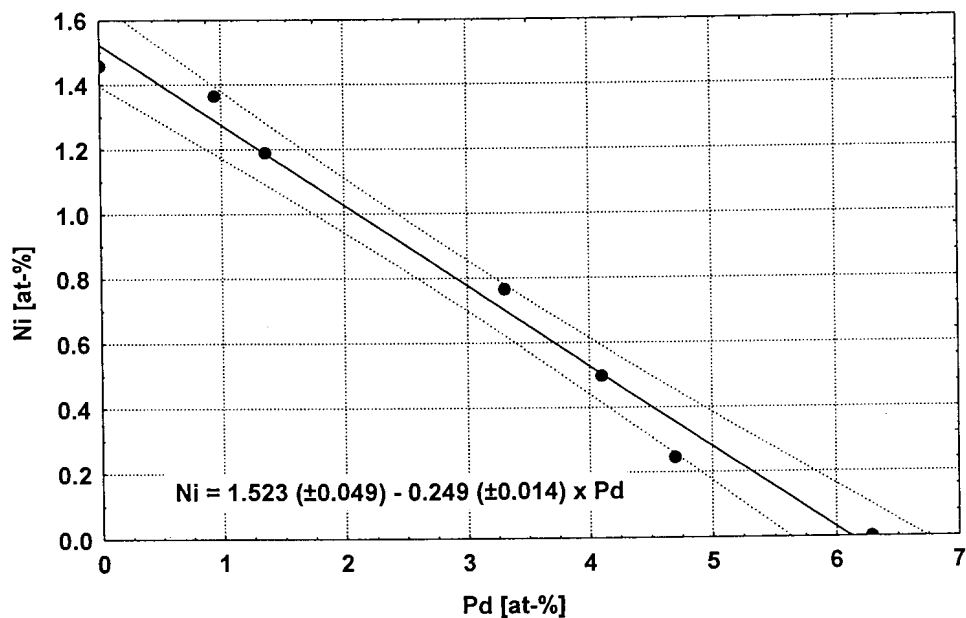


Figure 16 Ni-content versus Pd-content (in at-%) in “cooperite” formed at 1200°C. The solid line indicates the best linear fit and the stippled lines the 95% confidence interval according to the equation shown (N=7).

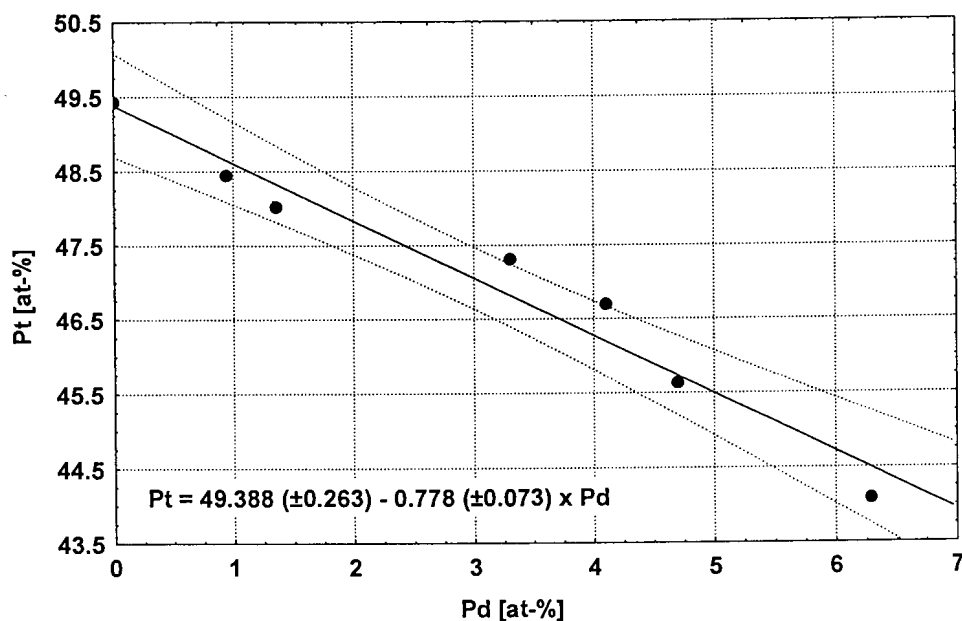


Figure 17 Pt-content versus Pd-content (in at-%) in “cooperite” formed at 1200°C. The solid line indicates the best linear fit and the stippled lines the 95% confidence interval according to the equation shown (N=7).

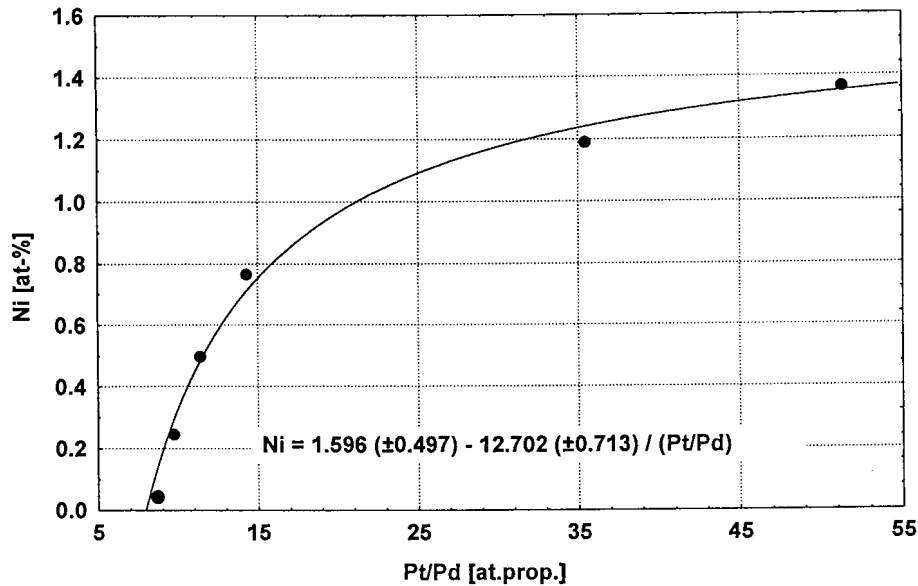


Figure 18 Ni-content versus Pt/Pd ratio (in atomic proportions) in “cooperite” formed at 1200°C. The solid line indicates the best fit according to the equation shown (N=6).

6.2.2 Melt at 1200°C

After quenching, a thin layer of sulphur on the capsule walls was observed in some charges. The amount of visible sulphur on the capsule walls increases with increasing Pd-content at constant bulk S-content in the charge.

The amount of free sulphur after quenching seems not to be due to a surplus of sulphur which was not able to react with the metals present. Two possible interpretations of this observation are:

- (i) The sulphur on the capsule walls is due to a release of elemental sulphur on quenching in analogy to the phase-relations in the Ni-Pd-S system (Karup-Møller & Makovicky, 1993) (see also Figures 5 & 6, Chapter 2). In this investigation at 1200°C, the proportions of melt (58 - 82 per cent, estimated using the lever rule), as well as the Pd-content in the melt, increase in the quenched experiments with increasing bulk Pd-content. Karup-Møller & Makovicky (1993) showed that at 900°C, the central portion of the system Pd-Ni-S is dominated by

a sulphide melt which extends from the Ni-S join to the Pd-S join. At the Ni-S join the melt contains between ~30 and ~46 at-% S and at the Pd-S join between ~8.5 to ~45 at-% S. In the central portion of the stability field of the melt, the melt can contain between 20 and 50 at-% sulphur; i.e. there is a drop of maximum S-content in the melt from the central portion towards the Pd-S- and the Ni-S joins. This shift in maximum S-solubility in the melt with variation in Pd/Ni ratio - and in this investigation with additional variation of Pt-content - could cause the expulsion of elemental sulphur on quenching which, in the rapid process of quenching, cannot combine with any of the crystallizing phases, and condenses on the capsule walls.

- (ii) The sulphur on the tube walls may be interpreted to be condensed vapour as described by Arnold & Malik (1975) for the NiS-S system and by Arnold (1971) for the FeS-S system. Arnold & Malik (1975) proposed to correct the combined condensed phases (solid and/or liquids) for the loss of sulphur by weighing of the sulphur in each cooled charge. In the system Pt-Pd-Ni-S, cooperite is a stoichiometric mono-sulphide and only the melt portion should be corrected for sulphur loss. The amount of sulphur condensed on the capsule wall lies, however, within the weighing uncertainty and a correction of the S-content of the melt would be inaccurate.

Spearman rank correlation (Ott, 1988) between the S-content and the Pd-content shows a strong negative correlation of $r = -0.96$. Between the S- and Ni-content there is a strong positive correlation of $r = 0.96$. Between S-content and the Pd/Ni ratio the Spearman correlation is $r = -0.94$. There is no significant correlation between the S-content and Pt-content. The relationship between the Pd-, Ni-, and S-contents in the melt at 1200°C can be visualized in the following 3D scatter plot (Fig.19).

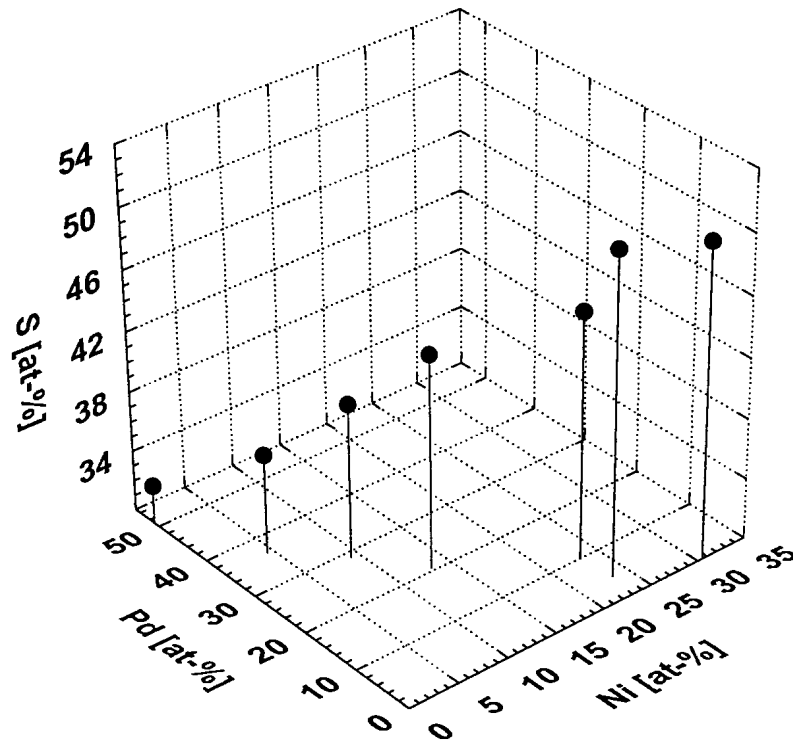


Figure 19 3D scatterplot of Pd-, Ni-, and S-content (in at-%) in melt coexisting with “cooperite” at 1200°C (N=7).

6.2.3 Relationships at 1200°C

Examination of Figure 14 indicates that the Pd-content of “cooperite” and the Pd-content of the coexisting melt have a strong positive linear relationship. The Pd-content of “cooperite” and the Ni-content of the coexisting melt, show a strong negative, linear relationship. The relationship of the Pt-content of “cooperite” and the Pd- and Ni-content of the coexisting melt is antipathetic to that of the Pd-content of “cooperite”. The Pt-content of the melt shows no systematic relationship with the Pt-, Pd-, or Ni-content of the “cooperite”, due to its erratic compositional variation within the melt. The compositional relationship of the Pd-content of “cooperite” and the Pd-content of the coexisting melt at 1200°C is illustrated in Figure 20.

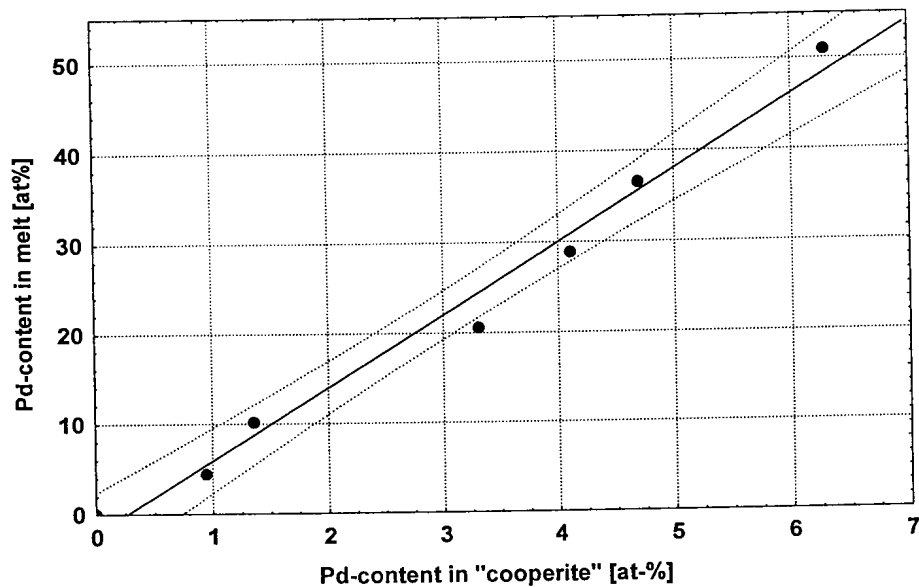


Figure 20 Pd-content in melt versus Pd-content in “cooperite” at 1200°C (in at-%). The solid line indicates the best linear fit and the stippled lines the 95% confidence interval of that fit (N=7).

6.3 THE 1100°C ISOTHERMAL SECTION

The two phases observed at 1100°C are “cooperite” and a melt. Compared to the phase relations at 1200°C, the compositional field of the melt is reduced and that of “cooperite” is enlarged.

The compositional relationship between the two phases is shown in Figure 21 and the compositions of melt and coexisting “cooperite” are presented in Table 7. Photomicrograph 3 shows the typical texture of “cooperite” and the coexisting melt at 1100°C, which is very similar to that at 1200°C (see Photomicrograph 2).

The PdS-NiS join is occupied by a melt with a maximum solubility of 9.0 at-% Pt along the PtS-NiS join as well as along the PtS-PdS join. Contrary to the observations at 1200°C, the Pt-content decreases slightly to a minimum of 3.5 at-% Pt towards the central portion of the melt field along the PdS-NiS join at 1100°C. The maximum solubility of Ni in ideal, Pd-free “cooperite”, coexisting with Pd-free melt along the PtS-NiS join, is 2.7 at-%. The Pd-content limit in Ni-free “cooperite”, coexisting with Ni-free melt at 1100°C, lies at 12.8 at-% (Fig.21 & Table 7).

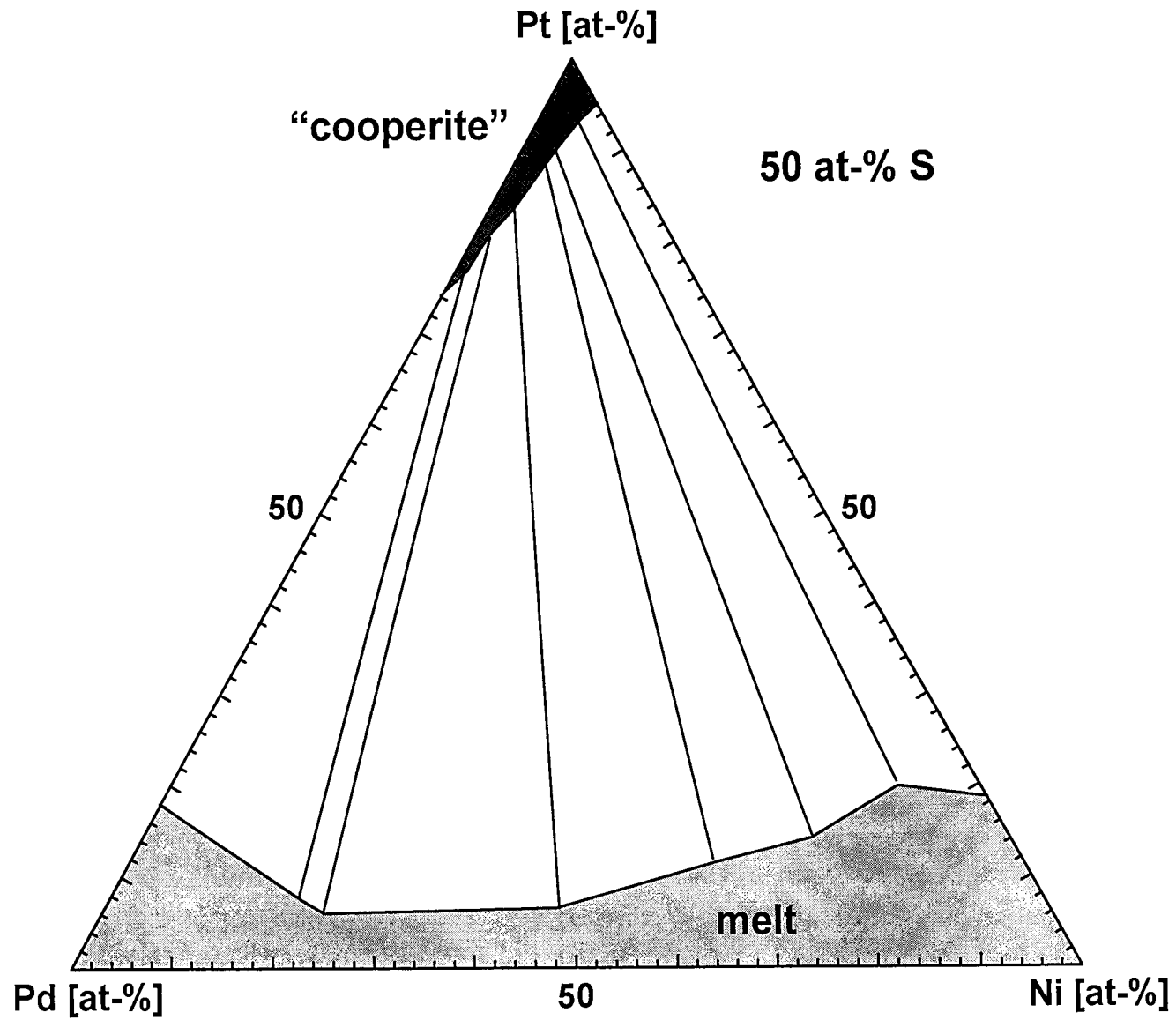
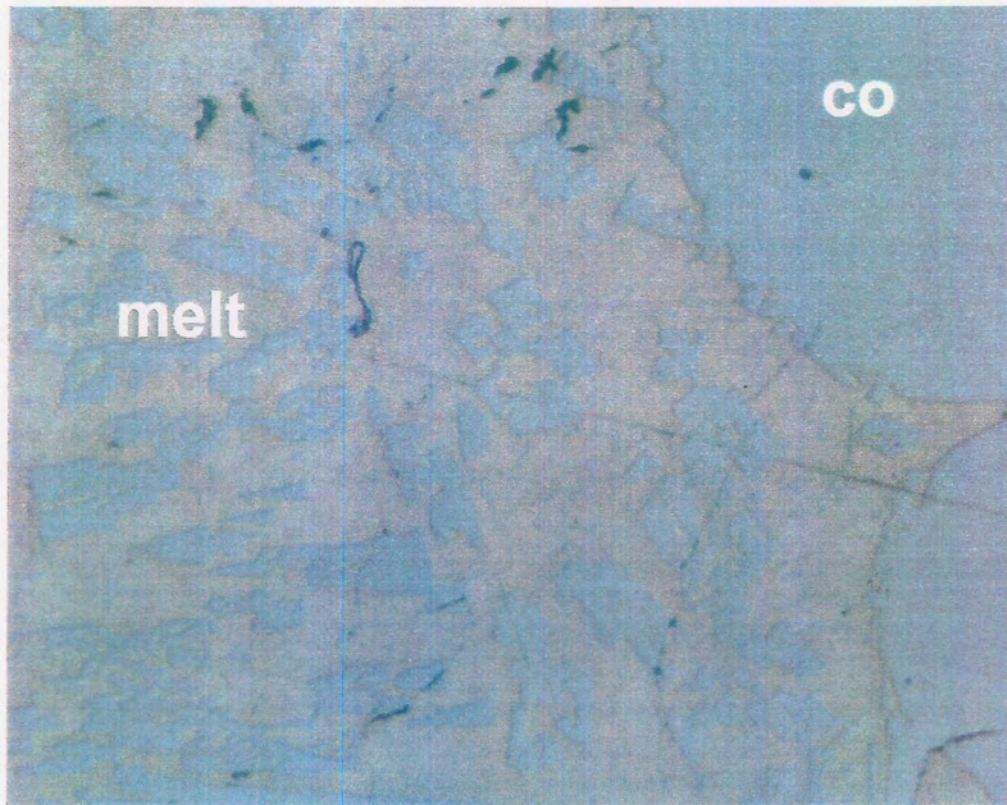


Figure 21 Phase relations in the system PtS-PdS-NiS in cation proportions at 1100°C



Photomicrograph 3 "Cooperite" (co) and coexisting melt at 1100°C of experiment SV337 (long side of the photomicrograph is 0.35 mm).

Table 7: Mean (arithmetic) compositions of phases in the system PtS-PdS-NiS at 1100°C in weight per cent (wt%) and atomic per cent (at%). Values in parenthesis show the standard deviation at the 1 σ level. N = number of analyses per experiment.

Sample	Phases		Pt	Pd	Ni	S	TOTAL
SV337	"Cooperite"	wt%	83.43 (0.37)	1.41 (0.33)	1.04 (0.08)	13.74 (0.15)	99.62
		at%	48.20 (0.32)	1.49 (0.34)	2.00 (0.15)	48.31 (0.29)	(N=17)
	Melt	wt%	31.75 (3.08)	6.92 (1.28)	35.10 (3.09)	26.08 (1.45)	99.45
		at%	9.93 (1.19)	3.97 (0.81)	36.48 (2.55)	49.63 (2.02)	(N=10)
SV338	"Cooperite"	wt%	74.62 (0.37)	9.12 (0.32)	0.38 (0.06)	15.06 (0.26)	99.18
		at%	40.51 (0.41)	9.08 (0.29)	0.68 (0.10)	49.73 (0.40)	(N=35)
	Melt	wt%	9.79 (6.55)	61.62 (5.88)	10.51 (1.98)	17.72 (1.67)	99.64
		at%	3.69 (2.49)	42.55 (4.38)	13.15 (2.20)	40.61 (3.27)	(N=21)
SV339	"Cooperite"	wt%	78.48 (0.58)	7.10 (0.45)	0	15.23 (0.18)	100.82
		at%	42.61 (0.56)	7.07 (0.51)	0	50.32 (0.50)	(N=7)
SV340	"Cooperite"	wt%	70.84 (0.57)	13.43 (0.46)	0	16.02 (0.32)	100.29
		at%	36.71 (0.48)	12.76 (0.40)	0	50.53 (0.50)	(N=38)
	Melt	wt%	21.40 (6.94)	62.32 (6.73)	0	16.70 (0.61)	100.42
		at%	9.02 (3.09)	48.16 (4.58)	0	42.83 (1.72)	(N=16)
SV342	"Cooperite"	wt%	84.26 (0.79)	0	1.45 (0.04)	14.28 (0.16)	100.01
		at%	47.89 (0.35)	0	2.74 (0.06)	49.37 (0.32)	(N=33)
	Melt	wt%	30.56 (7.39)	0	40.53 (6.05)	28.78 (1.79)	100.21
		at%	8.98 (2.77)	0	39.57 (4.36)	51.45 (2.34)	(N=15)
SV1102	"Cooperite"	wt%	72.06 (0.29)	11.48 (0.41)	0.38 (0.02)	15.71 (0.36)	99.63
		at%	37.93 (0.58)	11.08 (0.39)	0.66 (0.04)	50.32 (0.57)	(N=117)
	Melt	wt%	10.99 (4.54)	61.38 (2.69)	8.80 (1.99)	18.19 (0.76)	99.36
		at%	4.17 (1.79)	42.72 (0.97)	11.10 (2.26)	42.01 (1.61)	(N=15)
SV1103	"Cooperite"	wt%	80.21 (0.21)	4.06 (0.35)	0.86 (0.03)	14.69 (0.38)	99.83
		at%	44.59 (0.41)	4.13 (0.32)	1.59 (0.05)	49.69 (0.59)	(N=96)
	Melt	wt%	18.84 (5.92)	26.75 (3.49)	28.21 (5.76)	25.44 (1.67)	98.98
		at%	5.95 (2.37)	15.50 (1.70)	29.63 (5.92)	48.92 (3.04)	(N=5)
SV1104	"Cooperite"	wt%	80.78 (0.29)	3.50 (0.28)	0.94 (0.07)	14.55 (0.28)	99.77
		at%	45.16 (0.57)	3.59 (0.26)	1.75 (0.12)	49.50 (0.54)	(N=44)
	Melt	wt%	23.59 (5.07)	17.54 (2.73)	33.88 (2.99)	24.68 (1.33)	99.69
		at%	7.40 (1.79)	10.10 (1.63)	35.35 (2.25)	47.15 (1.68)	(N=6)
SV1105	"Cooperite"	wt%	77.08(0.24)	7.11 (0.29)	0.65 (0.05)	15.16 (0.34)	99.99
		at%	41.78 (0.54)	7.06 (0.26)	1.17 (0.09)	49.99 (0.60)	(N=53)
	Melt	wt%	10.65 (7.62)	43.87 (8.41)	22.74 (9.28)	23.09 (1.29)	100.35
		at%	3.47 (2.78)	26.19 (6.36)	24.60 (8.64)	45.74 (1.89)	(N=21)

6.3.1 “Cooperite” at 1100°C

The Ni-content in “cooperite” at 1100°C decreases slightly with increasing Pd-content. Least square fittings of the data for “cooperite” (in cation per cent) lead to the following relationships at the 95% confidence level (Table 8):

Table 8: Type of best fit, equation for best fit at the 95% confidence level, equation number (No), and R²-values of best fits of elements analysed in “cooperite” formed at 1100°C.

Variables	Fit	Equation	No	R ²
Ni, Pt	Linear	$Ni = 0.007 (\pm 0.195) + 0.192 (\pm 0.024) \times Pt$	6	0.9115
Ni, Pd	Linear	$Ni = 2.469 (\pm 0.115) - 0.186 (\pm 0.015) \times Pd$	7	0.9910
Pt, Pd	Linear	$Pt = 48.596 (\pm 0.346) - 0.934 (\pm 0.046) \times Pd$	8	0.9857
Ni, Pt/Pd	Logarithmic			0.9149
	Inverse	$Ni = 2.130 (\pm 0.102) - 5.548 (\pm 0.586) / (Pt/Pd)$	9	0.9573
	Square root			0.8104

Equations 6 to 9 are shown graphically in Figures 22 to 25:

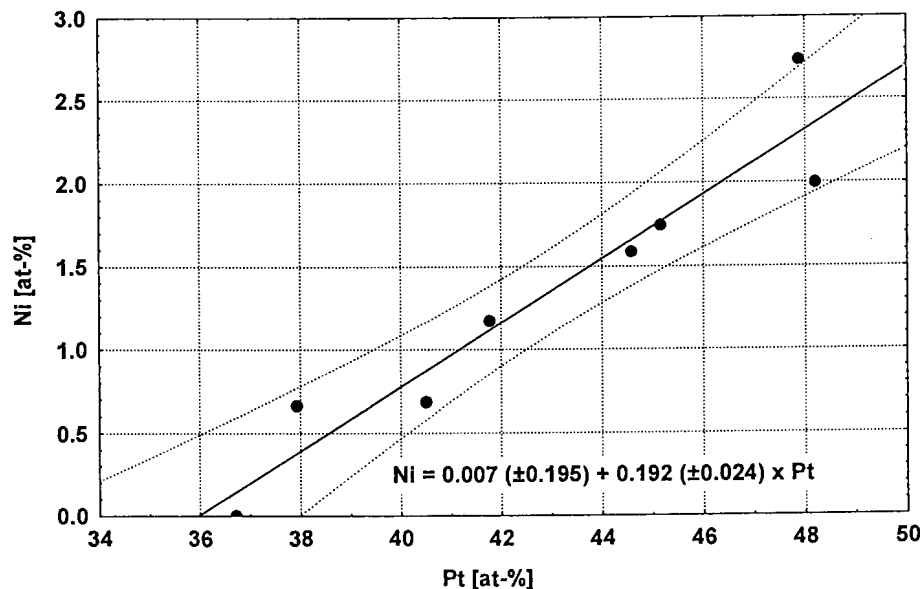


Figure 22 Ni-content versus Pt-content (in at-%) in “cooperite” formed in a Ni-saturated environment at 1100°C. The solid line indicates the best linear fit and the stippled lines the 95% confidence interval according to the equation shown (N=8).

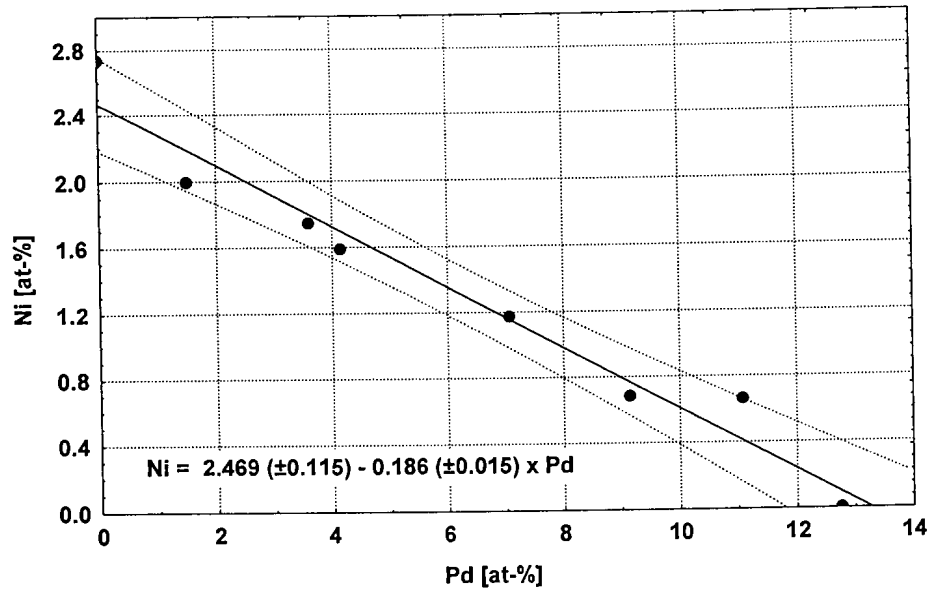


Figure 23 Ni-content versus Pd-content (in at-%) in “cooperite” formed in a Ni-saturated environment at 1100°C. The solid line indicates the best linear fit and the stippled lines the 95% confidence interval according to the equation shown (N=8).

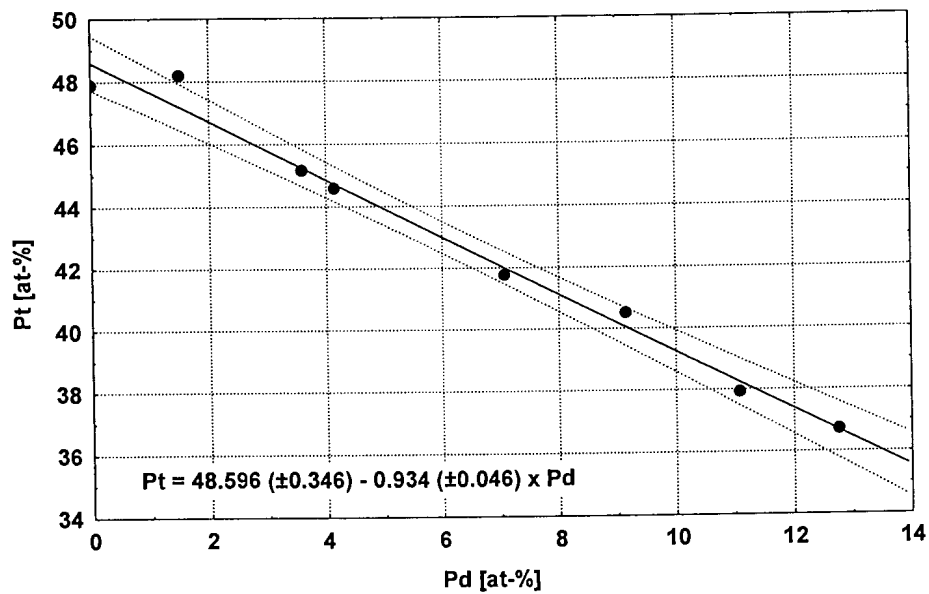


Figure 24 Pt-content versus Pd-content (in at-%) in “cooperite” formed in a Ni-saturated environment at 1100°C. The solid line indicates the best linear fit and the stippled lines the 95% confidence interval according to the equation shown (N=8).

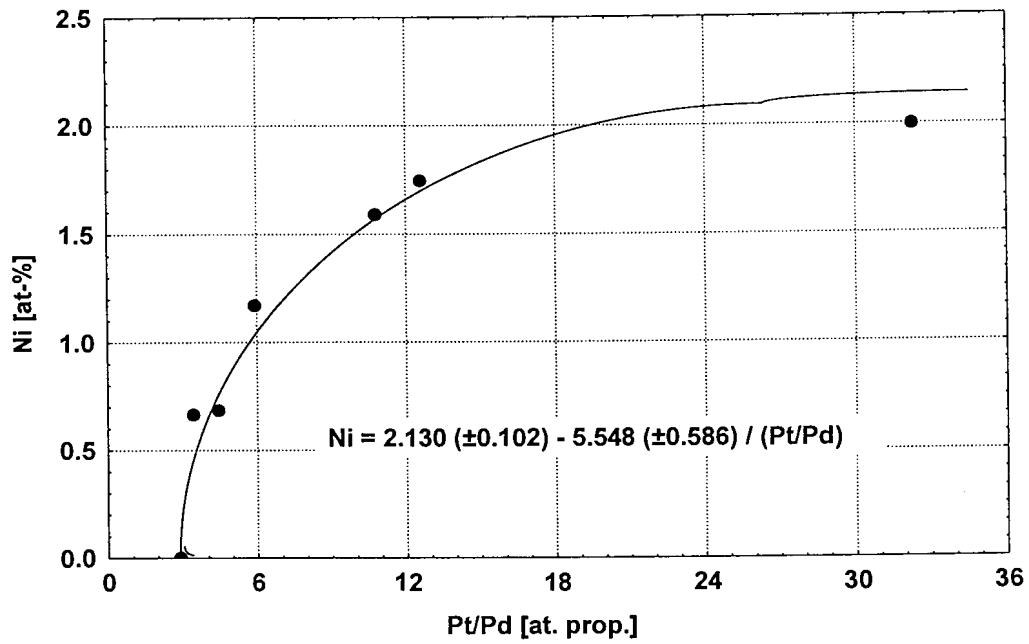


Figure 25 Ni-content versus Pt/Pd ratio (in atomic proportions) in “cooperite” formed in a Ni-saturated environment at 1100 °C. The solid line indicates the best fit according to the equation shown (N=7).

6.3.2 Melt at 1100°C

Analogous to the observations and discussions at 1200°C, a thin layer of sulphur was visible on the capsule wall exhibiting the same pattern after quenching at 1100°C. Spearman rank correlation between the S-content and the Pd-content shows a negative correlation of $r = -0.88$. Between the S- and Ni-content, there is a positive correlation of $r = 0.88$. Larger Spearman rank correlations are observed between the S-content and the Pd/Ni ratio ($r = -0.93$), which illustrates the dependance of the amount of sulphur on the capsule wall on the Pd/Ni-ratio of the charge. Higher Pd-content (i.e. lower Ni-content) in the melt results in lower S-content, which in turn is illustrated by the sulphur layer on the capsule wall. Correlation between the S-content and Pt-content is much weaker ($r = 0.57$).

The relationship between the Pd-, Ni-, and S-contents in the melt at 1100°C can also be visualized in the following 3D scatterplot (Fig. 26).

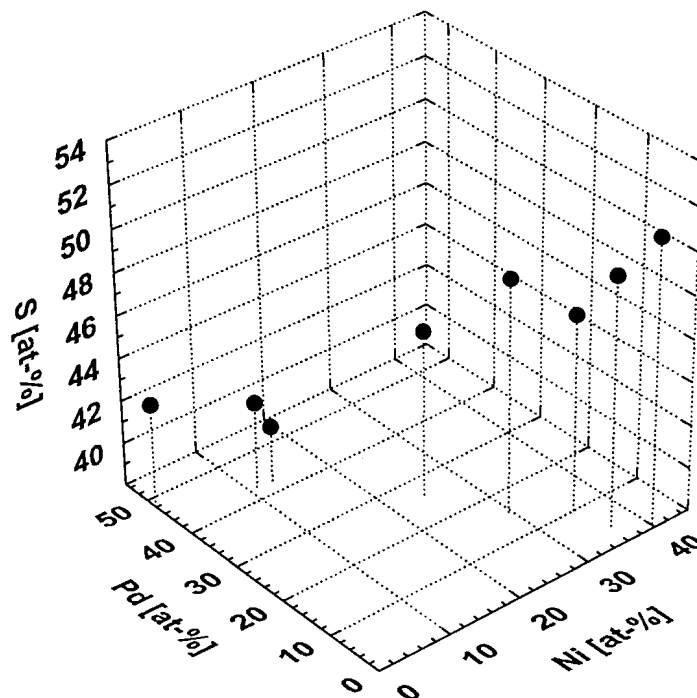


Figure 26 3D scatterplot of Pd-, Ni-, and S-content in at-% in melt coexisting with “cooperite” at 1100°C (N=8).

6.3.3 Relationships at 1100°C

Similar to the phase relations found at 1200°C, at 1100°C there is a strong positive linear relationship between the Pd-content of “cooperite” and the Pd-content of the coexisting melt, and a strong negative linear relationship between the Pd-content of “cooperite” and the Ni-content of the melt. Relationships between the Ni-content in the “cooperite” and the Pd- and Ni-contents in the melt show antipathetic behaviour to that of the Pd-content of “cooperite”. The Pt-content of the melt does not have a linear relationship with the Pt-, Pd-, or Ni- content of the “cooperite”, due to the complex variation of the Pt-content in the melt, as may be seen in Figure 21.

The relationship between the Pd-content in “cooperite” and the Pd-content of the melt resembles that at 1200°C and is illustrated in Figure 27.

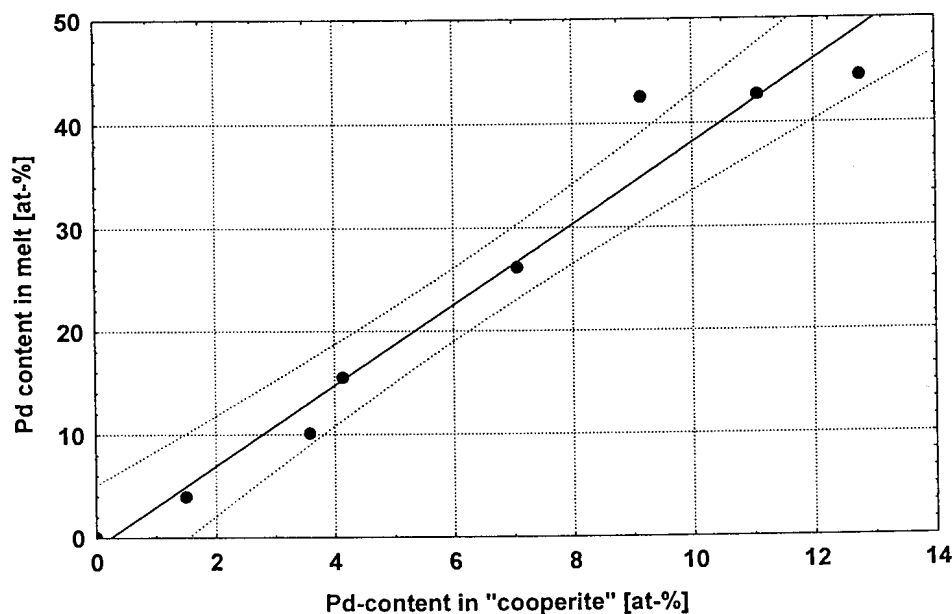


Figure 27 Pd-content in melt versus Pd-content in “cooperite” at 1100°C (in at-%). The solid line indicates the best linear fit and the stippled lines the 95-% confidence interval of the linear fit (N=8).

6.4 THE 1000°C ISOTHERMAL SECTION

At 1000°C, the compositional field of the melt is reduced further compared to that at 1100°C and - apart from “cooperite” and melt - a third phase corresponding to “braggite” appears. The compositional relationship between the three phases is shown in Figure 28 and the compositions of melt, “cooperite”, and “braggite” are summarized in Table 9.

Maximum solubility of Pt in the melt along the PtS-PdS join is 1.1 at-%, which is increasing with increasing Ni-content in the melt to a maximum of 4.0 at-% Pt along the PtS-NiS join. In the region where the melt coexists with “cooperite” and “braggite” (i.e. all three phases coexist), however, the Pt-content in melt declines to a minimum of 0.7 at-% (see Fig. 28). The maximum solubility of Ni in ideal, Pd-free “cooperite”, coexisting with Pd-free melt along the PtS-NiS join, is 3.3 at-%. The Pd-content in Ni-free “cooperite”, coexisting with Ni-free “braggite” at 1000°C, is 13.7 at-%, whilst the Pt-content in Ni-free “braggite”, coexisting with Ni-free “cooperite”, is 29.0 at-%. The Ni-content in both “cooperite” and “braggite” decreases with increasing Pd-content, but is higher in “braggite” than in “cooperite” (Fig. 29).

The textural relationship between coexisting “cooperite” and “braggite” is illustrated in Photomicrograph 4. The solidified melt shows a finer grained texture at 1000°C than at the higher temperatures discussed in the previous Chapters (Photomicrograph 5).

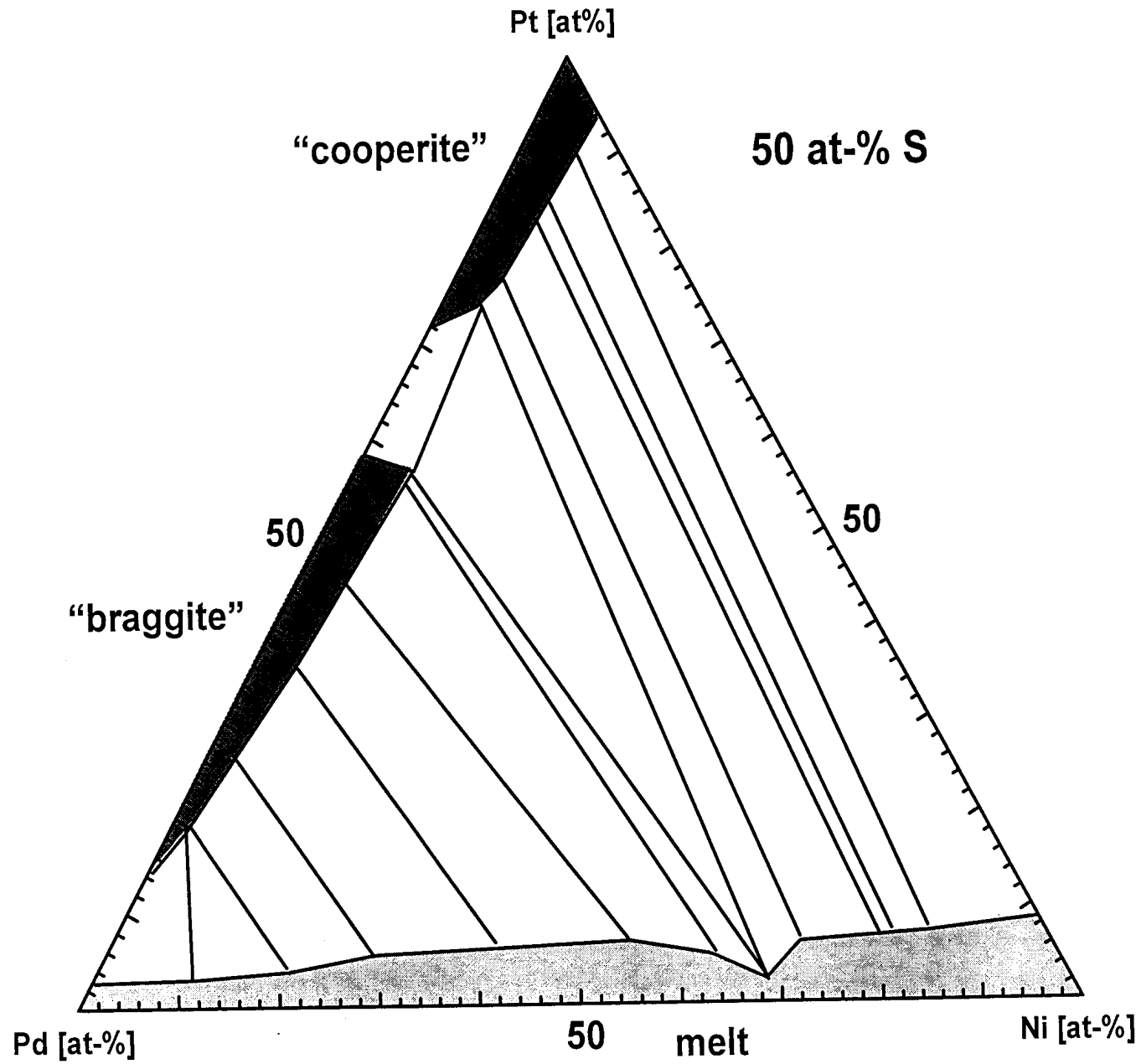


Figure 28 Phase relations in the system PtS-PdS-NiS in cation proportions at 1000°C.

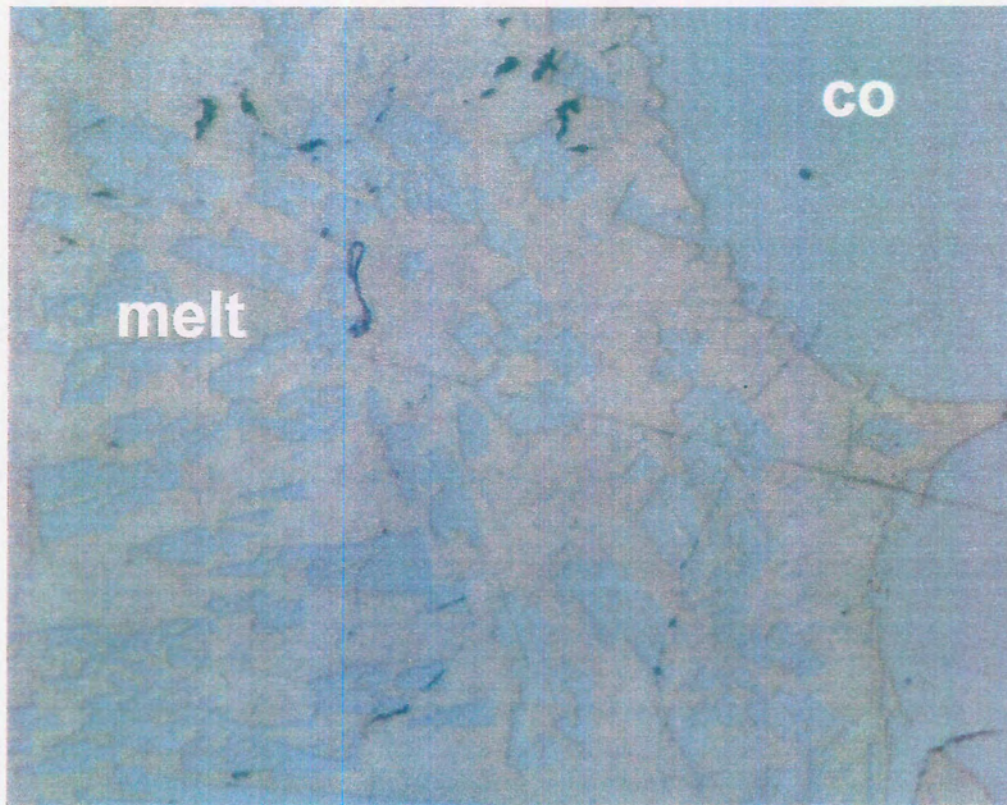
Table 9: Mean (arithmetic) compositions of phases in the system PtS-PdS-NiS at 1000°C in weight per cent (wt%) and atomic per cent (at%). Values in parenthesis show the standard deviation at the 1 σ level. N = number of analyses per experiment.

Sample	Phases		Pt	Pd	Ni	S	TOTAL
SV301	"Braggite"	wt%	24.06 (0.62)	54.39 (0.77)	0.55 (0.11)	21.47 (0.37)	100.47
		at%	9.39 (0.25)	38.92 (0.42)	0.71 (0.13)	50.98 (0.42)	(N=89)
	Melt	wt%	3.34 (1.86)	70.63 (1.80)	4.43 (1.07)	20.25 (0.94)	98.65
		at%	1.23 (0.69)	47.82 (1.27)	5.44 (1.32)	46.51 (1.93)	(N=9)
SV303	"Braggite"	wt%	18.41 (0.75)	60.02 (0.74)	0	21.03 (0.47)	99.54
		at%	7.17 (0.34)	42.87 (0.50)	0	49.86 (0.51)	(N=30)
	Melt	wt%	3.01 (0.62)	75.26 (1.75)	0	20.23 (0.23)	98.52
		at%	1.14 (0.23)	52.25 (0.79)	0	46.61 (0.90)	(N=3)
SV305	"Cooperite"	wt%	82.84 (0.70)	1.91 (0.45)	1.71 (0.06)	14.12 (0.15)	100.58
		at%	46.55 (0.38)	1.97 (0.45)	3.19 (0.13)	48.29 (0.29)	(N=9)
	Melt	wt%	15.06 (2.08)	10.40 (2.77)	44.25 (3.75)	29.66 (0.43)	99.88
		at%	4.16 (0.63)	5.27 (1.45)	40.66 (2.71)	49.91 (1.10)	(N=13)
SV306	"Cooperite"	wt%	78.77 (0.68)	5.25 (0.40)	1.61 (0.19)	14.56 (0.18)	100.18
		at%	43.20 (0.43)	5.28 (0.41)	2.93 (0.32)	48.59 (0.26)	(N=13)
	Melt	wt%	12.22 (2.07)	15.31 (1.93)	43.02 (2.28)	30.11 (0.64)	100.66
		at%	3.33 (0.69)	7.66 (1.33)	39.02 (1.87)	49.99 (1.28)	(N=20)
SV308	"Cooperite"	wt%	71.33 (0.80)	12.01 (0.46)	1.37 (0.10)	15.47 (0.35)	100.18
		at%	37.14 (0.59)	11.47 (0.42)	2.37 (0.16)	49.02 (0.66)	(N=51)
	Melt	wt%	12.71 (3.67)	32.20 (3.46)	29.70 (4.24)	26.19 (1.51)	100.79
		at%	3.85 (1.29)	17.90 (2.20)	29.93 (3.71)	48.32 (2.41)	(N=21)
SV309	"Cooperite"	wt%	73.99 (0.90)	9.58 (0.55)	1.37 (0.35)	15.11 (0.32)	100.05
		at%	39.34 (0.72)	9.34 (0.52)	2.42 (0.61)	48.89 (0.62)	(N=150)
	Melt	wt%	10.35 (4.47)	24.22 (1.77)	37.16 (4.32)	29.21 (1.40)	100.93
		at%	2.91 (1.36)	12.47 (1.19)	34.69 (3.04)	49.93 (1.70)	(N=26)
SV310	"Cooperite"	wt%	70.35 (0.10)	11.56 (0.46)	1.05 (0.04)	15.83 (0.41)	98.79
		at%	36.76 (0.41)	11.08 (0.49)	1.82 (0.06)	50.34 (0.78)	(N=6)
	"Braggite"	wt%	59.52 (0.75)	21.78 (0.74))	1.63 (0.29)	16.70 (0.49)	99.63
		at%	28.82 (0.59)	19.34 (0.84)	2.62 (0.61)	49.22 (0.96)	(N=58)
	Melt	wt%	3.87 (2.56)	32.16 (1.36)	41.71 (1.77)	23.97 (0.24)	101.72
		at%	1.11 (0.75)	16.98 (0.51)	39.91 (1.19)	42.00 (0.95)	(N=2)
SV311	"Braggite"	wt%	59.13 (0.55)	21.97 (0.58)	1.91 (0.19)	16.53 (0.24)	99.55
		at%	28.66 (0.29)	19.52 (0.49)	3.08 (0.28)	48.74 (0.57)	(N=7)
	Melt	wt%	7.64 (3.69)	32.67 (2.50)	32.73 (4.03)	27.93 (1.19)	100.97
		at%	2.21 (1.13)	17.30 (1.54)	31.41 (3.09)	49.08 (2.06)	(N=45)
SV312	"Braggite"	wt%	41.20 (0.69)	38.38 (0.67)	1.43 (0.19)	18.82 (0.45)	99.83
		at%	17.85 (0.35)	30.48 (0.55)	2.06 (0.28)	49.61 (0.69)	(N=54)
	Melt	wt%	8.19 (2.54)	48.25 (3.12)	18.70 (3.99)	24.99 (1.34)	100.13
		at%	2.63 (0.85)	28.46 (2.43)	19.99 (3.51)	48.92 (2.14)	(N=73)



Table 9 (continued):

Sample	Phases		Pt	Pd	Ni	S	TOTAL
SV313	"Braggite"	wt%	23.28 (0.56)	55.63 (0.72)	0.62 (0.16)	20.69 (0.65)	100.23
		at%	9.19 (0.31)	40.28 (0.71)	0.81 (0.21)	49.72 (0.89)	(N=35)
	Melt	wt%	4.66 (2.59)	63.59 (2.12)	8.64 (2.52)	22.44 (0.77)	99.33
		at%	1.63 (0.92)	40.69 (1.73)	10.02 (2.79)	47.66 (1.60)	(N=43)
SV314	"Braggite"	wt%	32.01 (0.77)	48.02 (0.75)	1.06 (0.21)	19.43 (0.56)	100.54
		at%	13.24 (0.39)	36.41(0.73)	1.46 (0.29)	48.89 (0.78)	(N=63)
	Melt	wt%	6.91 (2.27)	57.21 (2.02)	12.58 (2.64)	23.31 (0.68)	100.02
		at%	2.34 (0.79)	35.50 (1.74)	14.15 (2.68)	48.01 (1.30)	(N=35)
SV316	"Cooperite"	wt%	70.40 (0.76)	14.36 (0.43)	0	15.81 (0.22)	100.59
		at%	36.49 (0.57)	13.65 (0.41)	0	49.86 (0.29)	(N=16)
	"Braggite"	wt%	60.16 (0.77)	23.35 (0.75)	0	17.13 (0.19)	100.65
		at%	29.03 (0.41)	20.66 (0.69)	0	50.31 (0.21)	(N=18)
SV317	"Cooperite"	wt%	71.29 (0.62)	11.48 (0.47)	1.06 (0.06)	15.94 (0.44)	99.77
		at%	36.96 (0.73)	10.91(0.43)	1.83 (0.09)	50.29 (0.81)	(N=16)
	"Braggite"	wt%	58.91 (0.65)	21.83 (0.40)	2.00 (0.09)	17.57 (0.22)	100.69
		at%	27.72 (0.33)	18.84 (0.34)	3.13 (0.13)	50.31 (0.51)	(N=12)
	Melt	wt%	2.31 (1.34)	31.18 (3.83)	38.86 (1.84)	27.15 (1.22)	99.44
		at%	0.65 (0.36)	16.16 (2.27)	36.5 (1.28)	46.69 (1.22)	(N=11)
SV318	"Cooperite"	wt%	76.20 (0.67)	9.51 (0.46)	0	14.74 (0.30)	100.49
		at%	41.56 (0.32)	9.51 (0.51)	0	48.92 (0.66)	(N=18)
SV320	"Cooperite"	wt%	84.74 (0.54)	0	1.74 (0.20)	14.05 (0.24)	100.55
		at%	48.14 (0.56)	0	3.29 (0.31)	48.57 (0.36)	(N=14)
	Melt	wt%	15.47 (0.71)	0	52.77 (0.70)	32.57 (0.40)	100.81
		at%	3.98 (0.17)	0	45.08 (0.46)	50.94 (0.40)	(N=9)
SV1001	"Braggite"	wt%	50.12 (0.53)	30.56 (0.74)	1.65 (0.12)	17.69 (0.32)	99.83
		at%	22.86 (0.35)	25.55 (0.36)	2.50 (0.15)	49.09 (0.57)	(N=13)
	Melt	wt%	9.54 (1.55)	39.05 (3.23)	26.31 (1.51)	27.04 (0.87)	100.87
		at%	2.86 (0.71)	21.49 (2.49)	26.26 (1.49)	49.39 (1.01)	(N=12)



Photomicrograph 3 "Cooperite" (co) and coexisting melt at 1100°C of experiment SV337 (long side of the photomicrograph is 0.35 mm).

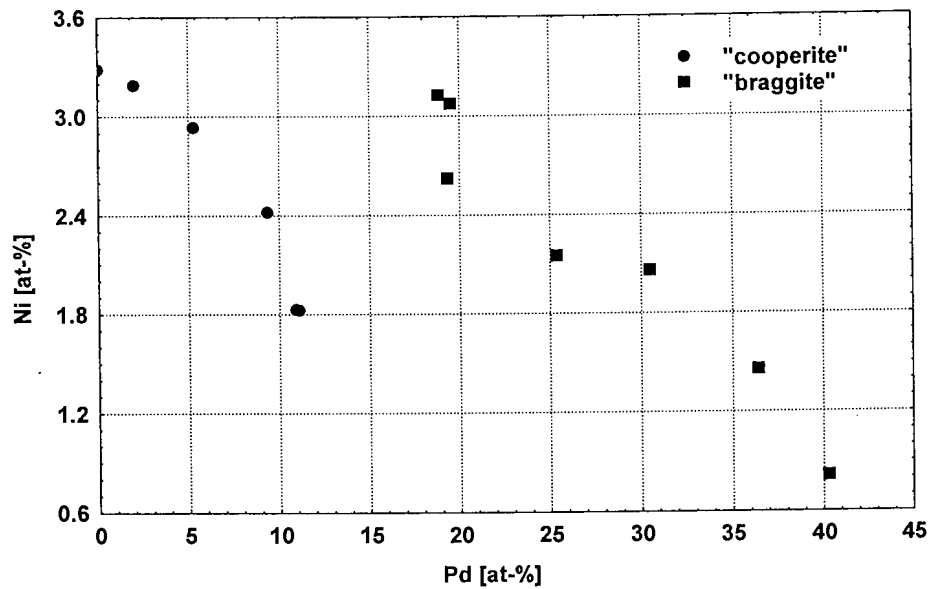


Figure 29 Ni-content versus Pd-content (in at-%) in “cooperite” and “braggite” formed at 1000°C.

6.4.1 “Cooperite” at 1000°C

The Ni-content in “cooperite” in a Ni-saturated environment at 1000°C decreases slightly with increasing Pd-content. Data for “cooperite” formed in a Ni-saturated environment (in cation per cent) lead to the following relationships at the 95% confidence level (Table 10):

Table 10: Type of best fit, equation for best fit at the 95% confidence level, equation number (No), and R²-values of best fits of elements analysed in “cooperite” formed at 1000°C.

Variables	Fit	Equation	No	R ²
Ni, Pt	Linear			0.9559
	Logarithmic			0.9679
	Inverse	$Ni = 8.223 (\pm 0.426) - 233.361 (\pm 17.507) / Pt$	10	0.9779
	Square root			0.9622
Ni, Pd	2 nd order polynomial	$Ni = 3.429 + 0.019 (\pm 0.043) \times Pd - 0.013 (\pm 0.004) \times Pd^2$	11	0.9860
Pt, Pd	Linear	$Pt = 48.433 (\pm 0.027) - 1.027 (\pm 0.035) \times Pd$	12	0.9954
Ni, Pt/Pd	Logarithmic			0.8449
	Inverse	$Ni = 3.528 (\pm 0.142) - 5.438 (\pm 0.632) / (Pt/Pd)$	13	0.9612
	Square root			0.7588

Equations 10 to 13 are shown graphically in Figures 30 to 33:

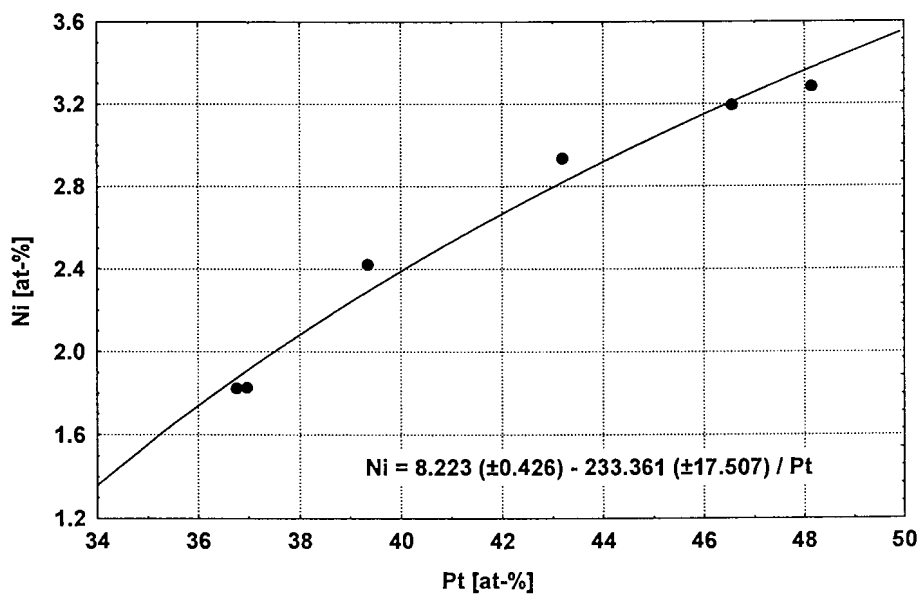


Figure 30 Ni-content versus Pt-content (in at-%) in “cooperite” formed in a Ni-saturated environment at 1000°C. The solid line indicates the best fit according to the equation shown (N=6).

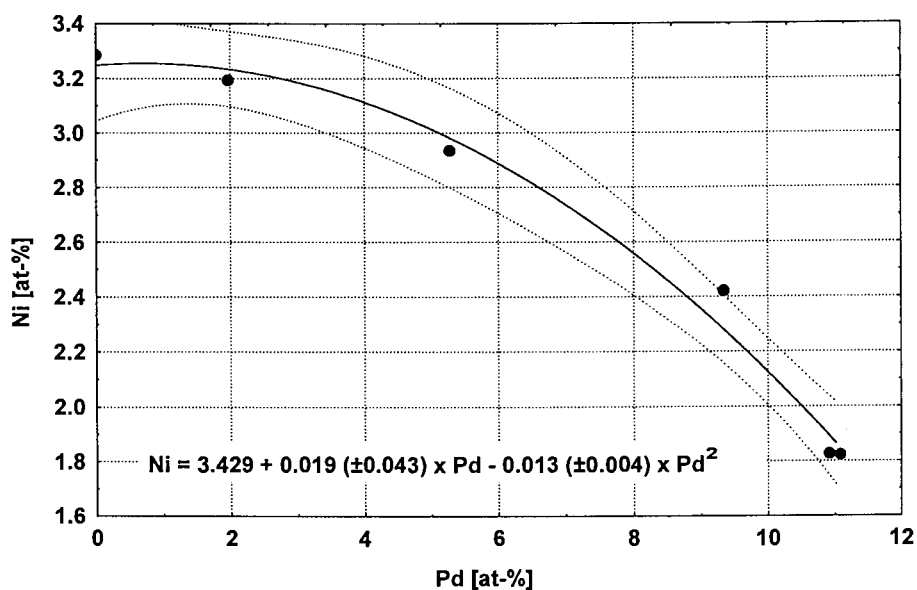


Figure 31 Ni-content versus Pd-content (in at-%) in “cooperite” formed in a Ni-saturated environment at 1000°C. The solid line indicates the best 2nd order polynomial fit and the stippled lines the 95% confidence interval according to the equation shown (N=6).

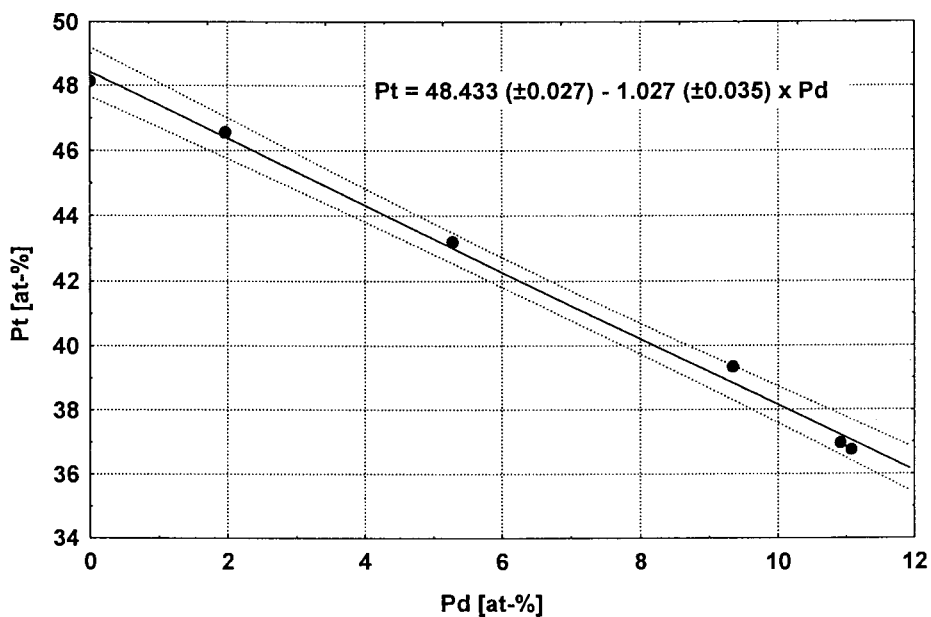


Figure 32 Pt-content versus Pd-content (in at-%) in “cooperite” formed in a Ni-saturated environment at 1000°C. The solid line indicates the best linear fit and the stippled lines the 95% confidence interval according to the equation shown (N=6).

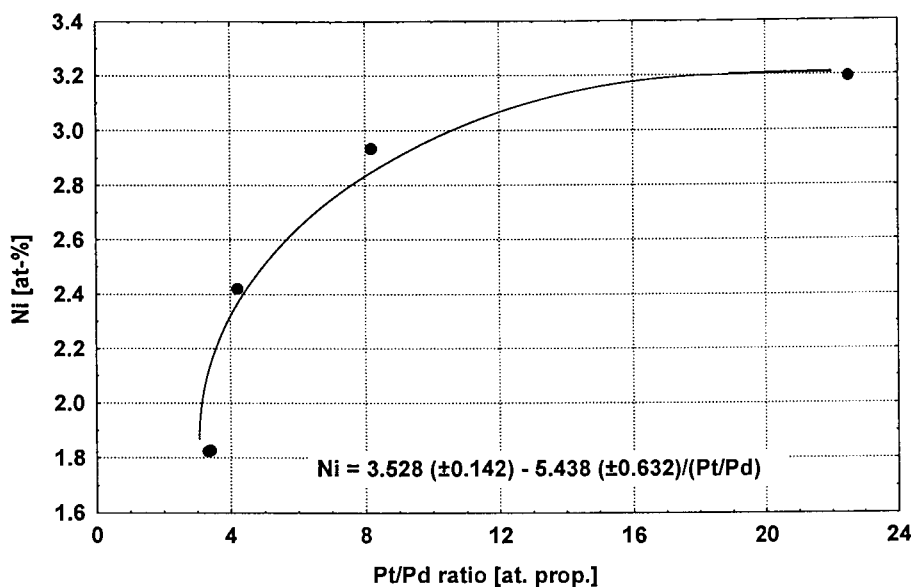


Figure 33 Ni-content versus Pt/Pd ratio (in atomic proportions) in “cooperite” formed in a Ni-saturated environment at 1000°C. The solid line indicates the fit according to the equation shown (N=5).

6.4.2 “Braggite” at 1000°C

In a Ni-saturated environment, the Ni-content in “braggite” decreases with increasing Pd-content. Least square fitting of the data (cation per cent) for “braggite formed in a Ni-saturated environment the following relationships at the 95% confidence level (Table 11):

Table 11: Type of best fit, equation for best fit at the 95% confidence level, equation number (No), and R²-values of best fits of elements analysed in “braggite” formed at 1000°C.

Variables	Fit	Equation	No	R ²
Ni, Pt	Linear	Ni= -0.307 (±0.147) + 0.124 (±0.007) x Pt	14	0.9823
Ni, Pd	Linear	Ni = 5.309 (±0.263) - 0.112 (±0.008) x Pd	15	0.9722
Pt, Pd	Linear	Pt= 45.802 (±0.989) - 0.912 (±0.032) x Pd	16	0.9940
Ni, Pt/Pd	Logarithmic	Ni =2.647 (±0.052) + 2.939 (±0.131)log ₁₀ (Pt/Pd)	17	0.9902
	Inverse			0.9645
	Square root			0.9633

Equations 14 to 17 are shown graphically in Figures 34 to 37:

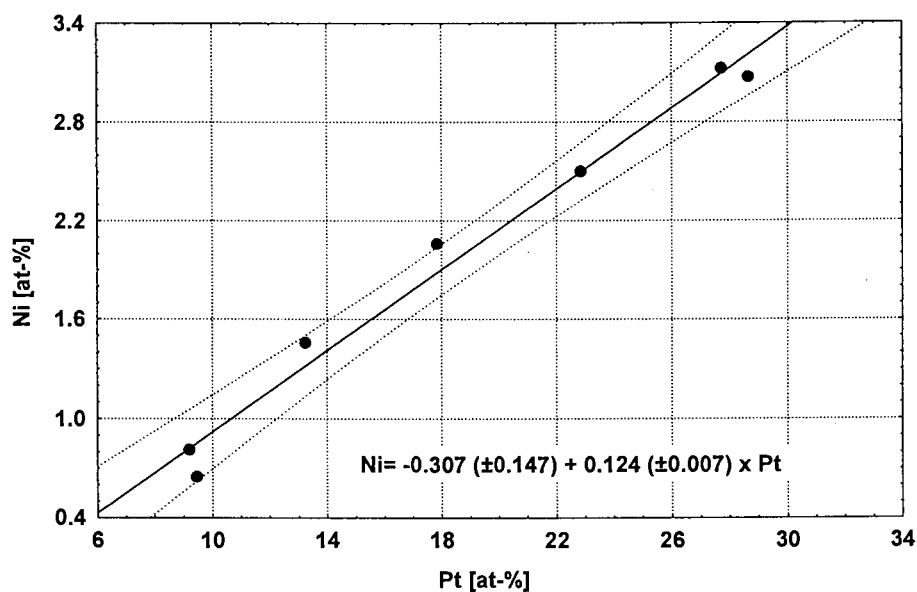


Figure 34 Ni-content versus Pt-content (in at-%) in “braggite” formed in a Ni-saturated environment at 1000°C. The solid line indicates the best linear fit and the stippled lines the 95% confidence interval according to the equation shown (N=7).

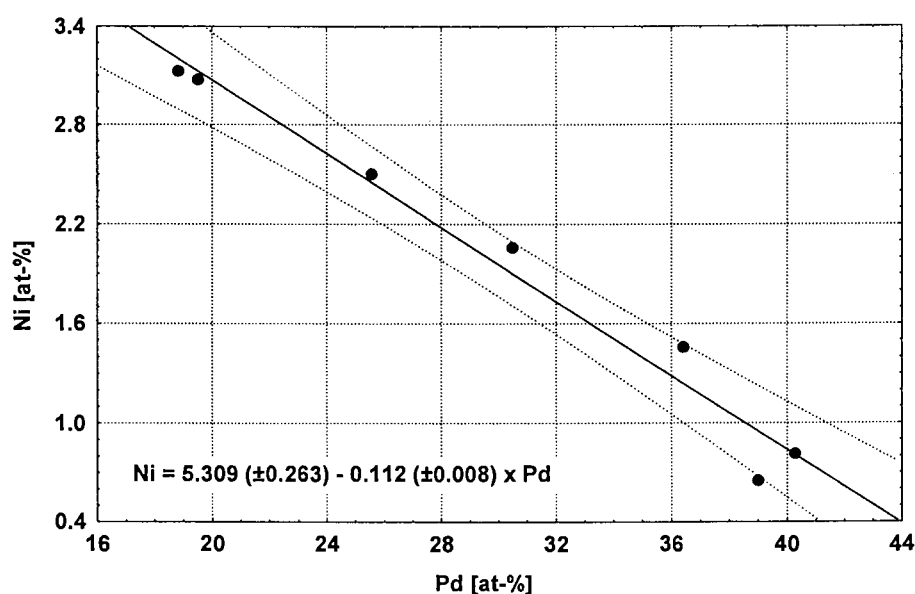


Figure 35 Ni-content versus Pd-content (in at-%) in “braggite” formed in a Ni-saturated environment at 1000°C. The solid line indicates the best linear fit and the stippled lines the 95% confidence interval according to the equation shown (N=7).

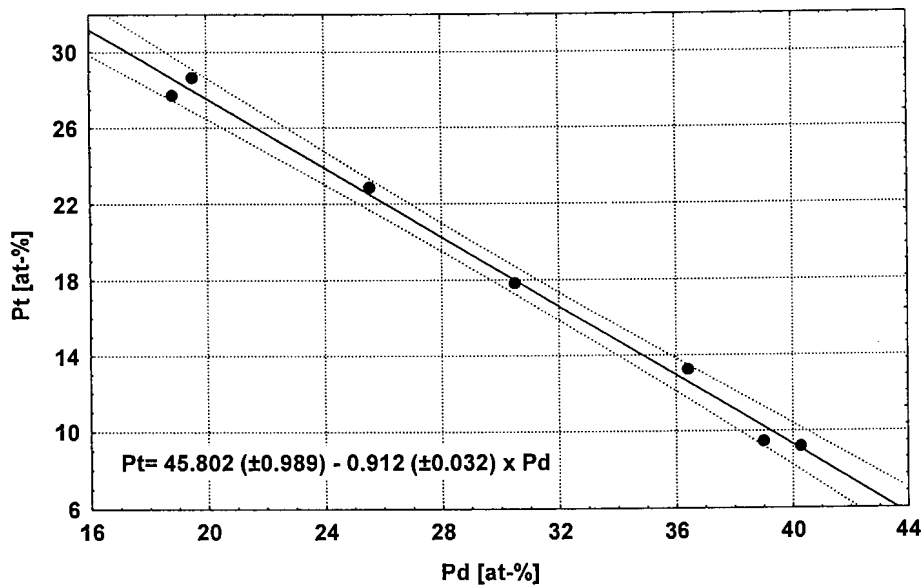


Figure 36 Pt-content versus Pd-content (in at-%) in “braggite” formed in a Ni-saturated environment at 1000°C. The solid line indicates the best linear fit and the stippled lines the 95% confidence interval according to the equation shown (N=7).

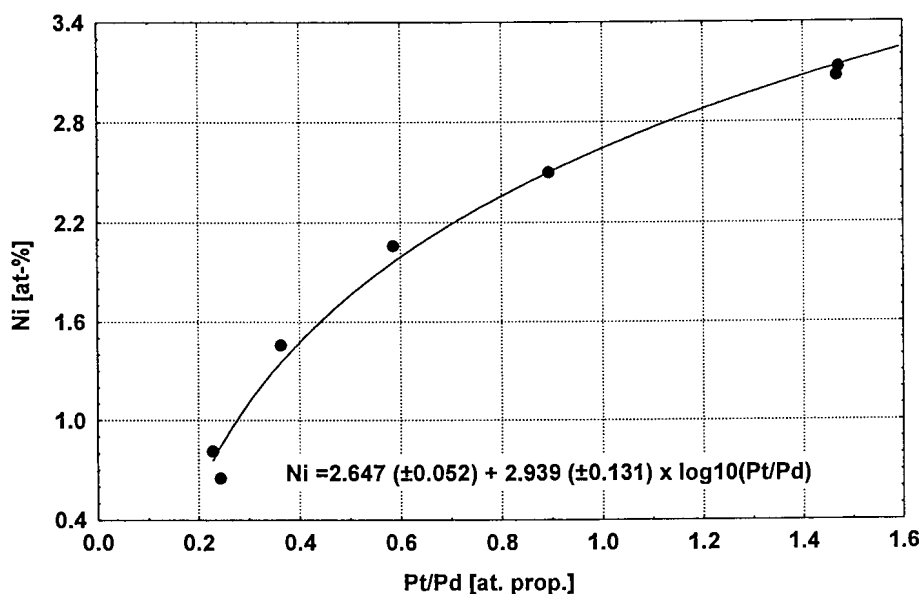


Figure 37 Ni-content versus Pt/Pd ratio (in atomic proportions) in “braggite” formed in a Ni-saturated environment at 1000°C. The solid line indicates the best logarithmic fit according to the equation shown (N=7).

6.4.3 Melt at 1000°C

Analogous to the observations at 1200°C and at 1100°C, and referring to the discussion in Chapter 6.2 (1200°C), a thin layer of sulphur was visible on the capsule walls of some of the experimental charges tempered at 1000°C.

The melt coexisting with “cooperite” and “braggite” (SV310 and SV317) contains abnormally low S-contents, compared to the rest of the melt phase at this temperature (see Fig. 28). Omitting these two experiments, there is a negative linear relationship between the S-content and the Pd-content and a positive linear relationship between S- and Ni-contents of the solidified melt.

The relationship between the Pd-, Ni-, and S-contents in the melt at 1000°C can be visualized in the following 3D scatterplot (Fig. 38).

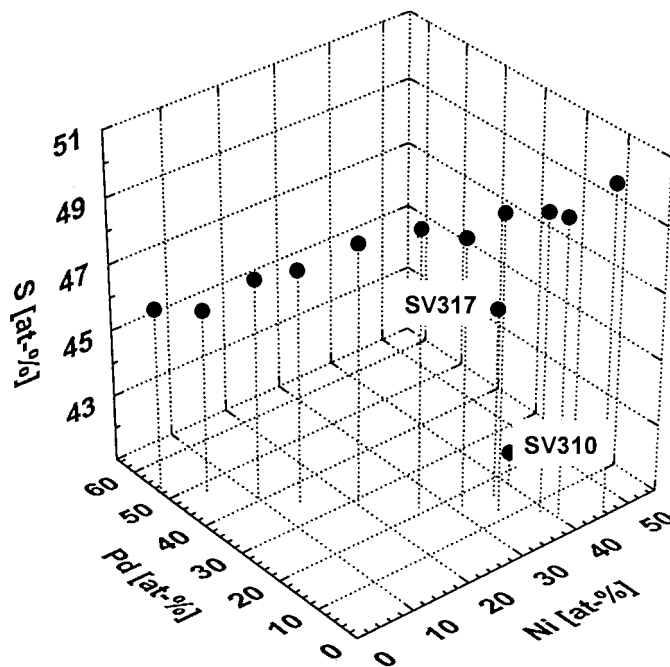


Figure 38 3D scatterplot of Pd-, Ni-, and S-content in at-% in melt at 1000°C coexisting with “cooperite” and/or “braggite”.

6.4.4 Relationships at 1000°C

In a Ni-saturated environment, there are strong positive linear relationships between the Pd-content of both “cooperite” as well as “braggite” and the Pd-content of the coexisting melt. There are strong negative linear relationships between Pd-content of the two minerals (“cooperite” and “braggite”) and the Ni-content of the coexisting melt, formed in a Ni-saturated environment. Comparable to the observations at 1200°C and at 1100°C, the Pt-content of the melt does not show any systematic relationship with the Pt-, Pd-, or Ni- content of the “cooperite” and “braggite”, due to the erratic compositional variation of Pt in the melt, as can be seen in Figure 28.

Least square fittings of the Pd-content of the melt and the Pd-content of “cooperite” and “braggite” individually, lead to the following linear equations at the 95% confidence level (in cation per cent):

$$\text{Pd}_{\text{“COOPERITE”}} = -0.544 (\pm 0.683) + 0.709 (\pm 0.059) \times \text{Pd}_{\text{MELT}} \quad (\text{Equation 18}) \quad R^2 = 0.9728$$

$$\text{Pd}_{\text{“BRAGGITE”}} = 4.828 (\pm 0.943) + 0.806 (\pm 0.035) \times \text{Pd}_{\text{MELT}} \quad (\text{Equation 19}) \quad R^2 = 0.9922$$

The relationship between the Pd-content in “cooperite” and “braggite” and the Pd-content of the melt is illustrated by Figure 39.

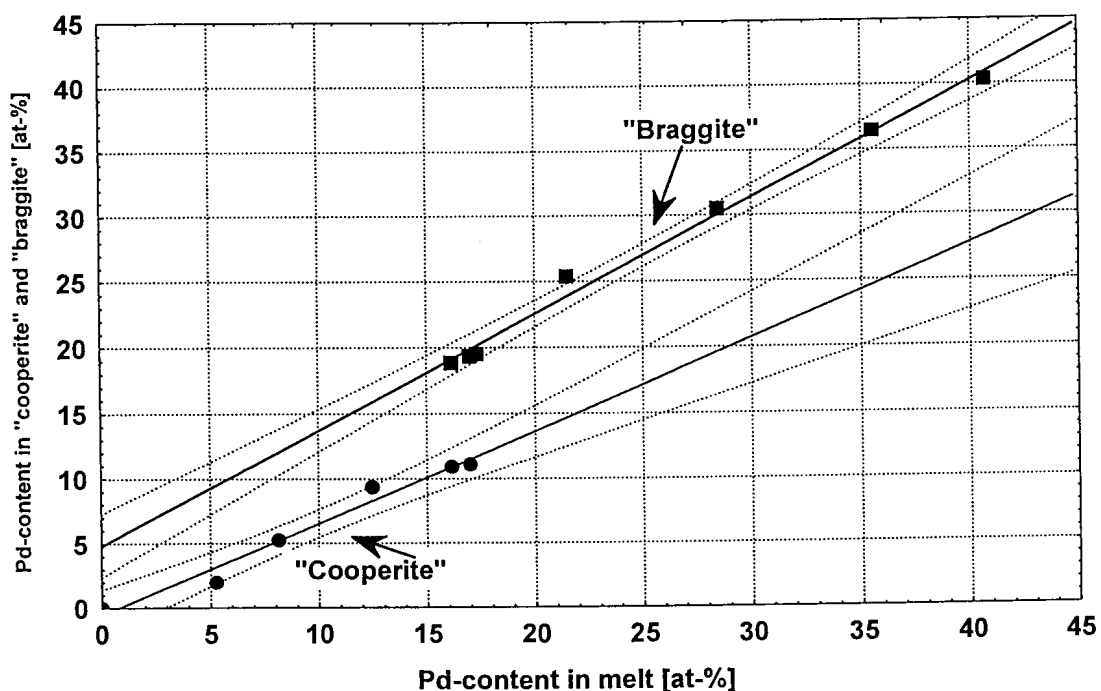


Figure 39 Pd-content in melt versus Pd-content in “cooperite” and “braggite” in a Ni-saturated environment at 1000°C (in at-%). The solid lines indicate the best linear fits and the stippled lines the confidence intervals at the 95 % level for the 2 populations individually.

6.5 THE 900°C ISOTHERMAL SECTION

At 900°C, the compositional field of the melt is reduced much further compared to that at 1000°C, especially on the Pd-rich side of the PdS-NiS join. The compositional field of “braggite-vysotskite” (see Chapter 3) stretches down to the PdS-NiS join. Ni_{1-x}S appears as another stable phase at this temperature.

The compositional relationship between the 5 phases (4 phases, if “braggite” and “vysotskite” are viewed as one iso-structural phase, see Chapter 3) is illustrated in Figure 40 and the compositions are summarized in Table 12. Totals lower than 97.0 wt-% were accepted for analysis of the solidified melt of experiments SV326, SV327, SV328, and SV917, due to porosity of the solidified melt.

Pt-free “vysotskite” which coexists with Pt-free melt, contains a maximum of 4.3 at-% Ni. Considering the analytical uncertainty of 0.3 wt-% at the 3 σ level (see Table 2, Chapter 5), this is in good agreement with results published for 900°C by Karup-Møller & Makovicky (1993), who obtained a maximum Ni content of 3.9 at-% (assuming some analytical uncertainty in those results). Pd-free “cooperite”, containing a maximum of 3.1 at-% Ni, coexists with Ni_{1-x}S, with a maximum solubility of 0.3 at-% Pt along the PtS-NiS join. Pt-free Ni_{1-x}S contains 0.6 at-% Pd, when coexisting with a melt containing 6.7 at-% Pd (Karup-Møller & Makovicky, 1993). This result is included in Figure 40.

The field of the solidified melt does not span across the entire PdS-NiS join as it does at the higher temperatures. The Ni-content of the melt varies between 25.8 and 43.3 at-%. Similar to the observation at 1000°C, the Pt-content in melt declines when coexisting with “cooperite” and “braggite” (i.e. all three phases coexist) (Fig. 40). The Ni-content in “cooperite” increases with increasing Pd-content, whereas the Ni-content decreases in “braggite-vysotskite” with increasing Pd-content (Fig. 41). The Ni-content is higher in “braggite-vysotskite” than in “cooperite”.

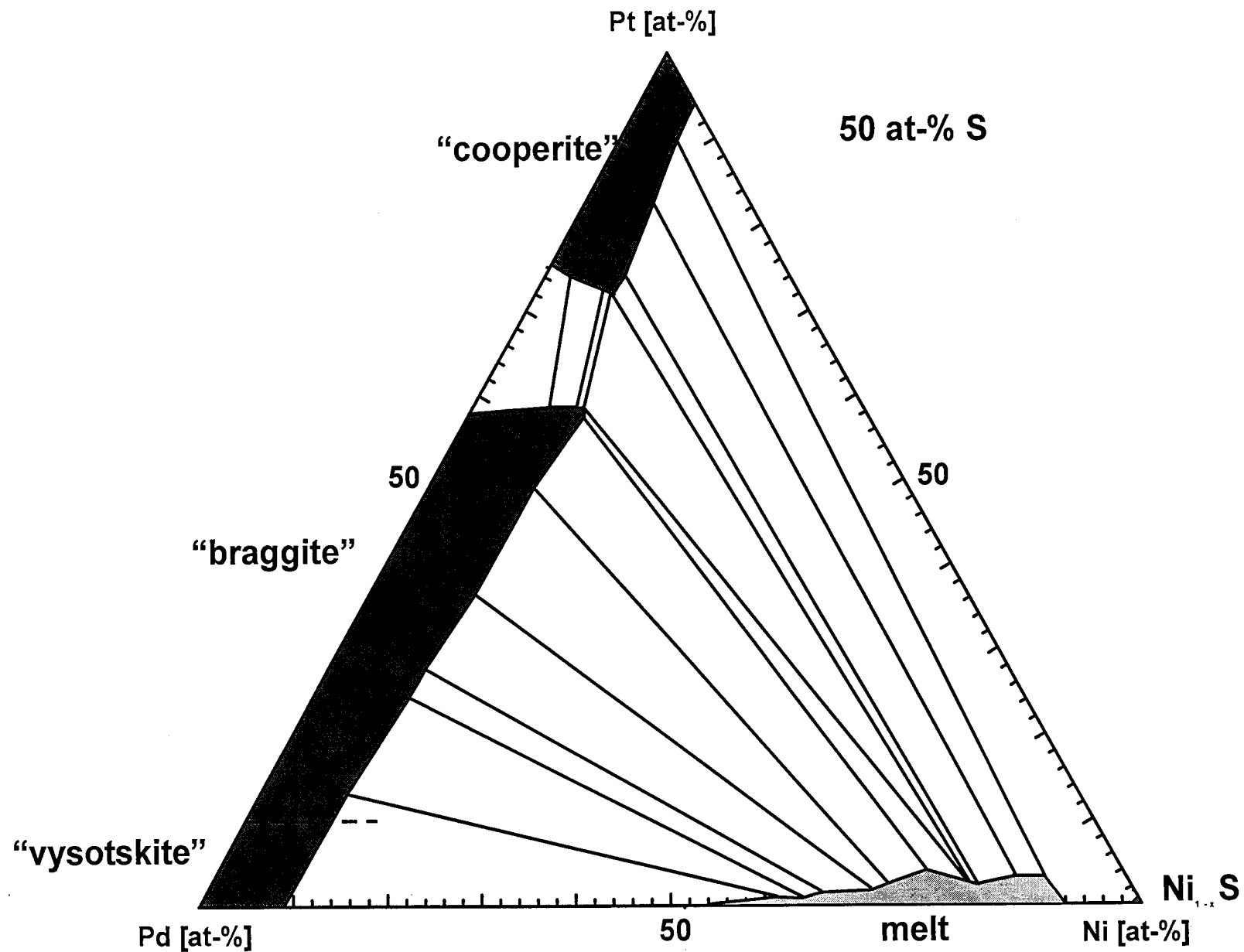


Figure 40 Phase relations in the system PtS-PdS-NiS in cation proportions cent at 900°C (the stippled line indicates the border between “braggite” and “vysotskite”).

Table 12: Mean (arithmetic) compositions of phases in the system PtS-PdS-NiS at 900°C in weight per cent (wt%) and atomic per cent (at%). Values in parenthesis show the standard deviation at the 1 σ level. N = number of analyses per experiment.

Sample	Phases		Pt	Pd	Ni	S	TOTAL
SV321	"Cooperite"	wt%	81.89 (0.72)	2.26 (0.57)	1.72 (0.16)	14.13 (0.23)	100.00
		at%	46.07 (0.61)	2.33 (0.58)	3.22 (0.31)	48.38 (0.43)	(N=28)
	Melt	wt%	7.34 (1.80)	9.65 (2.20)	49.76 (3.35)	32.10 (0.57)	98.84
		at%	1.90 (0.48)	4.59 (0.97)	42.87 (1.72)	50.64 (1.90)	(N=23)
SV322	"Cooperite"	wt%	77.94 (0.49)	5.43 (0.43)	2.16 (0.30)	15.06 (0.50)	100.53
		at%	41.74 (0.63)	5.33 (0.41)	3.84 (0.55)	49.08 (1.10)	(N=27)
	Melt	wt%	7.97 (5.74)	12.17 (3.75)	48.58 (5.84)	31.47 (1.52)	100.18
		at%	2.08 (1.58)	5.82 (1.82)	42.13 (3.65)	49.97 (2.34)	(N=26)
SV323	"Cooperite"	wt%	72.08 (0.78)	9.23 (0.45)	2.43 (0.13)	15.75 (0.47)	99.49
		at%	37.36 (0.82)	8.77 (0.39)	4.19 (0.27)	49.68 (0.90)	(N=38)
	Melt	wt%	5.79 (1.21)	19.03 (1.91)	43.24 (1.57)	31.06 (0.96)	100.01
		at%	1.54 (0.33)	9.26 (1.01)	39.03 (0.96)	50.17 (0.89)	(N=22)
SV324	"Cooperite"	wt%	71.06 (0.41)	9.95 (0.26)	2.45 (0.06)	15.56 (0.35)	99.02
		at%	36.99 (0.54)	9.50 (0.40)	4.24 (0.17)	49.28 (0.58)	(N=7)
	"Braggite"	wt%	61.40 (0.30)	16.39 (0.33)	3.91 (0.18)	17.36 (0.21)	99.07
		at%	29.23 (0.23)	14.30 (0.28)	6.19 (0.28)	50.28 (0.41)	(N=24)
	Melt	wt%	4.65 (1.65)	17.59 (11.36)	47.98 (10.10)	30.64 (2.61)	100.87
		at%	1.21 (0.44)	8.43 (6.13)	41.66 (6.33)	48.70 (1.77)	(N=15)
SV325	"Cooperite"	wt%	70.50 (0.21)	11.16 (0.32)	2.44 (0.03)	15.44 (0.34)	99.57
		at%	36.52 (0.40)	10.60 (0.30)	4.20 (0.06)	48.67 (0.59)	(N=16)
	"Braggite"	wt%	60.95 (0.69)	17.42 (0.63)	3.82 (0.15)	17.47 (0.60)	99.66
		at%	28.76 (0.41)	15.07 (0.70)	5.99 (0.19)	50.17 (0.91)	(N=27)
	Melt	wt%	7.03 (12.32)	19.73 (3.99)	39.69 (3.34)	29.48 (1.17)	95.88
		at%	1.98 (0.64)	10.20 (2.41)	37.21 (2.15)	50.61 (0.91)	(N=16)
SV326	"Braggite"	wt%	53.75 (0.51)	23.67 (0.76)	3.90 (0.11)	18.11 (0.45)	99.42
		at%	24.40 (0.43)	19.70 (0.55)	5.88 (0.19)	50.02 (0.62)	(N=12)
	Melt	wt%	4.18 (2.82)	25.10 (3.04)	36.95 (4.90)	27.30 (1.30)	93.54
		at%	1.23 (0.86)	13.57 (1.86)	36.21 (3.23)	48.99 (2.48)	(N=50)
SV327	"Braggite"	wt%	42.9 (0.72)	32.86 (0.68)	3.88 (0.26)	19.97 (0.52)	99.70
		at%	18.09 (0.30)	25.35 (0.76)	5.42 (2.31)	51.14 (0.68)	(N=12)
	Melt	wt%	2.61 (1.31)	25.07 (4.37)	38.09 (5.57)	28.65 (1.67)	94.42
		at%	0.75 (0.38)	13.15 (2.64)	36.22 (3.89)	49.88 (2.99)	(N=83)
SV328	"Braggite"	wt%	34.66 (0.74)	40.41 (0.64)	3.71 (0.13)	21.38 (0.19)	100.17
		at%	13.8 (0.31)	29.49 (0.32)	4.90 (0.16)	51.80 (0.19)	(N=18)
	Melt	wt%	3.24 (2.40)	32.00 (5.71)	31.57 (5.41)	25.36 (1.48)	92.11
		at%	1.01 (0.82)	18.27 (3.98)	32.67 (4.04)	48.05 (0.53)	(N=15)



Table 12 (continued):

Sample	Phases		Pt	Pd	Ni	S	TOTAL
SV330	"Braggite"	wt%	31.12 (0.57)	43.20 (0.56)	3.66 (0.05)	21.00 (0.15)	98.98
		at%	12.43 (0.26)	31.65 (0.36)	4.86 (0.07)	51.06 (0.21)	(N=27)
	Melt	wt%	2.23 (0.77)	31.85 (1.91)	34.87 (1.91)	28.34 (0.58)	97.29
		at%	0.64 (0.22)	16.73 (1.03)	33.21 (1.29)	49.42 (0.63)	(N=26)
SV331	"Cooperite"	wt%	70.69 (0.32)	12.90 (0.32)	0	15.69 (0.09)	99.29
		at%	37.24 (0.23)	12.47 (0.27)	0	50.30 (0.18)	(N=17)
	"Braggite"	wt%	59.44 (0.89)	22.78 (0.63)	0	17.52 (0.24)	99.73
		at%	28.60 (0.57)	20.10 (0.46)	0	51.30 (0.50)	(N=8)
SV332	"Cooperite"	wt%	70.40 (0.78)	12.30 (0.69)	0.91 (0.27)	16.17 (0.27)	99.78
		at%	36.22 (0.43)	11.60 (0.67)	1.56 (0.58)	50.62 (0.60)	(N=7)
	"Braggite"	wt%	60.36 (0.81)	19.13 (0.70)	2.65 (0.16)	18.03 (0.21)	100.18
		at%	28.19 (0.34)	16.40 (0.60)	4.12 (0.25)	51.29 (0.34)	(N=18)
SV334	"Cooperite"	wt%	78.1 (0.61))	7.36 (0.45)	0	14.27 (0.17)	99.74
		at%	43.77 (0.52)	7.56 (0.42)	0	48.66 (0.26)	(N=33)
SV335	"Braggite"	wt%	18.43 (0.22)	55.22 (0.12)	3.77 (0.01)	22.66 (0.01)	100.09
		at%	6.82 (0.08)	37.49 (0.09)	4.64 (0.01)	51.05 (0.02)	(N=2)
	Melt	wt%	0.23 (0.15)	35.86 (4.67)	35.42 (3.66)	28.80 (1.76)	100.31
		at%	0.06 (0.04)	18.32 (2.71)	32.80 (3.01)	48.82 (1.91)	(N=22)
SV336	"Cooperite"	wt%	85.36 (0.54)	0	1.66 (0.16)	14.04 (0.17)	101.09
		at%	48.4 (0.72)	0	3.13 (0.32)	48.46 (0.22)	(N=11)
	Ni _{1-x} S	wt%	1.29 (0.08)	0	64.67 (0.21)	36.86 (0.13)	102.82
		at%	0.29 (0.02)	0	48.79 (0.16)	50.92 (0.16)	(N=9)
SV917	"Vysotskite"	wt%	0	69.16 (0.37)	3.69 (0.15)	24.00 (0.49)	96.84
		at%	0	44.48 (0.36)	4.30 (0.19)	51.22 (0.44)	(N=15)
	Melt	wt%	0	44.22 (1.52)	25.78 (1.33)	26.00 (0.40)	97.01
		at%	0	24.95 (1.10)	26.37 (1.02)	48.69 (0.46)	(N=10)

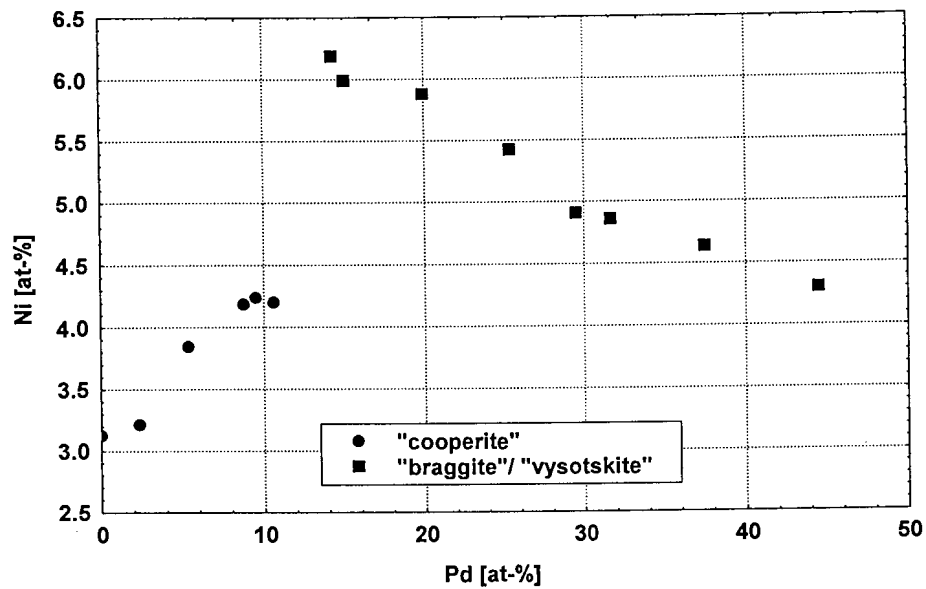
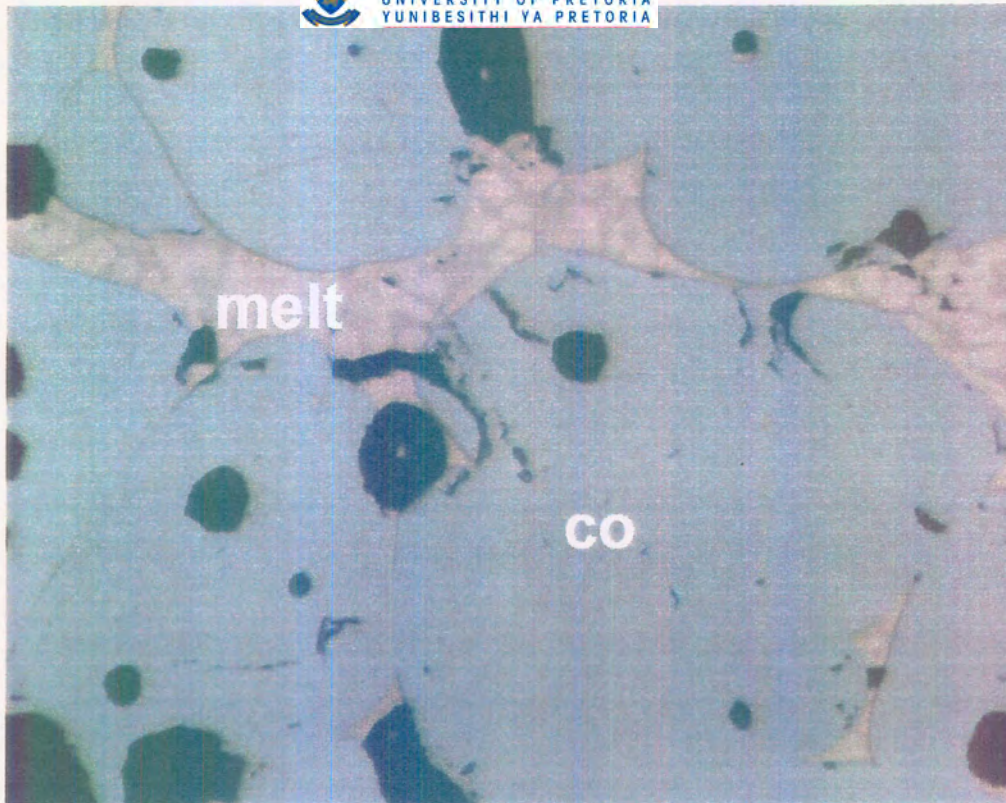
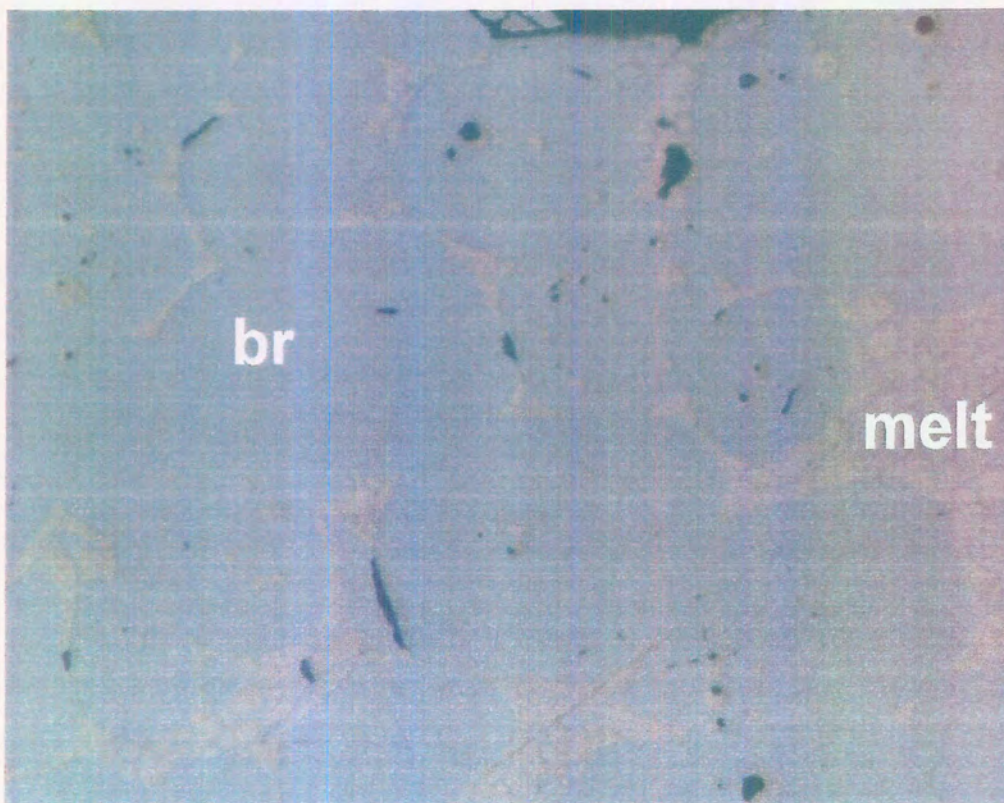


Figure 41 Ni-content versus Pd-content (in at-%) in "cooperite" and "braggite-vysotskite" formed at 900°C.

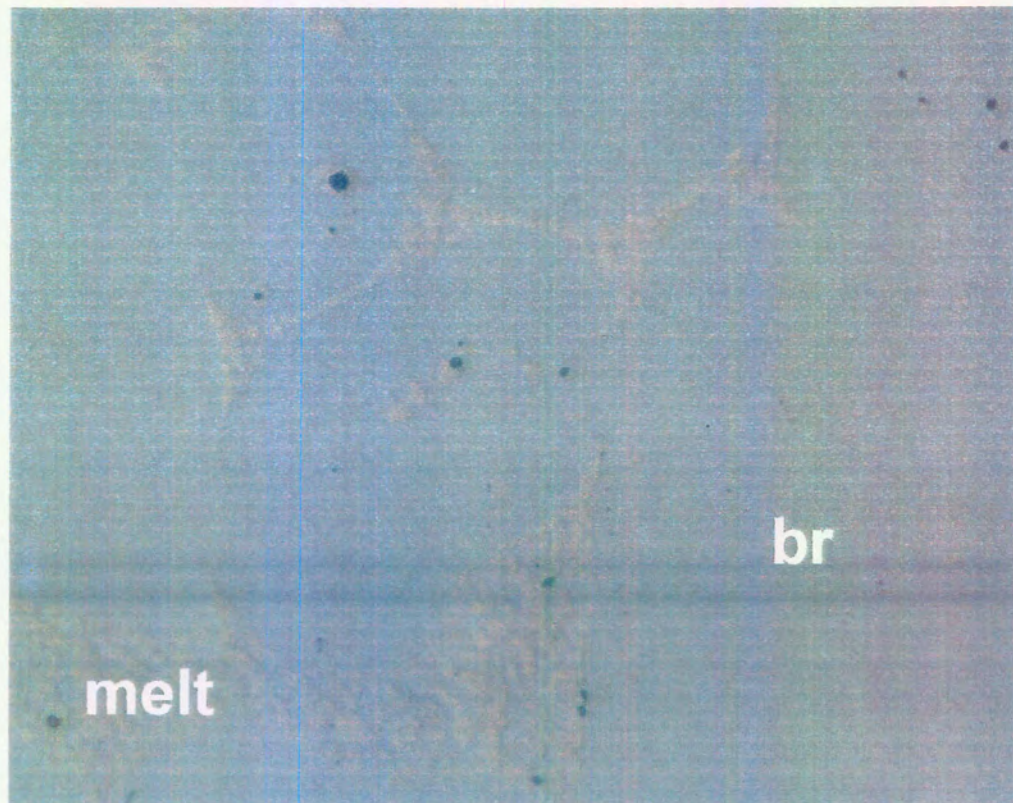
Photomicrographs 6 to 9 show the typical textures of "cooperite", "braggite", and the coexisting melt. The Pd-content of the solid phases and the melt increases from Photomicrograph 6 to 9, which is reflected in the overall colour of the melt. With increasing Pd-content, and with that, the decreasing Ni-content, the colour changes from yellowish to blue-grey. This is caused by the relative decrease of Ni-rich mono-sulphide phases in the solidified melt.



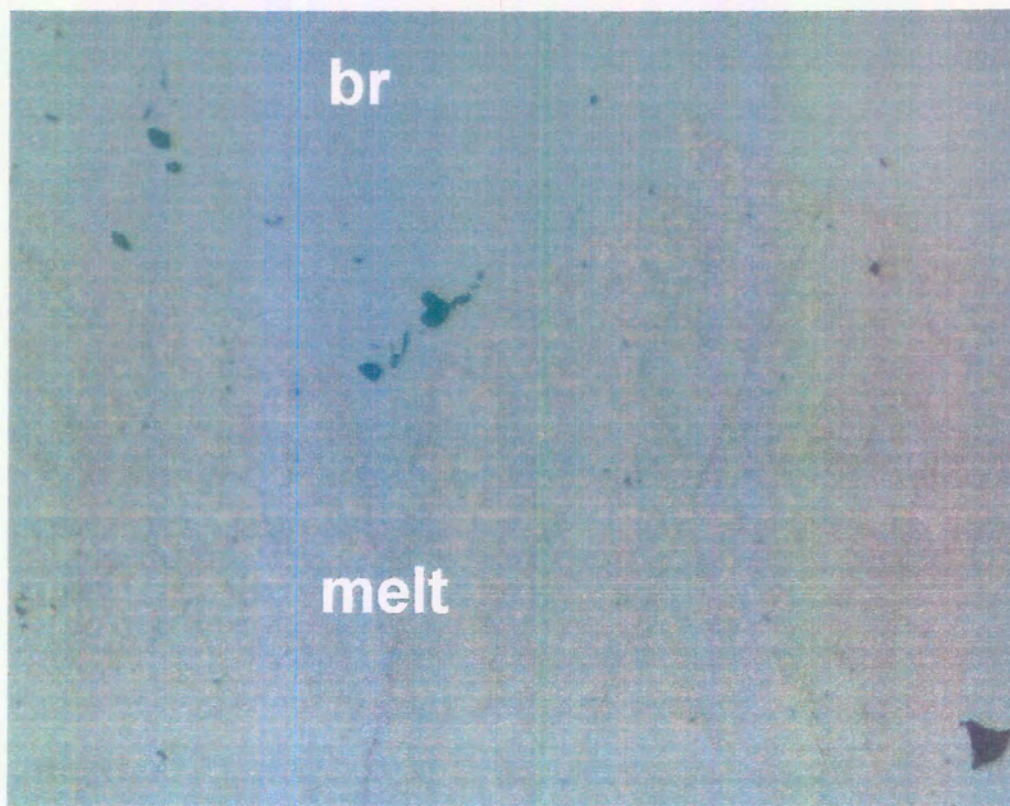
Photomicrograph 6 "Cooperite" (co) and coexisting melt at 900°C of experiment SV322 (long side of the photomicrograph is 0.35 mm).



Photomicrograph 7 "Braggite" (br) and coexisting melt at 900°C of experiment SV326 (long side of the photomicrograph is 0.35 mm).



Photomicrograph 8 “Braggite” (br) and coexisting melt at 900°C of experiment SV328 (long side of the photomicrograph is 0.35 mm).



Photomicrograph 9 “Braggite” (br) and coexisting melt at 900°C of experiment SV330 (long side of the photomicrograph is 0.35 mm).

6.5.1 “Cooperite” at 900°C

Contrary to the observations at 1200°C, 1100°C, and 1000°C, the Ni-content in “cooperite” formed in a Ni-saturated environment at 900°C increases slightly with increasing Pd content.

Least square fittings of the data for “cooperite” (in cation per cent) lead to the following linear relationships at the 95% confidence level:

Table 13: Type of best fit, equation for best fit at the 95% confidence level, equation number (No), and R²-values of best fits of elements analysed in “cooperite” formed at 900°C.

Variables	Fit	Equation	No	R ²
Ni, Pt	Linear	$Ni = 4.314 (\pm 0.049) - 0.099 (\pm 0.007) \times Pt$	20	0.9799
Ni, Pd	Linear	$Ni = 3.094 (\pm 0.095) + 0.116 (\pm 0.013) \times Pd$	21	0.9514
Pt, Pd	Linear	$Pt = 48.442 (\pm 0.417) - 1.192 (\pm 0.058) \times Pd$	22	0.9906
Ni, Pt/Pd	Linear	$Ni = 4.426 (\pm 0.046) - 0.062 (\pm 0.005) \times (Pt/Pd)$	23	0.9841

Equations 20 to 23 are presented graphically in Figures 42 to 45:

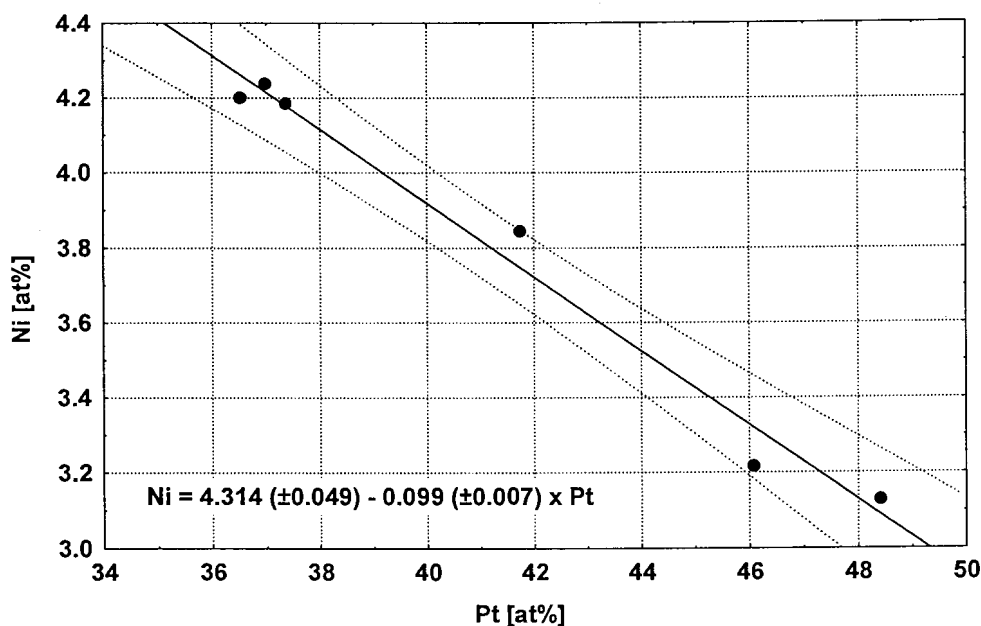


Figure 42 Ni-content versus Pt-content (in at-%) in “cooperite” formed in a Ni-saturated environment at 900°C. The solid line indicates the best linear fit and the stippled lines the 95% confidence interval according to the equation shown (N=6).

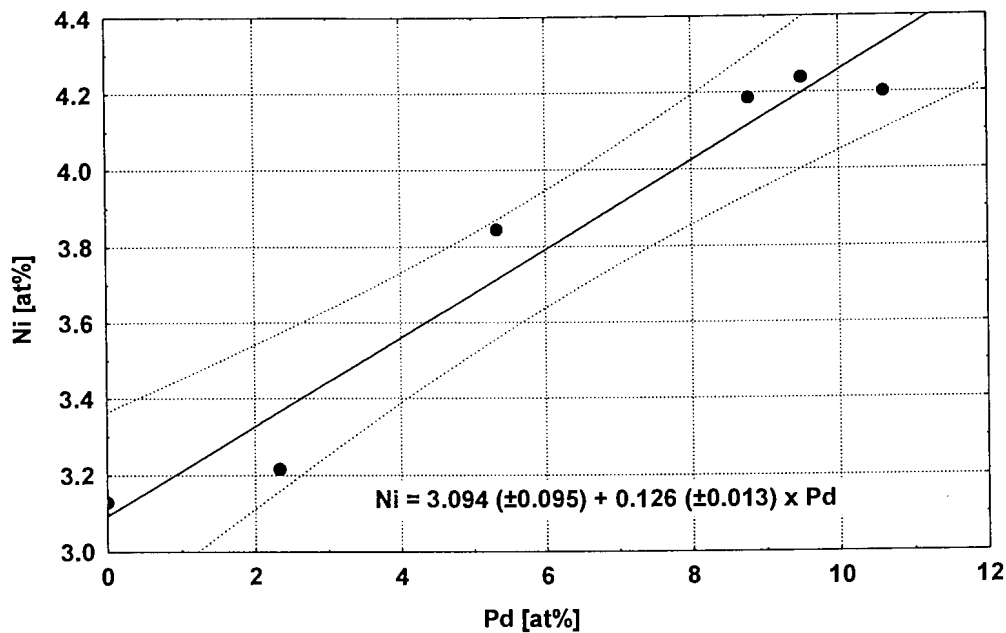


Figure 43 Ni-content versus Pd-content (in at-%) in “cooperite” formed in a Ni-saturated environment at 900°C. The solid line indicates the best linear fit and the stippled lines the 95% confidence interval according to the equation shown (N=6).

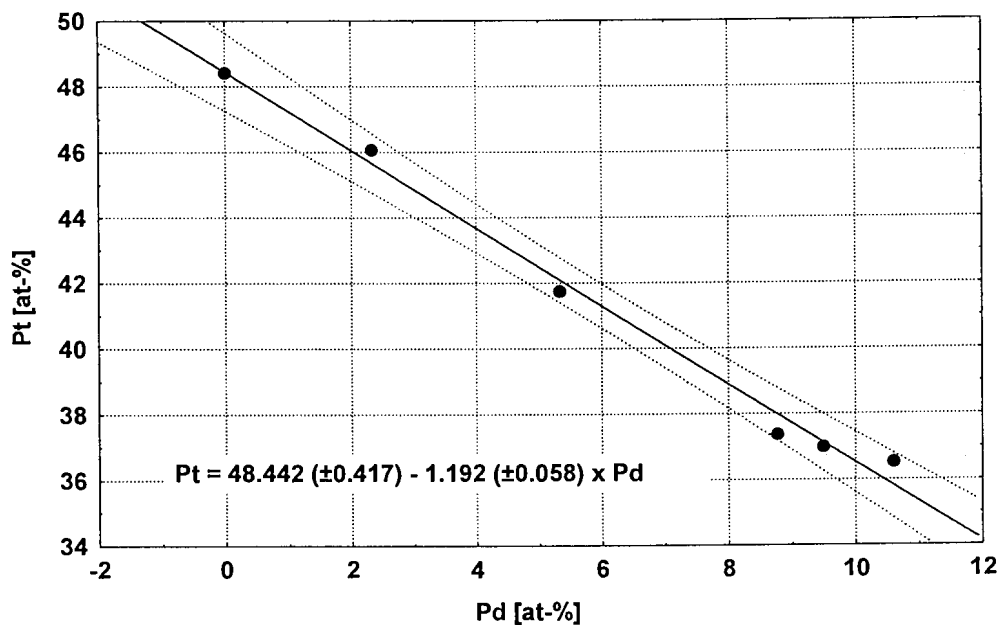


Figure 44 Pt-content versus Pd-content (in at-%) in “cooperite” formed in a Ni-saturated environment at 900°C. The solid line indicates the best linear fit and the stippled lines the 95% confidence interval according to the equation shown (N=6).

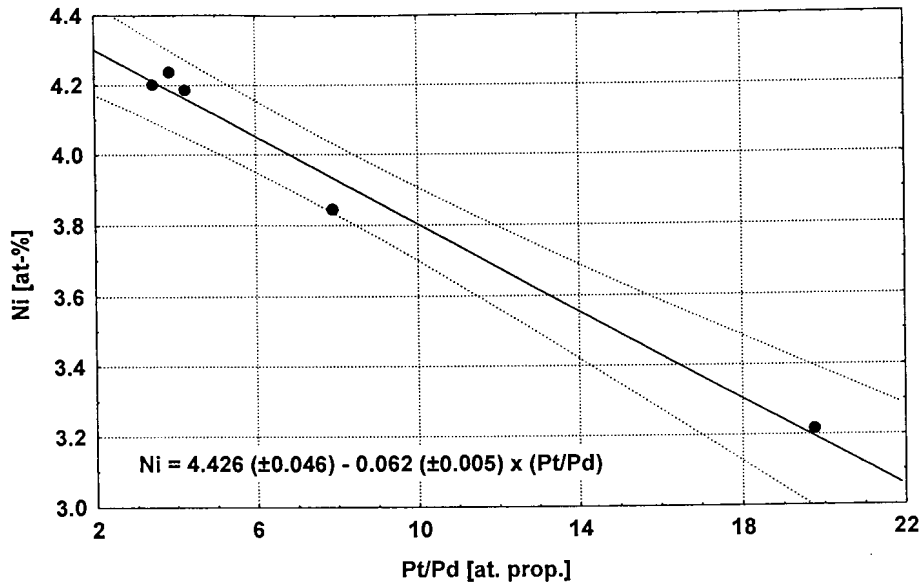


Figure 45 Ni-content versus Pt/Pd ratio (in atomic proportions) in “cooperite” formed in a Ni-saturated environment at 900°C. The solid line indicates the best linear fit and the stippled lines the 95% confidence interval according to the equation shown (N=6).

6.5.2 “Braggite” and “vysotskite” at 900°C

The Ni-content in “braggite-vysotskite” formed in a Ni-saturated environment at 900°C decreases slightly with increasing Pd content, but is higher than that at 1000°C. Least square fitting of the data (in cation per cent) for “braggite-vysotskite” formed in a Ni-saturated environment lead to the following relationships at the 95% confidence level (Table 14):

Table 14: Type of best fit, equation for best fit at the 95% confidence level, equation number (No), and R²-values of best fits of elements analysed in “braggite-vysotskite” formed at 900°C.

Variables	Fit	Equation	No	R ²
Ni, Pt	Linear	Ni= 4.180 (±0.084) + 0.065 (±0.004) x Pt	24	0.9742
Ni, Pd	Linear	Ni = 7.014 (±0.139) - 0.064 (±0.005) x Pd	25	0.9673
Pt, Pd	Linear	Pt = 43.257 (±0.037) - 0.977 (±0.013) x Pd	26	0.9988
Ni, Pt/Pd	Logarithmic			0.9528
	Inverse			0.7449
	Square root	Ni = 3.952 (±0.143) + 1.570 (±0.143) √(Pt/Pd)	27	0.9600

Equations 24 to 27 are presented graphically in Figures 46 to 49:

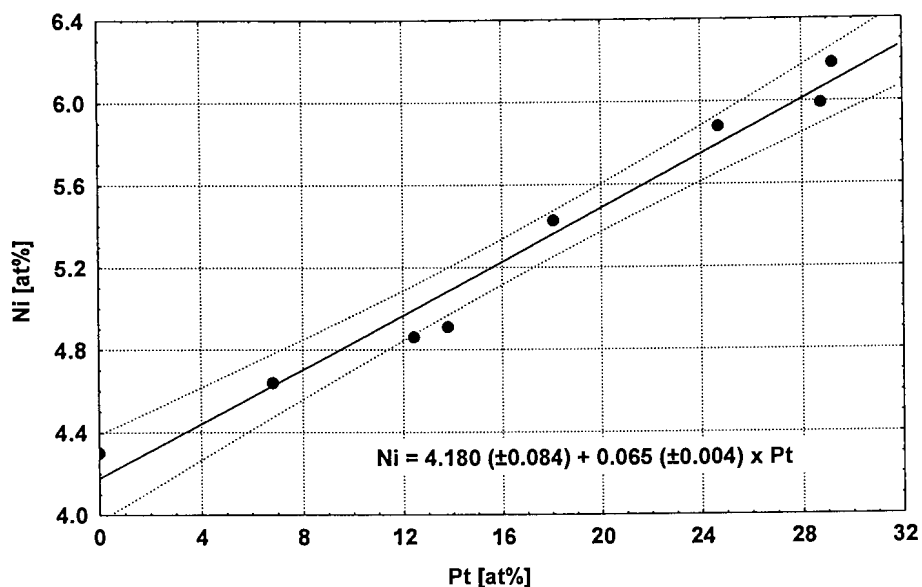


Figure 46 Ni-content versus Pt-content (in at-%) in “braggite-vysotskite” formed in a Ni-saturated environment at 900°C. The solid line indicates the best linear fit and the stippled line the 95% confidence interval according to the equation shown (N=8).

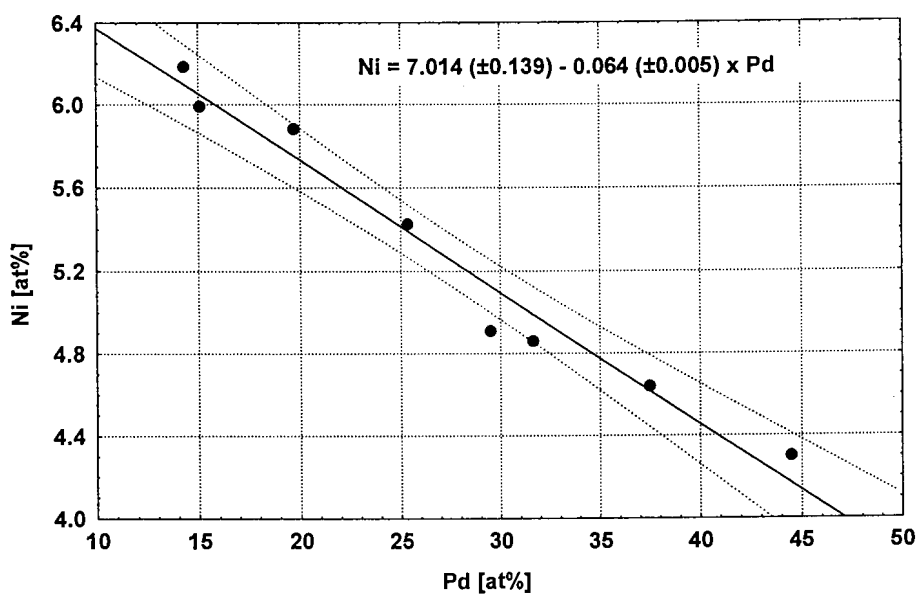


Figure 47 Ni-content versus Pd-content (in at-%) in “braggite-vysotskite” formed in a Ni-saturated environment at 900°C. The solid line indicates the best linear fit and the stippled line the 95% confidence interval according to the equation shown (N=8).

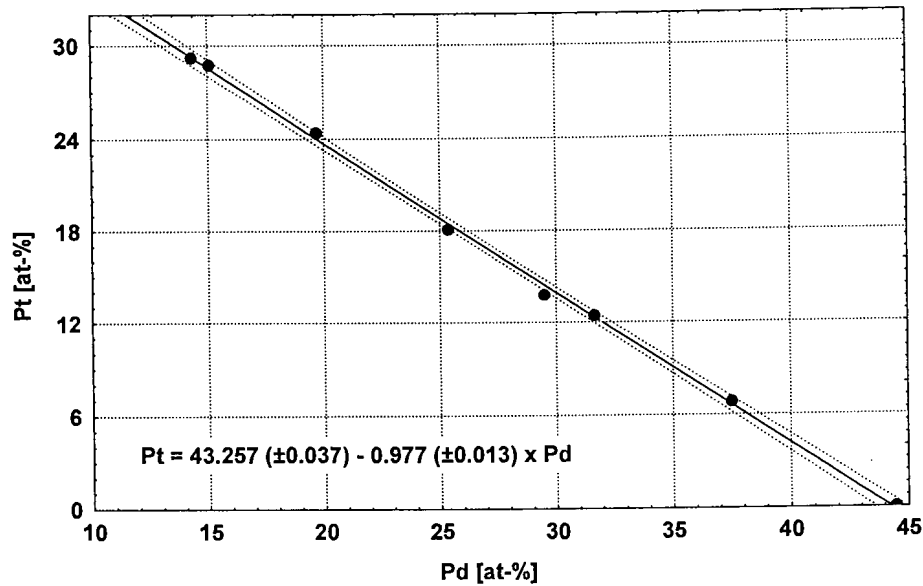


Figure 48 Pt-content versus Pd-content (in at-%) in “braggite-vysotskite” formed in a Ni-saturated environment at 900°C. The solid line indicates the best linear fit and the stippled line the 95% confidence interval according to the equation shown (N=8).

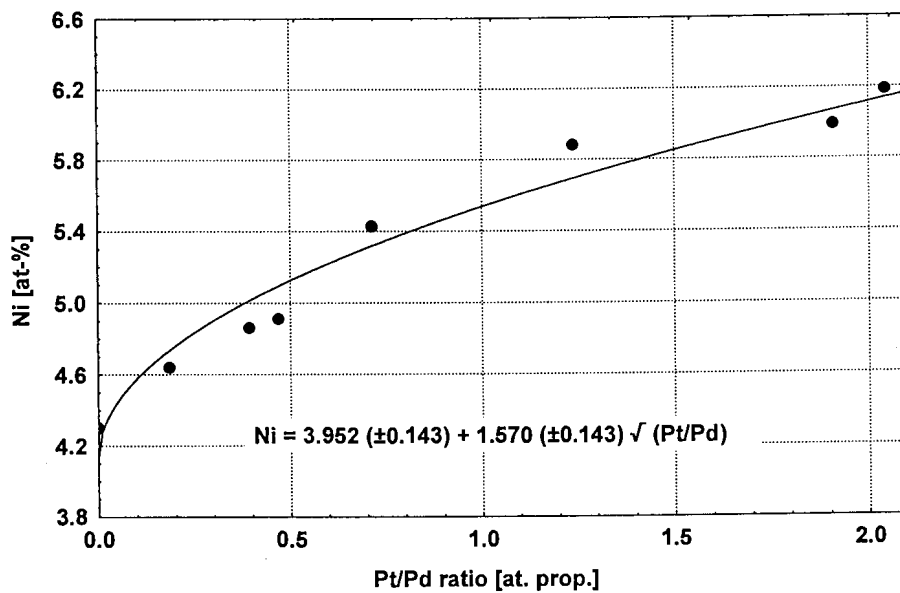


Figure 49 Ni-content versus Pt/Pd ratio (in atomic proportions) in “braggite-vysotskite” formed in a Ni-saturated environment at 900°C. The solid line indicates the best square root fit according to the equation shown (N=8).

6.5.3 Melt at 900°C

At 900°C the amount of sulphur visible on the glass capsule walls after quenching (as discussed in Chapter 6.2, 1200°C) is less than at the higher temperatures. This is reflected in the S-content of the solidified melt showing a smaller variation (48.1 at-% to 50.6 at-%) than at temperatures above 900°C. The relationships between the Pd- and S-content (Spearman correlation coefficient, $r = -0.71$), as well as between the S- and the Ni-content (Spearman correlation coefficient, $r = 0.74$), are not as pronounced at this temperature. This is also illustrated by the scatterplot below (Fig. 50). The Spearman correlation coefficients between the Ni-, Pd-, and S-content within the melt do not increase if the analyses of the melt are divided into two groups, i.e. coefficients calculated for a group in which the melt coexists with “cooperite”, and for another group in which the melt coexists with “braggite-vysotskite”.

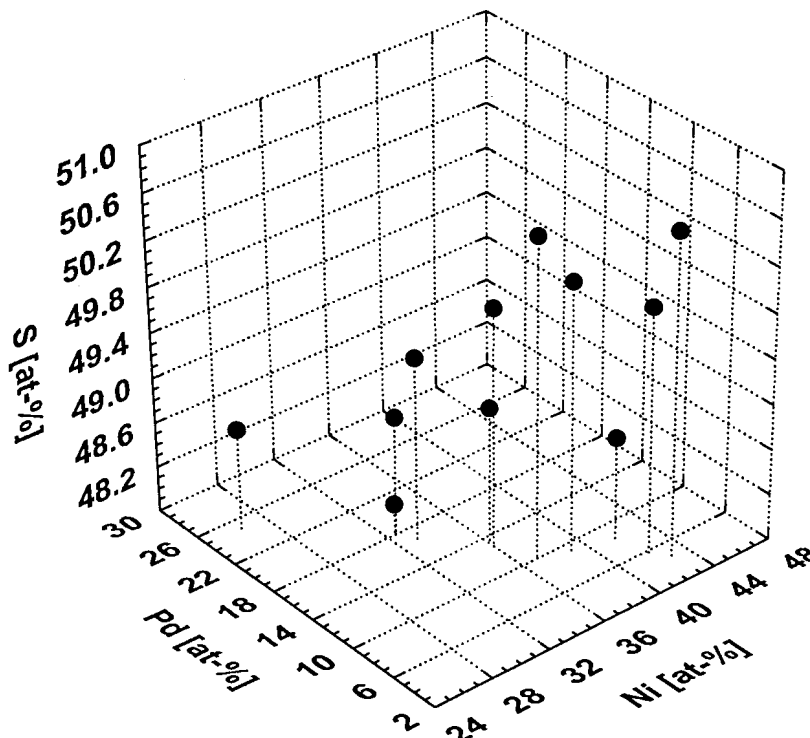


Figure 50 3D scatterplot of Pd-, Ni-, and S-content in at-% in melt at 900°C coexisting with “cooperite” and/or “braggite” or “vysotskite”.

At 800°C no melt phase is present and all “cooperite”, “braggite”, and “vysotskite”, formed under Ni-saturated conditions, coexist with $Ni_{1-x}S$.

Generally, two charges with constant Pt/Pd ratio, but varying Ni-content (25 and 10 at-%), were prepared. Nickel appears to act as a “flux” at this temperature, because in the experiments with low Ni-content in the charges, the quenched products displayed some degree of heterogeneity (if heterogeneity was detected, these experiments were discarded, i.e. Charges SV809, SV806, SV813, and SV804).

The compositional relationships are shown in Figure 51 and the experimental results are summarized in Table 15.

$Ni_{1-x}S$, which coexists with Pt-free “vysotskite” and Pd-free “cooperite” contains a maximum of 1.7 at-% Pd and 0.2 at-% Pt, respectively. Maximum solubility of Ni in ideal Pd-free “cooperite” along the PtS-NiS join is 4.5 at-%. The Pd-limit in Ni-free “cooperite”, coexisting with Ni-free “braggite” at 800°C is 12.6 at-%.

The Ni-content in both “cooperite” and “braggite-vysotskite”, formed in a Ni-saturated environment, remains fairly constant. The Ni-content ranges from 4.0 to 4.5 at-% Ni in “cooperite” and between 6.9 and 7.5at-% in “braggite-vysotskite”. These levels are slightly higher than at 900°C. In both mineral groups, there is a slight decline in Ni-content with increasing Pd-content. The Ni-content in the “cooperite” coexisting with “braggite”, however, drops sharply, compared to those coexisting only with $Ni_{1-x}S$. The same applies to the Ni-content in “braggite” coexisting with “cooperite” (see Fig. 52).

Photomicrographs 10 and 11 show the typical textures of “cooperite” with coexisting $Ni_{1-x}S$ and “vysotskite” with coexisting $Ni_{1-x}S$, respectively.

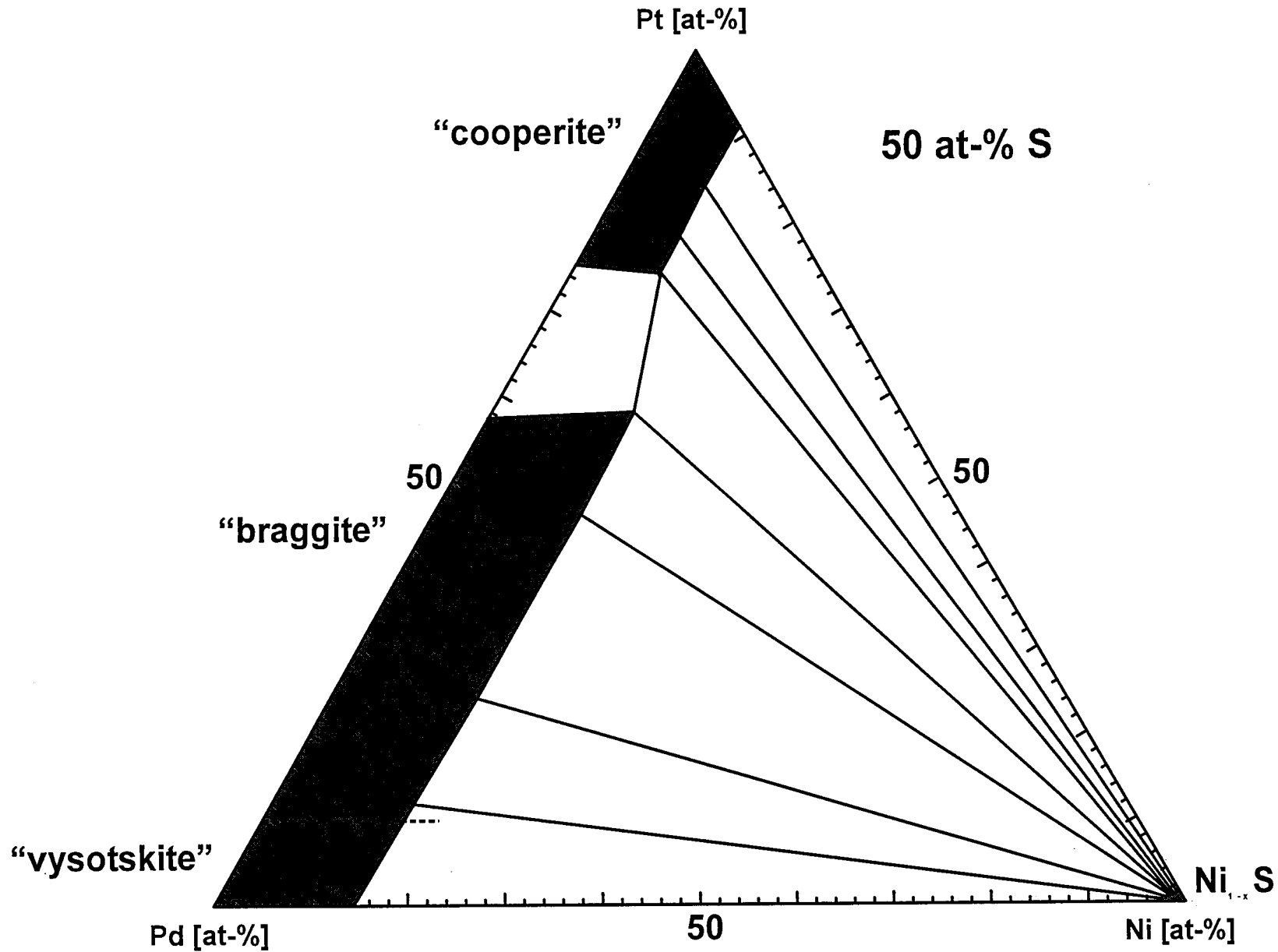


Figure 51 Phase relations in the system PtS-PdS-NiS in cation proportions at 800°C (the stippled line indicates the border between "braggite" and "vysotskite").

at%
0.16 (0.03)
0.25 (0.12)
48.35 (0.41)
51.24 (0.61)
(N=17)

Table 15: Mean (arithmetic) compositions of phases in the system PtS-PdS-NiS at 800°C in weight per cent (wt%) and atomic per cent (at%). Values in parenthesis show the standard deviation at the 1 σ level. N = number of analyses per experiment.

Sample	Phases		Pt	Pd	Ni	S	TOTAL
SV801	"Cooperite"	wt%	75.81 (0.67)	6.71 (0.43)	2.50 (0.15)	15.44 (0.27)	100.47
		at%	39.82 (0.41)	6.46(0.41)	4.36 (0.35)	49.35 (0.58)	(N=10)
	Ni _{1-x} S	wt%	0.73 (0.10)	0.87 (0.25)	64.12 (0.79)	34.42 (0.72)	100.22
		at%	0.17 (0.10)	0.38 (0.18)	50.16 (0.58)	49.30 (0.62)	(N=15)
SV807	"Braggite"	wt%	31.14 (0.84)	41.86 (0.77)	5.75 (0.27)	21.40 (0.60)	100.15
		at%	12.11 (0.53)	29.84 (0.58)	7.43 (0.29)	50.63 (0.72)	(N=30)
	Ni _{1-x} S	wt%	0.09 (0.28)	2.54 (0.25)	61.23 (0.17)	36.23 (0.47)	100.17
		at%	0.02 (0.15)	1.09 (0.52)	47.47 (0.46)	51.43 (0.31)	(N=8)
SV808	"Braggite"	wt%	52.07 (0.85)	24.20 (0.75)	5.15 (0.21)	18.78 (0.57)	100.20
		at%	22.85 (0.60)	19.48 (0.52)	7.51 (0.28)	50.16 (0.73)	(N=34)
	Ni _{1-x} S	wt%	0.41 (0.11)	1.89 (0.23)	61.92 (0.38)	35.91 (0.46)	100.13
		at%	0.10 (0.03)	0.81 (0.10)	48.06 (0.35)	51.03 (0.30)	(N=10)
SV810	"Braggite"	wt%	16.51 (0.85)	54.73 (0.76)	6.35 (0.13)	22.55 (0.63)	99.93
		at%	6.02 (0.31)	36.64 (0.56)	7.33 (0.18)	50.01 (0.64)	(N=17)
	Ni _{1-x} S	wt%	0.21 (0.05)	3.39 (0.13)	61.28 (0.84)	35.50 (0.12)	100.38
		at%	0.05 (0.01)	1.46 (0.05)	47.80 (0.34)	50.70 (0.47)	(N=4)
SV811	"Cooperite"	wt%	71.91 (0.54)	13.03 (0.82)	0	15.52 (0.32)	100.50
		at%	37.80 (0.40)	12.56 (0.79)	0	49.64 (0.73)	(N=7)
	"Braggite"	wt%	58.12 (0.64)	25.12 (0.64)	0	17.00 (0.38)	100.16
		at%	27.99 (0.62)	22.18 (0.42)	0	49.82 (0.61)	(N=13)
SV812	"Cooperite"	wt%	73.16 (0.54)	9.50 (0.27)	2.30 (0.08)	15.12 (0.36)	100.09
		at%	38.46 (0.52)	9.16 (0.23)	4.02 (0.15)	48.37 (0.59)	(N=21)
	"Braggite"	wt%	61.48 (0.77)	17.61 (0.74)	4.43 (0.10)	17.02 (0.32)	100.56
		at%	28.99 (0.57)	15.23 (0.52)	6.94 (0.17)	48.84 (0.50)	(N=15)
	Ni _{1-x} S	wt%	0.54 (0.10)	1.25 (0.11)	62.48 (0.50)	36.36 (0.22)	100.63
		at%	0.13 (0.04)	0.53 (0.05)	48.10 (0.46)	51.25 (0.51)	(N=5)
SV815	"Braggite"	wt%	0	69.34 (0.71)	6.49 (0.25)	24.36 (0.56)	100.21
		at%	0	42.82 (0.57)	7.26 (0.29)	49.92 (0.66)	(N=64)
	Ni _{1-x} S	wt%	0	3.91 (0.24)	60.39 (0.40)	35.46 (0.98)	99.77
		at%	0	1.69 (0.11)	47.37 (0.74)	50.93 (0.80)	(N=11)
SV816	"Cooperite"	wt%	83.34 (0.66)	0	2.41 (0.19)	14.37 (0.46)	100.13
		at%	46.61 (0.95)	0	4.48 (0.28)	48.91 (0.79)	(N=12)
	Ni _{1-x} S	wt%	0.69 (0.25)	0	63.26 (0.86)	36.73 (0.06)	100.78
		at%	0.16 (0.06)	0	48.39 (0.36)	51.45 (0.33)	(N=6)
SV819	"Cooperite"	wt%	78.52 (0.70)	3.61 (0.46)	2.48 (0.39)	15.51 (0.36)	100.13
		at%	41.82 (0.98)	3.53 (0.41)	4.39 (0.47)	50.27 (0.70)	(N=21)
	Ni _{1-x} S	wt%	0.70 (0.15)	0.58 (0.09)	63.05 (0.75)	36.49 (0.53)	100.85
		at%	0.16 (0.03)	0.25 (0.12)	48.35 (0.41)	51.24 (0.61)	(N=17)

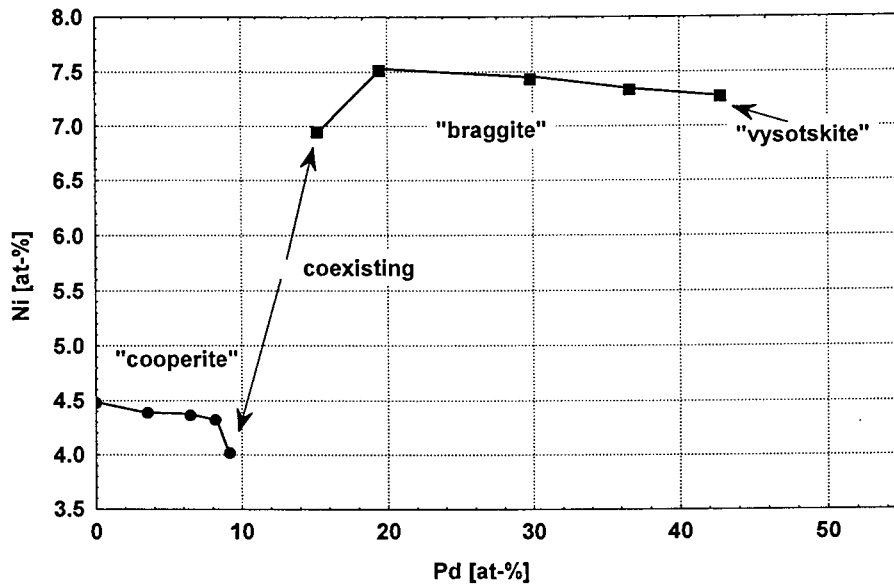
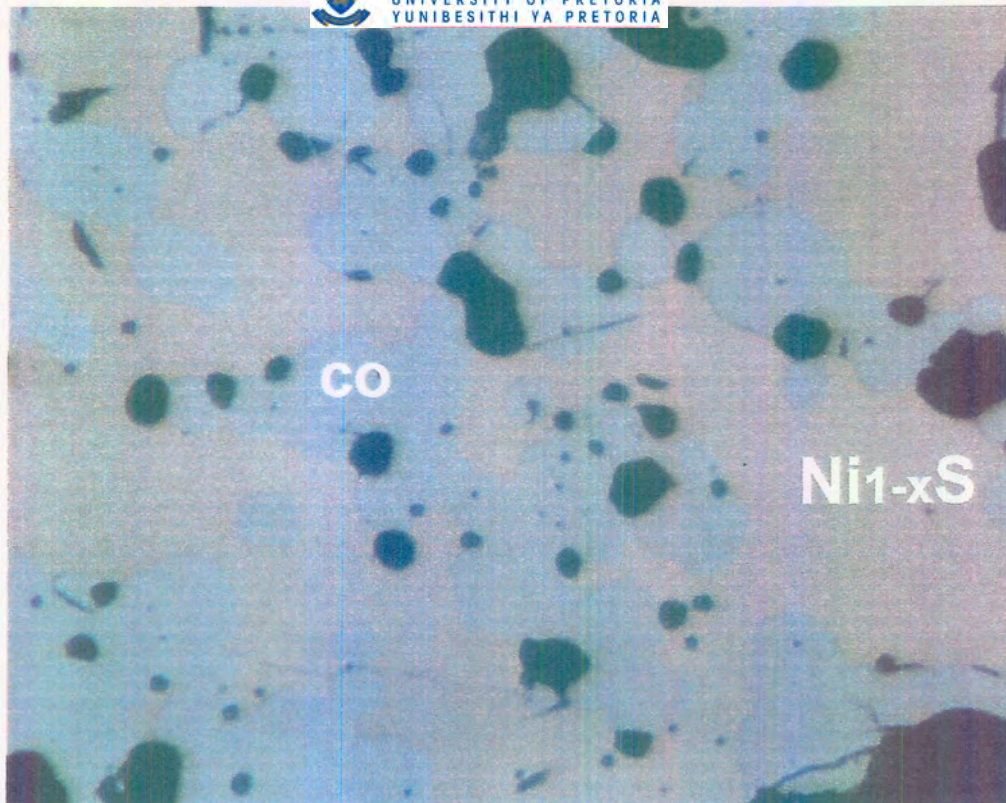
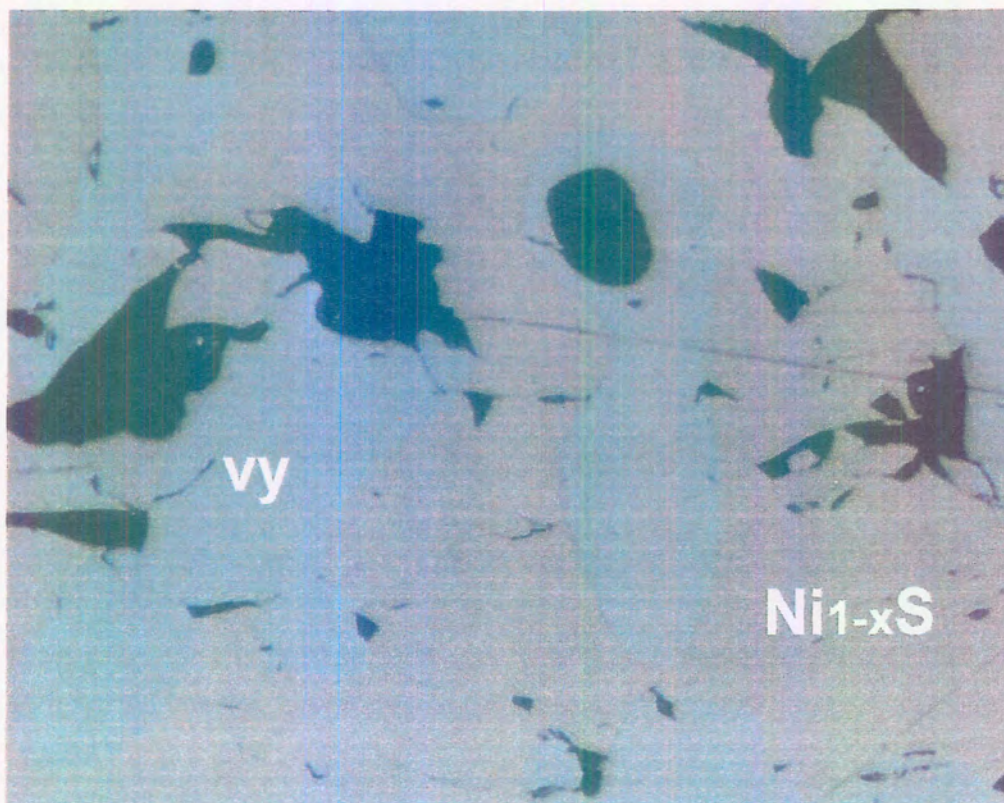


Figure 52 Ni-content versus Pd-content (in at-%) in “cooperite”, “braggite”, and “vysotskite” formed in a Ni-saturated environment at 800°C. The solid lines connect the data points of “cooperite” and “braggite-vysotskite” individually.



Photomicrograph 10 "Cooperite" (co) and coexisting $Ni_{1-x}S$ at $800^{\circ}C$ of experiment SV805 (long side of the photomicrograph is 0.35 mm).



Photomicrograph 11 "Vysotskite" (vy) and coexisting $Ni_{1-x}S$ at $800^{\circ}C$ of experiment SV815 (long side of the photomicrograph is 0.35 mm).

6.6.1 “Cooperite” at 800 °C

The Ni content in “cooperite”, formed in a Ni-saturated environment, decreases slightly with increasing Pd-content. Least square fitting of the data for “cooperite”, not coexisting with “braggite” (in cation per cent), lead to the following linear relationships at the 95% confidence level:

Table 16: Type of best fit, equation for best fit at the 95% confidence level, equation number (No), and R²-values of best fits of elements analysed in “cooperite” formed at 800 °C.

Variables	Fit	Equation	No	R ²
Ni, Pt	Linear	$Ni = 4.285 (\pm 0.008) + 0.018 (\pm 0.001) \times Pt$	28	0.9906
Ni, Pd	Linear	$Ni = 4.472 (\pm 0.014) - 0.018 (\pm 0.003) \times Pd$	29	0.9631
Pt, Pd	Linear	$Pt = 46.147 (\pm 0.635) - 0.989 (\pm 0.115) \times Pd$	30	0.9734

In “cooperite” formed at 800 °C, no well-defined relationship could established between the Ni-content and the Pt/Pd ratio.

Equations 28 to 30 are presented graphically in Figures 53 to 55 below.

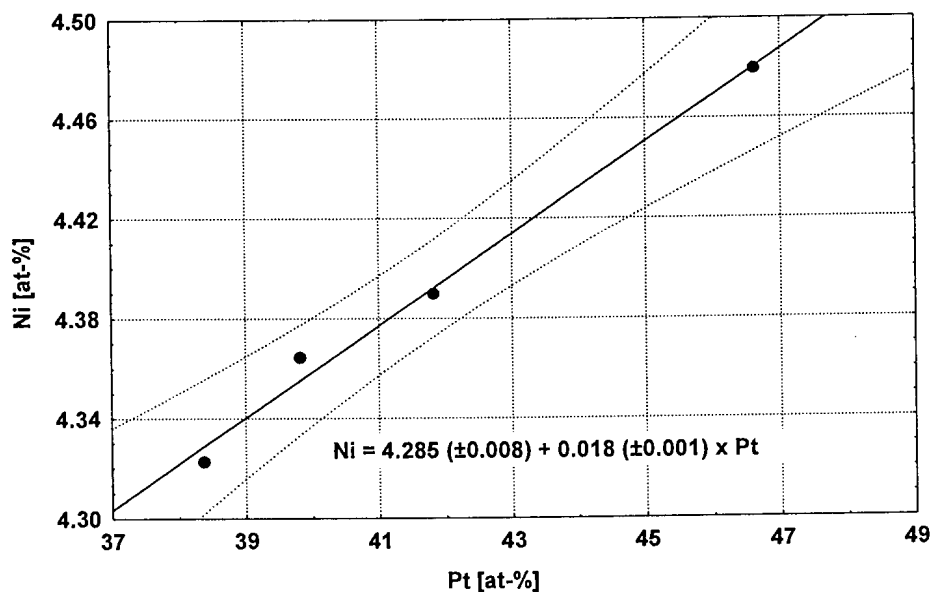


Figure 53 Ni-content versus Pt-content (in at-%) in “cooperite” formed in a Ni-saturated environment at 800 °C. The solid line indicates the best linear fit and the stippled lines the 95% confidence interval according to the equation shown (N=4).

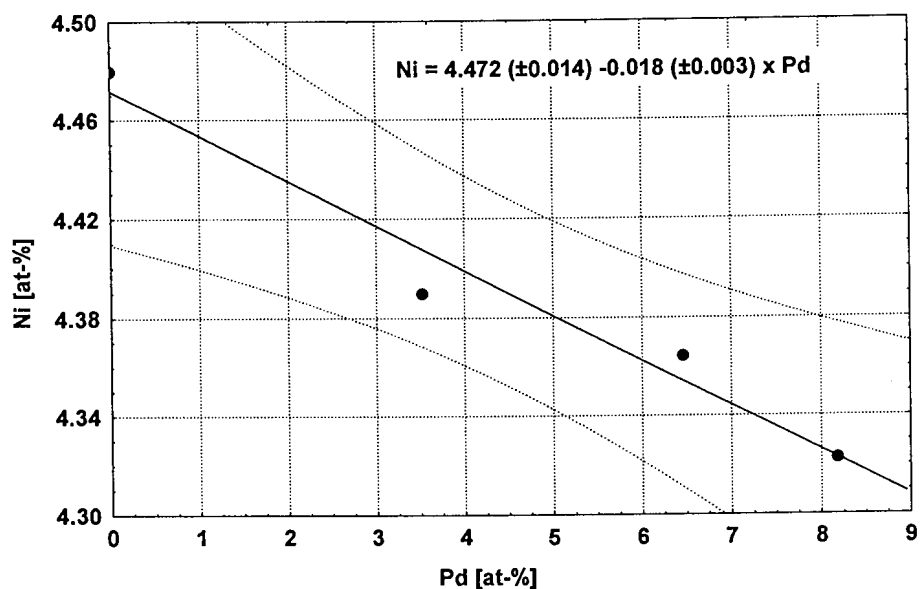


Figure 54 Ni-content versus Pd-content (in at-%) in “cooperite” formed in a Ni-saturated environment at 800°C. The solid line indicates the best linear fit and the stippled lines the 95% confidence interval according to the equation shown (N=4).

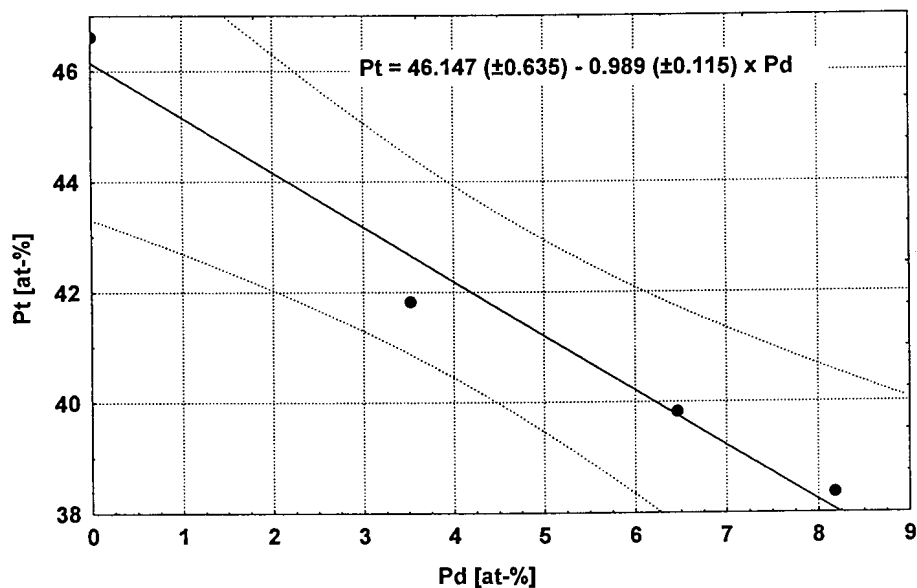


Figure 55 Pt-content versus Pd-content (in at-%) in “cooperite” formed in a Ni-saturated environment at 800°C. The solid line indicates the best linear fit and the stippled lines the 95% confidence interval according to the equation shown (N=4).

6.6.2 “Braggite” and “vysotskite” at 800°C

The Ni-content in “braggite-vysotskite” in a Ni-saturated environment decreases slightly with increasing Pd content, but is higher than that at 900°C. Least square fitting of the data of “braggite-vysotskite” formed in a Ni-saturated environment at 800°C, excluding the “braggite” coexisting with “cooperite” (in cation per cent), lead to the following Equations (at the 95% confidence level) (Table: 17):

Table 17: Type of best fit, equation for best fit at the 95% confidence level, equation number (No), and R²-values of best fits of elements analysed in “braggite-vysotskite” formed at 800°C.

Variables	Fit	Equation	No	R ²
Ni, Pt	Linear	$Ni = 7.270 (\pm 0.016) + 0.011 (\pm 0.001) \times Pt$	31	0.9761
Ni, Pd	Linear	$Ni = 7.734 (\pm 0.016) - 0.011 (\pm 0.001) \times Pd$	32	0.9845
Pt, Pd	Linear	$Pt = 41.628 (\pm 0.690) - 0.975 (\pm 0.021) \times Pd$	33	0.9990

As in the case of “cooperite” discussed above, no pronounced relationship between the Ni-content and the Pt/Pd ratio in “braggite-vysotskite” could be established.

Equations 31 to 33 are presented graphically in Figures 56 to 58.

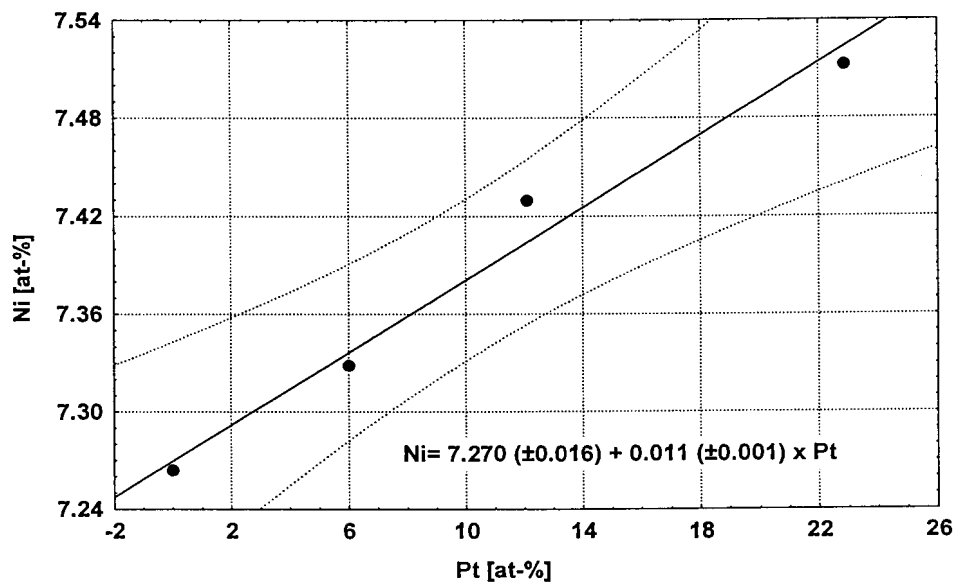


Figure 56 Ni-content versus Pt-content (in at-%) in “braggite-vysotskite” formed in a Ni-saturated environment at 800°C. The solid line indicates the best linear fit and the stippled lines the 95% confidence interval according to the equation shown (N=4).

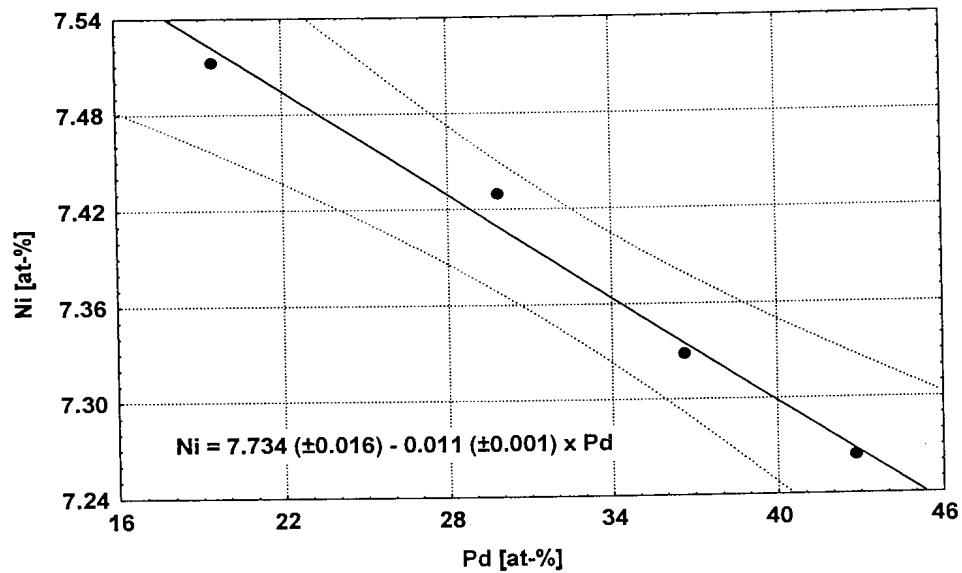


Figure 57 Ni-content versus Pd-content (in at-%) in “braggite-vysotskite” formed in a Ni-saturated environment at 800°C. The solid line indicates the best linear fit and the stippled lines the 95% confidence interval according to the equation shown (N=4).

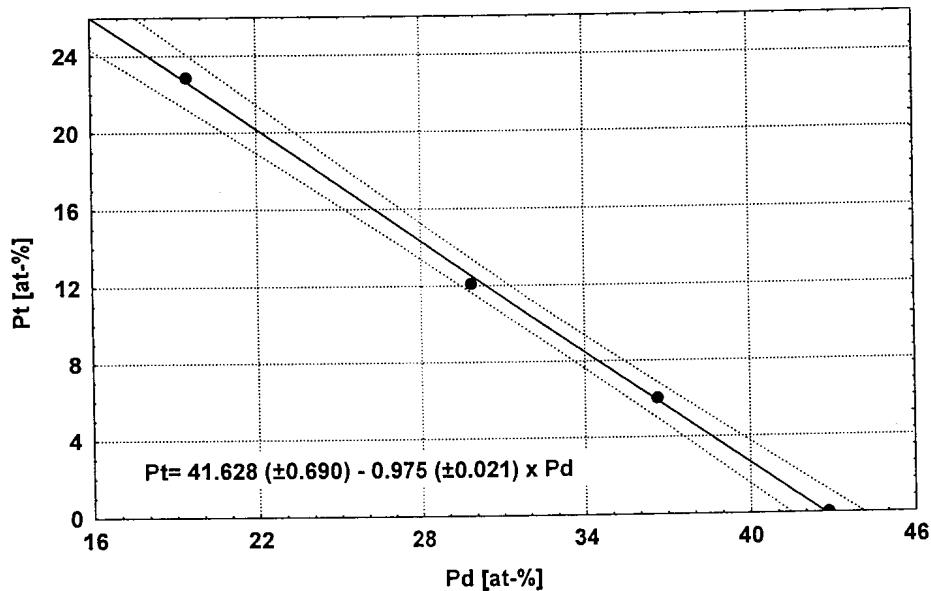


Figure 58 Pt-content versus Pd-content (in at-%) in “braggite-vysotskite” formed in a Ni-saturated environment at 800°C. The solid line indicates the best linear fit and the stippled lines the 95% confidence interval according to the equation shown (N=4).

6.6.3 Ni_{1-x}S at 800°C

At 800°C, the stability field of Ni_{1-x}S is very restricted. The compositional variation of Ni_{1-x}S at 800°C, is illustrated graphically in Figure 59.

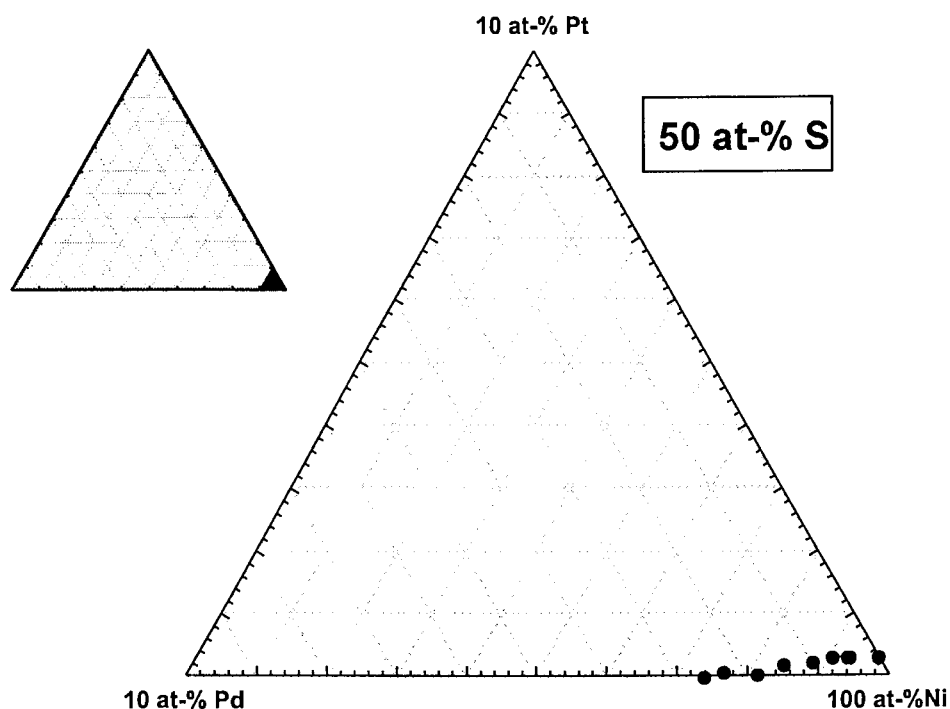


Figure 59 Compositional variation of Ni_{1-x}S (in cation proportions) coexisting with “cooperite”, “braggite”, or “vysotskite” at 800°C.

The Pt-content in Ni_{1-x}S, formed in a Pt- and Pd-saturated environment at 800°C, increases with increasing Ni-content. This rise is much more pronounced in Ni_{1-x}S coexisting with “braggite-vysotskite” than in Ni_{1-x}S coexisting with “cooperite” (Fig. 60). The Pd-content in Ni_{1-x}S coexisting with “braggite-vysotskite” decreases with increasing Ni-content and increases slightly with increasing Ni-content, when coexisting with “cooperite” (Fig. 61).

In Ni_{1-x}S coexisting with “braggite-vysotskite” at 800°C, the Pd-content decreases with increasing Pt-content and increases with increasing Pt-content, when coexisting with “cooperite” (Fig. 62).

It must, however, be pointed out, that the variation in Pt-content in Ni_{1-x}S, coexisting with “cooperite” lies within the analytical uncertainty (3σ) of 0.10 wt-% (~0.03 at-%) Pt and

the variation in Ni-content in $Ni_{1-x}S$ coexisting with “braggite-vysotskite” lies within the analytical uncertainty (3σ) of 0.84 wt-% (~ 0.7 at-%) Ni.

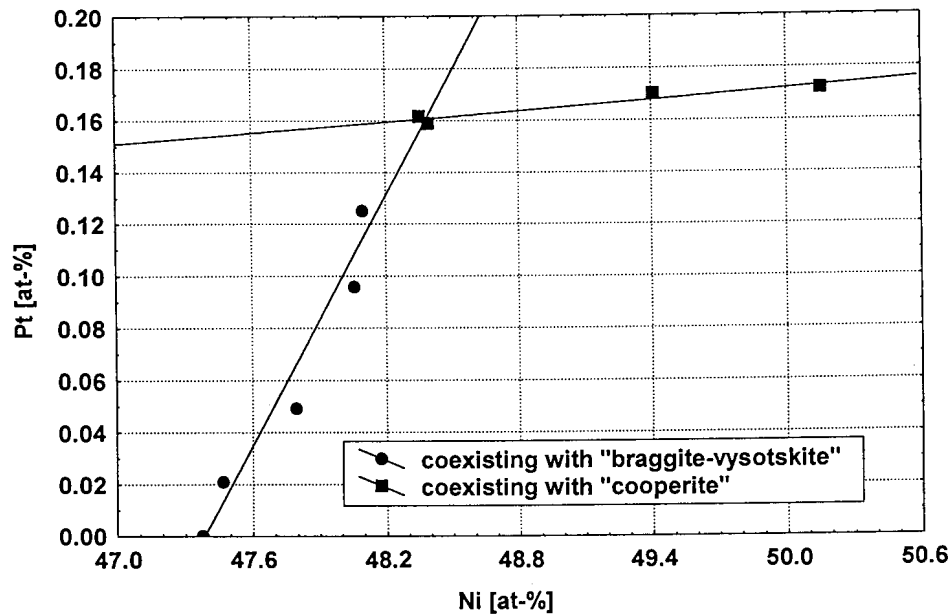


Figure 60 Pt-content versus Ni-content (in at-%) in $Ni_{1-x}S$ coexisting with “cooperite” or “braggite-vysotskite” at 800°C. The solid lines indicate the best linear fits for the 2 populations individually.

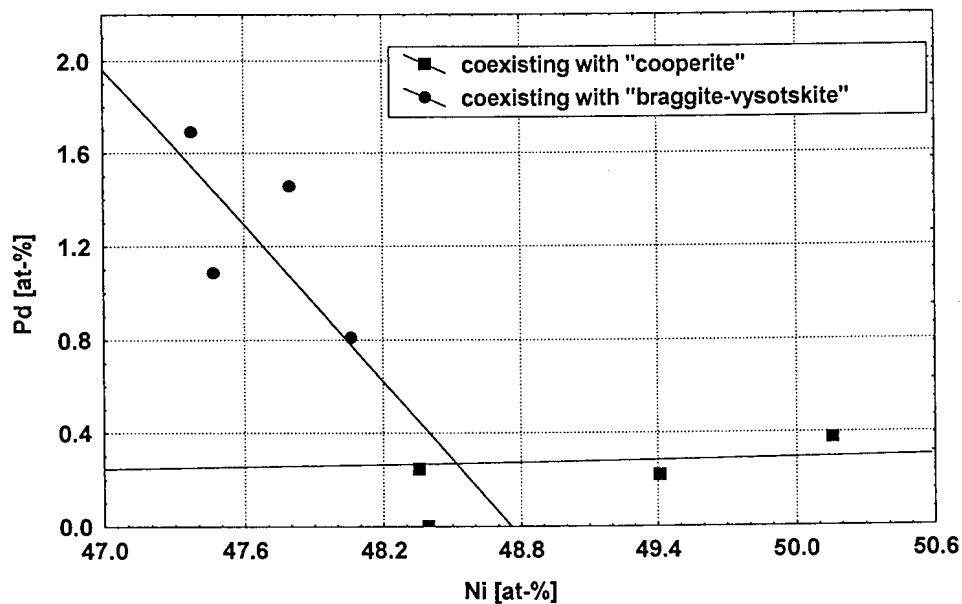


Figure 61 Pd-content versus Ni-content (in at-%) in $Ni_{1-x}S$ coexisting with “cooperite” or “braggite-vysotskite” at 800°C. The solid lines indicate the best linear fits for the 2 populations individually.

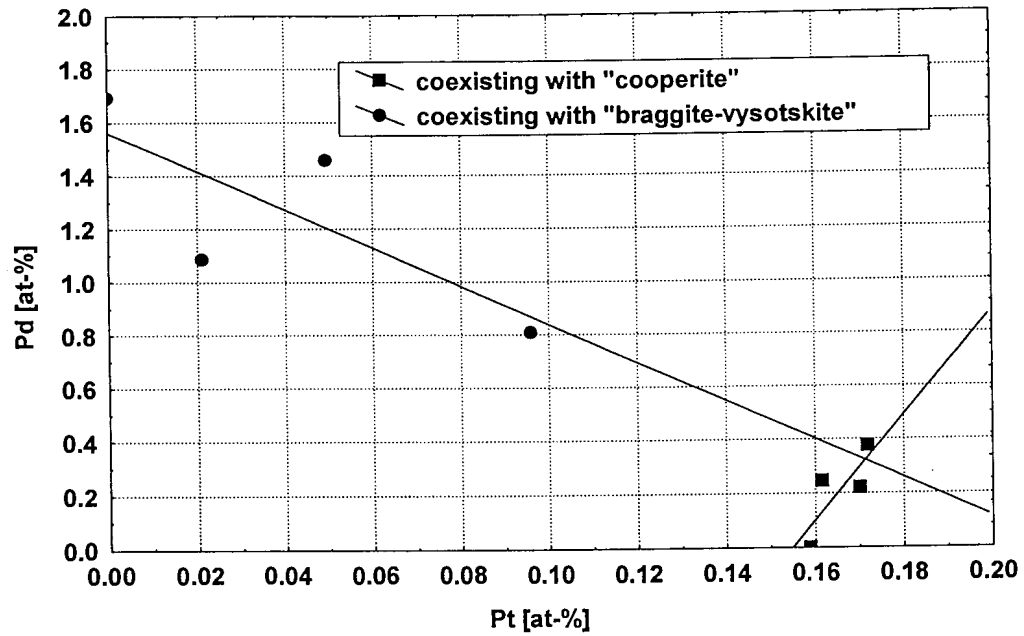


Figure 62 Pt-content versus Pd-content (in at-%) in $Ni_{1-x}S$ coexisting with "cooperite" or "braggite-vysotskite" at 800°C. The solid lines indicate the best linear fits for the 2 populations individually.

6.6.4 Relationships at 800°C

There is a positive relationship between the Pd-content of $Ni_{1-x}S$ and the Pd-content of the coexisting “cooperite”, braggite” and “vysotskite” (see Fig. 63).

The relationships between the Pt-content of $Ni_{1-x}S$ and the Pt-content of the coexisting “cooperite”, braggite”, and “vysotskite” are much more erratic. The same applies to the relationship between the Ni-content of $Ni_{1-x}S$ and the Ni-content of the coexisting “cooperite”, “braggite”, and “vysotskite”.

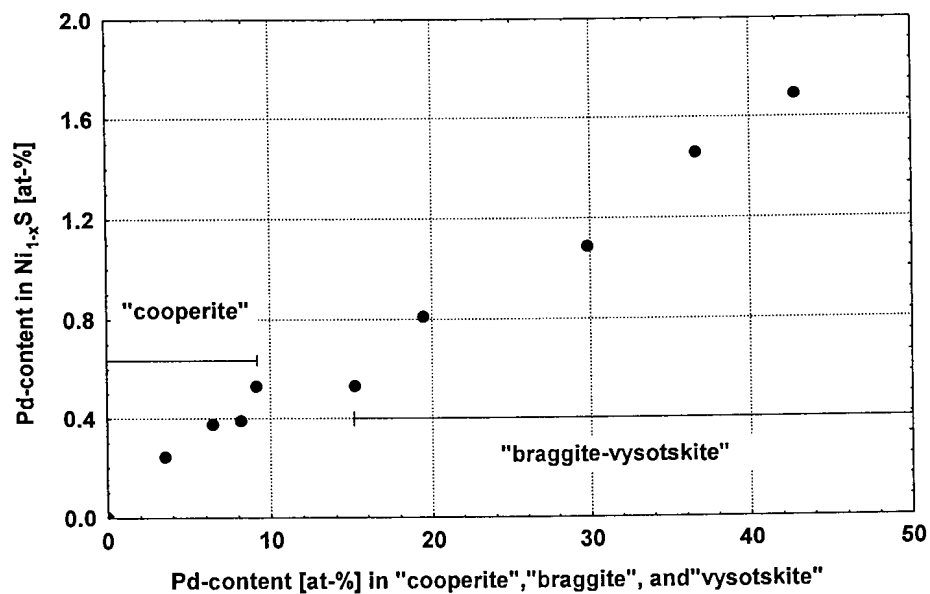


Figure 63 Pd-content (in at-%) in $Ni_{1-x}S$ versus Pd-content in “cooperite”, “braggite” and “vysotskite” at 800°C.

6.7 THE 700°C ISOTHERMAL SECTION

At 700°C, “cooperite”, “braggite”, and “vysotskite”, which formed in a Ni-saturated environment, coexist with Ni_{1-x}S .

The compositional relationships are shown in Figure 64 and the experimental results are summarized in Table 18.

Ni_{1-x}S , which coexists with Pt-free “vysotskite” and Pd-free “cooperite”, contains a maximum of 1.0 at-% Pd and 0.1 at-% Pt, respectively. Maximum solubility of Ni in ideal Pd-free “cooperite” along the PtS-NiS join is 3.7 at-%. The Pd-limit in Ni-free “cooperite”, coexisting with Ni-free “braggite” at 700°C, is 13.1 at-%. The Ni-content in both “cooperite” and “braggite-vysotskite”, formed in a Ni-saturated environment, remains fairly constant, ranging from 3.07 to 3.7 at-% Ni in the former and between 8.1 and 8.7 at-% Ni in the latter. The Ni-content in “braggite-vysotskite” is slightly higher than that at 800°C, whereas the Ni-content in “cooperite” is slightly lower than that at 800°C. In both mineral groups, there is a slight decline in Ni-content with increasing Pd-content.

The phase relations of coexisting “cooperite” and “braggite” at 700°C are a little different to those at 800°C. At 700°C, “cooperite”, coexisting with “braggite” synthesised under slightly Ni-undersaturated conditions (implying they do not coexist with Ni_{1-x}S), contains significantly higher amounts of Pd (13.1 at-% Pd) than that formed under Ni-saturated conditions (5.3 at-% Pd).

Photomicrograph 12 shows the typical texture of “cooperite” coexisting with “braggite” and Ni_{1-x}S .

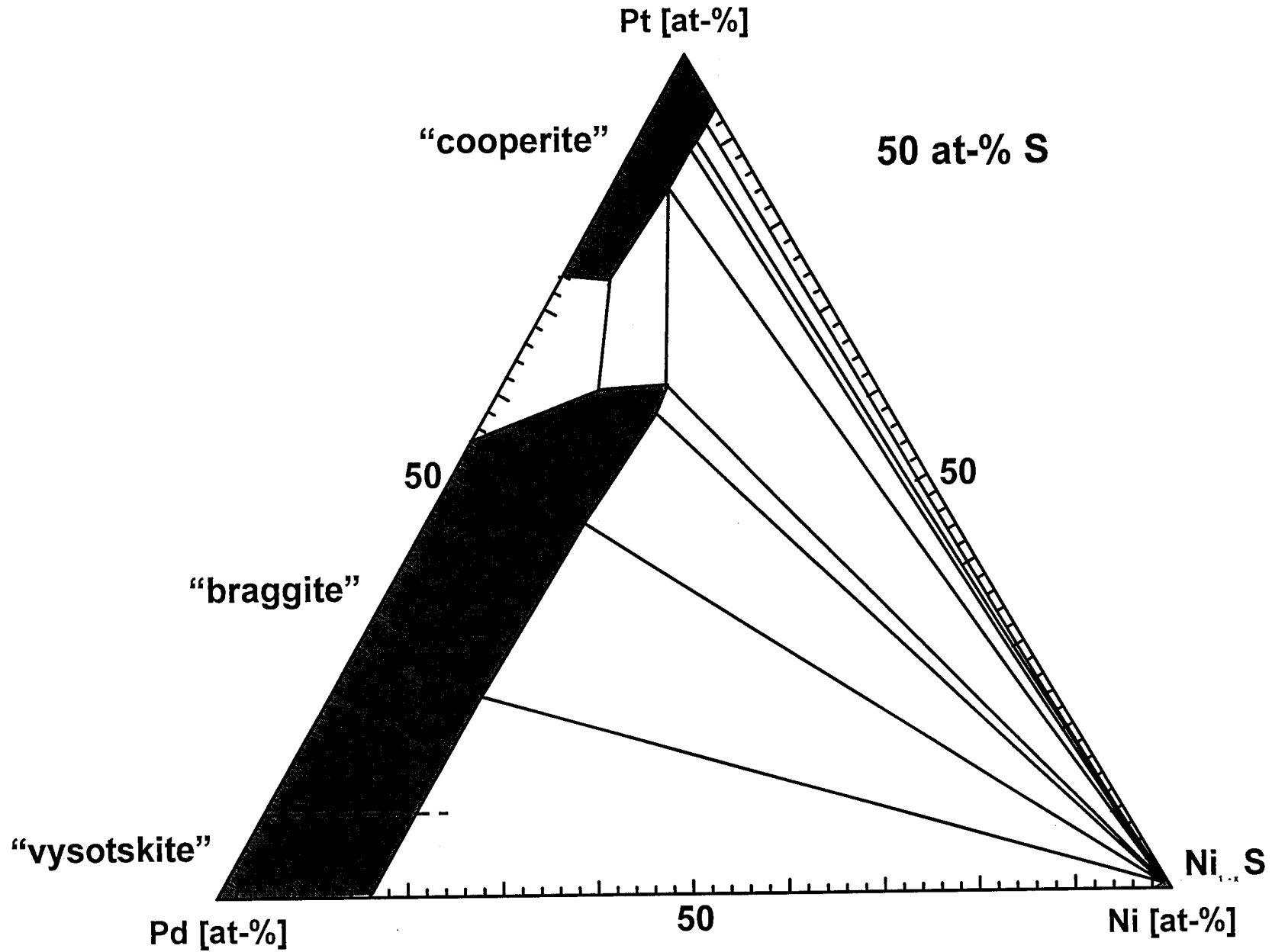


Figure 64 Phase relations in the system PtS-PdS-NiS in cation proportions at 700°C (the stippled line indicates the border between “braggite” and “vysotskite”).

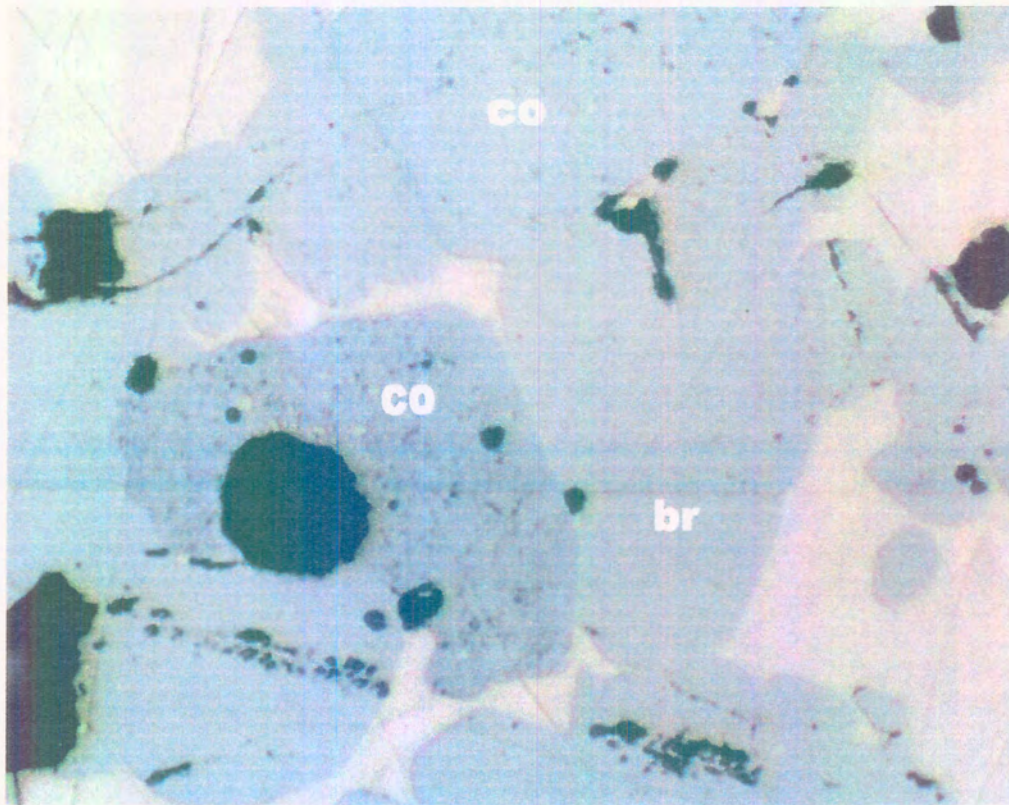
Table 18: Mean (arithmetic) compositions of phases in the system PtS-PdS-NiS at 700°C in weight per cent (wt%) and atomic per cent (at%). Values in parenthesis show the standard deviation at the 1 σ level. N = number of analyses per experiment.

Sample	Phases		Pt	Pd	Ni	S	TOTAL
SV701	"Braggite"	wt%	51.05 (0.70)	24.14 (0.53)	5.88 (0.13)	19.43 (0.12)	100.51
		at%	21.87 (0.36)	18.97 (0.36)	8.45 (0.16)	50.71 (0.18)	(N=19)
	Ni _{1-x} S	wt%	0.11 (0.06)	0.99 (0.14)	62.80 (0.51)	36.52 (0.85)	100.41
		at%	0.03 (0.01)	0.42 (0.06)	48.22 (0.72)	51.33 (0.75)	(N=9)
SV702	"Braggite"	wt%	62.75 (0.73)	14.31 (0.60)	5.85 (0.26)	18.06 (0.18)	100.97
		at%	28.64 (0.53)	12.08 (0.45)	8.65 (0.36)	50.63 (0.23)	(N=21)
	Ni _{1-x} S	wt%	0.17 (0.10)	0.54 (0.10)	63.37 (0.45)	36.23 (0.17)	100.31
		at%	0.04 (0.02)	0.23 (0.04)	48.73 (0.18)	51.00 (0.22)	(N=18)
SV703	"Cooperite"	wt%	78.87 (1.40)	4.90 (0.82)	1.76 (0.19)	15.18 (0.32)	100.70
		at%	42.39 (1.36)	4.83 (0.74)	3.14 (0.29)	49.64 (0.34)	(N=2)
	"Braggite"	wt%	63.78 (0.77)	13.20 (0.64)	5.58 (0.21)	17.89 (0.16)	100.44
		at%	29.61 (0.52)	11.24 (0.47)	8.61 (0.29)	50.54 (0.28)	(N=19)
	Ni _{1-x} S	wt%	0.26 (0.09)	0.43 (0.05)	63.76 (0.23)	36.63 (0.12)	101.09
		at%	0.06 (0.06)	0.18 (0.02)	48.62 (0.13)	51.14 (0.13)	(N=15)
SV704	"Cooperite"	wt%	79.85 (0.43)	4.28 (0.20)	1.70 (0.16)	14.87 (0.16)	100.70
		at%	43.42 (0.44)	4.28 (0.18)	3.07 (0.28)	49.23 (0.23)	(N=15)
	"Braggite"	wt%	64.14 (0.37)	12.42 (0.41)	5.62 (0.14)	17.94 (0.38)	100.12
		at%	29.87 (0.53)	10.60 (0.24)	8.70 (0.17)	50.83 (0.43)	(N=12)
	Ni _{1-x} S	wt%	0.20 (0.10)	0.42 (0.16)	63.79 (0.84)	36.68 (0.57)	101.09
		at%	0.05 (0.03)	0.18 (0.07)	48.60 (0.74)	51.17 (0.74)	(N=9)
SV705	"Cooperite"	wt%	85.03 (0.26)	0	1.97 (0.13)	14.29 (0.12)	101.31
		at%	47.63 (0.28)	0	3.67 (0.24)	48.70 (0.28)	(N=16)
	Ni _{1-x} S	wt%	0.30 (0.10)	0	63.15 (0.50)	36.01 (0.80)	99.51
		at%	0.07 (0.04)	0	48.89 (0.60)	51.04 (0.61)	(N=19)
SV707	"Cooperite"	wt%	70.77 (0.59)	13.85 (0.44)	0	15.99 (0.36)	100.61
		at%	36.58 (0.57)	13.13 (0.39)	0	50.29 (0.63)	(N=34)
	"Braggite"	wt%	57.85 (0.76)	26.46 (0.64)	0	17.03 (0.18)	100.73
		at%	27.55 (0.54)	23.10 (0.250)	0	49.35 (0.44)	(N=10)
SV708	"Cooperite"	wt%	71.35 (0.64)	11.64 (0.43)	1.62 (0.08)	16.36 (0.23)	100.96
		at%	36.10 (0.56)	10.80 (0.34)	2.72 (0.14)	50.38 (0.35)	(N=20)
	"Braggite"	wt%	62.89 (0.19)	16.67 (0.32)	3.38 (0.16)	17.86 (0.10)	100.86
		at%	29.47 (0.10)	14.33 (0.29)	5.26 (0.24)	50.94 (0.22)	(N=12)
SV710	"Cooperite"	wt%	81.56 (0.55)	2.41 (0.43)	1.90 (0.16)	14.83 (0.36)	100.69
		at%	44.68 (0.62)	2.42 (0.43)	3.46 (0.33)	49.44 (0.83)	(N=40)
	Ni _{1-x} S	wt%	0.31 (0.09)	0.56 (0.13)	63.35 (0.44)	36.25 (0.62)	100.48
		at%	0.07 (0.02)	0.24 (0.06)	48.68 (0.47)	51.01 (0.50)	(N=23)



Table 18 (continued):

Sample	Phases		Pt	Pd	Ni	S	TOTAL
SV711	"Cooperite"	wt%	82.20 (0.81)	1.73 (0.46)	1.80 (0.16)	14.49 (0.43)	100.21
		at%	45.79 (0.87)	1.77 (0.48)	3.33 (0.27)	49.11 (0.91)	(N=29)
	Ni _{1-x} S	wt%	0.42 (0.10)	0.50 (0.11)	63.35 (0.87)	35.95 (0.65)	100.21
		at%	0.10 (0.03)	0.21 (0.05)	48.89 (0.69)	50.80 (0.70)	(N=21)
SV712	"Cooperite"	wt%	82.95 (0.85)	1.04 (0.39)	1.86 (0.16)	14.41 (0.50)	100.26
		at%	46.41 (1.06)	1.07 (0.40)	3.46 (0.43)	49.06 (1.02)	(N=37)
	Ni _{1-x} S	wt%	0.43 (0.10)	0.29 (0.14)	64.55 (0.75)	36.02 (0.57)	101.26
		at%	0.10 (0.04)	0.12 (0.06)	49.35 (0.67)	50.43 (0.64)	(N=9)
SV713	"Braggite"	wt%	30.36 (0.75)	41.56 (0.55)	6.19 (0.12)	21.80 (0.38)	99.92
		at%	11.99 (0.34)	29.68 (0.34)	7.27 (0.17)	51.06 (0.43)	(N=13)
	Ni _{1-x} S	wt%	0.06 (0.03)	1.44 (0.10)	62.63 (0.33)	36.73 (0.33)	100.86
		at%	0.01 (0.01)	0.61 (0.04)	47.92 (0.25)	51.46 (0.22)	(N=23)
SV716	"Vysotskite"	wt%	0	68.48 (0.36)	7.35 (0.24)	24.66 (0.12)	100.49
		at%	0	41.85 (0.18)	8.14 (0.25)	50.01 (0.16)	(N=25)
	Ni _{1-x} S	wt%	0	2.33 (0.17)	61.32 (0.71)	36.54 (0.16)	100.19
		at%	0	0.99 (0.08)	47.35 (0.21)	51.66 (0.17)	(N=4)



Photomicrograph 12 Coexisting “cooperite” (co), “braggite” (br) and Ni_{1-x}S at 700°C of experiment SV703 (digitally enhanced, long side of the photomicrograph is 0.185 mm).

6.7.1 “Cooperite” at 700°C

The Ni-content in “cooperite” in a Ni-saturated environment decreases slightly with increasing Pd-content, but is lower than that at 800°C. Least square fitting of the data for “cooperite”, formed in a Ni-saturated environment (in cation per cent), lead to the following linear relationships at the 95% confidence level (Table: 19):

Table 19: Type of best fit, equation for best fit at the 95% confidence level, equation number (No), and R²-values of best fits of elements analysed in “cooperite” formed at 700°C.

Variables	Fit	Equation	No	R ²
Ni, Pt	Linear	$Ni = 2.440 (\pm 0.239) + 0.101 (\pm 0.026) \times Pt$	34	0.7919
Ni, Pd	Linear	$Ni = 3.620 (\pm 0.064) - 0.110 (\pm 0.022) \times Pd$	35	0.8647
Pt, Pd	Linear	$Pt = 47.534 (\pm 0.186) - 1.036 (\pm 0.061) \times Pd$	36	0.9862

No significant relationship between the Ni-content and the Pt/Pd ratio in “cooperite” could be established at this temperature.

Equations 34 to 36 are presented graphically in Figures 65 to 67.

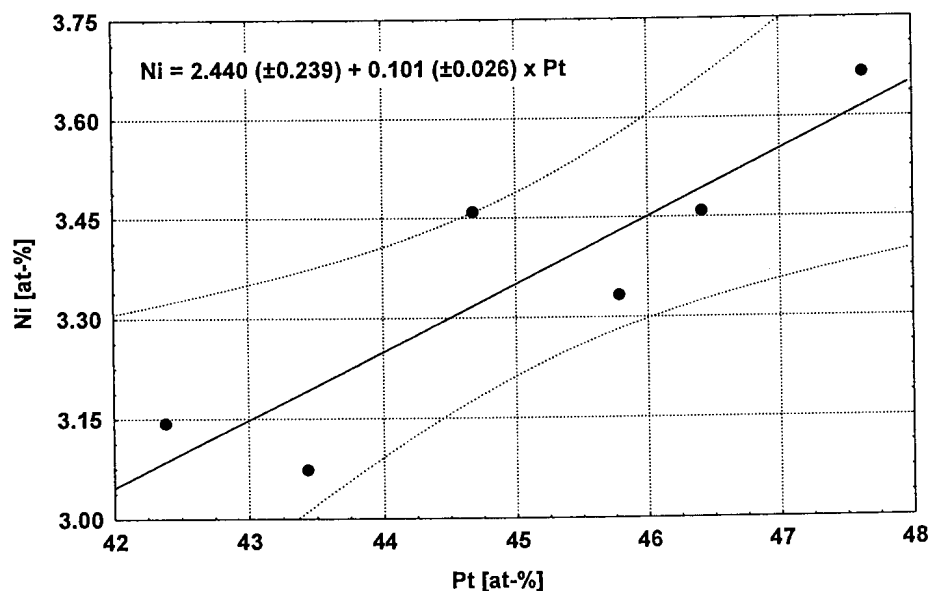


Figure 65 Ni-content versus Pt-content (in at-%) in “cooperite” formed in a Ni-saturated environment at 700°C. The solid line indicates the best linear fit and the stippled lines the 95% confidence interval according to the equation shown (N=6).

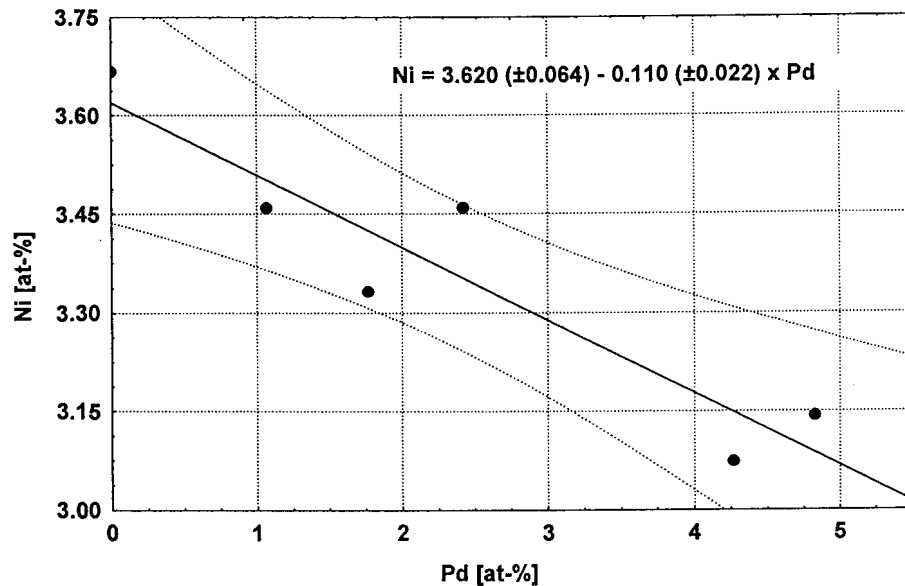


Figure 66 Ni-content versus Pd-content (in at-%) in “cooperite” formed in a Ni-saturated environment at 700°C. The solid line indicates the best linear fit and the stippled lines the 95% confidence interval according to the equation shown (N=6).

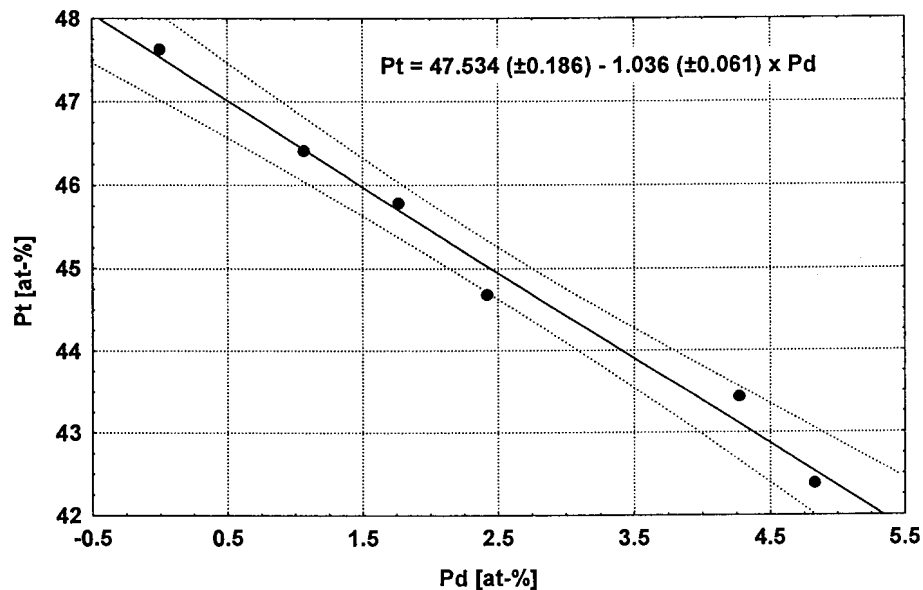


Figure 67 Pd-content versus Pt-content (in at-%) in “cooperite” formed in a Ni-saturated environment at 700°C. The solid line indicates the best linear fit and the stippled lines the 95% confidence interval according to the equation shown (N=6).

6.7.2 “Braggite” and “vysotskite” at 700°C

The Ni-content in “braggite-vysotskite” formed in a Ni-saturated environment decreases slightly with increasing Pd content, but is higher than at 800°C. Least square fitting of the data for “braggite-vysotskite” formed in a Ni-saturated environment at 700°C (in cation per cent) lead to the following equations at the 95% confidence level (Table 20):

Table 20: Type of best fit, equation for best fit at the 95% confidence level, equation number (No), and R²-values of best fits of elements analysed in “braggite-vysotskite” formed at 700°C.

Variables	Fit	Equation	No	R ²
Ni, Pt	Linear	$Ni = 7.936 (\pm 0.197) + 0.025 (\pm 0.009) \times Pt$	37	0.6815
Ni, Pd	Linear	$Ni = 8.938 (\pm 0.198) - 0.024 (\pm 0.008) \times Pd$	38	0.6727
Pt, Pd	Linear	$Pt = 40.263 (\pm 0.166) - 0.966 (\pm 0.007) \times Pd$	39	0.9998
Ni, Pt/Pd	Logarithmic	$Ni = 8.324 (\pm 0.076) + 0.982 (\pm 0.204) \log_{10} Pt/Pd$	40	0.8855
	Inverse			0.8686
	Square root			0.8549

Equations 37 to 40 are presented graphically in Figures 68 to 71 below.

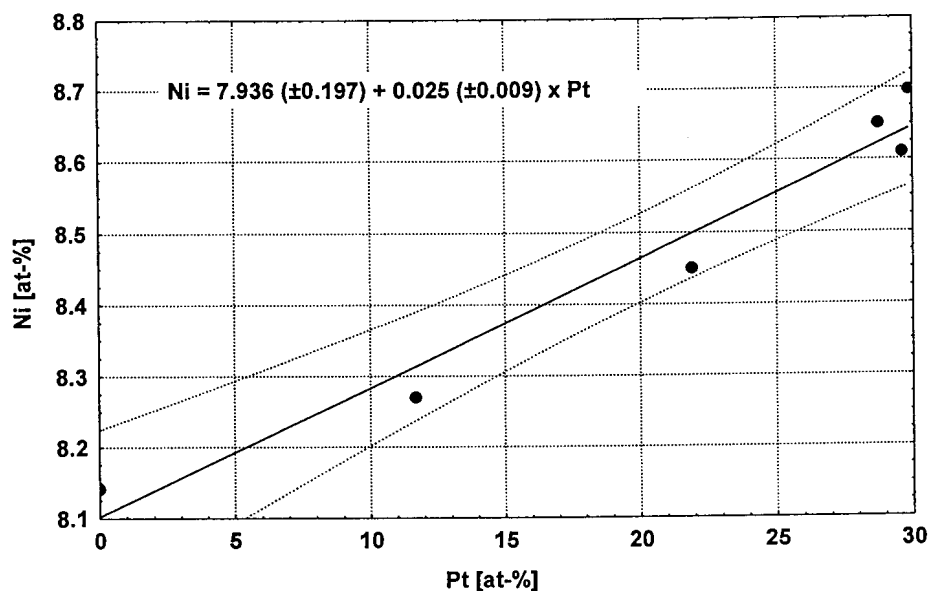


Figure 68 Pt-content versus Ni-content (in at-%) in “braggite-vysotskite” formed in a Ni-saturated environment at 700°C. The solid line indicates the best linear fit and the stippled lines the 95% confidence interval according to the equation shown (N=6).

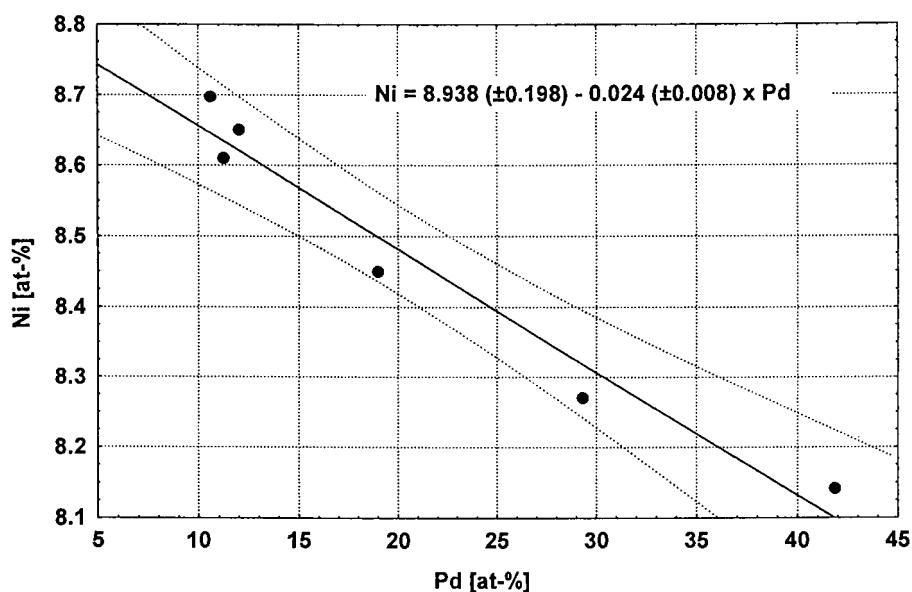


Figure 69 Pd-content versus Ni-content (in at-%) in “braggite-vysotskite” formed in a Ni-saturated environment at 700°C. The solid line indicates the best linear fit and the stippled lines the 95% confidence interval according to the equation shown (N=6).

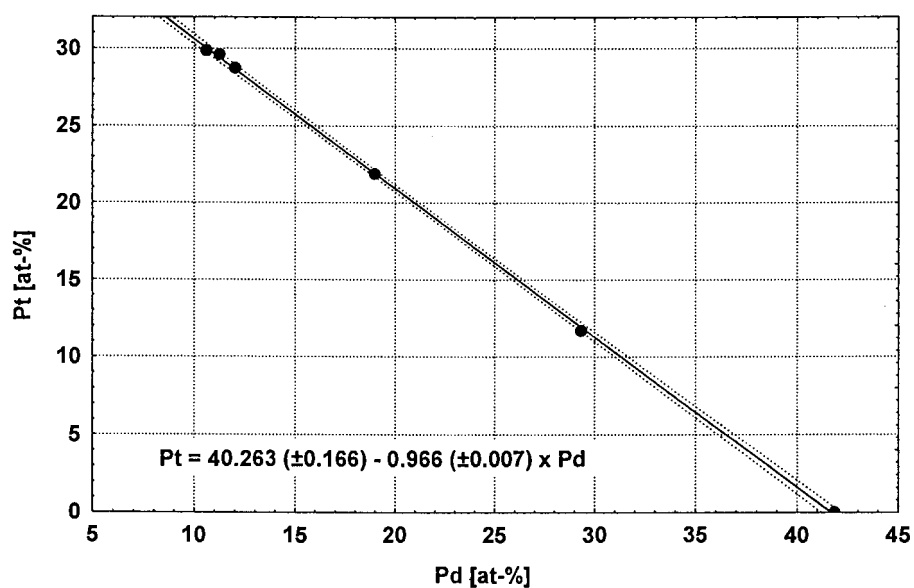


Figure 70 Pt-content versus Pd-content (in at-%) in “braggite-vysotskite” formed in a Ni-saturated environment at 700°C. The solid line indicates the best linear fit and the stippled lines the 95% confidence interval according to the equation shown (N=6).

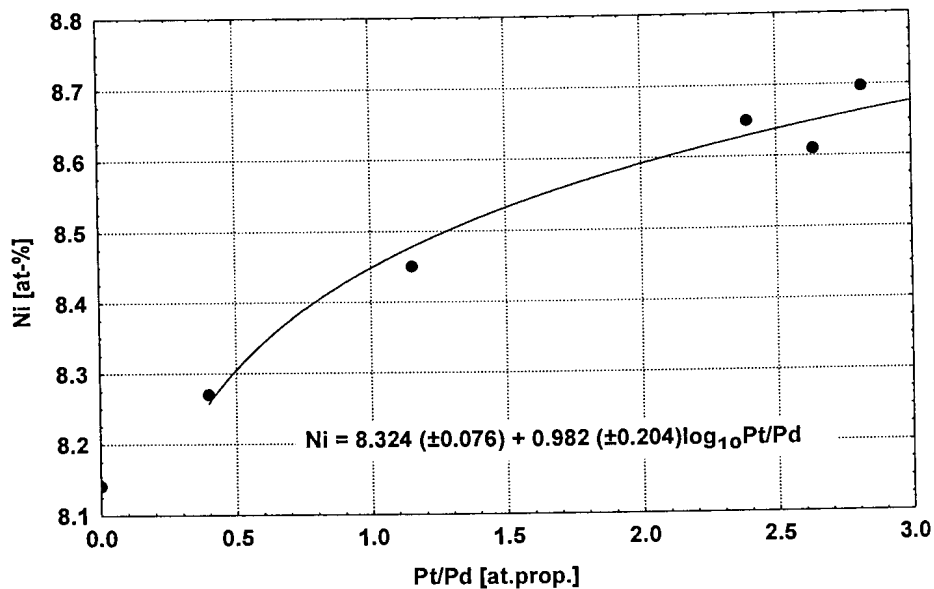


Figure 71 Ni-content (at-%) versus Pt/Pd ratio (in atomic proportions) in “braggite-vysotskite” formed in a Ni-saturated environment at 700°C. The solid line indicates the best fit according to the equation shown.

6.7.3 Ni_{1-x}S at 700°C

At 700°C, the compositional field of Ni_{1-x}S is even more restricted than that at 800°C. The Pt-content varies between 0 and 0.10 at-% and the Pd-content between 0 and 0.99 at-%. The compositional variation of Ni_{1-x}S at 700°C is graphically presented in Figure 72.

The variation in Pt-content in Ni_{1-x}S, coexisting with “cooperite” or with “braggite-vysotskite”, lies within the analytical uncertainty (3σ) of 0.10 wt-% (~0.03 at-%) Pt. Similarly, the variations in the Ni- and Pd-content in Ni_{1-x}S, coexisting with “cooperite”, lie within the analytical uncertainty (3σ) of 0.84 wt-% (~0.7 at-%) Ni and 0.25 wt-% (~0.23 at-%) Pd. In the case of Ni_{1-x}S coexisting with “cooperite”, the variation in Pd-content lies within the analytical uncertainty of 0.25 wt-% (~0.12 at-%) Pd. Therefore, only the relationship between the Pd- and Ni-content in Ni_{1-x}S, coexisting with “braggite-vysotskite” (the Pd-content decreases with increasing Ni-content), is presented graphically in Figure 73.

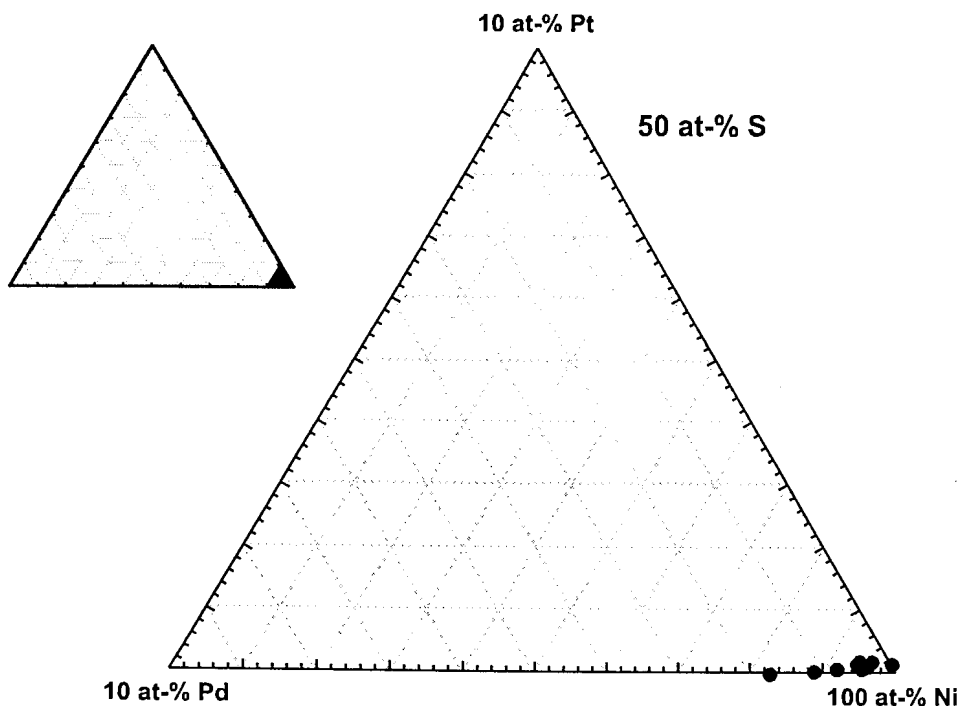


Figure 72 Compositional variation of Ni_{1-x}S (in cation proportions) coexisting with “cooperite”, “braggite”, or “vysotskite” at 700°C.

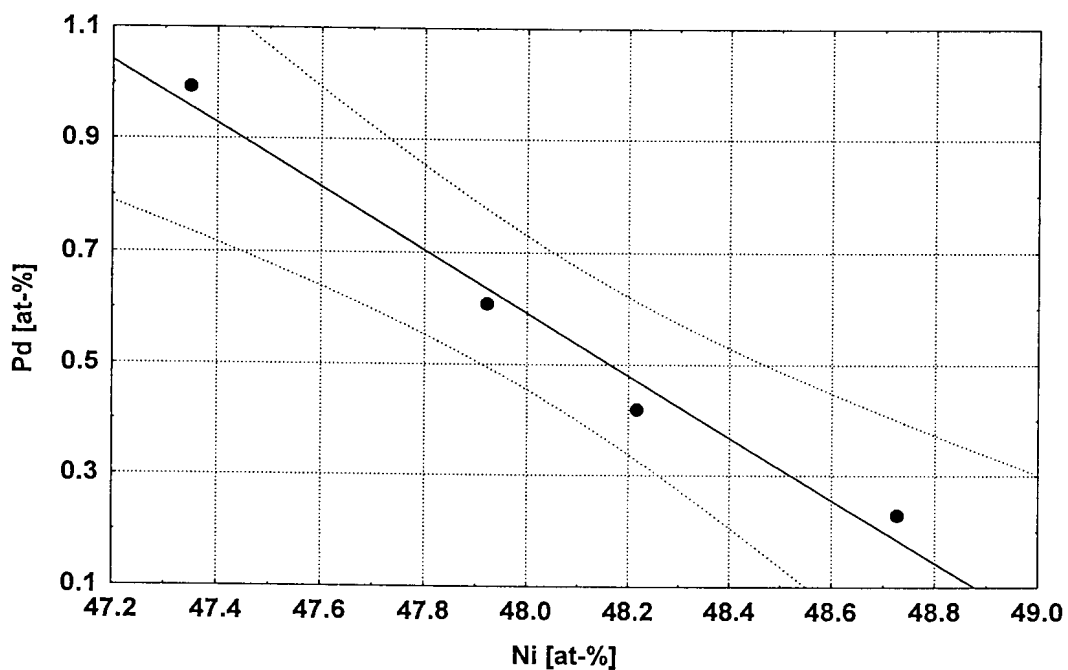


Figure 73 Pd-content versus Ni-content (in at-%) in Ni_{1-x}S coexisting with “braggite-vysotskite” at 700°C. The solid line indicates the best linear fit and the stippled lines the 95% confidence interval of that fit.

6.7.4 Relationships at 700°C

The Pd-content in $Ni_{1-x}S$ increases with increasing Pd-content of the “cooperite”, “braggite”, and “vysotskite” it is in equilibrium with (Fig. 74). This effect is more pronounced for $Ni_{1-x}S$ coexisting with “braggite-vysotskite” than that for $Ni_{1-x}S$ coexisting with “cooperite”. This is most likely due to the more restricted compositional variation of Pd (lying within the analytical uncertainty) in $Ni_{1-x}S$ coexisting with “cooperite”.

The relationship between the Pt-content of the two mineral groups ($Ni_{1-x}S$ and “cooperite”- “braggite”- “vysotskite”) cannot be resolved due to the analytical uncertainties as discussed in Chapter 5.8.3.

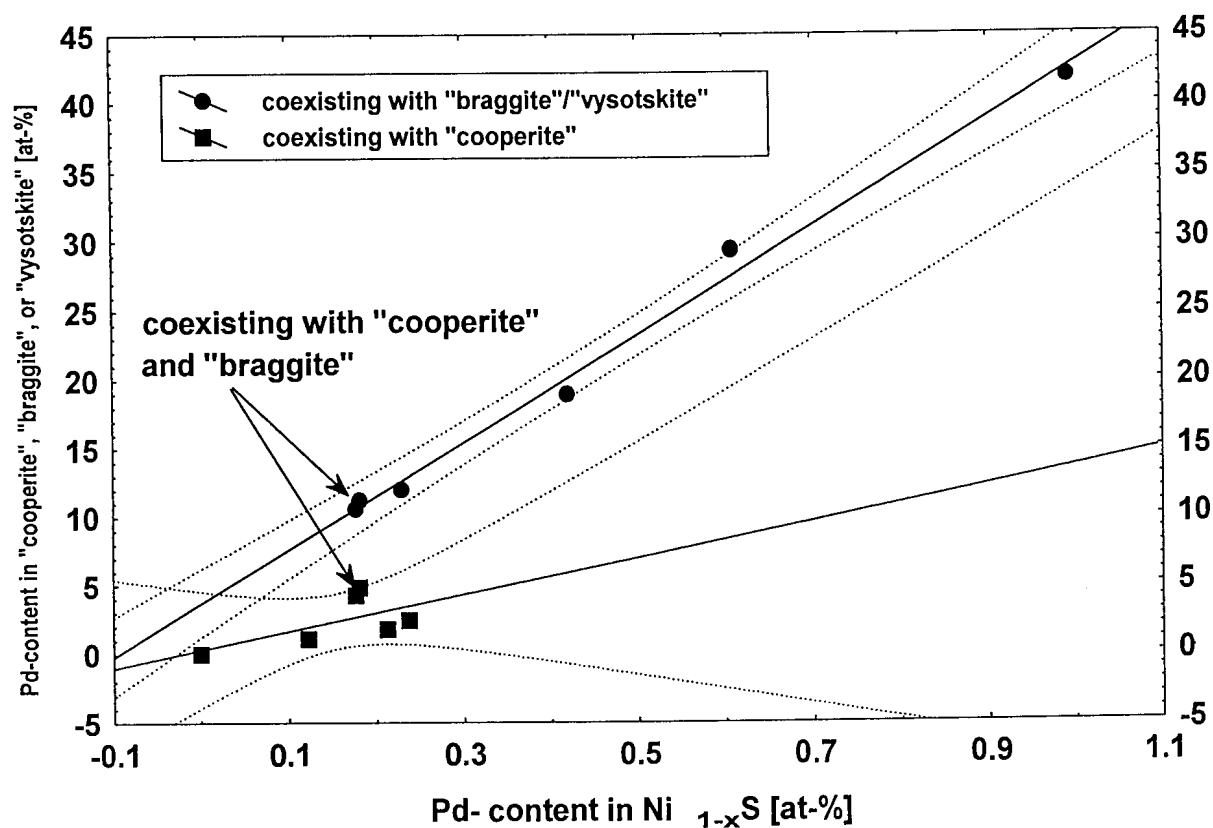


Figure 74 Pd-content in “cooperite”, “braggite”, or “vysotskite” versus Pd-content in $Ni_{1-x}S$ in at-% at 700°. The solid lines indicate the best linear fits and the stippled lines the 95% confidence intervals for the 2 populations individually.



CHAPTER 7

VARIABLE INITIAL SULPHUR CONTENT AT 1000 °C

7 VARIABLE INITIAL SULPHUR CONTENT AT 1000°C

Taylor (1985) showed that an increase in S-content within melts in the Pd-S system causes an increase in sulphur fugacity. In order to obtain an indication which effect the sulphur fugacity has on the system PtS-PdS-NiS, 2 to 3 charges containing between 47 and 52 at-% sulphur at constant Pt/Pd and Ni atomic ratios were prepared for experiments at 1000°C.

The phases observed in the experimental charges are “cooperite”, “braggite”, and a melt.

It was found that dividing the experiments into two groups, one where the initial S-content in the charge was above 50 at-% (Group **A** = above) and one where the S-content was below 50 at-% (Group **B** = below), aided in the illustration of the phase relationships. Figure 75 shows all experimental results in one diagram, the different initial sulphur contents of the charges shown in different colours. Figures 76 and 77 show the two groups individually.

The melt formed in the charges of group B shows a lower Pd/Ni ratio (in atomic proportions) than melt formed in Group A, when coexisting with braggite and/or cooperite of similar composition (see Figure 75). This is not a graphical or analytical artefact, as fixed Pd/Ni ratios (in wt-%) and varying S-content result in the same Pd/Ni ratios when converted into atomic proportions. The melts of the low sulphur charges also contain systematically slightly more Pt than the melt formed in the charges with high sulphur contents.

Comparable to the observations and discussions at 1200°C (Chapter 6.2), after quenching, a thin layer of sulphur was visible on the capsule walls. As at 1200°C, the amount of visible sulphur on the capsule walls increases with increasing Pd-content at constant overall S-content in the charge. In addition the amount of visible sulphur increases with increasing initial S-content of the charge.

The compositions of “cooperite”, “braggite”, and melt of these experiments are summarized in Table 21. Coexisting “cooperite”, “braggite” and melt are shown in Photomicrograph 13.

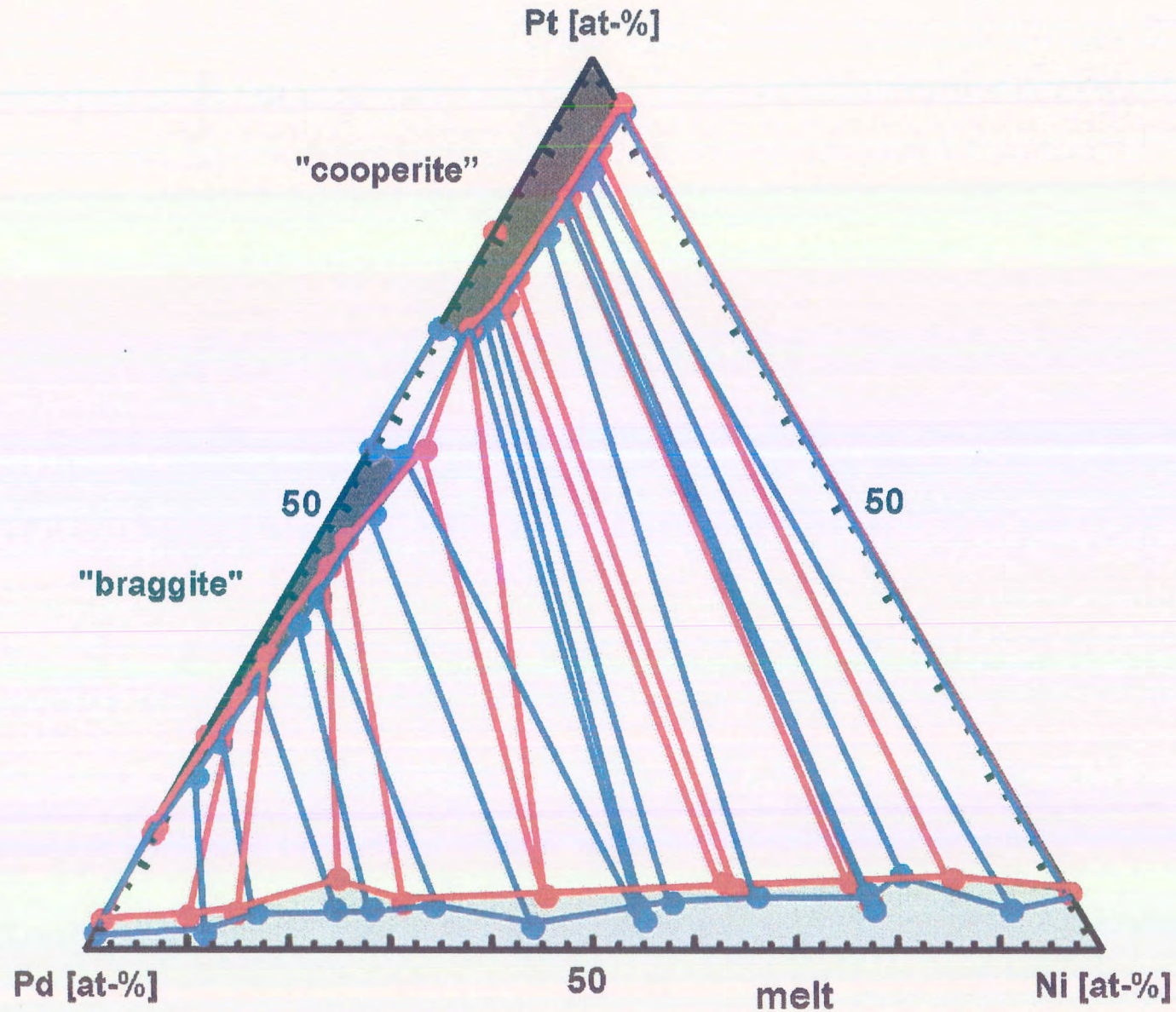


Figure 75 Phase relations in the system PtS-PdS-NiS in cation proportions at 1000°C. The red tie-lines and sample points represent experiments where the initial S-content in the charge was below 50 at-% and the blue tie-lines and sample points where the initial S-content in the charge was above 50 atomic percent.

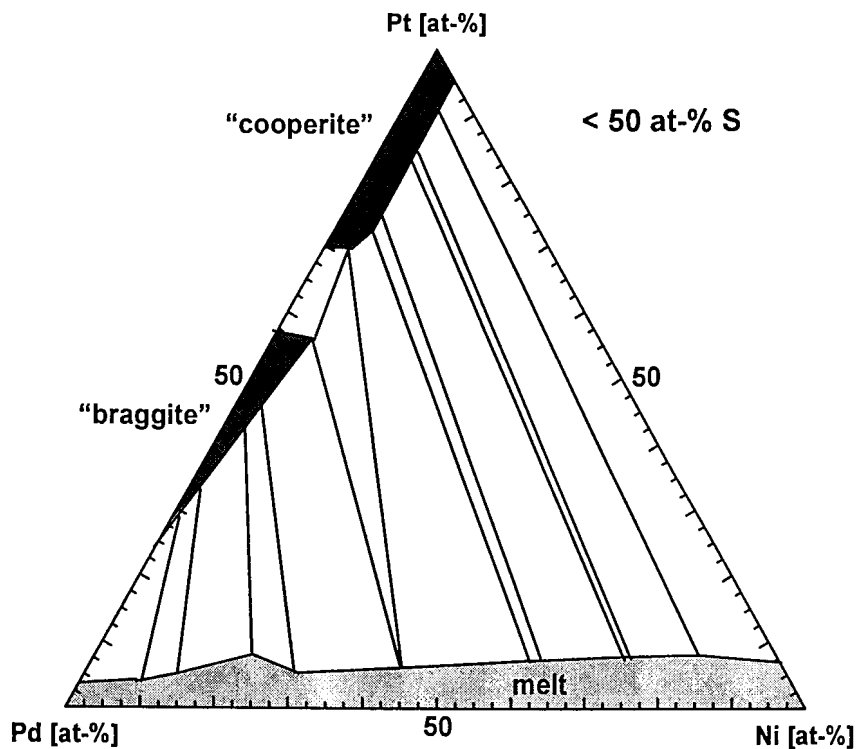


Figure 76 Phase relations in the system PtS-PdS-NiS in cation proportions at 1000°C of experiments where the initial S-content in the charge was below 50 at-%.

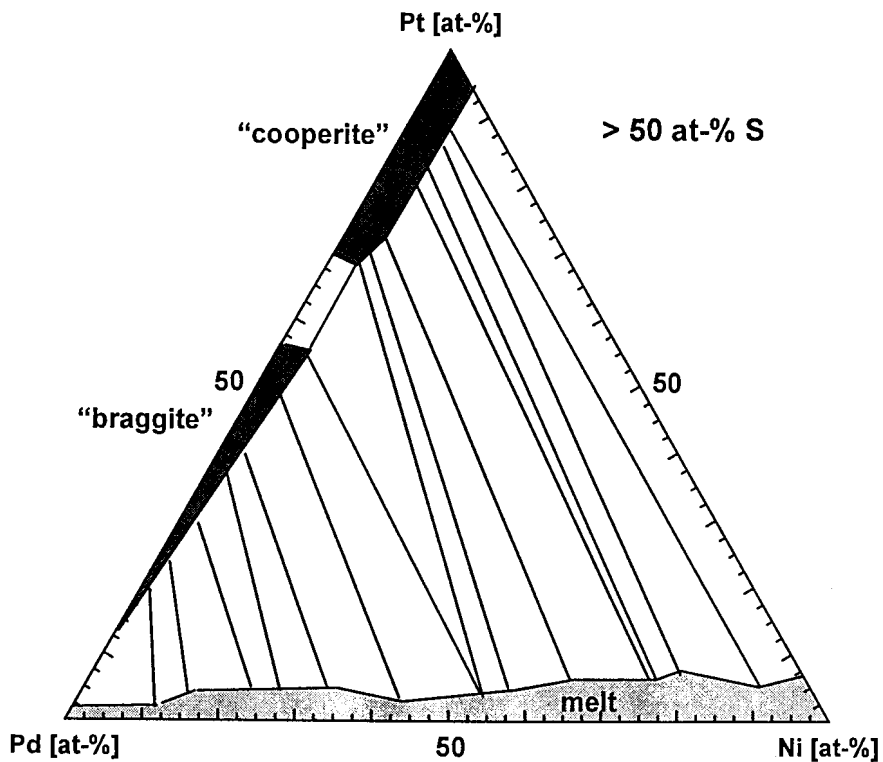


Figure 77 Phase relations in the system PtS-PdS-NiS in cation proportions at 1000°C of experiments where the initial S-content in the charge was above 50 at-%.

Table 21: Mean (arithmetic) compositions of phases in the system PtS-PdS-NiS at 1000°C with variable initial S-content in weight per cent (wt%) and atomic per cent (at%). Values in parenthesis show the standard deviation at the 1 σ level. N = number of analyses per experiment.

Sample	Phases		Pt	Pd	Ni	S	TOTAL
SV201	"Cooperite"	wt%	70.15 (0.34)	12.07 (0.23)	1.47 (0.03)	15.81 (0.35)	99.52
		at%	36.28 (0.18)	11.44 (0.20)	2.53 (0.05)	49.75 (0.69)	(N=55)
	Melt	wt%	10.11 (0.73)	28.40 (0.65)	31.91 (0.83)	28.90 (0.17)	99.32
		at%	2.94 (0.49)	15.13 (0.59)	30.82 (0.79)	51.11(0.24)	(N=19)
SV202	"Cooperite"	wt%	76.87 (0.85)	5.82 (0.44)	1.60 (0.14)	14.77 (0.19)	99.06
		at%	42.07 (0.51)	5.84 (0.41)	2.91 (0.18)	49.18 (0.37)	(N=62)
	Melt	wt%	9.69 (0.68)	19.58 (0.36)	39.94 (0.50)	28.89 (0.15)	98.10
		at%	2.74 (0.25)	10.14 (0.18)	37.48 (0.49)	49.64 (0.31)	(N=20)
SV205	"Cooperite"	wt%	72.01 (0.24)	10.24 (0.19)	1.42 (0.04)	15.24 (0.16)	98.89
		at%	38.25 (0.11)	9.97 (0.19)	2.51 (0.07)	49.26 (0.49)	(N=34)
	Melt	wt%	11.83 (0.92)	30.90 (0.86)	31.83 (0.65)	26.52 (0.23)	101.07
		at%	3.52 (0.31)	16.88 (0.42)	31.52 (0.65)	48.08 (0.44)	(N=34)
SV206	"Cooperite"	wt%	78.23 (0.69)	5.17 (0.31)	1.51 (0.16)	15.06 (0.20)	99.98
		at%	42.43 (0.65)	5.14 (0.30)	2.72 (0.30)	49.71(0.54)	(N=55)
	Melt	wt%	13.92 (2.09)	20.77 (0.87)	39.02 (1.43)	27.21 (0.37)	100.91
		at%	4.01 (0.84)	10.97 (0.44)	37.34 (1.39)	47.68 (0.50)	(N=26)
SV207	"Cooperite"	wt%	81.60 (0.85)	2.09 (0.32)	1.57 (0.15)	14.51 (0.17)	99.76
		at%	45.60 (0.49)	2.14 (0.33)	2.92 (0.31)	49.34 (0.52)	(N=51)
	Melt	wt%	14.59 (0.83)	10.92 (0.72)	45.83 (0.54)	28.74 (0.20)	100.08
		at%	4.03 (0.22)	5.53 (0.36)	42.10 (0.52)	48.34 (0.09)	(N=20)
SV209	"Cooperite"	wt%	70.51 (0.37)	11.61 (0.27)	1.44 (0.03)	15.51 (0.17)	99.08
		at%	36.92 (0.18)	11.15 (0.27)	2.51 (0.05)	49.42 (0.59)	(N=67)
	Melt	wt%	12.71 (1.07)	30.43 (0.72)	29.50 (1.34)	28.10 (0.44)	100.74
		at%	3.77 (0.38)	16.53 (0.33)	29.05 (1.33)	50.66 (0.21)	(N=23)
SV210	"Cooperite"	wt%	79.92 (0.85)	3.90 (0.44)	1.68 (0.15)	14.61 (0.37)	100.10
		at%	44.02 (0.44)	3.94 (0.43)	3.08 (0.31)	48.97 (0.99)	(N=129)
	Melt	wt%	14.13 (0.95)	14.40 (1.14)	39.03 (0.69)	30.27 (0.26)	97.85
		at%	4.81 (0.32)	8.99 (0.98)	44.18 (0.72)	42.01(0.32)	(N=21)
SV211	"Cooperite"	wt%	77.42 (0.85)	5.83 (0.44)	1.45 (0.30)	15.03 (0.37)	99.72
		at%	41.99 (0.49)	5.80 (0.44)	2.61 (0.58)	49.60 (0.99)	(N=135)
	Melt	wt%	8.22 (1.09)	19.62 (1.09)	40.59 (1.05)	30.43 (0.34)	98.86
		at%	2.26 (0.26)	9.88 (0.55)	37.03 (1.01)	50.83 (0.52)	(N=25)
SV212	"Cooperite"	wt%	75.12 (0.59)	17.26 (0.22)	1.63 (0.05)	15.38 (0.14)	99.40
		at%	40.08 (0.36)	7.10 (0.09)	2.89 (0.08)	49.93 (0.42)	(N=25)
	Melt	wt%	11.26 (1.37)	18.97 (0.95)	38.93 (1.19)	29.64 (0.16)	97.80
		at%	3.16 (0.48)	9.78 (0.46)	36.37 (1.13)	50.69 (0.29)	(N=16)



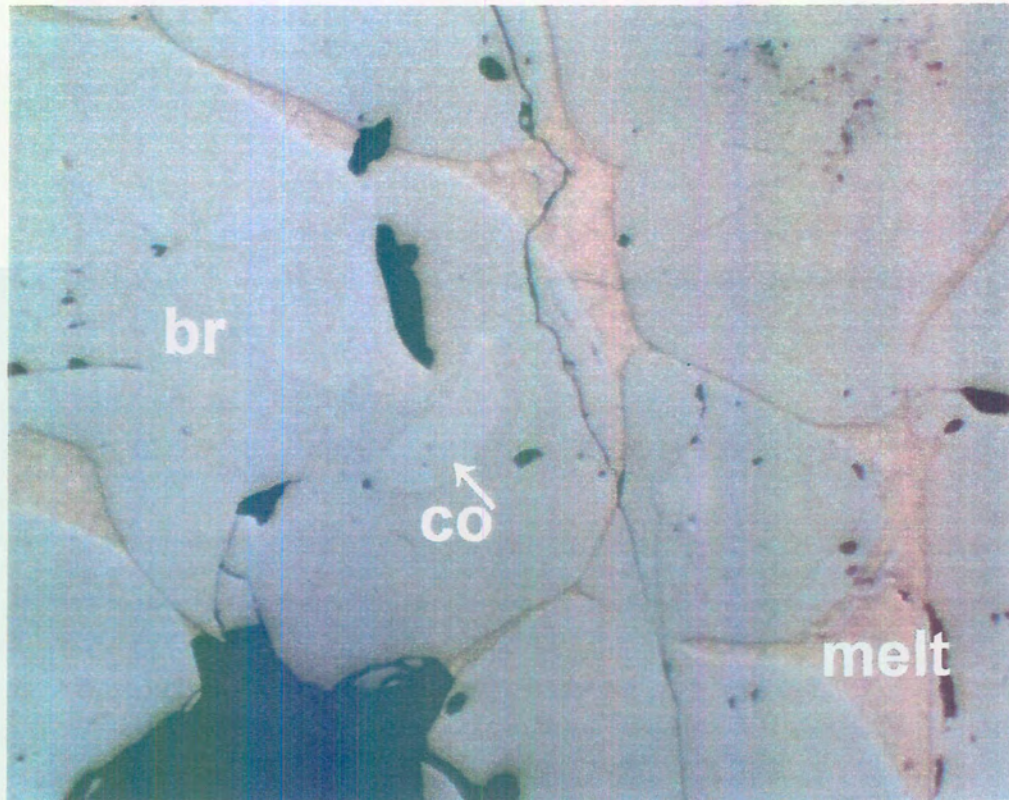
Table 21 (continued):

Sample	Phases		Pt	Pd	Ni	S	TOTAL
SV277	"Braggite"	wt%	57.62 (0.18)	24.46 (0.27)	0	16.68 (0.32)	98.76
		at%	28.25 (0.09)	21.99 (0.24)	0	49.76 (0.65)	(N=5)
	"Cooperite"	wt%	66.66 (0.58)	15.76 (0.59)	0	15.59 (0.21)	99.04
		at%	35.01 (0.29)	15.17 (0.58)	0	49.82 (0.45)	(N=29)
SV278	"Cooperite"	wt%	74.69 (0.85)	9.81 (0.44)	0	15.48 (0.46)	99.98
		at%	39.97 (0.48)	9.63 (0.43)	0	50.41 (0.96)	(N=144)
	Melt	wt%	16.27 (2.05)	59.74 (2.38)	0	11.70 (0.38)	87.72
		at%	8.26 (1.03)	55.60 (2.21)	0	36.14 (0.99)	(N=225)
SV279	"Cooperite"	wt%	84.81 (0.74)	0	1.62 (0.16)	14.19 (0.35)	100.62
		at%	48.04 (0.36)	0	3.05 (0.35)	48.91 (0.75)	(N=164)
	Melt	wt%	12.94 (9.47)	0	55.15 (6.49)	33.60 (2.42)	101.74
		at%	3.23 (3.12)	0	45.74 (5.21)	51.03 (3.87)	(N=172)
SV280	"Cooperite"	wt%	84.01 (0.57)	0	1.39 (0.15)	14.30 (0.24)	99.70
		at%	47.83 (0.39)	0	2.63 (0.30)	49.54 (0.65)	(N=181)
	Melt	wt%	13.42 (22.68)	0	56.97 (17.02)	29.25 (4.95)	100.03
		at%	3.52 (7.83)	0	49.73 (14.99)	46.75 (7.12)	(N=158)
SV284	"Braggite"	wt%	50.42 (0.77)	30.71 (0.71)	0.92 (0.04)	18.47 (0.23)	100.51
		at%	22.69 (0.32)	25.34 (0.68)	1.38 (0.07)	50.59 (0.62)	(N=206)
	Melt	wt%	8.30 (4.29)	56.79 (2.95)	13.57 (2.13)	23.47 (0.77)	102.13
		at%	2.76 (2.16)	34.67 (1.69)	15.02 (2.01)	47.55 (1.06)	(N=15)
SV285	"Cooperite"	wt%	67.92 (0.64)	14.46 (0.46)	1.07 (0.07)	15.90 (0.48)	99.36
		at%	34.88 (0.39)	13.61 (0.45)	1.83 (0.11)	49.68 (0.96)	(N=46)
	Melt	wt%	7.16 (1.40)	35.57 (2.21)	23.50 (1.47)	24.37 (1.12)	90.60
		at%	2.40 (0.66)	21.83 (1.64)	26.14 (1.51)	49.63 (1.55)	(N=18)
SV289	"Cooperite"	wt%	67.98 (0.39)	15.09 (0.19)	0.96 (0.13)	16.21 (0.16)	100.24
		at%	34.42 (0.20)	14.01 (0.18)	1.62 (0.23)	49.95 (0.39)	(N=52)
	"Braggite"	wt%	57.50 (0.77)	23.17 (0.47)	1.21 (0.13)	17.72 (0.16)	99.60
		at%	27.14 (0.38)	20.06 (0.45)	1.90 (0.23)	50.90 (0.41)	(N=141)
	Melt	wt%	5.96 (12.37)	42.46 (21.45)	28.69 (19.75)	22.76 (4.89)	100.00
		at%	1.88 (3.89)	24.51 (12.23)	30.02 (20.11)	43.60 (6.22)	(N=225)
SV290	"Cooperite"	wt%	68.08 (0.59)	14.48 (0.46)	0.94 (0.03)	16.42 (0.56)	99.92
		at%	34.44 (0.31)	13.43 (0.45)	1.58 (0.05)	50.55 (0.92)	(N=252)
	"Braggite"	wt%	59.11 (0.70)	22.20 (0.55)	1.74 (0.10)	17.21 (0.57)	100.27
		at%	45.39 (0.63)	4.44 (0.26)	0.56 (0.06)	49.61 (0.88)	(N=110)
	Melt	wt%	10.33 (2.25)	47.25 (1.05)	21.23 (1.71)	22.69 (0.27)	101.50
		at%	3.38 (0.99)	28.35 (0.59)	23.09 (1.73)	45.18 (0.52)	(N=18)
SV291	"Braggite"	wt%	52.01 (0.77)	27.59 (0.71)	1.33 (0.06)	18.32 (0.33)	99.26
		at%	23.80 (0.39)	23.15 (0.67)	2.02 (0.11)	51.02 (0.70)	(N=53)
	Melt	wt%	4.05 (10.27)	45.76 (16.66)	19.74 (18.96)	22.67 (3.80)	92.43
		at%	1.39 (3.15)	28.78 (8.68)	22.51 (16.23)	47.32 (5.56)	(N=46)



Table 21 (continued):

Sample	Phases		Pt	Pd	Ni	S	TOTAL
SV293	"Braggite"	wt%	45.18 (0.77)	35.59 (0.72)	1.15 (0.10)	18.62 (0.32)	100.54
		at%	19.85 (0.29)	28.68 (0.63)	1.68 (0.15)	49.79 (0.64)	(N=10)
	Melt	wt%	8.15 (11.41)	55.40 (17.54)	15.40 (17.26)	22.39 (3.37)	101.42
		at%	2.74 (4.01)	34.18 (9.66)	17.22 (18.22)	45.85 (5.66)	(N=207)
SV294	"Braggite"	wt%	17.97 (0.77)	60.53 (0.75)	0	21.13 (0.44)	99.68
		at%	6.98 (0.33)	43.10 (0.52)	0	49.93 (0.78)	(N=94)
	Melt	wt%	2.53 (0.56)	72.33 (2.71)	0	19.66 (0.78)	94.52
		at%	0.99 (0.31)	52.05 (1.97)	0	46.95 (1.28)	(N=16)
SV295	"Braggite"	wt%	41.49 (0.70)	38.10 (0.76)	0.97 (0.03)	19.26 (0.72)	99.83
		at%	17.90 (0.36)	30.14 (0.62)	1.39 (0.05)	50.57(1.23)	(N=202)
	Melt	wt%	6.94 (8.79)	57.91 (14.21)	11.78 (15.02)	23.53 (2.64)	100.15
		at%	2.35 (3.23)	35.94 (9.63)	13.25 (17.56)	48.46 (3.97)	(N=125)
SV296	"Braggite"	wt%	47.27 (0.77)	32.89 (0.74)	0.85 (0.05)	18.51 (0.40)	99.52
		at%	21.19 (0.32)	27.04 (0.69)	1.27 (0.07)	50.50 (0.81)	(N=161)
	Melt	wt%	12.11 (2.53)	59.20 (2.71)	9.58 (0.61)	20.67 (0.87)	101.56
		at%	4.35 (0.98)	39.01(1.56)	11.44 (0.75)	45.20 (1.55)	(N=15)
SV297	"Braggite"	wt%	35.05 (0.77)	44.01 (0.72)	0.85 (0.05)	19.97 (0.19)	99.88
		at%	14.60 (0.33)	33.61 (0.56)	1.18 (0.08)	50.61 (0.45)	(N=158)
	Melt	wt%	6.93 (7.81)	61.12 (12.74)	10.29 (13.84)	21.94 (2.86)	100.26
		at%	2.42 (3.02)	39.09 (7.91)	11.93 (14.22)	46.57 (4.52)	(N=36)
SV299	"Braggite"	wt%	28.13 (0.25)	49.49 (0.31)	0.68 (0.02)	20.52 (0.24)	98.83
		at%	11.43 (0.11)	36.89 (0.21)	0.92 (0.03)	50.76 (0.48)	(N=50)
	Melt	wt%	5.54 (1.44)	61.25 (0.96)	6.05 (1.41)	20.50 (0.37)	93.34
		at%	2.11 (0.71)	42.75 (0.77)	7.65 (1.69)	47.49 (0.78)	(N=20)
SV300	"Braggite"	wt%	38.41 (0.75)	41.60 (0.76)	0.51 (0.04)	19.68 (0.62)	100.19
		at%	16.27 (0.32)	32.30 (0.59)	0.72 (0.07)	50.71 (0.96)	(N=58)
	Melt	wt%	6.21 (2.10)	68.99 (1.09)	5.85 (0.70)	17.51 (0.64)	98.56
		at%	2.40 (0.96)	48.90 (0.95)	7.52 (0.81)	41.19 (0.98)	(N=15)
SV301	"Braggite"	wt%	24.24 (0.77)	54.24 (0.71)	0.49 (0.13)	21.32 (0.38)	100.29
		at%	9.50 (0.33)	38.99 (0.56)	0.64 (0.22)	50.87 (0.77)	(N=172)
	Melt	wt%	2.83 (1.64)	70.47 (1.46)	4.81 (1.02)	19.99 (0.90)	98.00
		at%	1.05 (0.76)	47.91 (0.96)	5.93 (1.36)	45.11 (1.47)	(N=20)
SV302	"Braggite"	wt%	33.79 (0.72)	44.93 (0.58)	0.30 (0.05)	20.16 (0.31)	99.18
		at%	14.09 (0.31)	34.35 (0.43)	0.42 (0.08)	51.15 (0.63)	(N=136)
	Melt	wt%	5.59 (1.10)	72.96 (0.83)	3.66 (0.39)	18.90 (0.42)	101.11
		at%	2.10 (0.52)	50.19 (0.56)	4.56 (0.49)	43.15 (0.82)	(N=17)
SV304	"Braggite"	wt%	29.29 (0.75)	50.51 (0.71)	0	20.21 (0.35)	100.01
		at%	11.96 (0.29)	37.82 (0.49)	0	50.22 (0.61)	(N=118)
	Melt	wt%	4.79 (4.04)	75.32 (8.08)	0	17.77 (5.06)	97.88
		at%	1.91 (1.86)	55.02 (5.93)	0	43.08 (7.22)	(N=97)



Photomicrograph 13 “Cooperite” (co), “Braggite” (br) and coexisting melt at 1000°C of experiment SV289 (digitally enhanced, long side of the photomicrograph is 1.10 mm).

Photomicrograph 14 Coexisting cooperite (co) and braggite (br) with chalcopyrite (cp) from the Maramba Reef under reflected light (digitally enhanced, the long side of the photomicrograph is 200µm long).



Page 123

Photomicrograph 15 Coexisting cooperite (co) and braggite (br) with chalcopyrite (cp) from the Maramba Reef under crossed nicols in reflected light (the long side of the photomicrograph is 200µm long).

Page 145

7.1 "BRAGGITE"

Figure 78 illustrates that "braggite" synthesized at 1000°C contains higher amounts of Ni at given Pt/Pd ratios in the initial charge, if formed under higher S-pressure. Furthermore, the Ni-content in the "braggite" increases with increasing Pt/Pd ratio at relatively constant S-pressure.

Within each group of constant bulk Pt/Pd ratio, the Pt/Pd ratio of the quenched "braggite" decreases with increasing sulphur fugacity (represented by the overall S-content of the initial charge) (Fig. 78). This is in accordance with thermodynamic data published by Barin et al. (1977)(Fig. 79), showing that PdS becomes stable at higher sulphur fugacities than PtS, implying that higher fS_2 will stabilize "braggite" with higher Pd-content.

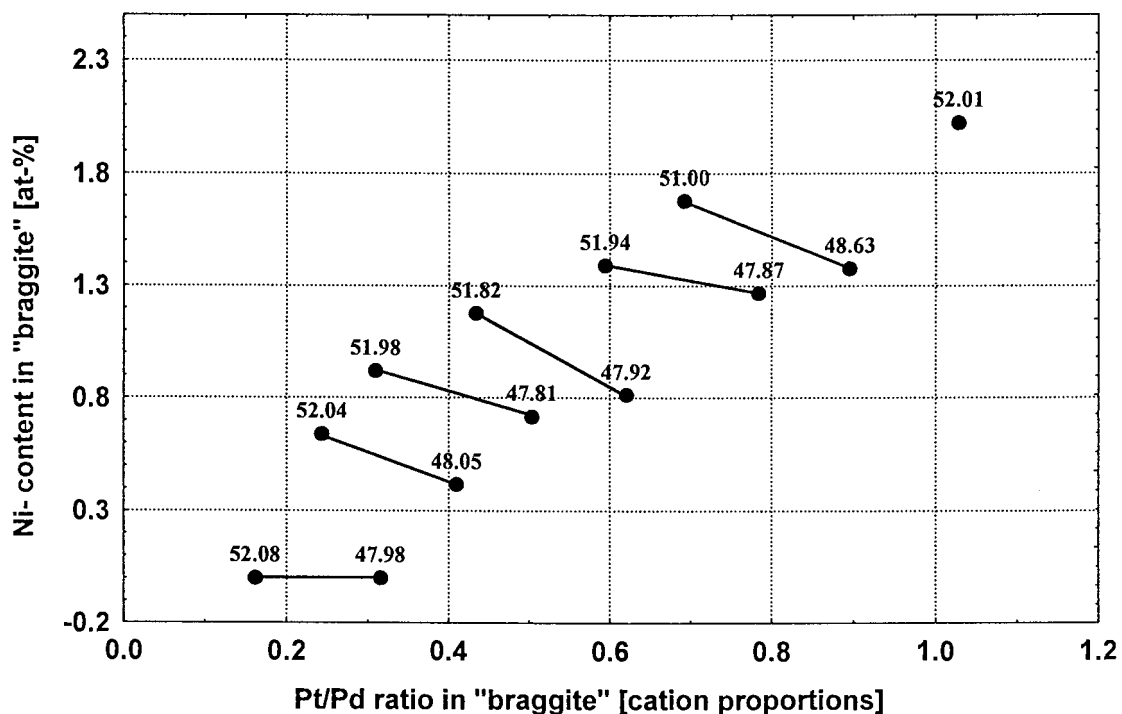


Figure 78 Pt/Pd ratio versus Ni-content in atomic proportions in "braggite" at 1000°C. Numbers above the symbols indicate the S-content in the initial charge. Tie-lines connect experiments of the same bulk Pt/Pd ratio.

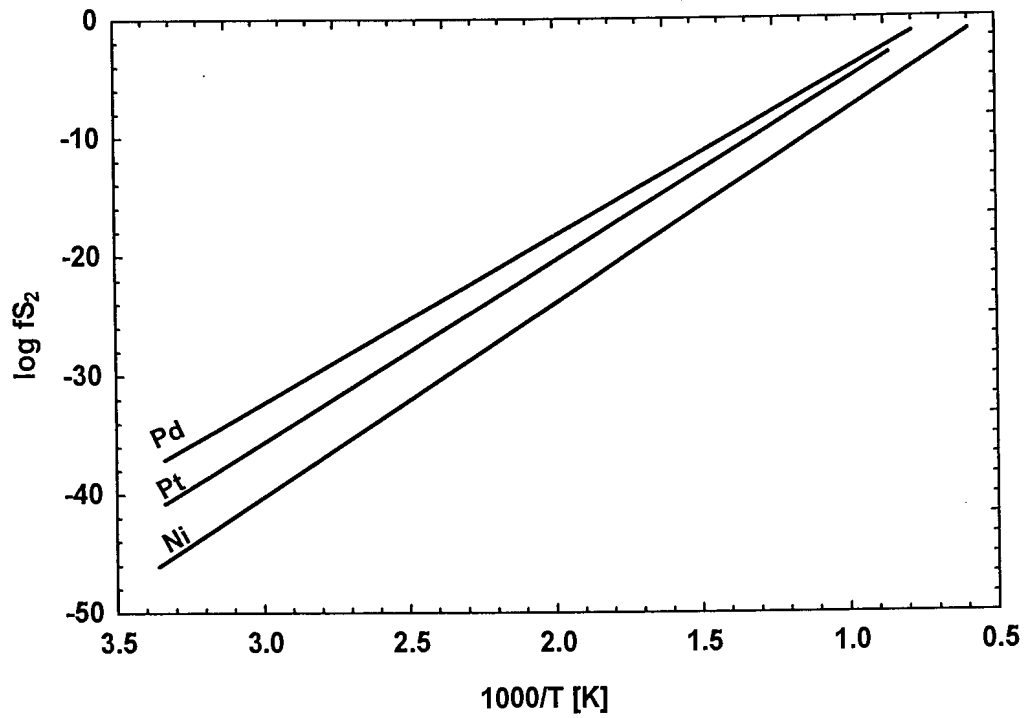


Figure 79 Sulphur pressures versus temperature for the equilibria Pd + S \leftrightarrow PdS, Pt + S \leftrightarrow PtS, and Ni + S \leftrightarrow NiS (data from Barin et al., 1977).

7.2 "COOPERITE"

In "cooperite" there is a similar dependence of the relationship between the Pt/Pd ratio and the Ni-content on the S-pressure as found in "braggite". The Ni-content increases with increasing Pt/Pd ratio. The effect, the sulphur fugacity exerts on the Pt/Pd ratio of "cooperite" increases with increasing Pt/Pd ratio of the "cooperite", i.e. the difference in Pt/Pd ratio between low and high sulphur charges, which initially contained the same Pt/Pd ratio, increases as the Pt/Pd ratio and the Ni-content of the "cooperite" increases (Fig. 80).

The tie line combining the data points with a Pt/Pd ratio between 5.6 and 8.2 in Figure 80 is not linear. This is most likely due to analytical errors, as the variation in Ni-content of these three data points of "cooperite" lies within the analytical uncertainty (3σ) of 0.16 wt-% (~0.33 at-%) Ni.

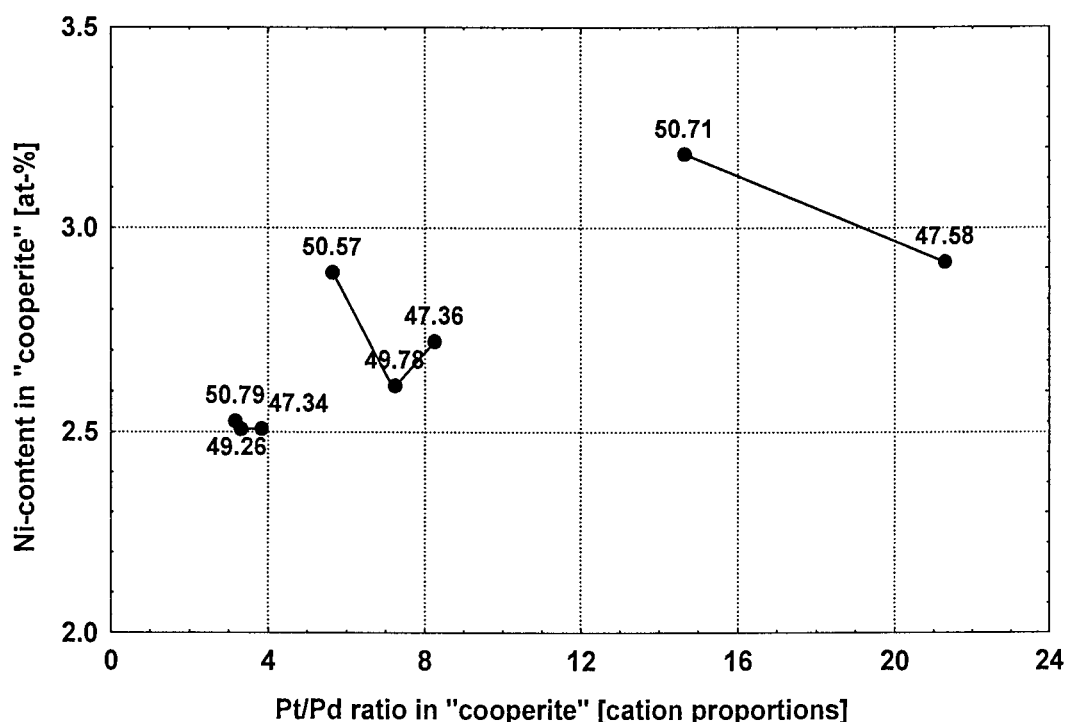


Figure 80 Pt/Pd ratio versus Ni-content in atomic proportions in "cooperite" at 1000°C. Numbers above the symbols indicate the S-content in the initial charge. Tie-lines connect experiments of the same initial Pt/Pd ratio.

CHAPTER 8

DISCUSSION: PART I

TEMPERATURE DEPENDENT TRENDS

8 DISCUSSION: PART I

TEMPERATURE DEPENDENT TRENDS

In this part of the discussion, the isothermal sections presented in Chapters 6.2 to 6.7 are combined and the effect of temperature on the compositions of “cooperite”, “braggite”, and “vysotskite” are discussed. Figure 81 shows a sketch of the stability fields from 1200°C to 700°C combined into one ternary diagram.

From Figure 81 it can be deduced that the compositional fields of “cooperite”, as well as that of “braggite-vysotskite”, become enlarged with decreasing temperature, whereas the compositional field of the melt shrinks with decreasing temperature, disappearing totally at 800°C. “Braggite” is only stable below 1100°C and “vysotskite” only below 1000°C.

“Cooperite” contains a maximum of 6.3 at-% Pd at 1200°C. From 1100°C down to 700°C, the maximum Pd-content remains fairly constant, ranging between 12.5 and 13.9 at-% in a Ni-free environment (Fig. 82). The maximum Pd-content of “cooperite” coexisting with “braggite”, in a Ni-saturated environment, decreases from 10.9 at-% at 1000°C to 4.8 at-% at 700°C (Fig. 83). In “braggite”, coexisting with “cooperite” in a Ni-free environment, the maximum Pd-content increases from 20.7 at-% Pd at 1000°C to 23.1 at-% Pd at 700°C, with a slight decrease to 20.1 at-% Pd at 900°C (Fig. 82). In a Ni-saturated environment, however, the Pd-content in “braggite”, in the assemblage with “cooperite”, decreases from 19.3 at-% (20.1 when Ni-free projected) Pd at 1000°C to 11.2 at-% (13.8, when Ni-free projected) at 700°C (see Fig. 83).

Figure 64 (Chapter 6.7) and Figure 83 imply that there is a relatively large difference in the Pd-limits at 700°C when coexisting “cooperite” and “braggite” have formed in a slightly Ni-undersaturated environment. This makes the application of the experimentally determined phase relations to natural systems at this temperature almost impossible, as a small variation in availability of Ni for incorporation in cooperite and braggite may change the phase relation between coexisting cooperite and braggite drastically.

The difference in maximum Ni-content in coexisting “cooperite” and “braggite” increases with decreasing temperature (Fig. 84).

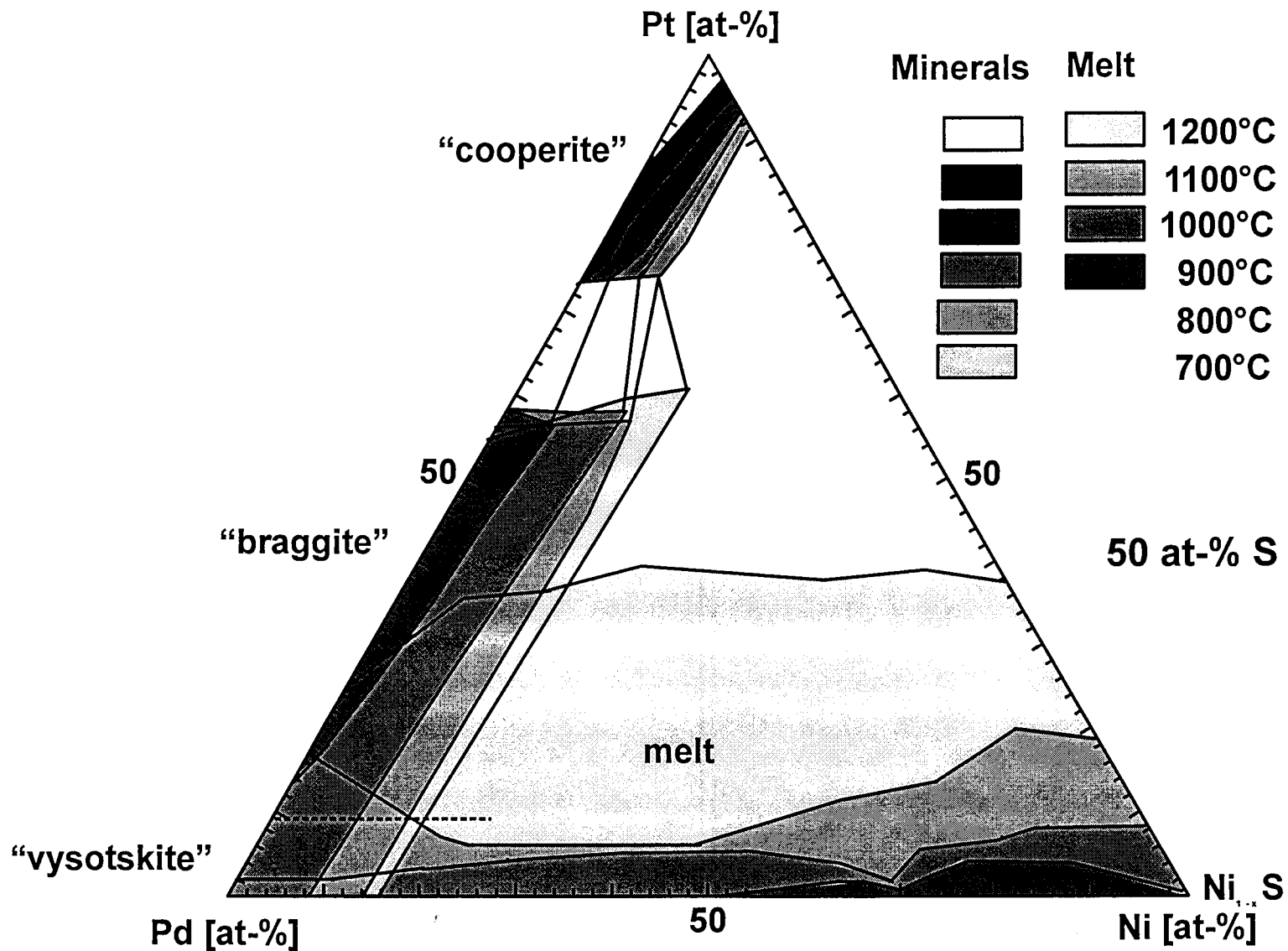


Figure 81 Sketch of phase relations in the system PtS-PdS-NiS in cation proportions from 1200°C to 700°C. Compositional fields of melts at the various temperatures stretch down to the Pd-Ni join. Compositional fields of "cooperite", "braggite", and "vysotskite" extend to the Pt-Pd join for the various temperatures. At 800°C and 700°C Ni_{1-x}S is stable. The tie lines combine coexisting "cooperite" and "braggite" formed in Ni-saturated environments at their respective temperatures. The stippled line indicates the border between "braggite" and "vysotskite".

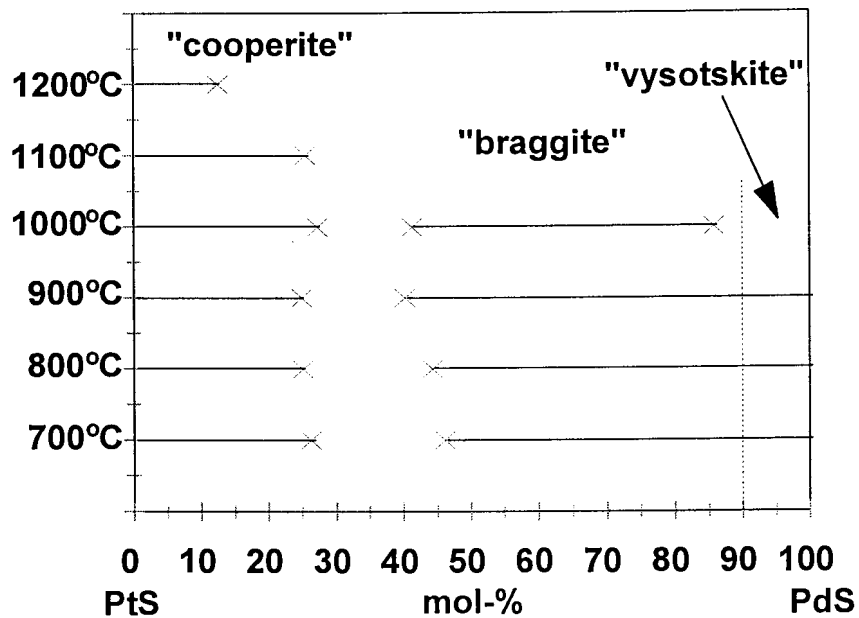


Figure 82 Stability ranges of "cooperite", "braggite", and "vysotskite" in mol-% formed in a Ni-free environment between 1200°C and 700°C.

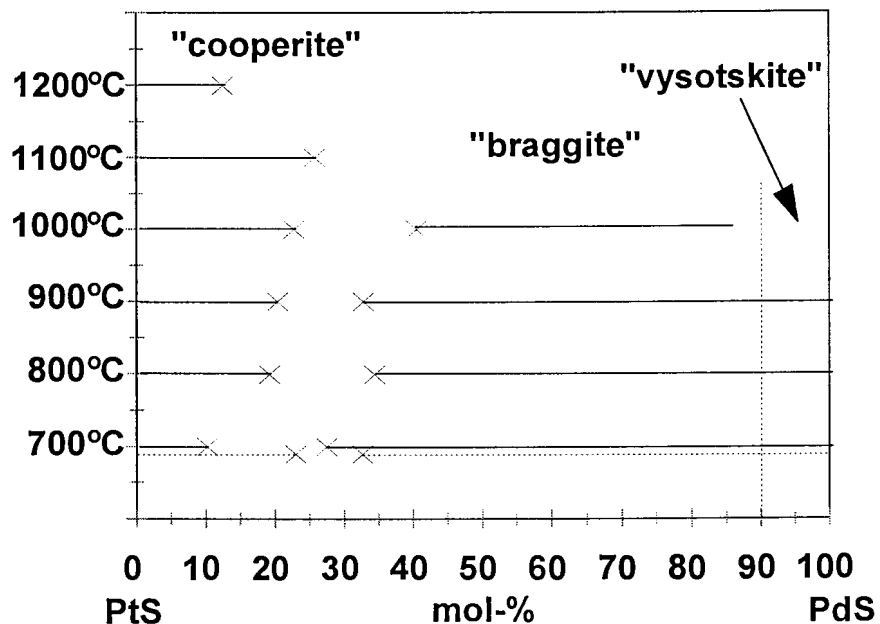


Figure 83 Ni-free projected stability ranges of "cooperite", "braggite", and "vysotskite" in mol-% formed in a Ni-saturated environment between 1200°C and 700°C. The horizontal stippled line indicates the stability range in a slightly Ni-undersaturated environment at 700°C.

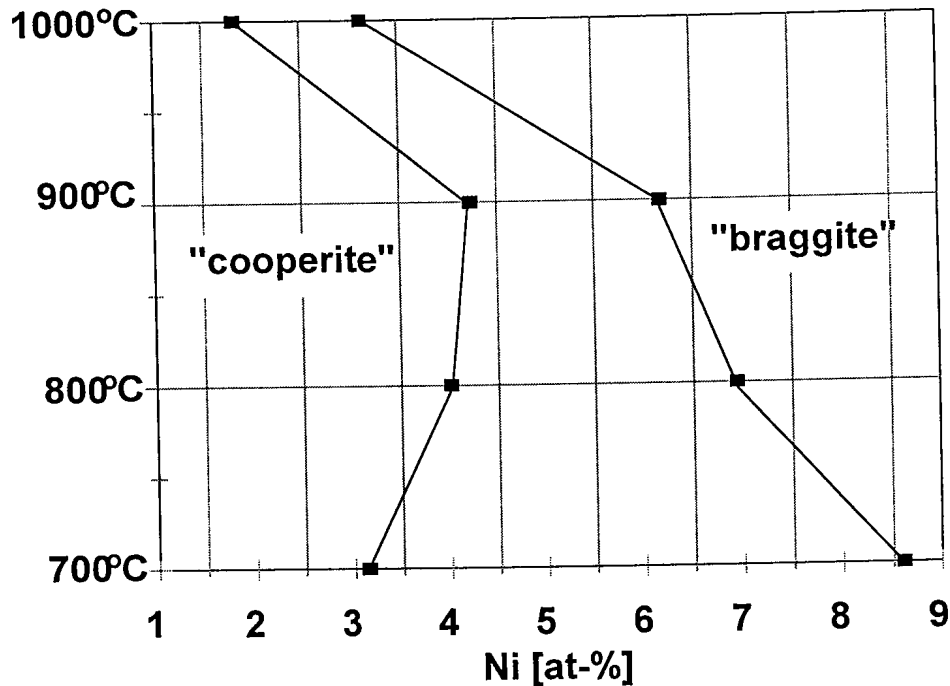


Figure 84 Ni-content (in at-%) in coexisting "cooperite" and "braggite" formed between 1000°C and 700°C in a Ni-saturated environment.

8.1 TRENDS IN "COOPERITE"- COMPOSITIONS

Between 1200°C and 1000°C, the Ni-content in "cooperite" increases with increasing temperature at relatively constant Pt-content. In "cooperite" formed at 700°C, the Ni-content is lower than that at 800°C, but again higher than that at 1000°C. The Ni-content also increases with increasing Pt-content. In "cooperite" formed at 900°C, however, the Ni-content decreases with increasing Pt-content (Fig. 85).

A reason for this rather complex behaviour of the Ni-content of "cooperite" might be found in the change of phase association at the various temperatures. Between temperatures of 1200°C and 1000°C, "cooperite" coexists with a sulphide melt. At 900°C Pd-free "cooperite" is associated with $Ni_{1-x}S$, whereas "cooperite" containing Pd coexists with a sulphide melt. At temperatures $\leq 800^\circ C$, "cooperite" coexists with $Ni_{1-x}S$. The relevant equations for the relationship between the Ni- and Pt-content are presented in the Chapters on the individual isothermal sections (Chapters 6.2 to 6.7).

Due to this complex relationship between the Ni-content and the temperature of formation of “cooperite”, no regression analysis in order to mathematically describe an association between composition of “cooperite” and temperature of synthesis was performed. To estimate the temperature of formation or equilibration of cooperite analyses from natural occurrences, Figure 85 may be used as an indicator. This method is, however only applicable in areas in Figure 85, where there is no overlap of regression lines, i.e. a cooperite containing 47 at-% Pt and 0.7 at-% Ni formed or equilibrated at a temperature of ~1200°C, whereas the formation or equilibration temperature of a cooperite containing 45 at-% Pt and 3 at-% Ni cannot be determined with certainty.

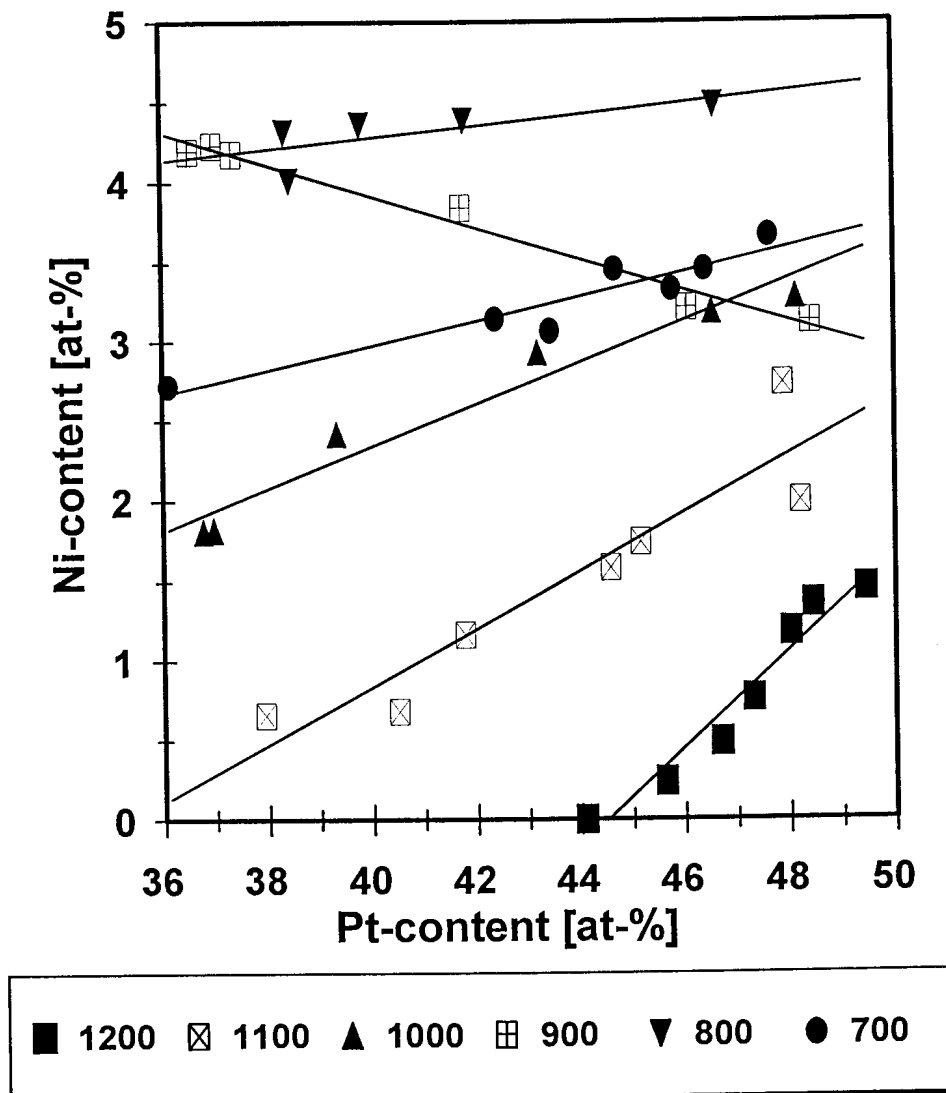


Figure 85 Ni-content versus Pt-content in “cooperite” in at-% formed between 1200°C and 700°C in a Ni-saturated environment. The solid lines show the best linear fits of the data for the various temperatures (°C) indicated in the legend.

Plotting Ni-content versus Pd-content data of the various temperatures, the lines of best linear fits display opposite slopes to those shown in Figure 85 and are not presented here.

8.2 TRENDS IN “BRAGGITE - VYSOTSKITE” COMPOSITIONS

Between 1000°C and 700°C the Ni-content in “braggite-vysotskite”, which formed in a Ni-saturated environment, increases with increasing temperature at constant Pt-contents. The Ni-content also increases with increasing Pt-content for most temperatures investigated in this study. Exceptions, however, are the compositions obtained for 800°C, where there is a slight decrease in Ni-content with increasing Pt-content of “braggite-vysotskite” (Fig. 86). The difference in the slope of the regression line between the Pt- and Ni-content at the various temperatures is possibly due to the change in phase associations occurring between 900°C and 800°C. At 900°C “braggite-vysotskite” is associated with a sulphide melt and at 800°C with Ni_{1-x}S .

The relevant equations for the relationship between the Ni- and Pt-content are presented in the chapters on the individual isothermal sections (Chapters 6.2 to 6.7).

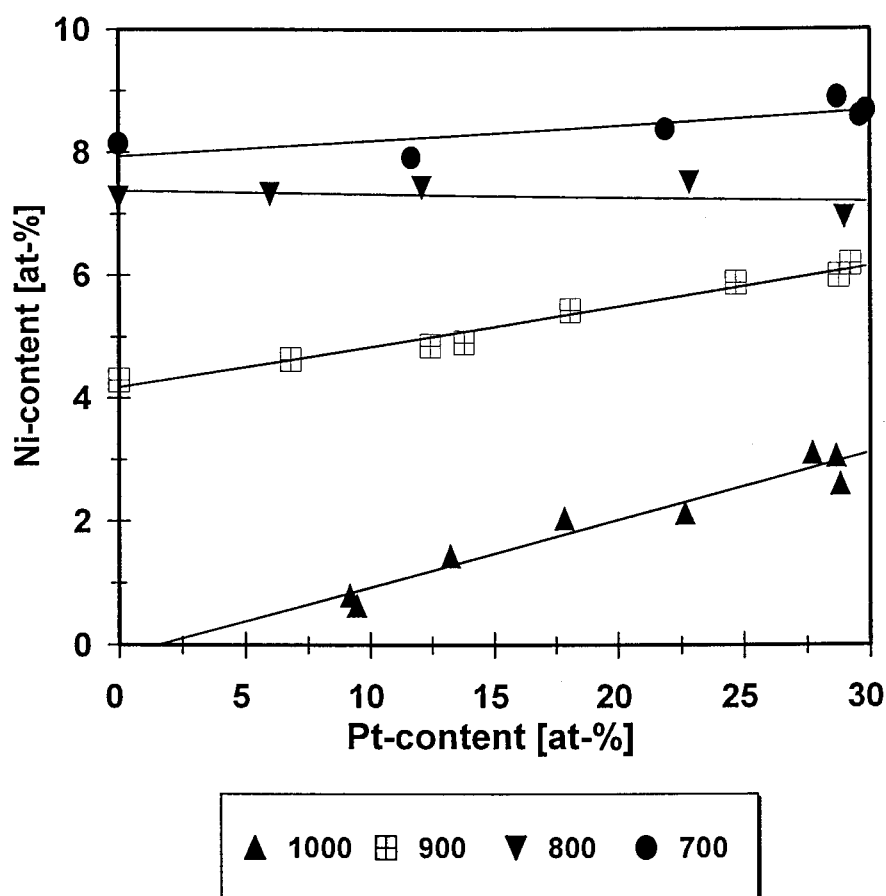


Figure 86 Ni-content versus Pt-content in “braggite-vysotskite” in at-% formed between 1000°C and 700°C in a Ni-saturated environment. The solid lines show the best linear fits of the data for the various temperatures (°C) indicated in the legend.

In order to deduce a relationship between temperature of formation and composition of “braggite” and “vysotskite”, all the compositions of “braggite” and “vysotskite” not coexisting with “cooperite” in a Ni-saturated environment obtained in this study between 1000°C and 700°C (above which “braggite” is not stable), were statistically evaluated. There is a significant Spearman correlation between the temperature of synthesis and the Ni-content (Table 22).

Table 22: Spearman correlation coefficients between temperature of synthesis and composition (at-%) of “braggite-vysotskite” not coexisting with “cooperite”, formed in a Ni-saturated environment between 1000°C and 700°C. The highlighted correlation coefficients are significant at a p -level ≤ 0.05 .

	Temperature
Pt	0.143494
Pd	0.180656
Ni	-0.965573

Exploring the best linear fit for the relationship between the temperature of formation and the Pt-, Pd-, and Ni content of “braggite-vysotskite”, using the formation temperature as the dependant variable and the Pt-, Pd-, and Ni-content as independent variables in a forward stepwise multiple linear regression analysis, led to the R^2 values shown in Table 23.

Table 23: Coefficient of determination (R^2) depending on variables used in a forward stepwise multiple linear regression analysis with temperature of synthesis as the dependant variable.

Variables in equation	R^2
Ni	0.9118
Ni, Pt	0.9205
Ni, Pd	0.9204
Ni, Pt, Pd	0.9205

From Table 23 it can be deduced, that the Ni-content alone of “braggite” may be used in the prediction of the temperature of formation or equilibration. Adding either the Pt- or the Pd-content to the equation improves the coefficient of determination only slightly. Including the Pt- and the Pd-content together with the Ni-content in an equation yields no improvement of the R^2 -value. Below, the equation (at the 95% confidence level) incorporating the Ni- and Pt-content in at-% is shown:

$$\begin{aligned} \text{Temp [C}^\circ] &= 1056.92 (\pm 20.36) \\ &+ 1.16 (0.85) \times \text{Pt} \\ &- 39.59 (\pm 2.84) \times \text{Ni} \end{aligned} \quad (\text{Equation 41}) \quad R^2 = 0.9205$$

A plot of the predicted temperature of formation versus the observed temperature of formation using Equation 41 is shown in Figure 87.

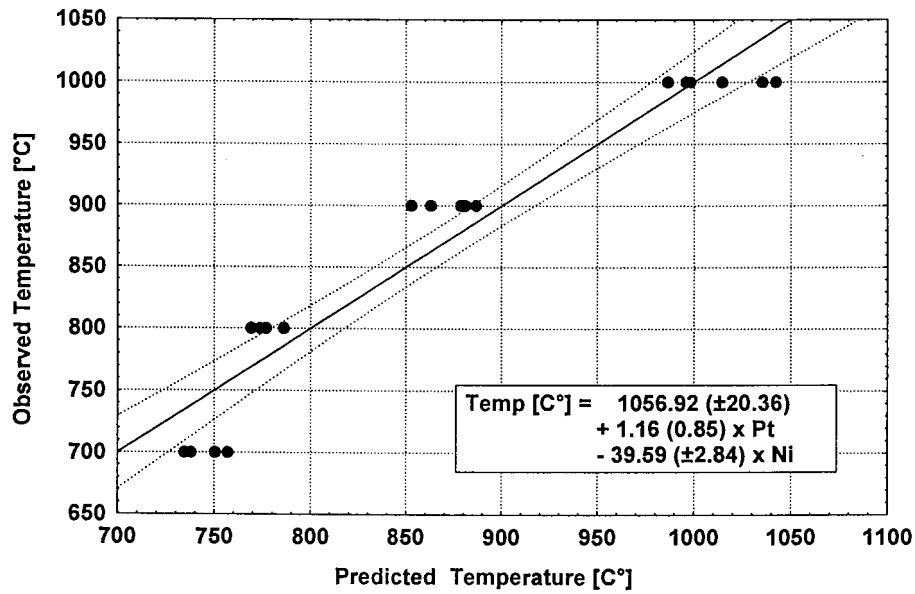


Figure 87 Predicted versus observed temperature of synthesis [°C] for “braggite” and “vysotskite” not coexisting with “cooperite”, formed in a Ni-saturated environment between 1000°C and 700°C, according to the linear equation shown. The solid line indicates the best linear fit and the stippled line the 95% confidence interval of the line.

Testing a quadratic ($y = a + bx^2$) relationship between the temperature of formation of “braggite-vysotskite” and the Pt-, Pd-, and Ni-content (using the formation temperature as the dependant variable and Pt-, Pd-, and Ni-content as independent variables) in a forward stepwise multiple regression analysis, led to the R^2 values shown in Table 24.

Table 24: Coefficient of determination (R^2) depending on quadratic variables used in a forward stepwise multiple regression analysis with temperature of synthesis as the dependant variable.

Variables in equation	R^2
Ni^2	0.9621
Ni^2, Pt^2	0.9753
Ni^2, Pd^2	0.973
Ni^2, Pt^2, Pd^2	0.9753

In Table 24 it is shown that the quadratic Ni-content of “braggite” may be used alone in the prediction of the temperature of formation or equilibration. The coefficient of determination is higher than that for the linear Equation 41. Adding either the quadratic Pt- or the Pd-content to the equation improves the coefficient of determination slightly. Using the quadratic Pt- and the Pd-content together with the quadratic Ni-content in an equation, does not improve the R^2 -value. The equation (at the 95% confidence level) incorporating the quadratic Ni- and Pt-content (in at-%) is:

$$\begin{aligned}
 \text{Temp [C}^\circ] &= 998.07 (\pm 7.88) \\
 &+ 0.05 (\pm 0.02) \times Pt^2 \\
 &- 4.24 (\pm 0.16) \times Ni^2 \quad \text{(Equation 42)} \quad R^2 = 0.9753
 \end{aligned}$$

A plot of the predicted temperature of formation versus the observed temperature of formation using Equation 42 is shown in Figure 88.

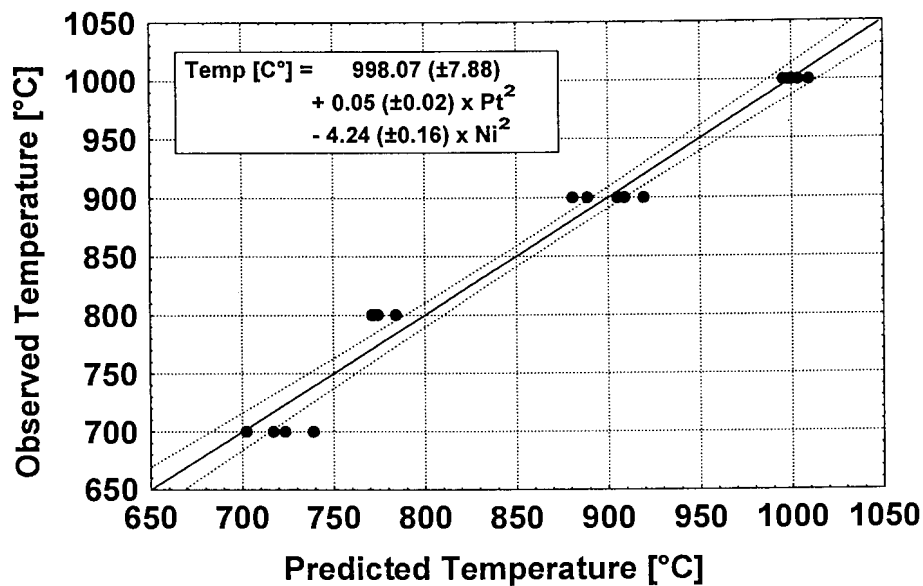


Figure 88 Predicted versus observed temperature of synthesis [°C] for “braggite” and “vysotskite” not coexisting with “cooperite”, formed in a Ni-saturated environment between 1000°C and 700°C, according to the quadratic equation shown. The solid line indicates the best fit and the stippled line the 95% confidence interval of the line.

Prediction of the formation- or equilibration temperature using Equation 42 yields a more accurate result than using Equation 41 (Figures 87 & 88). It is therefore recommended to use Equation 42 in the calculation of formation- or equilibration temperatures of natural braggite and vysotskite from their analyses. This equation is, however, derived from experimental results obtained for temperatures between 1000°C and 700°C and may not hold true for lower temperatures. I.e., using Equation 42, a Ni-content in braggite of more than ~9 at-% Ni yields a temperature below 700°C and may not be valid.

8.3 APPLICABILITY TO COOPERITE, BRAGGITE, AND VYSOTSKITE OCCURRING IN NATURE

Solubilities of Ni in “cooperite”, “braggite”, and “vysotskite” are sensitive to temperature and phase assemblages. Therefore, the mineral compositions have the potential to indicate at which stage of the development of the ore deposit these phases were exsolved, or suffered overprinting.

However, the Ni-content in “cooperite”, “braggite”, and “vysotskite” is a function of the activity of nickel sulphide in the system and therefore of the phase association in which these minerals occur. Temperatures of formation or equilibration can be affected by the Ni/Fe ratio in the base-metal sulphide assemblage. Makovicky et al. (1990) and Makovicky & Karup-Møller (1995) show that the Fe-content in the *monosulphide-solid-solution* (*mss*) and the melt associated with “vysotskite” influences the maximum solubility of Ni in “vysotskite”. The amounts of Pd, Fe, and Ni in the melt and the associated synthetic PdS are interrelated and the amount of Fe and Ni incorporated into synthetic PdS is a function of both the Fe/(Fe+Ni) and the (Fe+Ni)/Pd ratios (Makovicky & Karup-Møller, 1995). At 900°C the maximum solubility of Fe in synthetic Ni-free PdS is 0.4 at-% and that of Ni in Fe-free synthetic PdS is 3.9 at-%. For a Fe/(Fe+Ni) ratio (in at-prop.) of 0.76 in the melt, the Fe-content in synthetic PdS is 0.3 at-% and the Ni-content is 1.0 at-%, i.e. a small change in Fe-content is linked to a considerable decrease in the Ni-content. At 725°C, synthetic PdS coexisting with Ni_{1-x}S contains 8.2 at-% Ni, for 33.7 at-% Ni in *mss* there is 5.7 at-% Ni synthetic PdS, and for 8.2 at-% Ni in *mss* there is 1.4 at-% Ni in “vysotskite” (Makovicky & Karup-Møller, 1995).

The influence of other base metals has not been fully investigated yet.

Assuming that the incorporation of Pt into PdS does not change the general trends in the behaviour of Ni and Fe as discussed above, the following points concerning the applicability of the experimental results obtained in this thesis are made:

- (i) The temperature of formation or equilibration of cooperite occurring in a Ni-saturated environment can be estimated using Figure 85 according to Chapter 8.1.
- (ii) Presuming Ni-saturation, the temperature of formation or equilibration of braggite and vysotskite can be estimated using Equation 42 for estimated temperatures between 1000°C and 700°C.
- (iii) Formation- or equilibration temperatures of cooperite, braggite, and vysotskite formed in an $\text{Fe}\pm(\text{Cu})\pm(\text{Co})$ - saturated environment cannot be estimated using the data produced in this study as the maximum Ni-content in cooperite, braggite, and vysotskite may be lowered by the presence of Fe (Makovicky & Karup-Møller, 1995). Presuming that no elements other than Ni and Fe play a role in the compositional variation, maximum formation temperatures are, however, not influenced.

CHAPTER 9

DISCUSSION: PART II

APPLICATION TO NATURAL COOPERITE, BRAGGITE, AND VYSOTSKITE

9 DISCUSSION: PART II

APPLICATION TO NATURAL COOPERITE, BRAGGITE, AND VYSOTSKITE

In this Chapter, the results obtained from the experimental investigation of “cooperite”, “braggite”, and “vysotskite” are compared with compositions of naturally occurring phases, in order to give indications of their temperature of formation or equilibration. Analysis of cooperite, braggite, and vysotskite from 3 environments are considered:

- (i) Cooperite and braggite from the Merensky Reef, where coexisting cooperite and braggite as well as individually occurring cooperite- and braggite grains were encountered.
- (ii) Cooperite, braggite, and vysotskite from the UG-2 of two different BMS associations (one where the main Ni-bearing phase is millerite and one where the main Ni-bearing phase is pentlandite).
- (iii) Braggite and vysotskite from the Sompujärvi Reef of the Penikat Intrusion in northern Finland.

Analyses of cooperite, braggite, and vysotskite from selected localities taken from the literature are also discussed. It goes beyond the scope of this thesis to describe the geology of the deposits mentioned in the following discussion. Detailed descriptions of the geological environments can be found in the references cited.

9.1 BUSHVELD COMPLEX

9.1.1 Merensky Reef

Cooperite and braggite are frequently encountered in the silicate dominated Merensky Reef (Kinloch, 1982); occasionally, these two phases coexist (Merkle & Verryn, 1991; Verryn & Merkle, 1994). The PGMs in the Merensky Reef are associated with chalcopyrite, pentlandite, pyrrhotite, and minor pyrite (Brynard et al., 1976; Schwellnus et al., 1976; Vermaak & Hendriks, 1976; Mostert et al., 1982).

The compositional variation of 36 grains of coexisting braggite and cooperite from a production concentrate of the Merensky Reef (the origin of the material used in this investigation may not be disclosed) were determined along traverses across their mutual boundaries. In addition 5 and 6 individual grains of cooperite and braggite, respectively, were analysed. Selected analyses are presented in Table 25.

Table 25: Selected cooperite (co), braggite (br), and vysotskite (vy) analysis from the Merensky Reef (MR) and the UG-2 in association with pentlandite (pent) or millerite (mill).

Mineral		co	co	br	br	co	br	vy	br	vy	
Origin		MR	MR	MR	MR	UG-2	UG-2	UG-2	UG-2	UG-2	
Association		pent	pent	pent	pent	pent	pent	pent	mill	mill	
W	S	14.41	14.56	18.12	18.96	14.83	20.26	22.09	19.02	25.6	
	Rh	<0.11	<0.11	<0.11	<0.11	0.40	<0.11	<0.11	<0.11	0.16	
	Pd	0.80	1.31	19.92	21.45	2.57	23.29	43.55	25.69	60.46	
	Pt	83.81	83.92	57.15	53.38	80.43	47.55	25.43	52.20	1.25	
	Ni	0.58	0.53	4.24	5.67	0.53	7.63	8.85	3.90	12.28	
	Co	<0.02	<0.02	<0.02	<0.02	0.03	<0.02	<0.02	<0.02	<0.02	0.04
	Cu	0.04	<0.03	<0.03	<0.03	<0.03	0.32	0.06	0.03	0.3	
	Fe	<0.02	<0.02	0.14	0.05	0.47	1.37	0.52	0.12	0.57	
	Total		99.64	100.32	99.57	99.51	99.26	100.42	100.50	100.96	100.7
	A	S	50.1	50.15	50.45	50.8	50.24	50.39	49.58	50.65	49.92
Rh		-	-	-	-	0.42	-	-	-	0.1	
Pd		0.84	1.36	16.72	17.32	2.63	17.46	29.45	20.61	35.53	
Pt		47.89	47.5	26.16	23.51	44.77	19.44	9.38	22.84	0.4	
Ni		1.09	1	6.45	8.3	0.97	10.36	10.85	5.68	13.08	
Co		-	-	-	-	0.05	-	-	-	0.04	
Cu		0.07	-	-	-	-	0.4	0.07	0.04	0.3	
Fe		-	-	0.23	0.07	0.92	1.95	0.67	0.19	0.63	

Traverse analyses close to the grain boundary of coexisting braggite and cooperite were discarded if cooperite showed abnormally high Pd content, or if the Pd content in braggite was abnormally low compared with the rest of that particular grain. In such cases interference from the neighbouring grain was assumed. Analytical conditions are given in Chapter 5.

Profiles across the mineral boundaries of composite cooperite-braggite grains indicate that occasionally there is a change in composition of the minerals close to the mineral boundary. Abrupt and continuous changes over the whole mineral grain towards higher

and lower Pd content were observed in both minerals, but no systematic pattern of chemical variability in coexisting braggite and cooperite was detected. Compositional variation in braggite was usually found to be greater than in cooperite. Compositional variations were also observed by Cabri et al. (1978) in individual grains of braggite. This compositional variation is interpreted to reflect incomplete equilibration between, and within, the two phases. Different degrees of homogenization are attributed to differences in the cooling history (i.e., the effects of various postcumulus processes) of individual grains.

Figure 89 shows the compositional variation of braggite and cooperite from the Merensky Reef based on 766 analyses, while Photomicrographs 14 and 15 show coexisting cooperite and braggite from the Merensky Reef in plane polarized reflected light and under crossed nicols, respectively.

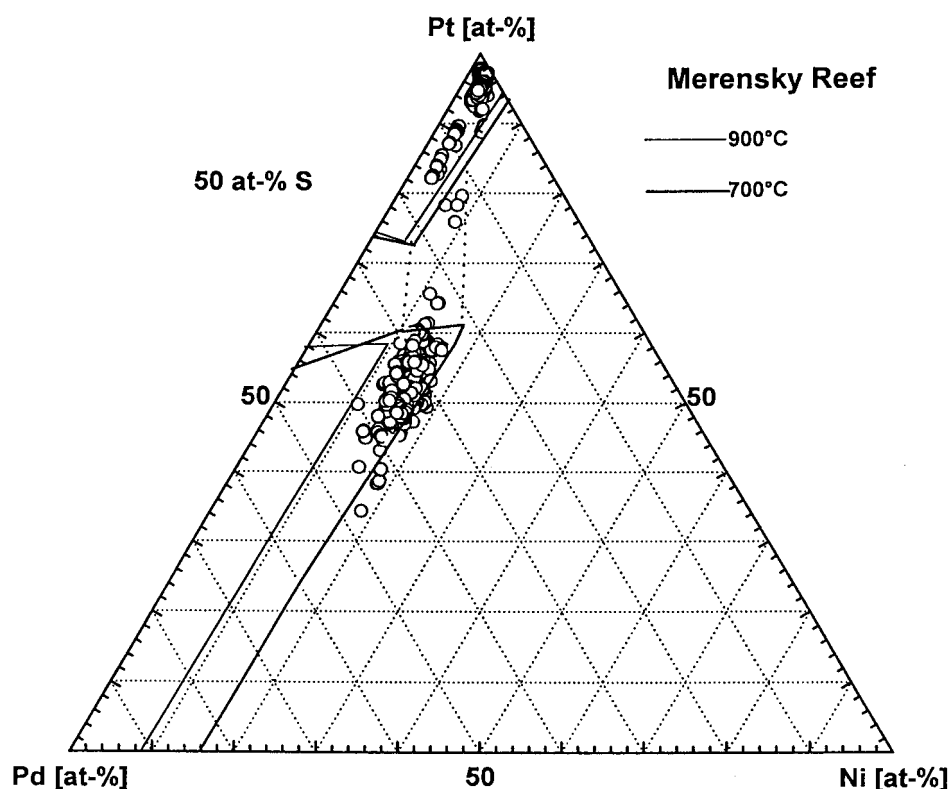
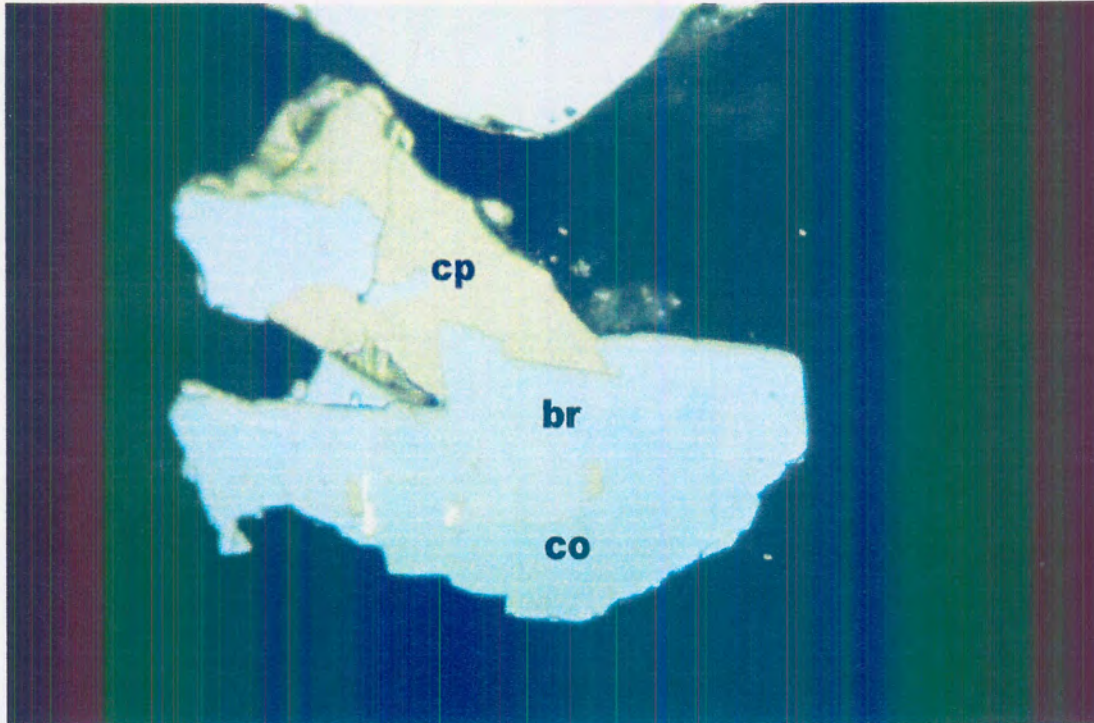
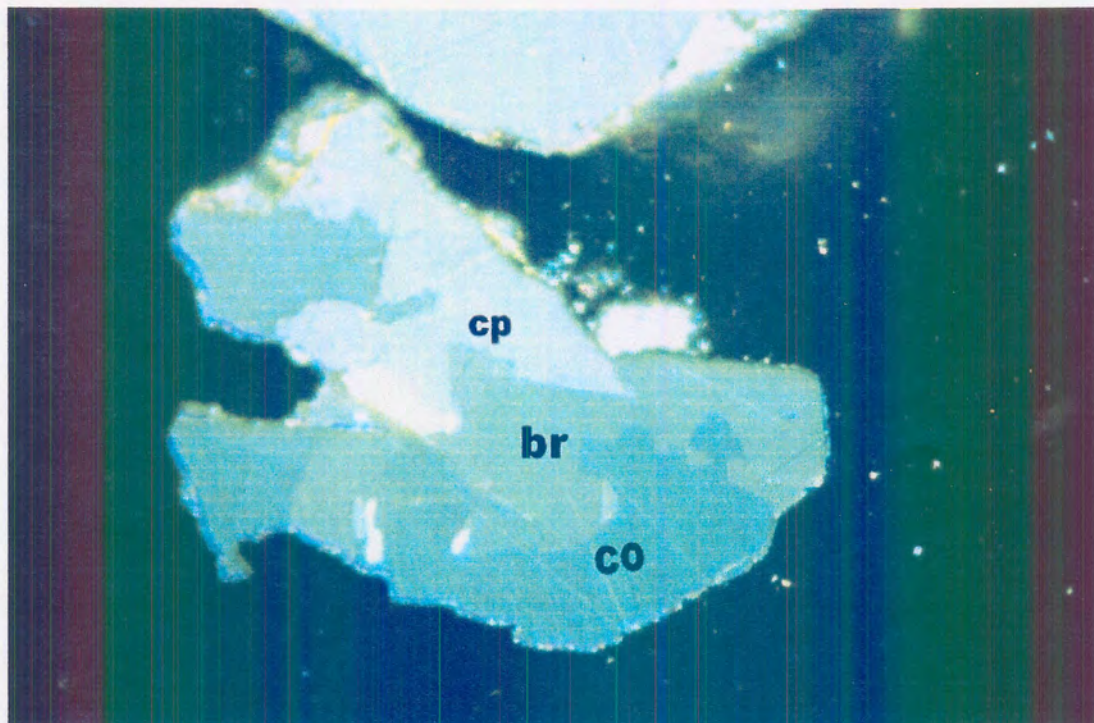


Figure 89 Compositional variation of cooperite and braggite from the Merensky Reef in cation proportions based on 766 analysis. The solid line indicates the compositional field established for 900°C and 700°C and the black stippled lines represent tie lines between coexisting “cooperite” and “braggite” synthesized at 700°C



Photomicrograph 14 Coexisting cooperite (co) and braggite (br) with chalcopyrite (cp) from the Merensky Reef under reflected light (digitally enhanced, the long side of the photomicrograph is 200 μ m long).



Photomicrograph 15 Coexisting cooperite (co) and braggite (br) with chalcopyrite (cp) from the Merensky Reef under crossed nicols in reflected light (the long side of the photomicrograph is 200 μ m long).

In Verryn and Merkle (1994), the compositional variation of cooperite and braggite from the Merensky Reef was interpreted to represent a coupled substitution of (Pd+Ni) for Pt. Based on a regression analysis of analytical results from the Merensky Reef, the Pd:Ni ratio in cooperite is approximately 9 :11 and in braggite the Pd:Ni ratio is about 7:3 (Verryn & Merkle, 1994). This experimental investigation, however, produced compositional trends which are not in accordance with the above trends. Assuming Ni-saturation, the analysis of cooperite and braggite from the Merensky Reef follow a trend experimentally established for temperatures between 900°C and 700°C (Fig. 89). As the analyses of braggite plot within the trend lines between 1200°C and 700°C established in this experimental investigation, it is possible to apply Equation 42 (Chapter 8.2). The use of Equation 42 results in the same temperature interval (Fig. 90) as deduced graphically from Figure 89.

It is, however, not possible to establish the BMS association of the cooperite and braggite grains analysed, as the individual and composite cooperite and braggite grains in the production concentrate from the Merensky Reef occur as isolated grains. The BMS minerals described from the Merensky Reef by various authors (e.g. Vermaak & Hendriks, 1976; Kingston & El-Dosuky, 1982; Mostert et al., 1982) are in decreasing abundance pyrrhotite, pentlandite, chalcopyrite, and pyrite, suggesting Fe-saturation. Referring to Chapter 8.3, the Fe-saturation may lower the Ni-content in cooperite and braggite at a given temperature, relative to that in a Ni-saturated environment. This indicates that these cooperite- and braggite grains from the Merensky Reef have formed below 900°C.

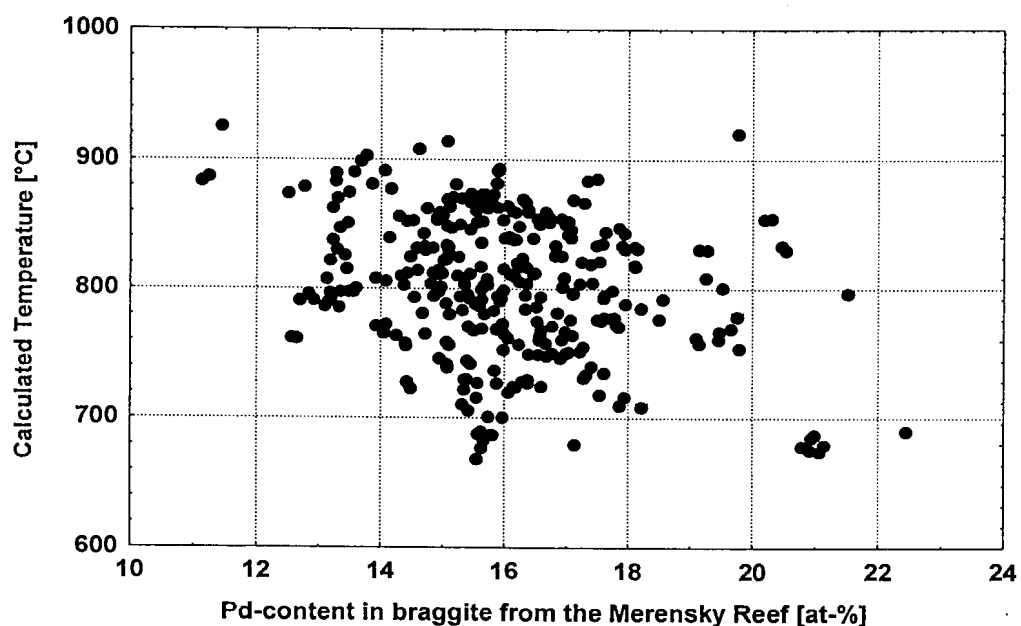


Figure 90 Pd-content (at-%) in braggite from the Merensky Reef versus temperature of formation or equilibration calculated according to Equation 42 ($\text{Temp [C}^\circ] = 998.07 (\pm 7.88) + 0.05 (\pm 0.02) \times \text{Pt}^2 - 4.24 (\pm 0.16) \times \text{Ni}^2$). Page 146

Looking at the individual composite grains of coexisting cooperite and braggite, which should have compositions at the Pd-limits on either side of the miscibility gap, it can be seen that this is not the case for some of the analyses from the Merensky Reef (Fig. 91). The cooperite analyses generally contain lower amounts of Pd than expected according to the experimental results of this study, and some of the braggite compositions fall into the miscibility gap. It is possible that the trend of coexisting “cooperite” and “braggite” observed at 700°C (i.e. in a Ni-saturated environment “braggite” coexists with “cooperite” containing less Pt than that formed in a slightly Ni-undersaturated environment, see Chapter 6.7) continues at lower temperatures. This could explain why some of the compositions of the coexisting cooperite and braggite analysed from the Merensky Reef fall “outside” the compositional variation established experimentally for temperatures between 1200°C and 700°C. Further investigations at lower temperatures and under hydrothermal conditions would be necessary to determine the effects postmagmatic alterations, such as hydrothermal- and metamorphic overprinting, might have on these coexisting cooperite and braggite pairs.

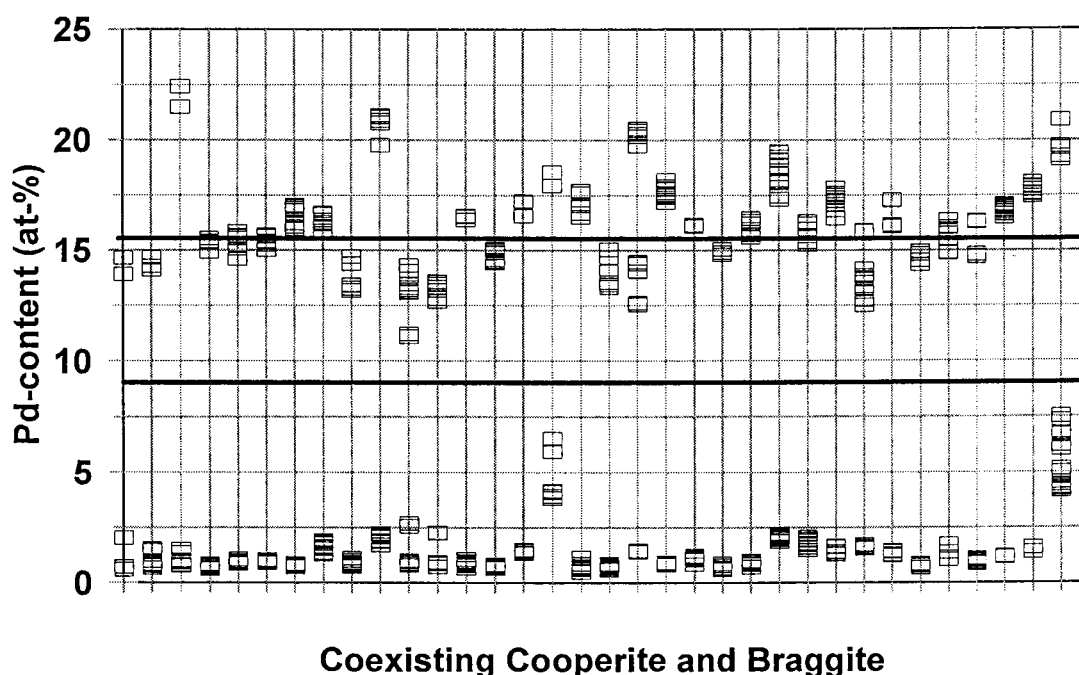


Figure 91 Pd-content in at-% of coexisting cooperite and braggite from the Merensky Reef. The solid black lines indicate the upper Pd-content limit for “cooperite” and the lower limit for “braggite” experimentally established at 800°C.

9.1.2 UG-2

Within the samples of the UG-2 chromitite of the Bushveld Complex, braggite and vysotskite are the most common phases in the system PtS-PdS-NiS (Kinloch, 1982). In the UG-2, the PGMs are associated with the BMSs pentlandite, pyrrhotite, chalcopyrite, millerite, and pyrite (McLaren and De Villiers, 1982).

For this study samples from the UG-2 in which cooperite, braggite, and vysotskite occur in two different BMS assemblages were selected (the origin of the material used in this investigation may not be disclosed). In one assemblage, the main Ni-bearing phase associated with cooperite, braggite, and vysotskite is pentlandite. In the other assemblage millerite and only traces of pentlandite are the main Ni-bearing phases associated with cooperite, braggite, and vysotskite. The different associations indicate different activity of NiS and could therefore be expected to have an effect on the Ni-content of the cooperite, braggite, and vysotskite. In the UG-2, the average grain sizes of cooperite, braggite, and vysotskite are smaller ($\pm 5\mu\text{m}$ in diameter) than in the Merensky Reef (often $>100\mu\text{m}$ in diameter). Compositional heterogeneity could therefore not be observed to the same degree as in the Merensky Reef. Selected analyses are given in Table 25.

Analyses of cooperite, braggite, and vysotskite coexisting with pentlandite or millerite are presented in Figure 92. There is a slight overlap in compositions between the two assemblages, but overall the braggite and vysotskite analyses of the millerite association plot on the Ni-poor side of those which are associated with pentlandite as the main Ni-bearing phase. Sulphide assemblages associated with chromitite layers of the Bushveld Complex are enriched in PGE, Ni, and Cu compared to typical magmatic sulphide assemblages (Von Gruenewaldt et al., 1986; Merkle, 1992; Penberthy & Merkle, 1999). Von Gruenewaldt et al. (1986) suggest that an interaction between chromite and sulphide may be responsible for the Fe-loss in the BMS assemblage. Therefore, presuming equilibrium after Fe-loss, the Fe-undersaturated - Ni-saturated assemblages make the trends, experimentally established in this study, applicable for cooperite, braggite, and vysotskite compositions of the UG-2 (see Chapter 8.3). Most of the braggite and vysotskite compositions associated with pentlandite (lower NiS-activity) follow the trend experimentally established for temperatures $\leq 700^\circ\text{C}$. Most of the braggite compositions associated with millerite (higher NiS-activity) follow the trend

established for temperatures between 800°C and 700°C.

This confirms the findings discussed in Verryn & Merkle (1994) stating: “The NiS activity in an environment in which only millerite forms is higher than that of an environment where pentlandite is present. The braggite and vysotskite grains in association with millerite, however, contain less NiS than those occurring together with pentlandite. This indicates that temperature of formation or equilibration, rather than NiS-activity, is the dominant factor for the Ni-content within braggite and vysotskite”.

In both associations the analyses plot more towards the lower temperature side (indicated by a relative increase in Ni-content) with increasing Pd-content of the braggite and vysotskite grains (Fig. 92). This could indicate that with cooling of the magma and/or ore forming solutions, braggite and vysotskite became richer in Pd.

Too few cooperite grains were encountered in the samples analysed from the UG-2, to justify a temperature determination.

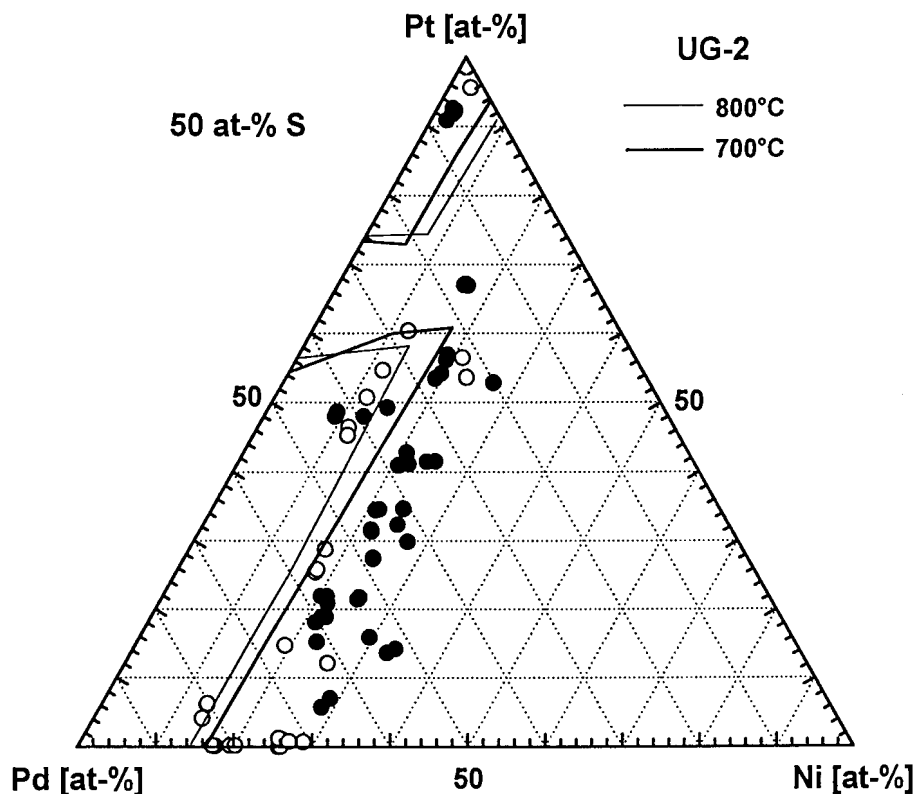


Figure 92 Compositional variation in cation proportions of cooperite, braggite, and vysotskite from the UG-2 (full circles are associated with pentlandite and open circles with millerite as the main Ni-bearing phase). The solid lines indicate the compositional trend established for 800°C and 700°C.

9.2 SOMPUJÄRVI REEF OF THE PENIKAT INTRUSION IN NORTHERN FINLAND

The Sompujärvi Reef (SJR) is the lowermost of the stratabound PGE mineralizations of the Sompujärvi Block within the Penikat Layered Intrusion in northern Finland (Alapieti and Lahtinen, 1986; Halkoaho, 1989 & 1994; Halkoaho et al., 1990). The Sompujärvi Reef has been subdivided into two main types, a chromite- and a sulphide type (Halkoaho, 1989; Halkoaho et al., 1990). The former is often richer in PGE (Halkoaho, 1994).

Samples used in this study, were obtained by Professor Roland K. W. Merkle during a Platinum Symposium Field trip from the open pit test mining at Kirakkajuppura. The material is similar to the SJR chromite-type previously described by (Halkoaho et al., 1990; Halkoaho, 1989 & 1994) (R.K.W. Merkle, personal communication). Only braggite and vysotskite, with strikingly low Ni-content, were observed in the samples analysed. Representative analyses are given in Table 26 and the compositional variation is shown in Figure 93 together with analyses from the literature of the AP 1 mineralization (Halkoaho, 1989), which is a sulphur richer environment.

Most data of braggite published by Halkoaho (1989) follow a trend similar to the one experimentally established in a Ni-saturated environment at 900°C (Fig. 93), whereas some of the Pt-poorer braggite and vysotskite follow a trend experimentally established in a Ni-saturated environment for $\leq 700^\circ\text{C}$. These temperatures could be affected by the Ni/Fe ratio in the BMS assemblage (Makovicky & Karup-Møller, 1995). However, analyses of braggite, vysotskite, and also cooperite failed to detect Fe in these minerals.

Analyses of braggite and vysotskite from the Sompujärvi Reef plot on the Ni-poor side of those taken from the literature for the AP 1 mineralization. According to the experimental results and assuming that the braggite and vysotskite formed in a Ni-saturated environment - not taking a possible effect of Fe-content into consideration - these compositions may be caused by the following two possibilities:

- (i) The braggite-vysotskite composition is only controlled by magmatic processes
- (ii) The originally magmatic braggite-vysotskite composition suffered metamorphic and/or hydrothermal overprinting.

Looking at scenario (i), that the braggite and vysotskite in the Sompujärvi Reef have formed under purely magmatic conditions in a Ni-saturated environment, their temperature of formation lies between the trends experimentally established for 1000°C and 900°C (Fig. 93).

There could, however, be a lack of Ni-bearing BMS, with which the braggite and vysotskite can equilibrate. Under those circumstances it is not possible to estimate a temperature of formation or equilibration for these Ni-poor braggites and vysotskites. Some analysis, however, do contain some Fe (38 of the 63 analyses contain up to 0.92 at-% Fe), which does have an influence on the Ni-content in phase relations in the system Pd-Ni-Fe-S (Makovicky et al., 1990; Makovicky & Karup-Møller, 1995), as discussed in Chapter 8.3. At 900°C, Pt-free vysotskite Pd-Ni-Fe-S in the system can contain a maximum of 0.36 at-% Fe, at 725°C 0.43 at-%, at 500°C 0.50 at-%, and at 400°C 0.70 at-% (Makovicky et al., 1990; Makovicky & Karup-Møller, 1995). At the maximum Fe-content, Pt-free vysotskite can be stable without any, or less Ni than established in the Fe-free PtS-PdS-NiS system.

Since not all analyses of braggite and vysotskite from the Sompujärvi Reef contain Fe, a more likely scenario is possibility (ii), that the originally magmatic braggite and vysotskite suffered overprinting by fluids (Merkle, publication in preparation) and the Ni was removed in that way and no temperature estimation is possible under those circumstances.



Table 26: Selected braggite (br) and vysotskite (vy) analysis from the Sompujärvi Reef of the Penikat Intrusion, Northern Finland.

Mineral		vy	vy	vy	br	br
W	S	23.12	22.42	20.87	20.83	19.91
	Rh	<0.11	0.18	0.12	<0.11	<0.11
	Pd	67.39	60.31	54.43	53.32	45.25
	Pt	6.79	13.64	21.06	24.48	31.4
	Ni	2.57	2.81	2.67	1.32	2.44
	Co	<0.02	<0.02	<0.02	<0.02	<0.02
	Cu	<0.03	<0.03	<0.03	0.04	<0.03
%	Fe	0.49	<0.02	0.17	<0.02	0.31
	Total	100.36	99.38	99.33	99.99	99.41
A	S	50.01	50.44	49.29	50	49.47
	Rh	-	0.12	0.09	-	-
	Pd	43.92	40.89	38.75	38.56	33.88
	Pt	2.41	5.04	8.18	9.66	12.82
	Ni	3.07	3.46	3.44	1.73	3.31
	Co	-	-	-	-	-
	Cu	-	-	-	0.05	-
%	Fe	0.61	-	0.24	-	0.44

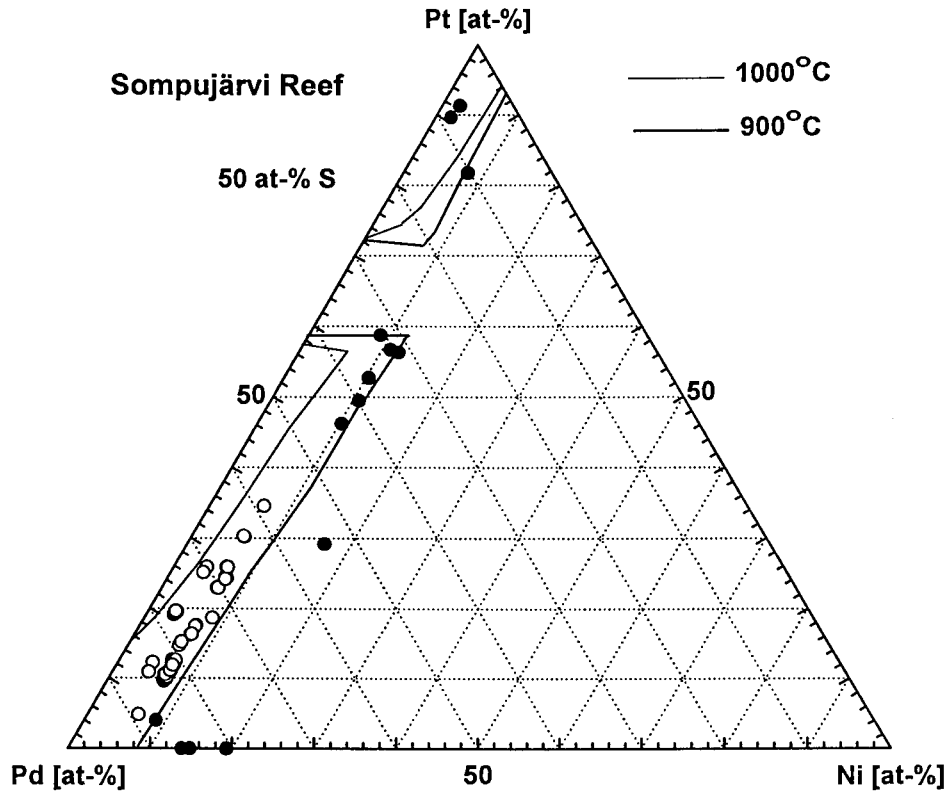


Figure 93 Compositional variation in cation proportions of braggite and vysotskite from the Sompujärvi Reef (this study = empty circles) and analysis from the AP 1 mineralization (from Halkoaho, 1989 = solid circles). The solid lines indicate the compositional trend established for 1000°C and 900°C.

9.3 SELECTED ANALYSES FROM THE LITERATURE

9.3.1 Placer Deposits

Cabri et al. (1996) published a comprehensive summary of analyses of cooperite and braggite from placer deposits throughout the world. In Figure 94 the analyses from Chindwin River Area in Burma, Borneo in Malaysia, Western Chukot in Russia, Chocó Area in Colombia, and the Esmeraldas Province in Ecuador are plotted (Cabri et al., 1996).

Cooperite and braggite (no vysotskite was observed) from placer deposits occur mainly in Pt-Fe nuggets and are rarely observed as discrete grains (Cabri et al., 1996). Most mineralogical and petrological studies of PGE-bearing grains and nuggets from worldwide deposits have confirmed a primary origin of PGM, which have formed under magmatic conditions in mafic to ultramafic intrusions (Cabri et al., 1996). The exact conditions (e.g. sulphur fugacity and Fe- and Ni-saturation) are, however, difficult to pinpoint. Therefore, an estimation of the temperature of formation or equilibration based on this study is not viable.

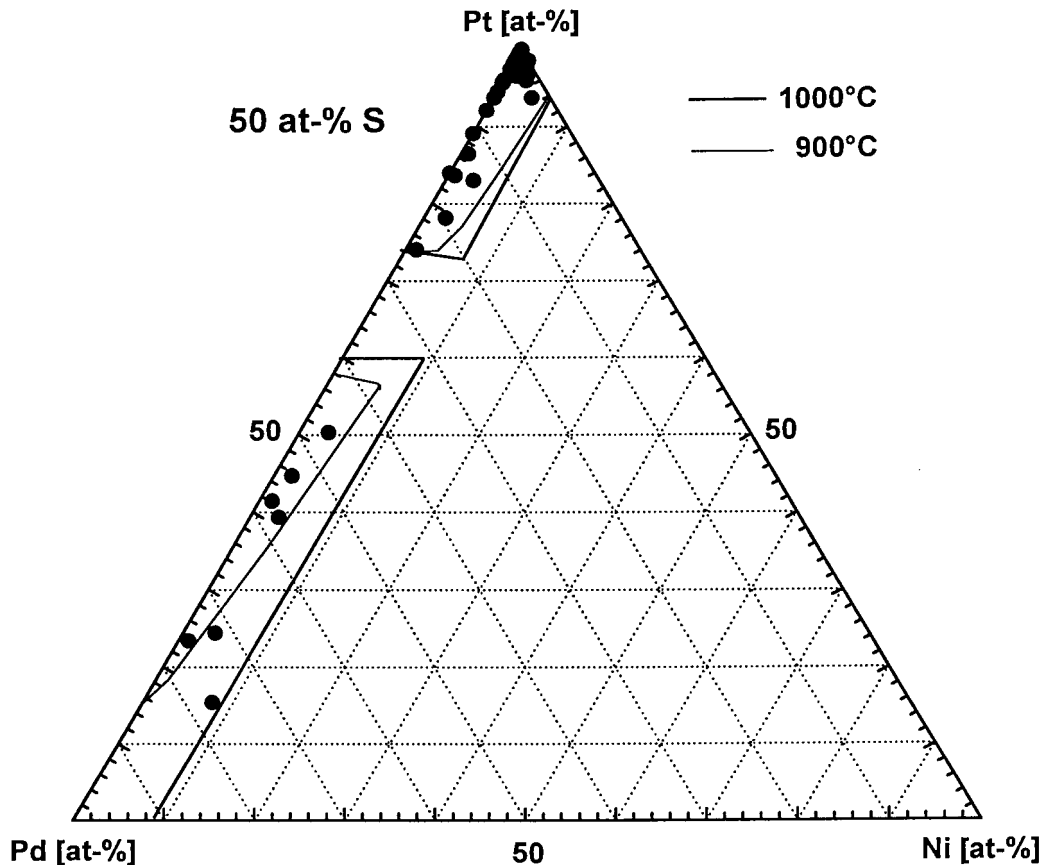


Figure 94 Compositional variation in cation proportions of cooperite and braggite from Placer deposits (from Cabri et al., 1996). The solid lines indicate the compositional trend established for 1000°C and 900°C.

9.3.2 The J-M Reef - Stillwater Complex, Montana

The J-M Reef of the Stillwater Complex is a striking counterpart of the Merensky Reef of the Bushveld Complex (Todd et al., 1982). Collectively cooperite, braggite, and vysotskite represent the most common PGE minerals at Stillwater. Analyses from the literature are presented graphically in Figure 95.

Cooperite seems to associate closely with Pt-Fe alloy, whereas braggite and vysotskite seem to be associated with millerite (Volborth et al., 1986). It could, therefore, be assumed that braggite and vysotskite formed under Ni-saturated conditions and, according to this experimental investigation, mostly at temperatures below 700°C.

The extremely Ni-poor cooperite associated with Pt-Fe alloy (Fig. 95) from the Stillwater

Complex may have formed under more Fe-rich conditions than braggite and vysotskite and temperature of formation or equilibration cannot be estimated. The slightly Ni-richer cooperite (Fig. 95) may have formed at temperatures below 900°C.

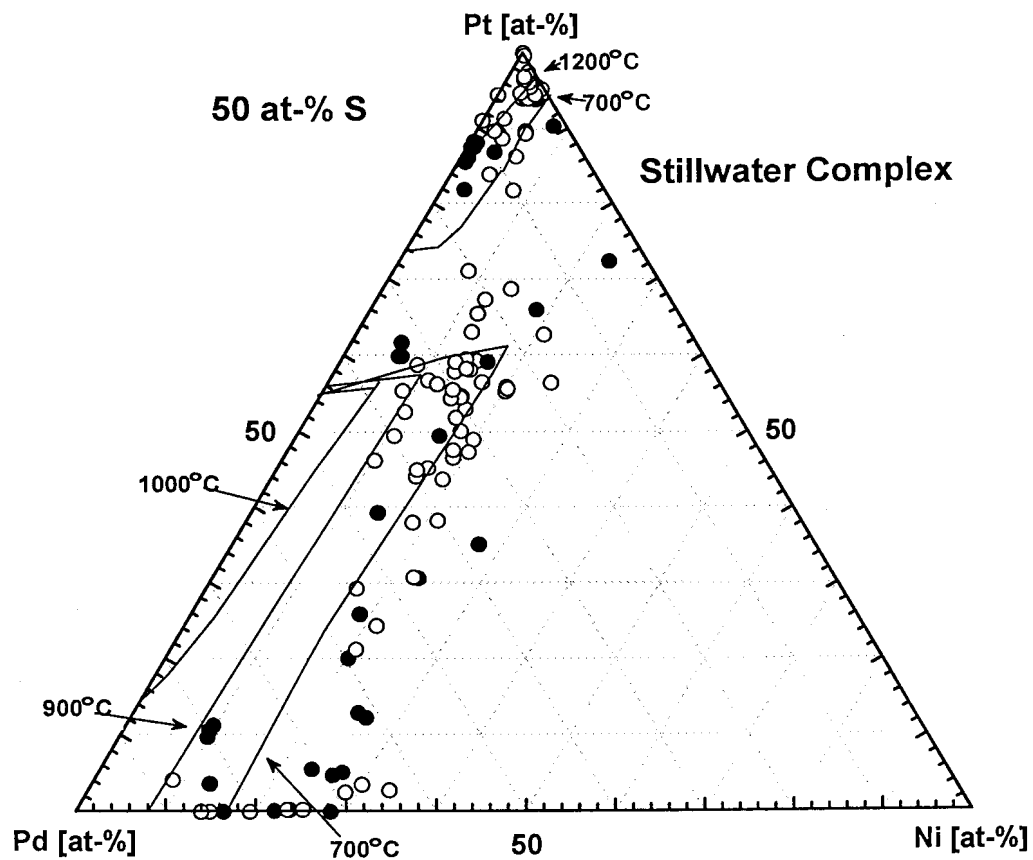


Figure 95 Compositional variation in cation proportions of cooperite, braggite, and vysotskite from layered intrusions taken from the literature. The solid circles are analyses from the Stillwater Layered Intrusion (Todd et al., 1982; Criddle & Stanley, 1985; Volboth et al., 1986) and the solid lines indicate the compositional trends established for the temperatures indicated.

9.3.3 Noril'sk

The Cu-Ni-PGE mineralization at Noril'sk occurs in three different ore types (Genkin & Evstigneeva, 1986) :

- (i) Disseminated sulphides consisting of pyrrhotite, pentlandite, and chalcopyrite. Pt- minerals (e.g. cooperite and Pt-Fe alloys) dominate over Pd-minerals.
- (ii) Massive ores consisting mainly of pyrrhotite, Pt-minerals predominate.
- (iii) Disseminated, vein-disseminated, and breccia ores consisting predominantly of pyrrhotite or chalcopyrite and contain cooperite, braggite, and vysotskite.

The association of cooperite, braggite, and vysotskite from Noril'sk with pyrrhotite suggests that these minerals formed under Fe-saturated conditions. Following the discussions in Chapter 8.3 only maximum formation temperatures can be estimated. Cooperite from Noril'sk may have formed at a maximum temperature of 700°C and braggite and vysotskite at temperatures below 700°C. According to Genkin & Evstigneeva (1986) the formation of Pt-Pd sulphides is manifested in the veinlet-disseminated and breccia ores from Noril'sk, supporting the low temperature of formation or equilibration deduced from this study for braggite and vysotskite. The Ni-content increases with increasing Pd-content in the analyses of braggite and vysotskite from Noril'sk, possibly indicating that the hydrothermal solution became enriched in Pd relative to Pt as the temperature decreased (Fig. 96).

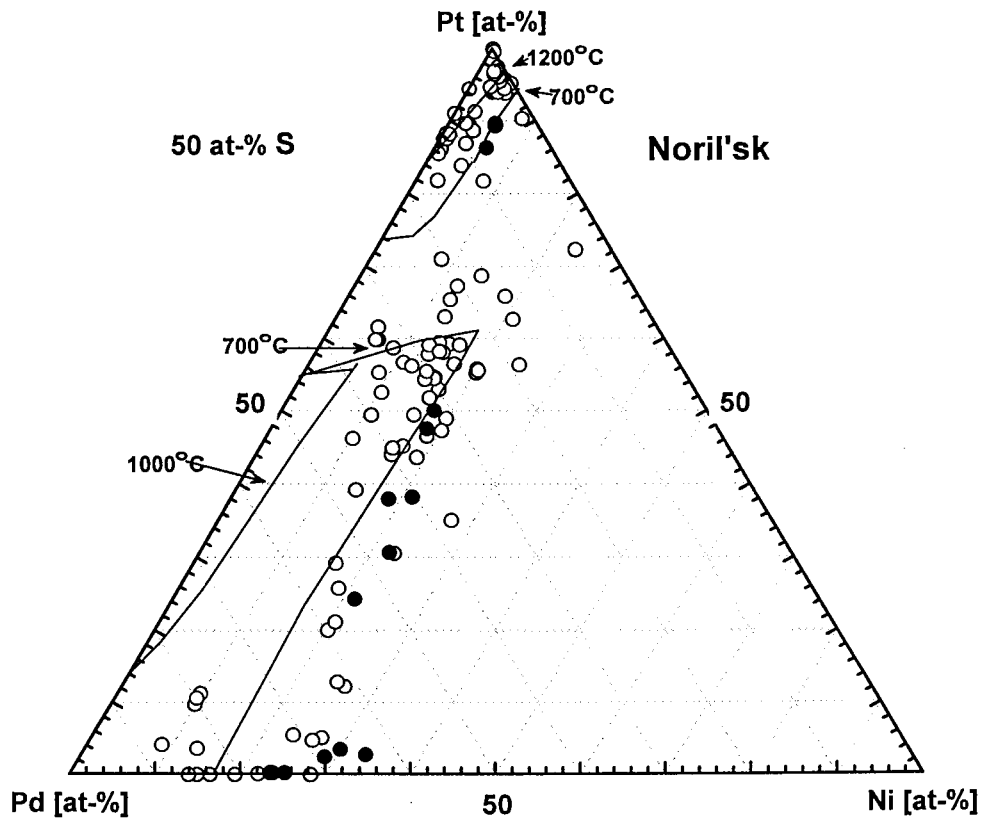


Figure 95 Compositional variation in cation proportions of cooperite, braggite, and vysotskite from layered intrusions taken from the literature. The solid circles are analyses from Noril'sk (Genkin & Evstigneeva, 1986; Laputina & Genkin, 1975; and unpublished data) and the solid lines indicate the compositional trends established for the temperatures indicated.

8.3.4 Bushveld Complex

Cooperite- and braggite analyses from the Bushveld Complex gathered from the literature (Fig. 97) originate from the Merensky Reef (Bannister & Hey, 1932; Schweltnus et al., 1976; Cabri et al., 1978; Kingston & El-Dosuky, 1982; Mostert et al., 1982; Criddle & Stanley, 1985; Tarkian, 1987). Most analyses of cooperite and braggite (except those falling into the field surrounded by the stippled line) in Figure 97 show similar compositional variations to those of cooperite and braggite from the Merensky Reef obtained in this study (see Chapter 9.1.1) and the discussion concerning the deduction of the temperature of formation or equilibration is applicable to the analyses from the literature as well, i.e. cooperite and braggite have formed or equilibrated at a temperature $\leq 900^\circ\text{C}$.

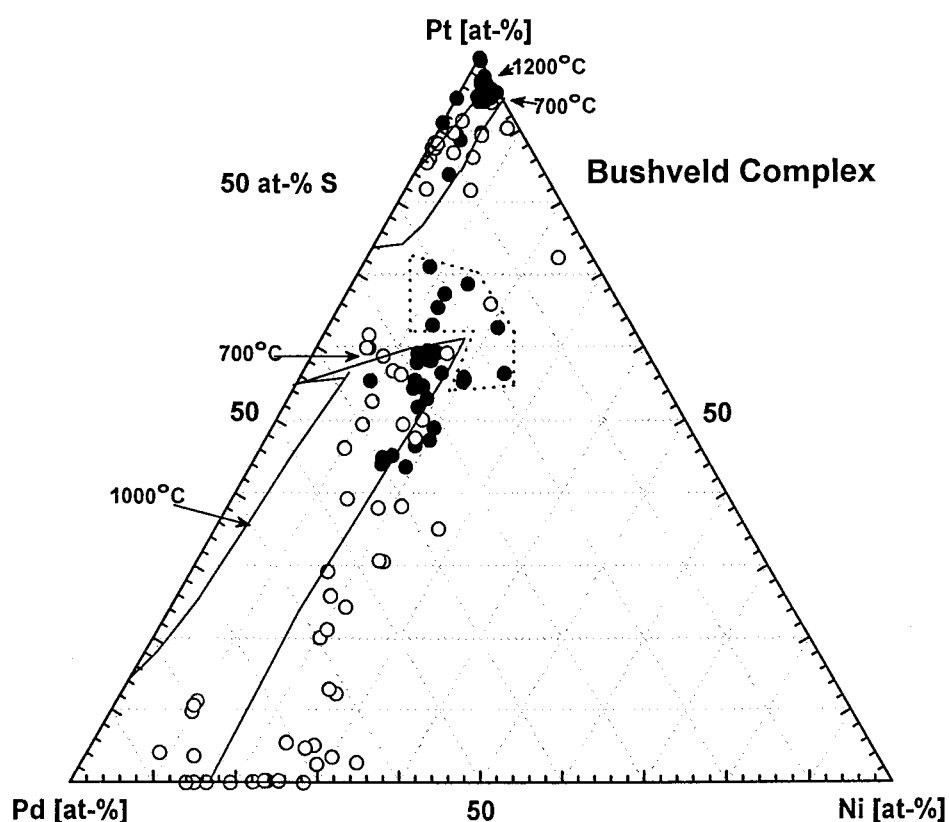


Figure 96 Compositional variation in cation proportions of cooperite, braggite, and vysotskite from layered intrusions taken from the literature. The solid circles are analyses from the Bushveld Complex (Bannister & Hey, 1932; Cabri et al., 1978; Criddle & Stanley, 1985; Kingston & El-Dosuky, 1982; Mostert et al., 1982; Schweltnus et al., 1976; Tarkian, 1987) and the solid lines indicate the compositional trends established for the temperatures indicated. Analyses falling into the field surrounded by the thick stippled line are referred to in the text.

9.3.5 “Problem Cases”

According to this experimental investigation, compositions represented by solid circles in Figure 98 should not be possible as they fall into the miscibility gap between cooperite and braggite or contain higher amounts of Ni than experimentally established. Analyses plotting on the Ni-rich side of the trend experimentally established in this study for 700°C are most likely due to formation or equilibration at temperatures below 700°C. The Pt/Pd ratio of analyses plotting outside, but close to the miscibility gap experimentally established, may be a result of the use of different standards in the calibration for the microprobe analysis than utilized in this study.

Analyses of the “problem cases” numbered 1 to 9 in Figure 98 followed by the reference originating from, are discussed individually below:

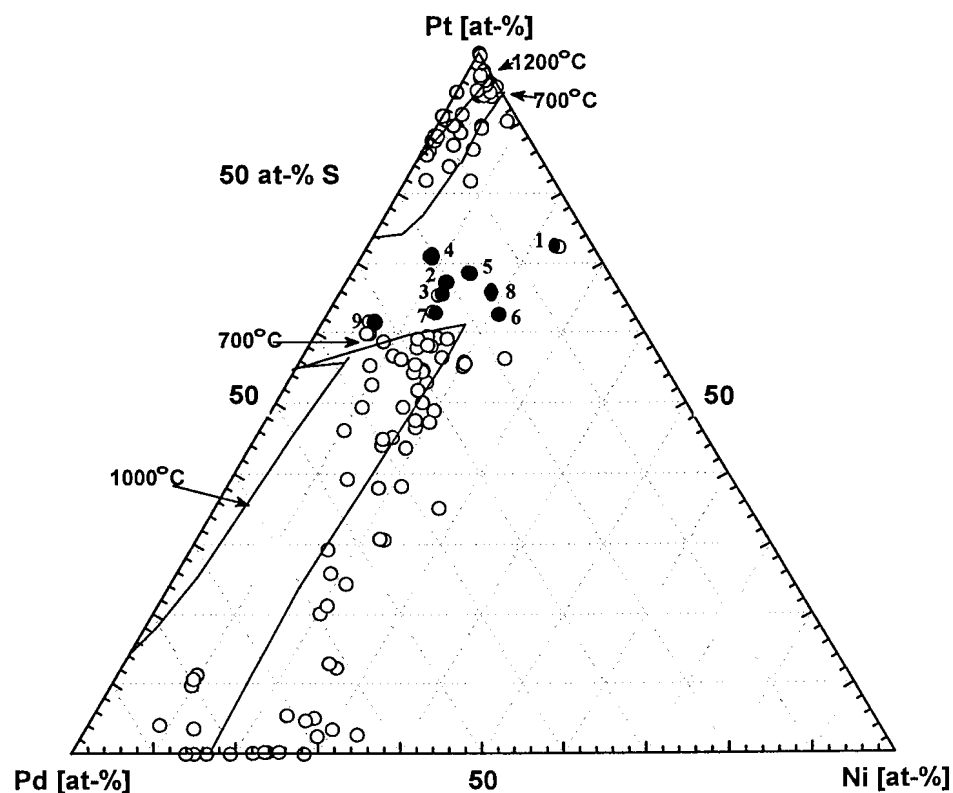


Figure 97 Compositional variation in cation proportions of cooperite, braggite, and vysotskite from layered intrusions taken from the literature. The solid circles are “problem” analyses and are discussed in the text. The solid lines indicate the compositional trends established for the temperatures indicated.

- 1** (Volboth et al., 1986)
The authors state that braggite often occurs associated with millerite, therefore analyses 1 could represent an analyses close to a grain boundary between cooperite and millerite, resulting in the abnormally high Ni-content through interference with the neighbouring millerite grain.
- 2 & 3** (Kingston & El-Dosuky, 1982)
The authors describe intergrowths of cooperite and braggite, therefore the analyses may represent analyses close to, or at the grain boundary between cooperite and braggite.
- 4, 5 & 8** (Schwellnus et al., 1976)
These analyses contain up to 1.1 wt-% Pb and 0.9 wt-% Bi possibly representing unusual conditions. The experimental results obtained in this study may, therefore, not be applicable. The analyses may also represent analyses close to grain boundaries between cooperite and braggite. Coexisting cooperite and braggite have, however, not been described by the authors.
- 6** (Mostert et al., 1982)
The analysis appears to be analytically sound and may represent a formation or equilibration temperature of the braggite grain below 700°C.
- 9** (Criddle & Stanley, 1985)
This analysis contains 54 at-% S and may therefore not be analytically correct.

CHAPTER 10

CONCLUSIONS

10 CONCLUSIONS

With reference to the objectives of this study cited in the introduction (Chapter 1) the following can be concluded:

(i) "To establish the temperature dependance of stability fields and phase relations of the mineral phases, as well as miscibility gaps between synthetic cooperite and braggite":

- ◆ Cooperite, braggite and vysotskite (natural and synthetic) have to be represented by the system PtS-PdS-NiS rather than Pt-Pd-S.
- ◆ There is a clearly defined miscibility gap between cooperite and braggite, but no evident gap exists between braggite and vysotskite. The miscibility gap between "cooperite" and "braggite" formed in a Ni-free environment becomes slightly larger with decreasing temperature. For "cooperite" and "braggite", formed in a Ni-saturated environment, the position of the miscibility gap between the two minerals shifts slightly to Pt-rich compositions with decreasing temperature.
- ◆ With decreasing temperature the compositional fields of "cooperite", as well as that of "braggite-vysotskite" become enlarged in the direction of the PtS - NiS join, whereas the compositional field of the melt shrinks with decreasing temperature, disappearing totally at 800°C. "Braggite" is only stable at temperatures below 1100°C and "vysotskite" only below 1000°C. "Cooperite" is stable at temperatures above 1200°C. The upper stability limit has not been determined..

(ii) "To investigate the influence of temperature on maximum Ni-solubility in cooperite, braggite, and vysotskite":

- ◆ The Ni-content of "braggite" and "vysotskite" with varying Pt/Pd ratios in a Ni-saturated environment is a function of temperature, i.e., a higher Ni-content indicates a lower equilibration temperature.

- ◆ In “cooperite”, there is a similar relationship between the Ni-content and the temperature of formation or equilibration, but this is only applicable between 1200° and 1000°C, because the Ni-content in “cooperite” increases with increasing temperature at a relatively constant Pt-content between 1200°C and 1000°C. In “cooperite” formed at 900°C, however, the Ni-content decreases with increasing Pt-content. In “cooperite” formed at 700°C, the Ni-content is lower than that at 800°C.

(iii) “To determine trends in Ni-content of synthetic cooperite, braggite, and vysotskite related to their Pt- and Pd-content and temperature of synthesis in order to estimate temperatures of formation or equilibration of naturally occurring cooperite, braggite, and vysotskite”:

- ◆ The compositions of “cooperite”, “braggite”, and “vysotskite”, have the potential to indicate at which stage of the development of an ore deposit these phases were exsolved or suffered overprinting by fluids:
 - ◆ The temperature of formation or equilibration of cooperite occurring in a Ni-saturated environment can be estimated using Figure 85 according to Chapter 8.1.
 - ◆ Assuming Ni-saturation, the temperature of formation or equilibration of braggite and vysotskite can be estimated using Equation 42 (i.e.: $\text{Temp [C}^\circ] = 998.07 (\pm 7.88) + 0.05 (\pm 0.02) \times \text{Pt}^2 - 4.24 (\pm 0.16) \times \text{Ni}^2$) for predicted temperatures between 1000°C and 700°C.
 - ◆ Formation- or equilibration temperatures of cooperite, braggite, and vysotskite formed in an Fe±(Cu)±(Co) - saturated environment cannot be estimated using the data produced in this study as the maximum Ni-content in cooperite, braggite, and vysotskite may be lowered by the presence of Fe. Assuming that no other elements play a role in the compositional variation, maximum formation temperatures are, however, not influenced.

- ◆ Maximum solubility of Pd in “cooperite” and maximum Pt-solubility in “braggite” of coexisting “cooperite” - “braggite” pairs, however, show only a limited sensitivity to temperature of formation and cannot be used with confidence as an indication for conditions of formation.

(iv) “To compare the results of the experimental investigation with compositions of naturally occurring phases determined in this study and compositions from the literature, in order to give indications of their temperature of formation or equilibration”:

- ◆ After establishment of the mineral association of cooperite, braggite, and vysotskite in the natural material studied, comparison of the experimental results with data of natural cooperite, braggite, and vysotskite of this study as well as data taken from the literature indicate that:
 - ◆ Cooperite- and braggite grains analysed in this study as well as those taken from the literature from the Merensky Reef have formed below 900°C.
 - ◆ Cooperite, braggite, and vysotskite from the UG-2 used in this study occur in two different BMS assemblages. In one assemblage, the main Ni-bearing phase associated with cooperite, braggite, and vysotskite is pentlandite; and in the other assemblage millerite and only traces of pentlandite are the main Ni-bearing phases associated with cooperite, braggite, and vysotskite. The different associations indicate different activity of NiS and could therefore be expected to have an effect on the Ni-content of the cooperite, braggite, and vysotskite. Most of the braggite and vysotskite compositions associated with pentlandite (lower NiS-activity) follow the trend experimentally established for temperatures $\leq 700^{\circ}\text{C}$. Most of the braggite compositions associated with millerite (higher NiS-activity) follow the trend established for temperatures between 800°C and 700°C. This indicates that temperature of formation or equilibration, rather than Ni-activity, is the dominant factor for the Ni-content within braggite and vysotskite from the UG-2 of the Bushveld Complex.



- ◆ Assuming that braggite and vysotskite of the Sompujavi Reef of the Penikat Intrusion have formed under purely magmatic conditions in a Ni-saturated environment their temperature of formation lies between 1000°C and 900°C. The originally magmatic braggite and vysotskite may, however, have suffered overprinting by fluids (Merkle, publication in preparation) and the Ni could have been removed in that way.
- ◆ Most analyses of braggite and vysotskite from placer deposits throughout the world published by Cabri et al. (1996) show very low Ni-contents. The exact conditions of formation or equilibration (e.g. sulphur fugacity and Fe- and Ni-saturation) are difficult to pinpoint. Therefore, estimation of formation- or equilibration temperatures based on this study is not possible
- ◆ Analysis of cooperite, braggite and vysotskite from Noril'sk taken from the literature indicate that cooperite from Noril'sk may have formed at a maximum temperature of 700°C and braggite and vysotskite at temperatures below 700°C.
- ◆ Braggite and vysotskite from the Stillwater Complex formed mostly at temperatures below 700°C. As most analyses of cooperite contain almost no Ni, a temperature of formation or equilibration cannot be estimated. Some slightly Ni-richer cooperite may have formed at temperatures below 900°C.

Further information emerging from this study:

- ◆ There are significant positive relationships between the Pd-content of “cooperite”, “braggite” and, “vysotskite” and the Pd-content of the coexisting melt or the Pd-content of the coexisting $Ni_{1-x}S$.
- ◆ The Pd- and Pt-content within “cooperite”, “braggite”, and “vysotskite” show strong negative correlations at all temperatures.
- ◆ $Ni_{1-x}S$ may act as a collector for Pd (2.1 at-% Pd at 900°C) but its significance decreases with decreasing temperatures (0.99 at-% Pd at 700°C). The solubility of Pt in $Ni_{1-x}S$ is not as high (0.29 at-% Pt at 900°C down to 0.07 at-%Pt at 700°).
- ◆ Sulphur fugacity has an effect on the system PtS-PdS-NiS:
 - ◆ The melt formed at 1000°C in the charges initially containing below 50 at-% S shows a lower Pd/Ni ratio (in at. prop.) than melt formed in charges initially containing more than 50 at-% S, when coexisting with braggite and/or cooperite of similar composition. The melts of the low sulphur charges also contain systematically slightly more Pt than the melt formed in the charges with an initially higher sulphur content.
 - ◆ “Braggite” synthesized at 1000°C contains higher amounts of Ni at given Pt/Pd ratios in the initial charge, if formed under higher S-pressure. The Ni-content in the “braggite” increases with increasing Pt/Pd ratio at relatively constant S-pressure.
 - ◆ Within each group of constant bulk Pt/Pd ratio, the Pt/Pd ratio of the quenched “braggite” decreases with increasing sulphur fugacity.
 - ◆ In “cooperite” synthesised at 1000°C, there is a similar dependance of the relationship between the Pt/Pd ratio and the Ni-content on the S-pressure as in “braggite”.

Recommendations for further investigations:

In order to understand fully the compositional variation of cooperite, braggite, and vysotskite, the following suggestions for further investigations are made:

- ◆ This experimental investigation was limited to the minerals “cooperite”, “braggite”, and “vysotskite” in the system PtS-PdS-NiS. The effect of S-content on the system was only touched on in the 1000°C isothermal section and should be investigated further.
- ◆ The influence of other cations such as Fe, Cu, and Co was not investigated. It is known that the presence of Fe in the system has a pronounced effect on the compositional variation of “vysotskite” (Makovicky et al., 1990; Karup-Møller & Makovicky, 1993; Makovicky & Karup-Møller, 1995). It can be assumed that this influence of Fe on the “vysotskite” composition also impacts on the “cooperite” and “braggite” compositions. As the association of PGE with sulphides, particularly pyrrhotite-pentlandite-chalcopyrite, is the most common and most important economic association of the PGE (Crocket, 1981), it will be necessary to study the influence of Fe as well as that of Cu on the system Pt-Pd-Ni-S.
- ◆ Another obstacle in using the high-temperature data presented in this study in the interpretation of geological occurrences of cooperite, braggite, and vysotskite are the problems of overprinting (e.g. hydrothermal overprinting) leading to later subsolidus reactions in the PGE deposits. The study of the system PtS-PdS-NiS should be expanded to temperatures below 700°C in order to determine whether the trends established between 1200°C and 700°C continue at lower temperatures.

CHAPTER 11

ACKNOWLEDGEMENTS

11 ACKNOWLEDGEMENTS

I am very grateful to my promoter, Professor Roland K. W. Merkle, for his moral support, advice, and intellectual assistance, which made this dissertation possible.

Financial support for the purchase of most of the very expensive raw materials needed in this study was given by Professor Roland K. W. Merkle and some raw material was donated by Amplats - thank you.

I also wish to thank the University of Pretoria for the opportunities, which were created for the further advancement of my education. Likewise I would like to thank my colleagues at the Department of Earth Sciences for their continuous encouragement.

The constructive comments by the external examiners Professor S. Karup-Møller and Professor M. Tarkian are greatly appreciated.

During the weeks, months and years of work on this journey, I discovered, that the journey could not be completed without the considerable sacrifice and teamwork of my husband, Steve. It is with deep admiration, that I thank Steve for his half of the work.

Last, but not least, I want to thank my children, Sandra, Nadine, and Mark for their patience.

CHAPTER 12

REFERENCES

12 REFERENCES

- Alapieti, T. & Lahtinen, J.J. (1986) Stratigraphy, petrology, and platinum-group element mineralization of the early Proterozoic Penikat layered intrusion, northern Finland. *Economic Geology*, **81**, 1126-1136.
- Arnold , R. G. (1971) Evidence for liquid immiscibility in the system FeS - S. *Economic Geology*, **66**, 1121-1130.
- Arnold , R.G. & Malik, O.P. (1975) The NiS-S System above 980°C - A Revision. *Economic Geology*, **70**, 176-182.
- Bannister, F.A. & Hey, M.H. (1932) Determination of minerals in platinum concentrates from the Transvaal by X-ray methods. *Mineralogical Magazine*, **28**, 188-206.
- Barin, O., Knacke, O. & Kubaschewski, O. (1977) **Thermochemical properties of inorganic substances (Supplement)**, Springer Verlag Berlin, Heidelberg, New York, 861pp.
- Barkov, A. Yu., Pakhomovskii, Y.A. & Men'shikov, Y.P. (1995) Zoning in the platinum-group sulphide minerals from the Lukkulaisvaara and Imandrovsky layered intrusions, Russia. *Neues Jahrbuch der Mineralogie, Abhandlungen*, **169(2)**, 97-117.
- Bruwer, J.S. (1996) **Experimental investigation of phase relations in the system Cu-Ni-S in the temperature range 1200°C to 700°C**. MSc Thesis, University of Pretoria, Pretoria, South Africa, 157 pp.
- Brynard, H.J., De Villiers, J.P.R. and Viljoen, E.A. (1976) A mineralogical investigation of the Merensky Reef at the Western Platinum Mine, near Marikana, South Africa. *Economic Geology*, **71**, 1299-1307.

- Cabri, L.J., Harris, D.C. & Weiser, T.W. (1996) Mineralogy and distribution of platinum-group mineral (PGM) placer deposits of the world. *Exploration and Mining Geology*, **5**, 73-167.
- Cabri, L.J., Laflamme, J.H.G., Steward, J.M., Turner, K. & Skinner, B.J. (1978) On cooperite, braggite, and vysotskite. *American Mineralogist*, **63**, 832-839.
- Cabri, L.J. & Laflamme, J.H.G. (1981) Analyses of Minerals Containing Platinum-Group Elements. In: **Platinum-Group Elements: Mineralogy, Geology, Recovery**, ed. by L.J. Cabri, CIM Special Volume 23, Chapter 8.
- Craig, J.R & Scott, S.D. (1974) Sulphide Phase Equilibria, In: **Sulphide Mineralogy**, ed. by P.H. Ribbe, Mineralogical Society of America, Washington DC, Vol.1 Chapter 5, C1-104.
- Criddle, A.J. & Stanley, J.S. (1985) Characteristic optical data for cooperite, braggite, and vysotskite. *Canadian Mineralogist*, **23**, 149-169.
- Crocket, J. H. (1981) Geochemistry of the Platinum-Group Elements. In: **Platinum-Group Elements: Mineralogy, Geology, Recovery**, ed. by L.J. Cabri, CIM Special Volume 23, Chapter 4.
- Genkin, A.D. & Evstigneeva, T.L. (1986) Associations of platinum-group minerals of the Noril'sk copper-nickel sulphide ores. *Economic Geology*, **81**, 1203-1212.
- Halkoaho, T. (1989) Ala-PeniKan Platinametalli-Mineralisaatiot Penikkain Kerrosintruusiossa. Raportti No: 2, Peräpohjan platinaprojekti, Oulun Yliopisto, Oulu, 221pp.
- Halkoaho, T.A.A., Alapieti, T.T. & Lahtinen, J.J. (1990) The Sompujärvi PGE reef in the Penikat layered intrusion, northern Finland. *Mineralogy Petrology*, **42**, 39-55.

- Halkoaho, T.A.A. (1994) The Sompujärvi and Ala-Penikat PGE reefs in the Penikat layered intrusion, northern Finland. *Acta Universitatis Ouluensis, Series A, Scientiae Renum Naturalium*, **249**, 1-122.
- Hansen, M. & Anderko, K. (1958) **Constitution of binary alloys**. 2nd ed.: New York, McGraw-Hill Book Co., 1305pp.
- Huhtelin, T.A., Alapieti, T.T. & Lahtinen, J.J. (1990) The Pasivaara PGE reef in the Penikat layered intrusion, northern Finland. *Mineralogy and Petrology*, **42**, 57-70.
- International Centre for Diffraction Data (ICDD) (1995) **Powder Diffraction File 2 (PDF2), Sets 1-45**, Newton Square Corporate Campus, USA.
- Kaiser, H. & Specker, H. (1956) Bewertung und Vergleich von Analysenverfahren. *Zeitschrift für Analytische Chemie*, **149**, 46-66.
- Karup-Møller, S. & Makovicky, E. (1993) The system Pd-Ni-S at 900°, 725°, 550°, and 400°C. *Economic Geology*, **88**, 1261-1268.
- Kingston, G.A. & El-Dosuky, B.T. (1982) A contribution on the platinum-group mineralogy of the Merensky Reef at the Rustenburg Platinum Mine. *Economic Geology*, **71**, 1299-1307.
- Kinloch, E.D., (1982) Regional trends in the platinum-group mineralogy of the Critical Zone of the Bushveld Complex, South Africa. *Economic Geology*, **77**, 1328-1347.
- Kullerud, G. & Yund, R.A. (1962) The Ni-S system and related minerals. *Journal of Petrology*, **3**, 126-175.
- Kullerud, G. (1971) Experimental techniques in dry sulphide research. In: **Research Techniques for High Pressure and High Temperature**, ed. by G.C. Ulmer, Springer Verlag, Berlin-Heidelberg-New York, 289-315.

- Laputina, I.P. & Genkin, A.D. (1975) Minerals of the braggite-vysotskite series. *Izomorpizm Mineraly*, Izdat. Nauka, 146-150 (in Russian).
- Lin R.Y., Hu, D. & Chang, Y.A. (1978) Thermodynamics and phase relationships of transition metal-sulphur systems: II. The nickel-sulphur system. *Metallurgical Transactions B*, **9B**, 531-538.
- Makovicky, E., Karup-Møller, S., Makovicky, M. & Rose-Hansen, J. (1990) Experimental studies on the phase systems Fe-Ni-Pd-S and Fe-Pt-Pd-As-S applied to PGE deposits. *Mineralogy and Petrology*, **42**, 307-319.
- Makovicky, E. & Karup-Møller, S. (1995) The system Pd-Fe-Ni-S at 900 and 725°C. *Mineralogical Magazine*, **59**, 685-702.
- Massalski T.B. (Ed) 1986) **Binary Alloy Phase Diagrams Volume 1**, American Society for Metals, 2 Volumes, Ohio, 2224pp.
- McLaren, C.H. & De Villiers, J.P.R. (1982) The platinum-group chemistry and mineralogy of the UG-2 chromitite layer of the Bushveld Complex. *Economic Geology*, **77**, 1348-1366.
- Merkle, R.K.W. & Verryn, S.M.C. (1991) Coexisting cooperite and braggite - new data. *Papers, International Congress on Applied Mineralogy, 1991*. Pretoria, South Africa, Paper **61**, 17pp.
- Merkle, R.K.W. (1992) Platinum-group minerals in the middle group of chromitite layers at Marikana, western Bushveld Complex: indications for collection mechanisms and postmagmatic modifications. *Canadian Journal of Earth Sciences*, **29**, 209-221.
- Merkle, R.K.W., Piki, R., Verryn, S.M.C. & De Waal, D. (1997) A Raman spectroscopic investigation of synthetic "cooperite", (Pt,Pd,Ni)S. *Neues Jahrbuch für Mineralogie Monatshefte*, 518-528.

- Merkle, R.K.W., Piki, R., Verry, S.M.C. & De Waal, D. (1999) Raman spectra of synthetic "braggite", (Pd,Pt,Ni)S. *Mineralogical Magazine*, **63(3)**, 363-367
- Moffat, W.G. (1984) **The Handbook of binary phase diagrams**, 3 Volumes. Schenectady, New York, General Electric Co.
- Moh, G.H. & Taylor, L.A. (1971) Laboratory techniques in experimental sulphide petrology. *Neues Jahrbuch für Mineralogie, Monatshefte*, 450-459.
- Mostert, A.B., Hofmeyr, P.K. & Potgieter, G.A. (1982) The platinum-group mineralogy of the Merensky Reef at the Impala Platinum Mines, Bophuthatswana. *Economic Geology*, **77**, 1385-1394.
- Nell, J. (1987) Phase Relations in the system Nickel-Copper-Sulphur-Ruthenium at 1200°C. Mintek Report No. M307, 8pp.
- Nickel, E.H. (1995) Mineral names applied to synthetic substances. *Canadian Mineralogist*, **33**, 1335.
- Ott, L. (1988) **An introduction to statistical methods and data analysis**, PWS-Kent Publishing company, Boston, Massachusetts, 835pp
- Penberthy, C.J. & Merkle R.K.W. (1999) Lateral variations in the platinum group element content and mineralogy of the UG2 Chromitite Layer, Bushveld Complex. *South African Journal of Geology*, **102(3)**, 240-250.
- Peyrerl, W. (1982) The influence of the Driekop dunite pipe on the platinum-group mineralogy of the UG-2 chromitite in its vicinity. *Economic Geology*, **77**, 1432-1438.
- Piki, R., de Waal, D., Merkle, R.K.W. & Verry, S.M.C. (1998) Raman spectra and factor group analysis of synthetic "braggite", (Pt,Pd,Ni)S. *Proceedings of the XVIth International Conference on Raman Spectroscopy*, Cape Town, Sept. 1998; **in press**

- Pikl, R., De Waal, D., Merkle, R.K.W. & Verryyn, S.M.C. (1999) Raman spectroscopic identification of synthetic "braggite" (Pd,Pt,Ni,S) samples in comparison with synthetic "cooperite". *Applied Spectroscopy*, **53(8)**, 927-930.
- Reid, A.M., le Roex, A.P. & Winter, W.E.L. (1988) Composition of gold grains in the Vaal Placer, Klerksdorp, South Africa, *Mineralium Deposita.*, **23**, 211-260.
- Schwellnus J.S.I, Hiemstra, S.A. & Gasparrini, E. (1976) The Merensky Reef at the Atok Platinum Mine and its environs. *Economic Geology*, **71**, 249-260.
- Skinner, B.J., Luce, F.D., Dill, J.A., Ellis, D.E., Hagan, H.A., Lewis, D.M., Odell, D.A., Sverjensky, D.A. & Williams, N. (1976) Phase relations in ternary portions of the system Pt-Pd-Fe-As-S. *Economic Geology*, **71**, 1469-1475.
- StatSoft, Inc. (1995). **STATISTICA for Windows** [Computer program manual]. Tulsa, OK: StatSoft, Inc., 2300 East 14th Street, Tulsa, OK, 74104-4442, (918) 749-1119, fax: (918) 749-2217, e-mail: info@statsoft.com, WEB: <http://www.statsoft.com>.
- Tarkian, M. (1987) Compositional variations and reflectance of the common platinum-group minerals. *Mineralogy and Petrology*, **36**, 169-190.
- Taylor, J.R. (1985) Phase relationships and thermodynamic properties of the Pd-S system. *Metallurgical Transactions B*. **16B**, 143-148.
- Todd, S.G., Keith, D.W., Le Roy, L.W., Schissel, D.J., Mann, E.L. & Irvine, T.N. (1982) The J-M platinum-palladium reef of the Stillwater Complex, Montana: I. Stratigraphy and petrology. *Economic Geology*, **77**, 1454-1480.
- Uytenbogaart W. & Burke, E.A.J (1971) **Tables for Microscopic Identification of Ore Minerals**. Elsevier Scientific Publishing Company, Amsterdam.

- Vermaak, C.F. & Hendriks, L.P. (1976) A review of the Mineralogy of the Merensky Reef, with Specific Reference to New Data on the Precious Metal Mineralogy. *Economic Geology*, **71**, 1244-1269.
- Verryn, S.M.C & Merkle, R.K.W. (1994) Compositional variation of cooperite, braggite, and vysotskite from the Bushveld Complex. *Mineralogical Magazine*, **58**, 223-234.
- Verryn, S.M.C & Merkle, R.K.W. (1996) Observations on factors affecting the compositional variation of synthetic "cooperite" in the system Pt-Pd-Ni-S at 1000°C. *Neues Jahrbuch für Mineralogie, Monatshefte*. **10**, 471-482.
- Verryn, S.M.C. and Merkle, R.K.W. (2000) Synthetic "cooperite", "braggite", and "vysotskite" in the system PtS-PdS-NiS at 1100°C, 1000°C, and 900°C. *Mineralogy and Petrology*, **68**, 63-73.
- Von Gruenewaldt, G., Hatton, C.J., Merkle, R.K.W. & Gain S.B. (1986) Platinium-Group Element - Chromitite Associations in the Bushveld Complex. *Economic Geology*, **81**, 1067-1079.
- Volborth, A., Tarkian, M., Stumpfl, E.F. & Housley, R.M. (1986) A Survey of the Pd-Pt mineralization along the 35 km Strike of the J-M Reef, Stillwater Complex, Montana. *Canadian Mineralogist*, **24**, 329-346.
- Westland, A.D. (1981) Inorganic Chemistry of the Platinum-Group Elements. In: **Platinum-Group Elements: Mineralogy, Geology, Recovery**, ed. by L.J. Cabri, CIM Special Volume 23, Chapter 2.
- Wiebke, F. & Laar, J. (1935) *Zeitschrift für anorganische Chemie*, **224**, 49-61.
- Zwiadadze, G.N., Gulyanitskaya, Z.F., Pavlyuchenko, N.M. & Blagoveshchenskaya, N.V. (1982) Examination of Cu-Pd-S and Ni-Pd-S Phase diagrams. *Russian Metallurgy - USSR*, **5**, 40-43

APPENDIX I

EXPERIMENTAL CHARGES

APPENDIX I: EXPERIMENTAL CHARGES

Information about composition, pre-reaction, tempering, and quenching of experimental charges made for the investigation of the system PtS-PdS-NiS at 1200°C, 1100°C, 1000°C, 900°C, 800°C, and 700°C are presented in Table 27.

Abbreviations used in Table 27:

- W = water
- WI = water and ice
- dupl. = duplicate charge
- S = free sulphur visible in charge after quenching

Table 27: Composition of charges, their pre-reaction-, tempering-, and quenching histories for the investigation of the 1200°C, 1100°C, 1000°C, 900°C, 800°C and 700°C isothermal sections.

1200°C

Nr	Weight measured (mg)				Total (mg)	Weight %				Pre-reaction		Temper days	Quench		Remarks	
	Pt	Pd	Ni	S		Pt	Pd	Ni	S	°C	days		°C	day		medium
SV120	143.7	63.9	0	42.6	250.2	57.43	25.54	0.00	17.03	700	53		1	W	05.02.99	S
SV120	145.6	55.2	5.7	43.4	249.9	58.26	22.09	2.28	17.37	700	53		1	W	05.02.99	S
SV120	148.3	45.3	11.4	44.5	249.5	59.44	18.16	4.57	17.84	700	53		1	W	05.02.99	S
SV120	151.7	36.0	17.7	45.4	250.8	60.49	14.35	7.06	18.10	700	53		1	W	05.02.99	S
SV120	154.8	24.5	24.6	46.4	250.3	61.85	9.79	9.83	18.54	700	53		1	W	05.02.99	Glass rod sucked up -loss of
SV120	157.5	15.5	29.9	47.1	250.0	63.00	6.20	11.96	18.84	700	53		1	W	05.02.99	S
SV120	160.0	7.6	34.6	47.9	250.1	63.97	3.04	13.83	19.15	700	53		1	W	05.02.99	material
SV120	162.1	0	39.5	48.5	250.1	64.81	0.00	15.79	19.39	700	53		1	W	05.02.99	S

1100°C

Nr	Weight measured (mg)				Total (mg)	Weight %				Pre-reaction		Temper days	Quench		Remarks	
	Pt	Pd	Ni	S		Pt	Pd	Ni	S	°C	days		°C	day		medium
SV337	134.9	14.1	48.6	52.7	250.3	53.90	5.63	19.42	21.05	800	62		10	W	20.10.97	S
SV338	118.6	64.6	17.8	48.8	249.8	47.48	25.86	7.13	19.54	800	62		10	W	20.10.97	S
SV339	186.3	25.7	0.0	38.4	250.4	74.40	10.26	0.00	15.34	800	62		10	W	20.10.97	S
SV340	112.1	91.8	0.0	46.3	250.2	44.80	36.69	0.00	18.51	800	62		10	W	20.10.97	S
SV341	44.3	160.7	26.2	70.2	301.4	14.70	53.32	8.69	23.29	800	62		10	W	20.10.97	exploded
SV342	153.5	0.0	46.3	50.8	250.6	61.25	0.00	18.48	20.27	800	62		10	W	20.10.97	S
SV343	173.7	18.0	15.7	42.7	250.1	69.45	7.20	6.28	17.07	800	62		10	W	20.10.97	exploded
SV344	110.6	32.6	52.2	56.0	251.4	43.99	12.97	20.76	22.28	800	62		10	W	20.10.97	exploded
SV345	145.0	42.5	17.5	47.3	252.3	57.47	16.85	6.94	18.75	800	62		10	W	20.10.97	Pt as Pt-foil
SV346	88.6	48.9	53.5	58.9	249.9	35.45	19.57	21.41	23.57	800	62		10	W	20.10.97	exploded
SV347	57.6	95.5	70.6	76.6	300.3	19.18	31.80	23.51	25.51	800	62		10	W	20.10.97	exploded
SV348	80.0	130.5	24.0	65.6	300.1	26.66	43.49	8.00	21.86	800	62		10	W	20.10.97	exploded
SV349	47.9	173.6	12.5	66.9	300.9	15.92	57.69	4.15	22.23	800	62		10	W	20.10.97	exploded
SV350	32.1	114.9	73.4	80.2	300.6	10.68	38.22	24.42	26.68	800	62		10	W	20.10.97	exploded
SV351	163.5	45.8	0.0	40.9	250.2	65.35	18.31	0.00	16.35	800	62		10	W	20.10.97	exploded
SV352	158.4	44.5	4.5	42.0	249.4	63.51	17.84	1.80	16.84	800	62		10	W	20.10.97	exploded
SV110	44.4	161.4	25.5	71.6	302.9	14.66	53.28	8.42	23.64	800	65		5	W	03.11.98	Dupl. SV341, S, only melt
SV110	158.3	44.5	4.8	42.2	249.8	63.37	17.81	1.92	16.89	800	65		5	W	03.11.98	Dupl. SV352, S
SV110	173.7	18.0	15.0	42.5	249.2	69.70	7.22	6.02	17.05	800	65		5	W	03.11.98	Dupl. SV343, S
SV110	132.3	39.3	61.4	67.0	300.0	44.10	13.10	20.47	22.33	800	65		5	W	03.11.98	Dupl. SV344, S
SV110	144.5	42.4	16.8	45.4	249.1	58.01	17.02	6.74	18.23	800	65		5	W	03.11.98	Dupl. SV345, S
SV110	79.7	130.9	24.3	56.0	290.9	27.40	45.00	8.35	19.25	800	65		5	W	03.11.98	Dupl. SV348, S, only melt

1000°C

Nr	Weight measured (mg)				Total (mg)	Weight %				Pre-reaction				Temper days	Quench		Remarks
	Pt	Pd	Ni	S		Pt	Pd	Ni	S	°C	days	°C	days		medium	date	
SV200	16.1	102.3	61.7	69.0	249.1	6.46	41.07	24.77	27.70	800	24	1200	1	38	WI	12.06.95	S, not in equilibrium
SV201	73.1	59.5	55.0	61.9	249.5	29.30	23.85	22.04	24.81	800	24	1200	1	38	WI	12.06.95	S
SV202	145.2	35.3	56.2	63.0	299.7	48.45	11.78	18.75	21.02	800	24	1200	1	38	WI	12.06.95	
SV203	133.7	13.9	48.2	54.0	249.8	53.52	5.56	19.30	21.62	800	24	1200	1	38	WI	12.06.95	S, not in equilibrium
SV204	16.6	106.6	64.4	62.5	250.1	6.64	42.62	25.75	24.99	800	24	1200	1	38	WI	12.06.95	S
SV205	75.5	61.5	56.2	55.4	248.6	30.37	24.74	22.61	22.28	800	24	1200	1	38	WI	12.06.95	unsealed in descicator 7 days, S
SV206	135.6	39.8	62.8	61.7	299.9	45.22	13.27	20.94	20.57	800	24	1200	1	38	WI	12.06.95	
SV207	137.7	14.3	49.3	48.9	250.2	55.04	5.72	19.70	19.54	800	24	1200	1	38	WI	12.06.95	S
SV208	16.2	104.2	62.4	66.6	249.4	6.50	41.78	25.02	26.70	800	24	1200	1	38	WI	12.06.95	S
SV209	74.0	60.2	55.8	59.5	249.5	29.66	24.13	22.36	23.85	800	24	1200	1	38	WI	12.06.95	S
SV210	128.3	19.6	49.8	53.5	251.2	51.07	7.80	19.82	21.30	800	24	1200	1	38	WI	12.06.95	S
SV211	111.5	32.5	51.2	55.6	250.8	44.46	12.96	20.41	22.17	800	24	1200	1	38	WI	12.06.95	S
SV212	109.8	32.7	51.1	57.1	250.7	43.80	13.04	20.38	22.78	800	24	1200	1	38	WI	12.06.95	
SV277	190.9	56.3	0.0	52.9	300.1	63.61	18.76	0.00	17.63	800	24	1200	1	40	WI	29.10.96	
SV278	196.4	58.6	0.0	45.9	300.9	65.27	19.47	0.00	15.25	800	24	1200	1	40	WI	29.10.96	
SV279	181.8	0.0	54.3	64.4	300.5	60.50	0.00	18.07	21.43	800	24	1200	1	40	WI	29.10.96	
SV280	187.0	0.0	56.2	56.5	299.7	62.40	0.00	18.75	18.85	800	24	1200	1	40	WI	29.10.96	
SV281	189.6	56.2	2.7	53.1	301.6	62.86	18.63	0.90	17.61	800	24	1200	1	40	WI	29.10.96	not in equilibrium
SV282	193.7	56.9	2.7	46.7	300.0	64.57	18.97	0.90	15.57	800	24	1200	1	40	WI	29.10.96	not in equilibrium
SV283	185.0	54.2	5.5	54.8	299.5	61.77	18.10	1.84	18.30	800	24	1200	1	40	WI	29.10.96	not in equilibrium
SV284	191.0	57.3	5.3	48.8	302.4	63.16	18.95	1.75	16.14	800	24	1200	1	40	WI	29.10.96	
SV285	182.2	53.5	9.3	55.3	300.3	60.67	17.82	3.10	18.41	800	24	1200	1	40	WI	29.10.96	
SV286	186.9	54.4	9.9	48.1	299.3	62.45	18.18	3.31	16.07	800	24	1200	1	40	WI	29.10.96	not in equilibrium
SV287	166.3	54.1	19.7	59.1	299.2	55.58	18.08	6.58	19.75	800	24	1200	1	40	WI	29.10.96	not in equilibrium
SV288	171.6	57.3	20.9	51.7	301.5	56.92	19.01	6.93	17.15	800	24	1200	1	40	WI	29.10.96	not in equilibrium
SV289	140.5	76.5	20.9	62.1	300.0	46.83	25.50	6.97	20.70	800	24	1200	1	40	WI	29.10.96	
SV290	144.9	78.6	22.2	55.3	301.0	48.14	26.11	7.38	18.37	800	24	1200	1	40	WI	29.10.96	
SV291	111.7	100.3	22.2	65.8	300.0	37.23	33.43	7.40	21.93	800	24	1200	1	40	WI	29.10.96	
SV292	114.6	105.2	22.9	58.1	300.8	38.10	34.97	7.61	19.32	800	24	1200	1	40	WI	29.10.96	not in equilibrium
SV293	78.0	128.7	23.4	67.0	297.1	26.25	43.32	7.88	22.55	800	24	1200	1	40	WI	29.10.96	
SV294	81.2	133.4	24.7	61.8	301.1	26.97	44.30	8.20	20.52	800	24	1200	1	40	WI	29.10.96	
SV295	77.7	136.8	17.7	68.8	301.0	25.81	45.45	5.88	22.86	800	24	1200	1	40	WI	29.10.96	
SV296	79.4	142.0	18.6	60.6	300.6	26.41	47.24	6.19	20.16	800	24	1200	1	40	WI	29.10.96	
SV297	75.4	145.3	11.7	67.3	299.7	25.16	48.48	3.90	22.46	800	24	1200	1	40	WI	29.10.96	
SV298	78.7	149.9	11.8	59.4	299.8	26.25	50.00	3.94	19.81	800	24	1200	1	40	WI	29.10.96	not in equilibrium
SV299	47.6	169.3	12.0	70.8	299.7	15.88	56.49	4.00	23.62	800	24	1200	1	40	WI	29.10.96	
SV300	49.7	177.7	12.5	62.8	302.7	16.42	58.71	4.13	20.75	800	24	1200	1	40	WI	29.10.96	
SV301	47.1	177.3	5.6	69.7	299.7	15.72	59.16	1.87	23.26	800	24	1200	1	40	WI	29.10.96	
SV302	48.9	183.6	6.1	61.7	300.3	16.28	61.14	2.03	20.55	800	24	1200	1	40	WI	29.10.96	
SV303	46.2	185.2	0.0	68.9	300.3	15.38	61.67	0.00	22.94	800	24	1200	1	40	WI	29.10.96	

SV304	47.4	191.4	0.0	60.4	299.2	15.84	63.97	0.00	20.19	800	24	1200	1	40	WI	29.10.96	
SV305	161.6	16.8	59.7	63.1	301.2	53.65	5.58	19.82	20.95	850	63	1100	1	56	W	09.10.97	
SV306	208.3	21.4	19.3	51.5	300.5	69.32	7.12	6.42	17.14	850	63	1100	1	56	W	09.10.97	
SV307	132.1	38.6	62.6	67.0	300.3	43.99	12.85	20.85	22.31	850	63	1100	1	56	W	09.10.97	S, not in equilibrium
SV308	174.1	51.3	21.0	55.6	302.0	57.65	16.99	6.95	18.41	850	63	1100	1	56	W	09.10.97	S
SV309	89.1	48.6	53.6	58.7	250.0	35.64	19.44	21.44	23.48	850	63	1100	1	56	W	09.10.97	S
SV310	118.6	64.6	17.8	48.8	249.8	47.48	25.86	7.13	19.54	850	63	1100	1	56	W	09.10.97	S
SV311	57.5	95.5	70.9	76.8	300.7	19.12	31.76	23.58	25.54	850	63	1100	1	56	W	09.10.97	S
SV312	79.8	130.6	24.9	65.9	301.2	26.49	43.36	8.27	21.88	850	63	1100	1	56	W	09.10.97	S
SV313	47.6	173.9	12.6	66.9	301.0	15.81	57.77	4.19	22.23	850	63	1100	1	56	W	09.10.97	S
SV314	44.8	161.2	26.0	70.0	302.0	14.83	53.38	8.61	23.18	850	63	1100	1	56	W	09.10.97	S
SV315	32.0	115.3	73.3	79.9	300.5	10.65	38.37	24.39	26.59	850	63	1100	1	56	W	09.10.97	S, not in equilibrium
SV316	163.2	45.8	0.0	40.6	249.6	65.38	18.35	0.00	16.27	850	63	1100	1	56	W	09.10.97	
SV317	158.2	45.0	4.9	44.0	252.1	62.75	17.85	1.94	17.45	850	63	1100	1	56	W	09.10.97	S
SV318	186.2	25.5	0.0	38.3	250.0	74.48	10.20	0.00	15.32	850	63	1100	1	56	W	09.10.97	
SV319	112.1	91.9	0.0	46.2	250.2	44.80	36.73	0.00	18.47	850	63	1100	1	56	W	09.10.97	not in equilibrium
SV320	153.4	0.0	46.3	50.4	250.1	61.34	0.00	18.51	20.15	850	63	1100	1	56	W	09.10.97	S
SV100	112.5	99.7	22.4	65.2	299.8	37.53	33.26	7.47	21.75	800	65	1100	1	55	W	12.06.98	S

900°C

Nr	Weight measured (mg)				Total (mg)	Weight %				Pre-reaction				Temper days	Quench		Remarks
	Pt	Pd	Ni	S		Pt	Pd	Ni	S	°C	days	°C	day		medium	date	
SV321	135.0	14.1	48.9	52.8	250.8	53.38	5.92	19.50	21.05			1200	1	60	W	11.05.97	S
SV322	173.7	18.0	15.9	42.8	250.4	69.37	7.19	6.35	17.09			1200	1	60	W	11.05.97	
SV323	110.5	32.5	51.6	55.4	250.0	44.20	13.00	20.64	22.16			1200	1	60	W	11.05.97	S
SV324	144.6	42.6	16.7	45.8	249.7	57.91	17.06	6.69	18.34			1200	1	60	W	11.05.97	S
SV325	89.2	49.2	53.5	58.6	250.5	35.61	19.64	21.36	23.29			1200	1	60	W	11.05.97	S
SV326	118.8	64.4	17.8	48.6	249.6	47.60	25.80	7.13	19.47			1200	1	60	W	11.05.97	S
SV327	57.7	95.7	70.3	76.7	300.4	19.21	31.86	23.40	25.53			1200	1	60	W	11.05.97	S
SV328	79.9	130.3	24.1	65.5	299.8	26.65	43.46	8.04	21.85			1200	1	60	W	11.05.97	S
SV329	44.0	160.9	25.7	69.6	300.2	14.66	53.60	8.56	23.18			1200	1	60	W	11.05.97	S, not in equilibrium
SV330	32.2	115.1	73.0	79.9	300.2	10.73	38.34	24.32	26.62			1200	1	60	W	11.05.98	S
SV331	163.3	45.9	0.0	40.7	249.9	65.35	18.37	0.00	16.29			1200	1	60	W	11.05.98	
SV332	158.9	45.0	4.7	42.8	251.4	63.21	17.90	1.87	17.05			1200	1	60	W	11.05.78	S
SV333	0.0	139.4	76.8	83.9	300.1	0.00	46.45	25.59	27.96			1200	1	60	W	11.05.97	S, not in equilibrium
SV334	186.2	25.5	0.0	38.2	249.9	74.51	10.20	0.00	15.29			1200	1	60	W	11.05.97	
SV335	112.2	91.3	0.0	46.1	249.6	44.95	36.58	0.00	18.47			1200	1	60	W	11.05.97	S charge broke after pre reaction, resealed in other
SV336	153.4	0.0	46.6	50.7	250.7	61.19	0.00	18.59	20.22			1200	1	60	W	11.05.97	
SV917	0.0	179.3	42.0	77.7	299.0	0.00	59.97	14.05	25.99	800	78	860	53	30	W	22.01.99	tube
SV918	63.0	159.2	11.8	64.9	298.9	21.08	53.26	3.95	21.71	800	78	860	53	30	W	22.01.99	not in equilibrium

800 °C

Nr	Weight measured (mg)				Total (mg)	Weight %				Pre-reaction		Temper days	Quench		Remarks
	Pt	Pd	Ni	S		Pt	Pd	Ni	S	°C	days		°C	days	
SV801	134.6	14.6	48.5	52.9	250.6	53.71	5.83	19.35	21.11			78	W	02.09.98	
SV802	173.6	18.4	15.4	43.1	250.5	69.30	7.35	6.15	17.21			78	W	02.09.98	not in equilibrium
SV803	110.3	33.1	51.1	56.7	251.2	43.91	13.18	20.34	22.58			78	W	02.09.98	not in equilibrium
SV804	144.9	42.4	16.7	45.5	249.5	58.08	16.99	6.69	18.24			78	W	02.09.98	not in equilibrium
SV805	106.8	58.1	64.4	70.4	299.7	35.64	19.39	21.49	23.49			78	W	02.09.98	
SV806	118.5	65.9	18.5	50.6	253.5	46.75	26.00	7.30	19.96			78	W	02.09.98	not in equilibrium
SV807	57.8	95.4	70.1	76.5	299.8	19.28	31.82	23.38	25.52			78	W	02.09.98	
SV808	79.8	130.3	24.0	65.8	299.9	26.61	43.45	8.00	21.94			78	W	02.09.98	
SV809	44.1	161.2	25.6	70.3	301.2	14.64	53.52	8.50	23.34			78	W	02.09.98	not in equilibrium
SV810	32.4	115.5	77.3	79.7	304.9	10.63	37.88	25.35	26.14			78	W	02.09.98	
SV811	163.6	46.4	0.0	41.2	251.2	65.13	18.47	0.00	16.40			78	W	02.09.98	
SV812	162.1	35.4	11.4	43.6	252.5	64.20	14.02	4.51	17.27			78	W	02.09.98	
SV813	0.0	139.0	76.6	83.3	298.9	0.00	46.50	25.63	27.87			78	W	02.09.98	not in equilibrium
SV814	165.6	38.2	5.1	41.3	250.2	66.19	15.27	2.04	16.51			78	W	02.09.98	not in equilibrium
SV815	0.0	180.0	42.9	77.5	300.4	0.00	59.92	14.28	25.80			78	W	02.09.98	
SV816	153.4	0.0	46.4	50.4	250.2	61.31	0.00	18.55	20.14			78	W	02.09.98	
SV817	119.5	25.4	50.2	54.8	249.9	21.19	53.13	4.13	21.56	700	78	61	W	08.07.99	not in equilibrium
SV818	127.3	19.5	49.2	54.3	250.3	50.86	7.79	19.66	21.69	700	78	61	W	08.07.99	not in equilibrium
SV819	148.3	4.1	47.3	51.3	251	59.08	1.63	18.84	20.44	700	78	61	W	08.07.99	

700 °C

Nr	Weight measured (mg)				Total (mg)	Weight %				Pre-reaction		Temper days	Quench		Remarks		
	Pt	Pd	Ni	S		Pt	Pd	Ni	S	°C	days		°C	days		medium	date
SV701	0.0	140.1	77.0	84.2	301.3	0.00	46.50	25.56	27.95	700	43	1200	1	42	W	04.02.99	
SV702	32.6	115.1	74.0	80.5	302.2	10.79	38.09	24.49	26.64	700	43	1200	1	42	W	04.02.99	
SV703	57.3	95.4	70.2	77.4	300.3	19.08	31.77	23.38	25.77	700	43	1200	1	42	W	04.02.99	
SV704	80.3	78.0	68.4	74.6	301.3	26.65	25.89	22.70	24.76	700	43	1200	1	42	W	04.02.99	
SV705	89.5	48.6	53.9	58.5	250.5	35.73	19.40	21.52	23.35	700	43	1200	1	42	W	04.02.99	
SV706	110.5	32.4	51.1	55.9	249.9	44.22	12.97	20.45	22.37	700	43	1200	1	42	W	04.02.99	not in equilibrium
SV707	120.0	25.1	50.4	55.1	250.6	47.89	10.02	20.11	21.99	700	43	1200	1	42	W	04.02.99	
SV708	127.3	19.6	49.6	53.7	250.2	50.88	7.83	19.82	21.46	700	43	1200	1	42	W	04.02.99	
SV709	134.5	14.0	48.9	52.7	250.1	53.78	5.60	19.55	21.07	700	43	1200	1	42	W	04.02.99	not in equilibrium
SV710	140.0	10.0	47.7	52.1	249.8	56.04	4.00	19.10	20.86	700	43	1200	1	42	W	04.02.99	
SV711	145.1	6.4	47.2	51.5	250.2	57.99	2.56	18.86	20.58	700	43	1200	1	42	W	04.02.99	
SV712	148.8	3.6	47.1	51.2	250.7	59.35	1.44	18.79	20.42	700	43	1200	1	42	W	04.02.99	
SV713	154.2	0.0	45.0	50.9	250.1	61.66	0.00	17.99	20.35	700	43	1200	1	42	W	04.02.99	
SV714	166.2	29.4	14.6	40.2	250.4	66.37	11.74	5.83	16.05	700	43	1200	1	42	W	04.02.99	not in equilibrium
SV715	172.2	32.5	4.5	40.2	249.4	69.05	13.03	1.80	16.12	700	43	1200	1	42	W	04.02.99	not in equilibrium
SV716	173.5	36.5	0.0	39.9	249.9	69.43	14.61	0.00	15.97	700	43	1200	1	42	W	04.02.99	

APPENDIX II

REFEREED PUBLICATIONS

RESULTING FROM THIS

STUDY

Compositional variation of cooperite, braggite, and vysotskite from the Bushveld Complex

SABINE M. C. VERRYIN AND ROLAND K. W. MERKLE

Department of Geology, University of Pretoria, Pretoria, 0002 South Africa

Abstract

The compositions of coexisting and individual cooperite (ideally PtS) and braggite (ideally (Pt,Pd)S) grains from the Merensky Reef of the Bushveld Complex, as well as cooperite, braggite and vysotskite (ideally PdS) grains from the UG-2 of the Bushveld Complex were investigated. There is a clearly defined miscibility gap between cooperite and braggite, but no evident gap between braggite and vysotskite. Partition coefficients between cooperite and braggite are determined on coexisting phases. The $K_D^{\text{braggite/cooperite}}$ in atomic ratios are estimated to be 0.54 for Pt, 15.81 for Pd and 5.93 for Ni. For Rh and Co the $K_D^{\text{cooperite/braggite}}$ are estimated to be > 1.40 and > 1.46 respectively. No systematic behaviour is detected for Fe and Cu. Coupled substitutions of Pd + Ni for Pt in cooperite and braggite/vysotskite are indicated. Within the cooperite of the Merensky Reef, the Pd:Ni ratio is approximately 9:11. The substitution trend in braggite, which extends to vysotskite in the UG-2, is dependent on the base-metal sulphide (BMS) association. If pentlandite is the dominant Ni-bearing BMS, the Pd:Ni ratio is about 7:3 in the Merensky Reef and in the UG-2. Millerite as the dominant Ni-bearing BMS in the UG-2 changes this ratio to 3:1. It is concluded that the Ni-content in braggite/vysotskite from BMS assemblages does not depend on the NiS activity, but rather on temperature of formation.

KEYWORDS: cooperite, braggite, vysotskite, Merensky Reef, Bushveld Complex, UG-2.

Introduction

COOPERITE, braggite and vysotskite have been described from many localities throughout the world — amongst others, from the Merensky Reef of the Bushveld Complex (e.g. Brynard *et al.*, 1976; Schweltnus *et al.*, 1976; Kingston and El-Dosuky, 1982; Mostert *et al.*, 1982), from the UG-2 (e.g. Kinloch, 1982; McLaren and De Villiers, 1982; Peyerl, 1982), from the Stillwater Complex (e.g. Todd *et al.*, 1982; Volborth *et al.*, 1986), and from Noril'sk (e.g. Genkin and Evstigneeva, 1986).

Amongst the platinum-group minerals (PGM) in the UG-2 and the Merensky Reef, these three minerals are the dominant ore minerals (Kinloch, 1982). From an economic point of view, cooperite, braggite and vysotskite are therefore probably the most important minerals in ores of the platinum-

group elements (PGE). They are also the most common minerals in the system Pt-Pd-S.

Although cooperite (ideally PtS) and braggite (ideally (Pt,Pd)S) have been synthesized by Skinner *et al.* (1976) at 1000°C, and cooperite, braggite, and vysotskite (ideally PdS) by Cabri *et al.* (1978) at 800°C in the Ni-free system, analyses of natural cooperite, braggite, and vysotskite typically contain significant amounts of Ni.

The description of the optical properties of the minerals, particularly those of cooperite and braggite, has caused a considerable amount of confusion in the past. Quantitative and descriptive data given for braggite often correspond to the properties of cooperite, whereas several descriptions of cooperite do not correspond to either of the two minerals. Therefore Criddle and Stanley (1985) reinvestigated the three minerals with the

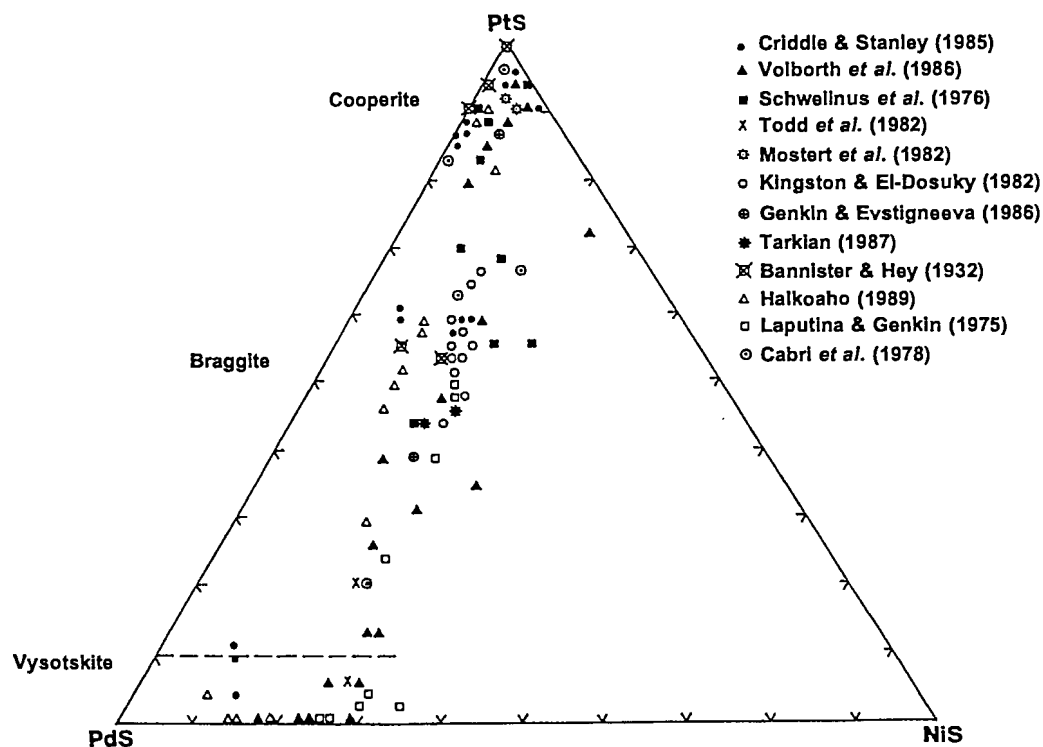


Fig. 1. Compositional variation of 133 braggite, cooperite and vysotskite analyses from various localities (in mol. %; owing to overlap, 36 projection points hidden; the stippled line indicates the arbitrary border between braggite and vysotskite).

aid of reflectivity measurements of analysed grains. Cabri *et al.* (1978) summarized existing compositional data, and Tarkian (1987) also presented compositional data as well as reflectance data. In our investigation it was observed that the frequency of twinning in large grains may aid distinction of braggite and cooperite minerals. Only 3 out of 185 cooperite grains, but 40 out of 161 braggite grains were found to be twinned.

Figure 1 summarizes the compositional variations of cooperite, braggite and vysotskite in the system PtS-PdS-NiS taken from the literature. Cooperite and braggite seem to be separated by a miscibility gap, and there seems to be a continuous solid solution between braggite and vysotskite. An arbitrary content of 10 mol. % PtS is taken as the upper limit for vysotskite compositions (Cabri *et al.*, 1978).

Despite their wide distribution, cooperite and braggite are rarely observed in physical contact with each other. Until the investigation of Merkle and Verryin (1991), which concentrated on

material from the Merensky Reef of the Bushveld Complex, the compositions of coexisting braggite and cooperite had not been addressed.

This investigation forms part of a larger programme to investigate the compositions of cooperite, braggite, and vysotskite from different mineralizations and mineral assemblages. Here we report on the compositions of coexisting braggite and cooperite; and those of individual cooperite, braggite and vysotskite grains; inter-element relationships; the verification of the miscibility gap between cooperite and braggite; and provide partition coefficients between the two minerals where possible.

Samples

The samples used in this investigation originate from various localities of the Merensky Reef and the UG-2 of the Bushveld Complex. Within the samples of the UG-2 chromitite, braggite and



TABLE 1. Analytical conditions, detection limits (3 sigma level in wt.%) and reproducibilities (1 sigma, determined according to Kaiser and Specker (1956) in wt.%; N = 60 (n.d. = not determined).

Element	Standard	Analysing Crystal	X-Ray Line	Detection Limit	Reproducibility	
					Braggite	Cooperite
Pt	Pt _{0.7} Pd _{0.3} S	LIF	L α	n.d.	0.2564	0.2840
Pd	Pt _{0.7} Pd _{0.3} S	PET	L α	0.150	0.1952	0.1141
Ni	Ni	LIF	K α	0.022	0.0656	0.0102
S	Pt _{0.7} Pd _{0.3} S	PET	K α	n.d.	0.1183	0.1177
Cu	CuFeS ₂	LIF	K α	0.030	0.0634	0.0076
Fe	FeS	LIF	K α	0.022	0.0158	0.0050
Co	CoS ₂	LIF	K α	0.023	n.d.	0.0086
Rh	Rh	PET	L α	0.112	n.d.	0.0430
						(N=16)
As	PtAs ₂	TAP	L α	0.055	n.d.	n.d.

vysotskite are the most common phases in the system PtS-PdS-NiS (Kinloch, 1982). Here the PGM are associated with the base-metal sulphides (BMS) pentlandite, pyrrhotite, chalcopyrite, millerite, and pyrite (McLaren and De Villiers, 1982). In contrast, cooperite and braggite are frequently encountered in the silicate dominated Merensky Reef samples (Kinloch, 1982); occasionally, these two phases coexist. The PGM in the Merensky Reef are associated with chalcopyrite, pentlandite, pyrrhotite and minor pyrite (Brynard *et al.*, 1976; Schweltnus *et al.*, 1976; Vermaak and Hendriks, 1976; Mostert *et al.*, 1982).

Analytical methods

The compositional variation of 36 grains of coexisting braggite and cooperite from the Merensky Reef were determined along traverses across their mineral boundaries with a JEOL 733 microprobe at the University of Pretoria. In addition, five and six individual grains respectively of cooperite and braggite from the Merensky Reef were analysed and 49 grains of cooperite, braggite and vysotskite from the UG-2. The accelerating potential was 20 kV and the beam current 5×10^{-8} A. Counting times were 20 s at the peak positions and 10 s for symmetrical backgrounds. The elements analysed were Pt, Pd, Ni, S, Cu, Fe, Co, Rh, and As. Arsenic is hardly ever present in quantities above the detection limit (0.055 wt.%) and therefore omitted in the tables and calculations. Technical data of the analyses are given in Table 1 and a selection of representative analyses is given in Table 2.

A non-linearity in the determination of Pd, similar to the problem for Au-Ag alloys encountered by Reid *et al.* (1988), was observed and corrected as discussed in Merkle and Verry

(1991). After correction for Pd, analyses with totals between 98.5 and 101.5 wt.% were used for further calculations. Traverse analyses close to the grain boundary of coexisting braggite and cooperite were discarded for calculation of the means, if cooperite showed abnormally high Pd contents or if the Pd concentrations in braggite were abnormally low compared with the rest of that particular grain. In such cases interference from the neighbouring grain was assumed, because of the large excitation area of about 2.5 μ m (primary and fluorescent radiation) at 20 kV.

Compositions of coexisting braggite and cooperite (Merensky Reef)

Profiles across the mineral boundaries of composite cooperite-braggite grains indicate that there is occasionally a change in composition of the minerals close to the mineral boundary. Abrupt and continuous changes over the whole mineral grain towards higher and lower Pd contents were observed in both minerals, but no systematic pattern of chemical variability in coexisting braggite and cooperite was detected. Compositional variation in braggite was usually found to be greater than in cooperite. Compositional variations were also observed by Cabri *et al.* (1978) in individual grains of braggite. The compositional variation is interpreted to reflect incomplete equilibration between, and within, the two phases in response to the reduced stability fields of braggite and cooperite on cooling (see below). Different degrees of homogenization are attributed to differences in the cooling history (i.e. the effects of various postcumulus processes) of individual grains.

Figure 2 shows the compositional variation of coexisting and discrete braggite and cooperite

TABLE 2. Selected cooperite (co), braggite (br), and vysotskite (vy) analysis from the Merensky Reef (MR) and the UG-2 chromitite in assemblages containing pentlandite (pent) or millerite (mill).

Mineral Origin Association		co MR pent	co MR pent	br MR pent	br MR pent	co UG-2 pent	br UG-2 pent	vy UG-2 pent	br UG-2 mill	vy UG-2 mill
W e i g h t	S	14.41	14.56	18.12	18.96	14.83	20.26	22.09	19.02	25.60
	Rh	<0.11	<0.11	<0.11	<0.11	0.40	<0.11	<0.11	<0.11	0.16
	Pd	0.80	1.31	19.92	21.45	2.57	23.29	43.55	25.69	60.46
	Pt	83.81	83.92	57.15	53.38	80.43	47.55	25.43	52.20	1.25
	Ni	0.58	0.53	4.24	5.67	0.53	7.63	8.85	3.90	12.28
	Co	<0.02	<0.02	<0.02	<0.02	0.03	<0.02	<0.02	<0.02	0.04
	Cu	0.04	<0.03	<0.03	<0.03	<0.03	0.32	0.06	0.03	0.30
	% Fe	<0.02	<0.02	0.14	0.05	0.47	1.37	0.52	0.12	0.57
	Total	99.64	100.32	99.57	99.51	99.26	100.42	100.50	100.96	100.66
	A t o m i c %	S	50.099	50.148	50.445	50.797	50.238	50.394	49.582	50.646
Rh		-	-	-	-	0.423	-	-	-	0.098
Pd		0.842	1.355	16.716	17.319	2.625	17.458	29.454	20.607	35.529
Pt		47.894	47.496	26.157	23.513	44.773	19.436	9.380	22.842	0.401
Ni		1.092	1.001	6.453	8.299	0.973	10.363	10.845	5.675	13.079
Co		-	-	-	-	0.052	-	-	-	0.043
Cu		0.072	-	-	-	-	0.395	0.068	0.043	0.296
% Fe		-	-	0.230	0.072	0.916	1.954	0.670	0.186	0.633

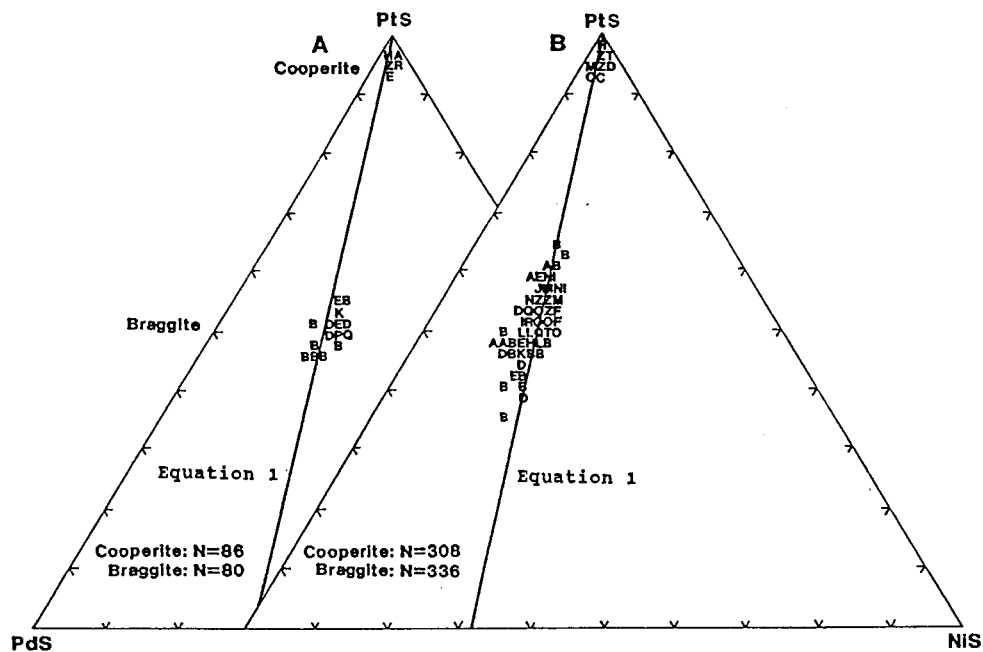


FIG. 2. Compositional variation of discrete (A) and coexisting (B) braggite and cooperite from the Merensky Reef in the PtS–PdS–NiS diagram (in mol. %; A = 1 observation, B = 2 observations, etc., Z = 26 and more). Equation 1 is graphically represented by the solid line.

grains from the Merensky Reef based on 810 analyses. The fields of the discrete (Fig. 2A) and the coexisting grains (Fig. 2B) show a complete overlap. The range in the PdS component of the individual braggite grains, however, is smaller (45–55 mol. %) than that of braggite coexisting with cooperite. Here the PdS content ranges from 35 to 65 mol. %. This difference is likely to be due to the smaller number of individual grains analysed.

When compared to compositions of braggite and cooperite from various other localities (Fig. 1), the compositional range of the two minerals observed in this investigation is seen to be more restricted and better defined. Figure 1 indicates a range of 28–90 mol. % PdS in braggite and up to 20 mol. % PdS in cooperite. In this investigation, a maximum of 8 mol. % PdS was observed in cooperite.

It is also evident from Fig. 2 that braggite contains significantly more Ni than the cooperite. A clearly visible miscibility gap, as previously described by Cabri *et al.* (1978), exists between the two minerals, most likely because of the different crystallography of the two minerals. Cooperite belongs to space group *P42/mmc* and braggite to *P42/m* (Bannister and Hey, 1932). This miscibility gap between coexisting braggite and cooperite (Fig. 2) is much larger than is indicated in literature analyses (Fig. 1). If the possibility of mixed analyses is excluded, the mineral compositions that lie inside the gap probably represent grains that formed at high temperatures which permitted a higher degree of solid solution. Fast cooling or different degrees of postmagmatic overprinting (e.g. through hydrothermal fluids) may have a profound effect on the exsolution and the development of a clear miscibility gap. The difference in the miscibility gaps of Figs. 1 and 2 implies that these gaps depend on the temperature at which equilibration ceases (see discussion below).

Inter-element relations of coexisting cooperite and braggite (Merensky Reef)

Cooperite and braggite have distinct compositional ranges, which make differences in their inter-element relations likely. The spot analyses taken from 36 coexisting grains of cooperite and braggite of the Merensky Reef were averaged for each phase in each grain. As the elements Pt, Pd, and Ni are the only elements, apart from S, that are always present in quantities above the detection limits, their inter-element relations will be discussed first.

Braggite. A Spearman correlation coefficient (Table 3) of $r = -0.8569$ between Pt and Pd (see also Fig. 3A) indicates a substitution of Pt and Pd.

TABLE 3. Spearman correlation coefficients (error probabilities underneath) calculated from analyses in at. % ($N = 36$) of braggite coexisting with cooperite of the Merensky Reef.

	Pd	Ni	Pd + Ni
Pt	-0.85689 0.0001	-0.65611 0.0001	-0.94826 0.0001
Pd		0.30888 0.0668	0.95084 0.0001
Ni			0.56113 0.0004

Pt and Ni also show a negative correlation, with a coefficient $r = -0.6561$ (Fig. 3B). A rather weak positive correlation of $r = 0.3089$ (Fig. 3C) between Pd and Ni indicates that the inter-element relations are not restricted to a 1:1 substitution of Pt and Pd. If a coupled substitution of Pt for Pd + Ni is assumed and tested for the degree of correlation, the correlation coefficient improves to -0.9483 (Fig. 3D). The small deviation from an ideal relation is likely to be caused not by an even more complex substitution involving additional elements, but rather by the unavoidable analytical uncertainties. A least-squares fitting of the data leads to Equation 1 (at the 95% confidence level) for the substitution of Pt by Pd + Ni in braggite in atomic proportions.

$$\text{Pt} = (0.68 \pm 0.03) \times \text{Pd} + (0.32 \pm 0.03) \times \text{Ni} \quad (1)$$

The same relation (without the error margin) can be derived graphically by drawing a line in Fig. 2 from the PtS-corner through the mean of the braggite population to the PdS–NiS join.

Fe and Cu show a fairly weak positive correlation ($r = 0.5879$; $N = 10$) within the braggite when present in quantities above the detection limit (Table 1). In eight grains, only Fe was detected and in three grains only was Cu detected.

Cooperite. For cooperite (Table 4), the Spearman correlation between Pt and Pd is well developed ($r = -0.7663$), whereas correlations between Ni and Pt ($r = -0.3776$) and Ni and Pd ($r = 0.4224$) are weaker. If the same type of coupled substitution as shown for braggite is assumed and the correlation between Pt and Pd + Ni is tested, a marginally higher coefficient results than that between Pt and Pd alone ($r = -0.7866$). This indicates that Pt, here also, is most likely to be substituted by Pd + Ni. However, due to the lower concentrations of Pd and Ni in cooperite (i.e., larger relative analytical uncertainty) and the restricted compositional range, the correlation coefficients for cooperite are less clearly defined

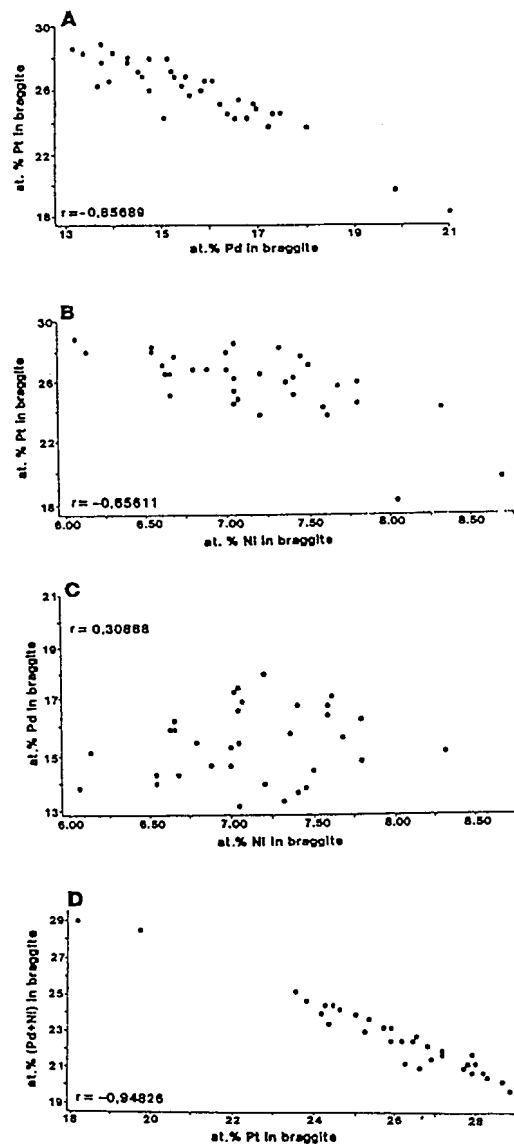


FIG. 3. Scatter plots (in atomic per cent) of Pt versus Pd (A), Pt versus Ni (B), Pd versus Ni (C), and Pt versus Pd+Ni (D) in braggite from the Merensky Reef.

than they are for braggite. A formula for the substitution, calculated as for the braggite (at the 95% confidence level), would be:

$$\text{Pt} = (0.45 \pm 0.09) \times \text{Pd} + (0.55 \pm 0.09) \times \text{Ni} \quad (2)$$

Spearman correlation coefficients (Table 4) imply a negative correlation ($r = -0.5077$)

between Co and Pt and positive correlations between Co and Pd ($r = 0.3670$), and between Co and Ni ($r = 0.5297$). This suggests a possible substitution of Co for Pt. Rhodium correlates positively with Pt ($r = 0.4336$) and negatively with Pd ($r = -0.4755$), indicating a substitution of Rh for Pd. The correlation between Rh and Ni is very poor. We may therefore be dealing with a more complex systematic substitution of Pd+Ni+Co for Pt+Rh, but our data do not permit a more rigorous evaluation of this aspect. A further positive correlation is indicated between the amounts of Fe in cooperite and Ni in coexisting braggite ($r = 0.4990$, $N = 23$).

Dependence of braggite compositions on BMS assemblages (UG-2)

From the UG-2 of the Bushveld Complex, we selected samples in which cooperite, braggite, and vysotskite occur in two different BMS assemblages. In one assemblage, the Ni-bearing phase is pentlandite and in the other one millerite with only traces of pentlandite. The distinct associations indicate different activity of NiS and could therefore be expected to have an effect on the Ni-proportion of Pt-Pd-Ni sulphides. In the UG-2, the average grain sizes of braggite, cooperite and vysotskite are smaller ($\pm 5 \mu\text{m}$ in diameter) than in the Merensky Reef (often $>100 \mu\text{m}$ in diameter). Compositional heterogeneity could therefore not be observed to the same degree as in the Merensky Reef. Analyses of cooperite, braggite, and vysotskite coexisting with pentlandite are presented in Fig. 4. Spearman correlation coefficients (Table 5) between Pt, Pd, Ni and Pd+Ni indicate the same coupled substitution of Pd+Ni for Pt as for the braggite of the Merensky Reef (Table 3), which also coexists with pentlandite. Mathematically, the Pd/Ni ratio is also very similar to that of the Merensky Reef (Equation 3).

$$\text{Pt} = (0.67 \pm 0.06) \times \text{Pd} + (0.33 \pm 0.06) \times \text{Ni} \quad (3)$$

Figure 4 indicates that the trend established for braggite continues right down to vysotskite and that there is no significant difference between the Merensky Reef and UG-2 trends.

In contrast, Fig. 5 shows compositions of cooperite, braggite, and vysotskite from the UG-2 in association with millerite. The analyses all plot on the Ni-poor side of the trend established for the pentlandite association (Equations 1 and 3). For the millerite association the Pd/Ni ratio can be expressed as follows:

$$\text{Pt} = (0.75 \pm 0.10) \times \text{Pd} + (0.25 \pm 0.10) \times \text{Ni} \quad (4)$$

COOPERITE, BRAGGITE AND VYSOTSKITE

TABLE 4. Spearman correlation coefficients from analyses of cooperite (in at. %), coexisting with braggite of the Merensky Reef. Error probabilities and the number of observations underneath.

	Pd	Ni	Co	Rh	Pd+Ni
Pt	-0.76628 0.0001 36	-0.37761 0.0232 36	-0.50769 > 0.0638 14	0.43357 0.1591 12	-0.78662 0.0001 36
Pd		0.42239 0.0103 36	0.36703 0.1967 14	-0.47552 0.1182 12	0.96834 0.0001 36
Ni			0.52967 0.0514 14	0.18881 0.5567 12	0.54100 0.0007 36
Co				0.20000 0.5796 10	

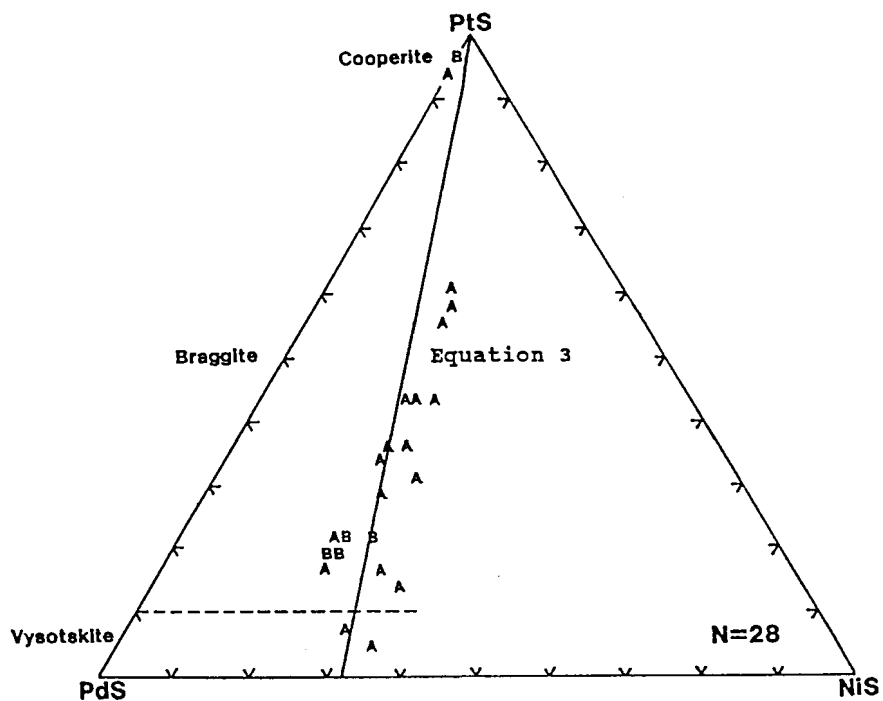


FIG. 4. Compositional variation of 28 cooperite, braggite and vysotskite grains from the UG-2 associated with pent landite (in mol. %, A = 1 observation, B = 2 observations). Equation 3 is graphically represented by the solid line.

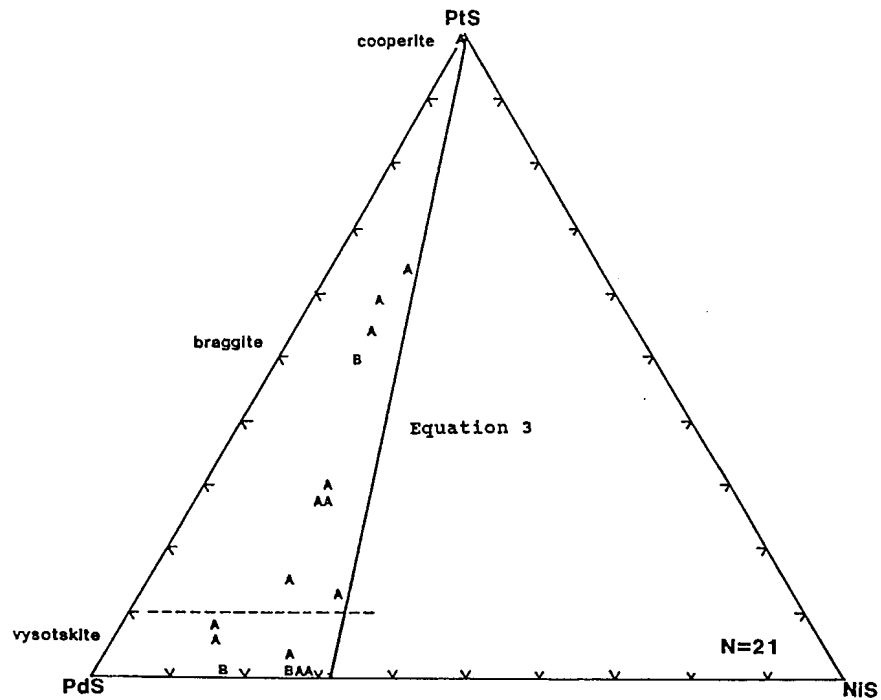


FIG. 5. Compositional variation of 21 cooperite, braggite and vysotskite grains from the UG-2 associated with millerite (in mol. %, A = 1 observation, B = 2 observations). Equation 3 is graphically represented by the solid line.

In the investigated samples, the millerite occurs as grains of up to several hundred μm with rare pentlandite inclusions. Phase relations within the Fe-Ni-S system do not change significantly between 600 and 300°C (Vaughan and Craig, 1978). Pentlandite exsolves from the monosulphide solid solution (mss) below 610°C (Kullerud, 1963). For bulk sulphide compositions signifi-

cantly more Ni-rich than normal magmatic sulphides, the mss can be expected to decompose below 300°C and millerite should coexist with an Fe-rich and a S-rich phase. However, this was not observed in the samples investigated. Naldrett and Lehmann (1988) and Naldrett *et al.* (1989) demonstrated that the Fe content in BMS assemblages can be reduced through absorption of Fe by chromite, as was suggested by Von Gruenewaldt *et al.* (1986). Merkle (1992) showed that hydrothermal fluids can have an even more pronounced effect and lead to further reduction in the proportion of sulphidic Fe.

In localized areas of chromitite layers, the loss of Fe may progress to such a degree, that we are effectively dealing with the pure Ni-S system. The Fe-loss results in a relative increase in S and at temperatures above 379°C, Ni_{1-x}S should crystallize instead of stoichiometric millerite. With cooling of the system below 379°C millerite is the stable phase, which should exhibit exsolution of a S-richer phase if it had formed from the non-stoichiometric Ni_{1-x}S (Kullerud and Yund, 1962). Exsolutions, which should easily be observed due

TABLE 5. Spearman correlation coefficients from analyses of braggite of the UG-2 in association with pentlandite (in atomic per cent, N = 25, error probabilities underneath).

	Pd	Ni	Pd + Ni
Pt	-0.8608 0.0001	-0.6508 0.0004	-0.9762 0.0001
Pd		0.3377 0.0988	0.9054 0.0001
Ni			0.6139 0.0011

TABLE 6. $K_D^{\text{braggite/cooperite}}$ with respective standard deviations (s_{KD}), 68% confidence level.

	atomic		mass	
	K_D	s_{KD}	K_D	s_{KD}
Pt	0.54	0.05	0.69	0.04
Pd	15.81	5.48	19.92	6.84
Ni	5.93	0.85	7.49	1.18

to the large size of the millerite grains, were not once encountered in the samples investigated.

The phase relations in the systems Fe-Ni-S and Ni-S discussed above indicate that we are dealing with millerite that formed at temperatures below 379°C. It can be assumed that the PGM which coexist with millerite are in equilibrium with millerite and reflect the compositional characteristics of PGM formed, or equilibrated, at temperatures below 379°C. The NiS-activity, in an environment in which only millerite forms, is higher than that of an environment where pentlandite is present. The braggite and vysotskite grains in association with millerite, however, contain less NiS than those occurring together with pentlandite. This indicates that temperature of formation or equilibration, rather than Ni-activity, is the dominant factor for the Ni-concentration within braggite and vysotskite.

Partition coefficients

Partition coefficients can only be estimated from coexisting phases that are in equilibrium, therefore only the analytical results obtained from samples of the Merensky Reef can be used. As discussed above, the spot-analyses of the grains of coexisting braggite and cooperite were averaged. From these averages, partition coefficients (K_D) were calculated (Table 6).

The element concentrations, and from them the partition coefficients, can also be derived by linear

regression in the form of

$$\text{atomic \% in braggite} = a + b \times \text{atomic \% in cooperite} \quad (5)$$

where a is the intercept and b the slope of the regression line. In Table 7 the respective values for a and b for Pt, Pd and Ni, with their standard errors, are presented together with Spearman correlation coefficients. As the values of the 36 grains used for calculations in Table 7 are already mean values of a number of spot analyses, the standard deviations indicated in Table 7 might in actual fact be conservative, because the means on which the calculations are based already do have a variance. Rh and Co seem to have a higher affinity for cooperite than for braggite. Rhodium was detected only three times in braggite, and Co twice compared with 12 and 14 times respectively in cooperite. For individual pairs of cooperite and braggite, the $K_D^{\text{cooperite/braggite}}$ of Rh and Co were calculated from the available analytical results, as well as the lower limit of detection (LLD) (Table 1) for those mineral pairs where the respective concentrations of the elements were below the LLD for one of the minerals. Involvement of the LLD for one of the minerals, mostly braggite, results in minimum values for the K_D . The estimated $K_D^{\text{cooperite/braggite}}$ for Rh was determined to be > 1.11 (by mass) and > 1.40 (atomic ratio). For Co the $K_D^{\text{cooperite/braggite}}$ was estimated > 1.17 (mass ratio) and > 1.46 (atomic ratio). For Fe and Cu no systematic behaviour was detected. The ratios of these two elements between braggite and cooperite vary from 0.07 to 7.00 by mass for Fe and 0.17 to 4.49 by mass for Cu, indicating that these elements do not have a preferred affinity for any one of the two minerals.

Implications for phase relations

Skinner *et al.* (1976) reported ternary phase relations for the system Pt-Pd-S at 1000°C and Cabri *et al.* (1978) at 800°C. Three phases could be distinguished — a solid solution between Pt and

TABLE 7. Spearman correlation coefficients r with error probabilities e_r and slopes b and intercepts a of regression lines with standard error s_b and s_a for the concentration in atomic per cent Pt, Pd and Ni between braggite and cooperite.

	r	e_r	b	s_b	a	s_a
Pt	0.3426	0.0408	0.94	0.54	-18.63	25.49
Pd	0.4860	0.0027	1.97	0.63	13.52	0.74
Ni	-0.0378	0.8266	-0.51	0.69	7.80	0.85

Pd and two sulphides. The first sulphide is a solid solution with a structure identical to cooperite, extending from PtS to $(Pt_{0.7}Pd_{0.3})S$ at 1000°C and to $(Pt_{0.54}Pd_{0.46})S$ at 800°C (Fig. 6). At 1000°C the braggite-like phase ranges from $(Pt_{0.4}Pd_{0.6})S$ to $(Pd_{0.84}Pt_{0.16})S$ but does not reach the composition PdS. At 1000°C PdS is not stable but the upper stability limit of PdS is not clear; temperatures of 912°C (Skinner *et al.*, 1976) and 970°C (Barin *et al.*, 1977) are reported. At 800°C the braggite-like solid solution ranges from PdS to $(Pd_{0.76}Pt_{0.24})S$.

The Ni-free projected data from our samples of the Merensky Reef, as well as the UG-2, indicate cooperite to range from PtS to $(Pt_{0.94}Pd_{0.06})S$ and braggite from $(Pt_{0.74}Pd_{0.26})S$ to PdS in the case of the UG-2. It can be assumed that the 'freezing' temperature of this system lies well below 800°C. Looking at the compositional ranges at the different temperatures it seems unusual that the stability field for cooperite should be larger at a lower temperature. The solid solution ranges, as well as the positions of the miscibility gaps require further investigation.

Summary and conclusion

In summary, this investigation yielded the following results:

(1) Natural cooperite, braggite and vysotskite are best represented by the system Pt-Pd-Ni-S. There is a clearly defined miscibility gap between cooperite and braggite, but no evident gap exists between braggite and vysotskite.

(2) Coexisting cooperite and braggite grains permitted an approximation of partition coefficients. The $K_D^{cooperite/braggite}$ in atomic proportions were estimated to be 0.54 for Pt, 15.81 for Pd and 5.93 for Ni. Rh and Co seem to have a higher affinity for cooperite and the $K_D^{braggite/cooperite}$ in atomic proportions are > 1.40 for Rh and > 1.46 for Co. For Fe and Cu no systematic behaviour was detected.

(3) A coupled substitution of Pd + Ni for Pt with a Pd:Ni ratio of approximately 9:11 (Equation 2) is indicated within cooperite. This substitution may also include Rh and Co.

(4) In braggite the same coupled substitution of Pd + Ni for Pt is evident. It has been shown here, that the Pd:Ni ratio can be changed by postmagmatic processes, which are reflected in the BMS assemblages. If the Ni-bearing phase in association with the PGM is pentlandite, the Pd:Ni ratio is about 7:3 (Equations 1 and 3, Figs. 2 and 4). However, if the Ni-bearing phase is millerite, the Pd:Ni ratio changes and the analyses plot on the Ni-poor side of the trend established for the pentlandite association (Equation 4, Fig.

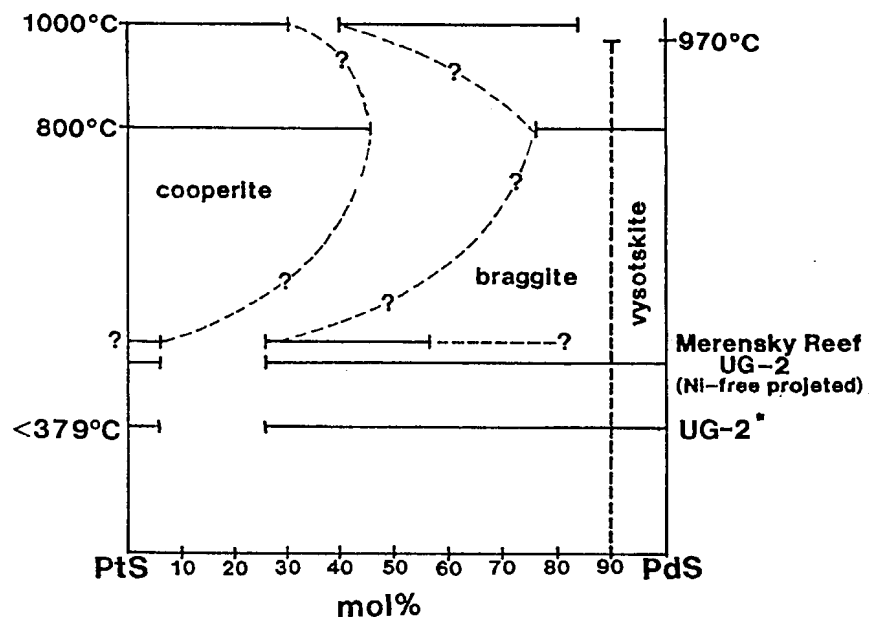


FIG. 6. Stability of cooperite, braggite and vysotskite at 1000°C (after Skinner *et al.*, 1976), at 800°C (after Cabri *et al.*, 1978) and Ni-free projected data from the Merensky Reef and the UG-2 of the Bushveld Complex (*implied by millerite stability).



5). These trends extend right down to vysotskite. The dependence of the Pd:Ni ratio on BMS assemblages indicates that temperature of formation or re-equilibrium rather than the availability of NiS plays the dominant role in the Ni-content of braggite.

(5) The data taken from the literature (Fig. 1) suggest that not all braggites and vysotskites follow the trends derived from our analyses. This, however, could be attributed to variables like temperature of formation and different cooling histories.

(6) The compositional variability of cooperite and braggite/vysotskite at different temperatures (Fig. 6) requires experimental confirmation.

Acknowledgements

The authors thank H. E. Horsch for her assistance with the microprobe analyses, L. J. Cabri for synthetic standards, and M. van Leeuwen for drafting the diagrams. The constructive comments of L. J. Cabri, A. J. Criddle and S. J. Edwards are greatly appreciated.

References

- Bannister, F.A. and Hey, M.H. (1932) Determination of minerals in platinum concentrates from the Transvaal by X-ray methods. *Mineral. Mag.*, **28**, 188–206.
- Barin, I., Knacke, O. and Kubaschewski, O. (1977) *Thermochemical properties of inorganic substances (Supplement)*. Springer Verlag Berlin, Heidelberg, New York.
- Brynard, H. J., de Villiers, J. P. R. and Viljoen, E. A. (1976) A mineralogical investigation of the Merensky Reef at the Western Platinum Mine, near Marikana, South Africa. *Econ. Geol.*, **71**, 1299–307.
- Cabri, L. J., Laflamme, J. H. G., Steward, J. M., Turner, K. and Skinner, B. J. (1978) On cooperite, braggite, and vysotskite. *Amer. Mineral.* **63**, 832–9.
- Criddle, A. J. and Stanley, J. S. (1985) Characteristic optical data for cooperite, braggite and vysotskite. *Canad. Mineral.*, **23**, 149–69.
- Genkin, A. D. and Evstigneeva, T. L. (1986) Associations of platinum-group minerals of the Noril'sk copper-nickel sulfide ores. *Econ. Geol.*, **81**, 1203–12.
- Halkoaho, T. (1989) *Ala-Penikan platinametallimineralisaatiot Penikkain kerrosintruusiossa*. Raportti no 2, Peräpohjan platinaprojekti, Oulun Yliopisto, 173 pp.
- Kaiser, H. and Specker, H. (1956) Bewertung und Vergleich von Analysenverfahren. *Z. anal. Chem.*, **149**, 46–66.
- Kingston, G. A. and El-Dosuky, B. T. (1982) A contribution on the platinum-group mineralogy of the Merensky Reef at the Rustenburg Platinum Mine. *Econ. Geol.*, **71**, 1299–307.
- Kinloch, E. D. (1982) Regional trends in the platinum-group mineralogy of the Critical Zone of the Bushveld Complex, South Africa. *Econ. Geol.*, **77**, 1328–47.
- Kullerud, G. (1963) Thermal stability of pentlandite. *Canad. Mineral.*, **7**, 353–66.
- Kullerud, G. and Yund, R. A. (1962) The Ni–S system and related minerals. *J. Petrol.*, **3**, 126–75.
- Laputina, I. P. and Genkin, A. D. (1975) Minerals of the braggite–vysotskite series. *Izomorpizm Mineraly, Izdat. Nauka*, 146–50 (in Russian).
- McLaren, C. H. and De Villiers, J. P. R. (1982) The platinum-group chemistry and mineralogy of the UG-2 chromitite layer of the Bushveld Complex. *Econ. Geol.*, **77**, 1348–66.
- Merkle, R.K.W. (1992) Platinum-group minerals in the middle group of chromitite layers at Marikana, western Bushveld Complex: indications for collection mechanisms and postmagmatic modification. *Canad. J. Earth Sci.*, **29**, 209–21.
- Merkle, R. K. W. and Verryin, S. M. C. (1991) Coexisting cooperite and braggite — new data. *Papers, International Congress on Applied Mineralogy, 1991*, Pretoria, South Africa, Paper 61, 17 pp.
- Mostert, A. B., Hofmeyr, P. K. and Potgieter, G. A. (1982) The platinum-group mineralogy of the Merensky Reef at the Impala Platinum Mines, Bophuthatswana. *Econ. Geol.*, **77**, 1385–94.
- Naldrett, A. J. and Lehmann, J. (1988) Spinel non-stoichiometry as the explanation for Ni-, Cu- and PGE-enriched sulfides in chromitites. In *Geoplatinum '87*. (H. M. Prichard, P. J. Potts, J. F. W. Bowles and S. J. Cribb, eds.). Elsevier, Amsterdam, 93–109.
- Naldrett, A. J., Lehmann, J. and Augé, T. (1989) Spinel non-stoichiometry and reactions between sulphides, with examples from ophiolite complexes. In *Magmatic sulphides — the Zimbabwe volume*. (M. D. Prendergast and M. J. Jones, eds.). The Institution of Mining and Metallurgy, London, 221–7.
- Peyerl, W. (1982) The influence of the Driekop dunite pipe on the platinum-group mineralogy of the UG-2 chromitite in its vicinity. *Econ. Geol.*, **77**, 1432–8.
- Reid, A. M., le Roex, A. P. and Minter, W. E. L. (1988) Composition of gold grains in the Vaal Placer, Klerksdorp, South Africa. *Mineral. Dep.*, **23**, 211–7.



- Schwellnus J. S. J., Hiemstra, S. A. and Gasparrini, E. (1976) The Merensky Reef at the Atok Platinum Mine and its environs. *Econ. Geol.*, **71**, 249–60.
- Skinner, B. J., Luce, F. D., Dill, J. A., Ellis, D. E., Hagen, H. A., Lewis, D. M., Odell, D. A., Sverjensky, D. A. and Williams, N. (1976) Phase relations in ternary portions of the system Pt–Pd–Fe–As–S. *Econ. Geol.*, **71**, 1469–75.
- Tarkian, M. (1987) Compositional variations and reflectance of the common platinum-group minerals. *Mineral. and Petrol.*, **36**, 169–90.
- Todd, S. G., Keith, D. W., Le Roy, L. W., Schissel, D. J., Mann, E. L. and Irvine, T. N. (1982) The J-M platinum-palladium reef of the Stillwater Complex, Montana: I. Stratigraphy and petrology. *Econ. Geol.*, **77**, 1454–80.
- Vaughan, D. J. and Craig, J. R. (1978) *Mineral chemistry of metal sulfides*. Cambridge University Press, xv + 493 pp.
- Vermaak, C. F. and Hendriks, L. P. (1976) A review of the mineralogy of the Merensky Reef with specific reference to new data on the precious metal mineralogy. *Econ. Geol.*, **71**, 1244–69.
- Volborth, A., Tarkian, M., Stumpfl, E. F. and Housley, R. M. (1986) A Survey of the Pd-Pt mineralization along the 35 km strike of the J-M Reef, Stillwater Complex, Montana. *Canad. Mineral.*, **24**, 329–46.
- Von Gruenewaldt, G., Hatton, C. J., Merkle, R. K. W. and Gain, S. B. (1986) Platinum-group element–chromitite associations in the Bushveld Complex. *Econ. Geol.*, **81**, 1067–79.

[Manuscript received 16 November 1992:
revised 4 August 1993]



Observations on Factors Affecting the Compositional Variation of Synthetic "Cooperite" in the System Pt-Pd-Ni-S at 1000 °C

By Sabine M. C. Verryn and Roland K. W. Merkle, Pretoria

With 6 figures and 2 tables in the text

VERRYN, S. M. C. & MERKLE, R. K. W.: Observations on Factors Affecting the Compositional Variation of Synthetic "Cooperite" in the System Pt-Pd-Ni-S at 1000 °C. - N. Jb. Miner. Mh. 1996, H. 10, 471-482; Stuttgart 1996.

Abstract: Experimental results on synthetic "cooperite" at 1000 °C are presented. The two phases observed in the experiments are "cooperite" and a melt. The Pt/Pd ratio of "cooperite" and the coexisting melt show a strong positive correlation ($r = 0.93$) and are dependant on the initial Pt/Pd ratio of the experimental charges. The maximum Pd-concentration at 1000 °C can be in excess of 11.4 atomic per cent. Within each group of constant initial Pt/Pd ratio, the Pt/Pd ratio of the quenched "cooperite" decreases with decreasing sulphur fugacity. With excess Ni in the charges, the Ni-content varies between 2.5 and 3.2 atomic per cent. The Ni-content increases slightly with increasing Pt/Pd ratio at constant S-pressure and with increasing S-pressure at constant Pt/Pd ratio.

Key words: Pt-Pd-Ni-S, phase relations, experimental investigations, synthetic "cooperite".

Introduction

Natural cooperite (ideally PtS), braggite ((Pt,Pd)S) and vysotskite (ideally PdS) have been described from various localities throughout the world, including the Merensky Reef and the UG-2 chromitite layer of the Bushveld Complex (e.g., BRYNARD et al. 1976, SCHWELLNUS et al. 1976, KINGSTON & EL-DOSUKY 1982, KINLOCH 1982, McLAREN & DE VILLIERS 1982, MOSTERT et al. 1982, PEYERL 1982, VERRYN & MERKLE 1994), the Stillwater Complex (e.g., TODD et al. 1982, VOLBOTH et al. 1986), Noril'sk (e.g., GENKIN & EVSTIGNEVA 1986), the Lukkulaisvaara and Imandrosky layered intrusions (BARKOV et al. 1995) and Penikat (ALAPIETI & LAHTINEN 1986, HALKOaho et al. 1990, HUHTELIN et al. 1990). Previous investigations of the compositional variation of cooperite, braggite, and vysotskite from the Bushveld Complex (VERRYN & MERKLE 1994) and of Ni-poor braggite in the Sompujärvi mineralization of the Penikat intrusion (MERKLE et al., in preparation) implied that the mineral chemistry of the system PtS-PdS-NiS is not sufficiently understood and should be com-

prehensively investigated. The system Pd–Ni–S was investigated by KARUP-MØLLER & MAKOVICKY (1993) up to 900 °C, and the system Ni–NiS–PtS–Pt by GULYANITSKAYA et al. (1979). Experimental investigations by SKINNER et al. (1976) at 1000 °C and CABRI et al. (1978) at 800 °C concentrated on the PtS–PdS join and were not exploring the possible influence of Ni on thermal stabilities and miscibility ranges of minerals in the system. Looking at the mineral compositions of braggite and cooperite from the Bushveld (VERRYN & MERKLE 1994), Pd/Ni ratio remains fairly constant, but varies for different base metal assemblages (Fig. 1). This was interpreted as a systematic substitution of Pd + Ni

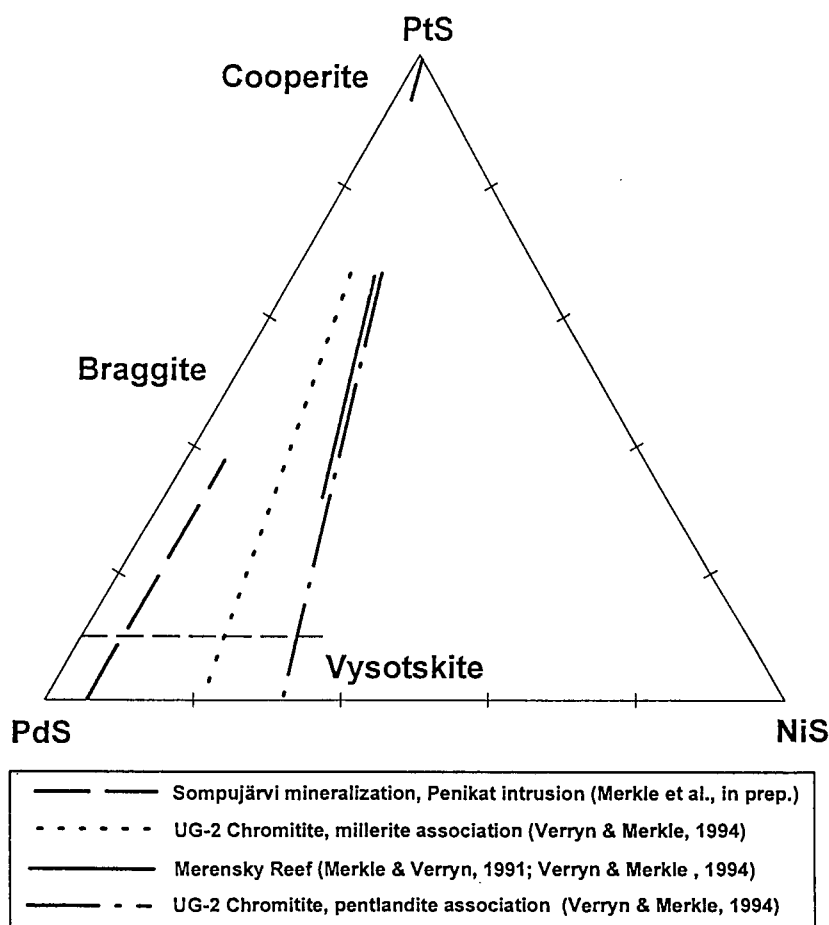


Fig. 1. Schematic illustration of the compositional variation of cooperite, braggite, and vysotskite from the Merensky Reef and the UG-2 chromitite of the Bushveld Complex, and from the Sompujärvi mineralization, Penikat intrusion.

for Pt the amount of Ni substitutable seems to be a function of temperature (rather than the activity of NiS). In cooperite, the chemical variations were rather small, limiting the confidence in any implied substitution trends. It became apparent during the analytical investigation of braggite from Sompujärvi (Penikat intrusion, Finland) that the relationships established from the Bushveld Complex are not the only possible systematic relationship of cation concentrations in braggite. Here it was found that braggite displays approximately constant Ni proportions, while the Pt/Pd ratio is variable (MERKLE et al., in preparation). In this mineralization, cooperite was not observed, but this deviation from the rules which apparently control the mineral chemistry of cooperite and braggite from the Bushveld Complex, was taken into account in the planning of experimental investigations of the system Pt–Pd–Ni–S.

The investigation presented here is based on experiments at 1000 °C, which form part of a larger evaluation of the phase relations in the system PtS–PdS–NiS at several other temperatures.

Experimental techniques

All experiments were conducted under dry conditions following standard procedures in evacuated quartz–glass capsules (MOH & TAYLOR 1971, KULLERUD 1971).

13 Charges of 200–300 mg each were prepared and were sealed under a vacuum of $\sim 8 \times 10^{-2}$ millibar.

Metal and metal/sulphur ratios were varied in order to obtain an indication of the effects of sulphur pressure, Ni-activity, and initial Pt/Pd ratio. All charges initially contained 47–51 atomic per cent sulphur, 24.0–26.5 atomic per cent Ni (which is in excess of the amount of Ni that can be accommodated by cooperite, see Fig. 1), and Pt/Pd atomic ratios ranging from 0.08 to 5.25 (i.e., 1.9 to 22.0 atomic per cent Pt and 3.9 to 24.2 atomic per cent Pd).

An excess of sulphur can cause experimental difficulties in dry sulphide research. Sulphur-vapour pressures are not known very accurately (NELL 1987), but to avoid failure of the glass containers due to high sulphur vapour-pressures, the charges were pre-reacted at 800 °C for 24 days. After further tempering for 8 hours at 1200 °C to achieve quick homogenization in the melt stage without excessive growths of cooperite, the charges were reacted for 38 days at 1000 °C, before being quenched in ice-water.

Analytical techniques

Polished sections of the quenched products were studied by reflected light microscopy. The compositional variation of the products was determined by electron microprobe analysis on a JEOL 733 microprobe in wavelength-dis-

persive mode. The accelerating potential was 20 kV and the beam current 2×10^{-8} A. Multiple spot analyses were taken on "cooperite". Synthetic PdS (L_{α} line) was used for Pd, the K_{α} line for S on the same standard, synthetic $Pt_{0.7}Pd_{0.3}S$ (L_{α} line) for Pt and synthetic NiS (K_{α} line) for Ni. Solidified melts were analysed by scanning multiple preselected areas using a quenched melt with known composition as a standard (MERKLE et al., in preparation). Reproducibilities at the 1 sigma level are given in Table 1. Analyses with totals between 98.5 and 101.5 weight per cent were considered in the following discussions. A summary of the analytical results in atomic proportions is given in Table 2.

Table 1. Reproducibilities (1 sigma, determined according to KAISER & SPECKER 1956) for analyses of synthetic "cooperite" and solidified melt in atomic per cent.

	Synthetic "Cooperite"	Solidified Melt
Pt	0.207	0.017
Pd	0.167	0.007
Ni	0.051	0.014
S	0.167	0.014

Table 2. Mean experimental results of the system PtS–PdS–NiS at 1000 °C in atomic per cent. * Indicates the presence of visible sulphur after quenching (values in parentheses show the standard deviations at the 1 σ level).

Sample No.	Phase	No. of analysis	Pt (at %)	Pd (at %)	Ni (at %)	S (at %)
SV200*	Melt	20	1.99 (0.090)	22.93 (0.453)	25.38 (0.554)	49.70 (0.180)
SV201*	"Cooperite"	45	36.13 (0.275)	11.39 (0.203)	2.52 (0.042)	49.95 (0.303)
	Melt	20	2.93 (0.225)	15.14 (0.378)	30.81 (0.591)	51.12 (0.173)
SV202*	"Cooperite"	23	41.66 (0.202)	5.92 (0.187)	2.90 (0.060)	49.52 (0.177)
	Melt	20	2.74 (0.202)	10.14 (0.290)	37.48 (0.286)	49.65 (0.188)
SV203*	"Cooperite"	27	44.15 (0.450)	3.07 (0.213)	3.15 (0.162)	49.64 (0.253)
	Melt	14	2.81 (0.340)	4.48 (0.347)	39.28 (0.290)	53.44 (0.222)
SV204*	Melt	20	2.08 (0.159)	23.65 (0.856)	26.80 (0.573)	47.48 (0.509)
SV205*	"Cooperite"	14	38.06 (0.171)	9.95 (0.140)	2.50 (0.056)	49.49 (0.161)
	Melt	20	3.47 (0.333)	16.93 (0.400)	31.56 (0.564)	48.06 (0.300)
SV206	"Cooperite"	45	42.44 (0.280)	5.08 (0.190)	2.67 (0.061)	49.81 (0.265)
	Melt	14	4.05 (0.251)	10.65 (0.252)	37.44 (0.416)	47.86 (0.245)
SV207	"Cooperite"	25	45.32 (0.231)	2.18 (0.159)	2.96 (0.087)	49.57 (0.197)
	Melt	20	4.03 (0.241)	5.54 (0.367)	42.09 (0.346)	48.34 (0.258)
SV208*	Melt	20	2.15 (0.250)	23.36 (0.620)	25.18 (0.810)	49.30 (0.305)
SV209*	"Cooperite"	45	36.85 (0.296)	11.07 (0.243)	2.51 (0.053)	49.58 (0.212)
	Melt	18	3.80 (0.375)	16.68 (0.527)	28.77 (0.795)	50.75 (0.161)
SV210*	"Cooperite"	17	42.55 (0.250)	4.32 (0.242)	3.07 (0.082)	50.06 (0.353)
	Melt	20	3.98 (0.295)	7.48 (0.614)	36.51 (0.439)	52.03 (0.216)
SV211*	"Cooperite"	19	40.47 (0.484)	6.78 (0.224)	2.97 (0.062)	49.79 (0.308)
	Melt	18	2.12 (0.117)	9.98 (0.616)	37.26 (0.572)	50.65 (0.202)
SV212*	"Cooperite"	24	40.05 (0.261)	7.10 (0.220)	2.89 (0.082)	49.96 (0.256)
	Melt	14	3.29 (0.233)	9.93 (0.362)	36.07 (0.460)	50.72 (0.195)

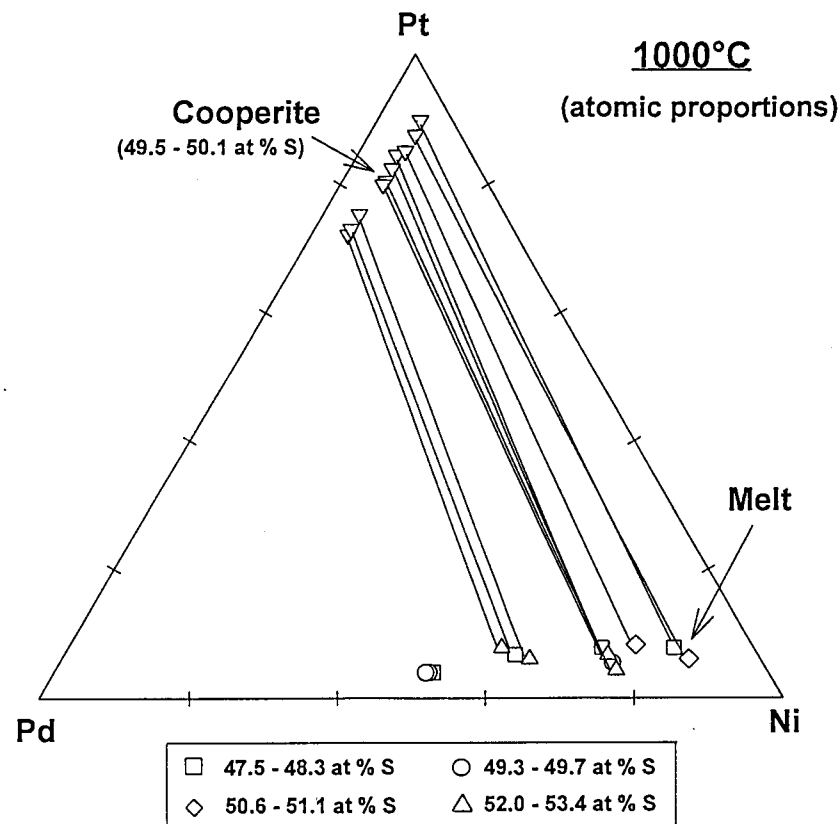


Fig. 2. Compositional variation of "cooperite" and coexisting melt in the system Pt–Pd–Ni–S at 1000 °C in atomic per cent.

Discussion of phase relationships

At 1000 °C in a "NiS-saturated" environment the following observations emerged:

1. The two phases recognized are "cooperite" and a melt. The compositional relationship between the "cooperite" and the coexisting melt is shown in Fig. 2. No "cooperite" formed at Pt/Pd ratios in the initial charge of 0.085 (i.e., 1.95 to 2.06 atomic per cent Pt and 22.64 to 24.24 atomic per cent Pd). The Pt/Pd ratios of cooperite and the coexisting melt exhibits a strong positive correlation of $r = 0.93$ (Fig. 3).
2. "Cooperite" displays a relatively constant Ni-content of 2.5 to 3.2 atomic per cent and a maximum Pd content of 11.4 atomic per cent in our experi-

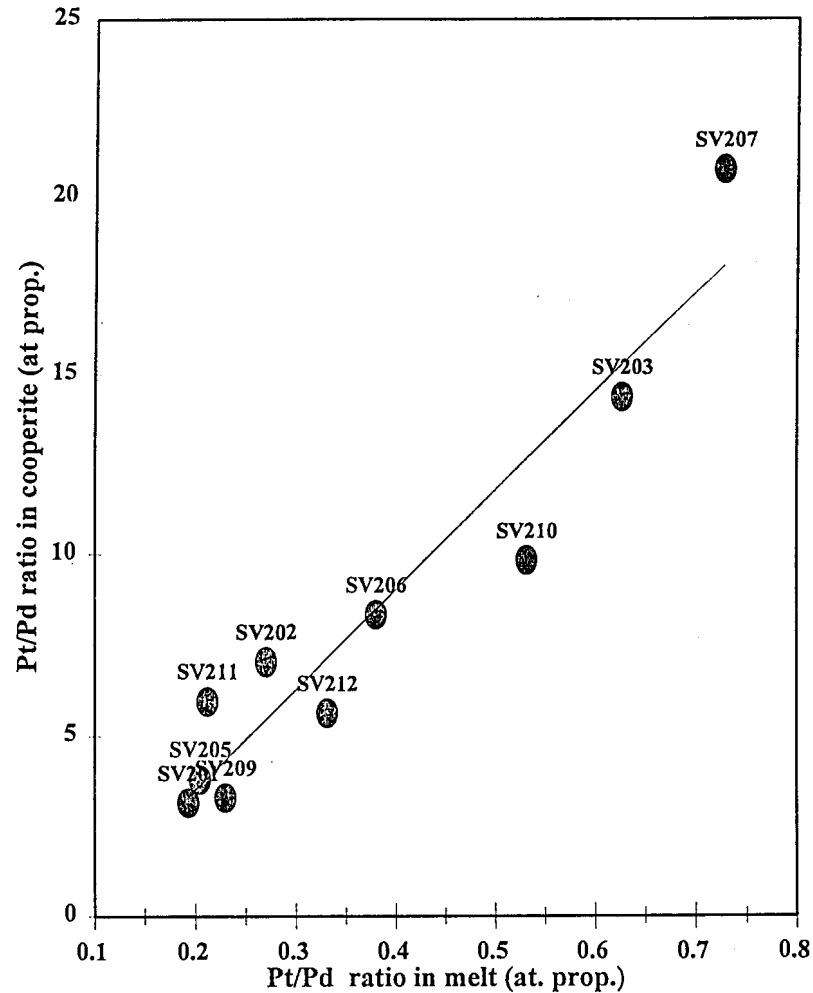


Fig. 3. Pt/Pd ratio in "cooperite" versus Pt/Pd ratio in melt in atomic proportions (the solid line indicates the best linear fit).

ments to date. The true limit of Pd solubility in "cooperite" at this temperature has not yet been determined.

- "Cooperite" synthesized at 1000 °C contains higher amounts of Ni at given Pt/Pd ratios if formed under higher S-pressure. Ni in the "cooperite" increases with increasing Pt/Pd ratio at relatively constant S-pressure (Fig. 4). The former is in disagreement with the findings in natural cooperites and braggites from the Merensky Reef and the UG-2 of the Bushveld

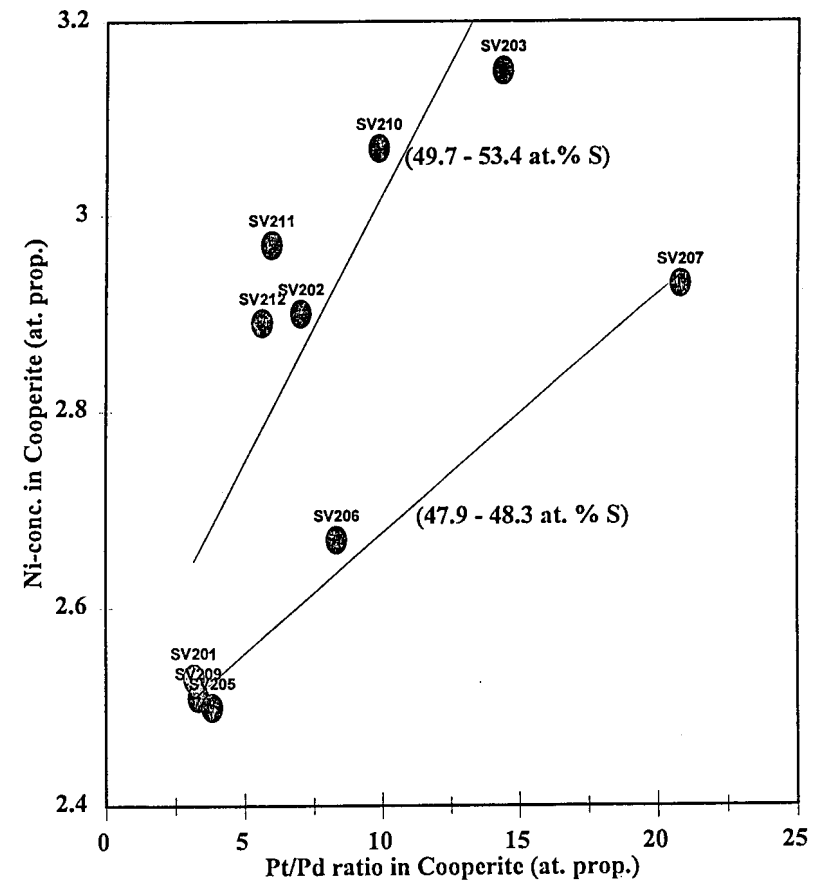


Fig. 4. Ni-concentration versus Pt/Pd ratio in "cooperite" (in atomic proportions), solid lines indicate best linear fits for two groups of sulphur concentrations in coexisting melt (in parenthesis, atomic per cent), experiment numbers are indicated above symbols.

Complex (VERRYN & MERKLE 1994). Here the Ni content increased significantly with decreasing Pt/Pd ratio. This might, however, be due to different temperatures of formation and/or equilibration, as well as availability of Ni. On the other hand, braggite might follow a trend different from that of cooperite.

- Analytical results of S-content of the "cooperite" vary between 49.49 and 50.06 atomic per cent. The S-content of the solidified melt lies between 47.86 and 53.44 atomic per cent for individual analysis, showing a strong positive correlation ($r = 0.89$) with the initial S-content of the charge.



5. After quenching, a thin layer of sulphur on the capsule walls was observed in some charges according to the following pattern:

The amount of visible sulphur on the capsule walls increases with increasing Pd-content at constant overall S-content in the charge. Additionally, the higher the overall S-content, the more visible S.

The amount of free sulphur after quenching (even at proportions below 50 atomic per cent) seems not to be due to a surplus of sulphur which was not able to react with the metals present. Two possible interpretations of this observation are:

(1) The sulphur on the capsule walls is due to a release of elemental sulphur on quenching in analogy to the phase-relations in the Ni-Pd-S system (KARUP-MØLLER & MAKOVICKY 1993). At 1000 °C, the proportions of melt (58–82 per cent, estimated using the lever rule), as well as the Pd-concentration in the melt, increase in the quenched experiments with increasing Pd-content. KARUP-MØLLER & MAKOVICKY (1993) showed that at 900 °C, the central portion of the system Pd-Ni-S is dominated by a sulphide melt which extends from the Ni-S join to the Pd-S join. At the Ni-S join the melt lies between ~30 and 46 atomic per cent S and at the Pd-S join between ~18.5 to 45 atomic per cent S. In the stability field of the melt, between $Pd_{0.15}Ni_{0.35}S$ and $Pd_{0.28}Ni_{0.22}S$ the melt contains between ~20 and 50 atomic per cent sulphur resulting in a drop of S-content from 50 atomic per cent at $Pd_{0.15}Ni_{0.35}S$ to 46 atomic per cent at the Ni-S join.

We believe that this change in maximum S-solubility in the melt can cause the expulsion of elemental sulphur on quenching which, in the rapid process of quenching, cannot combine with any of the crystallizing phases, and condenses on the capsule walls.

(2) The sulphur on the tube walls may be interpreted to be condensed vapour as described by ARNOLD & MALIK (1975) for the NiS-S system and by ARNOLD (1971) for the FeS-S system. ARNOLD & MALIK (1975) proposed to correct the combined condensed phases (solid and/or liquids) for the loss of sulphur by weighing of the sulphur in each cooled charge. In the system Pt-Pd-Ni-S, cooperite is a stoichiometric monosulphide and only the melt portion should be corrected for sulphur loss. The amount of sulphur condensed on the capsule wall lies, however, within the uncertainty of the scale and a correction of the S-content of the melt would be inaccurate.

6. TAYLOR (1985) showed that within melts in the Pd-S system an increase in S-content causes an increase in sulphur fugacity. In order to obtain an indication which effect the sulphur fugacity has on the system Pt-Pd-Ni-S, charges containing between 47 and 51 atomic per cent sulphur at constant Pt/Pd and Ni atomic ratios were prepared. Within each group of constant initial Pt/Pd ratio, the Pt/Pd ratio of the quenched "cooperite" decreases

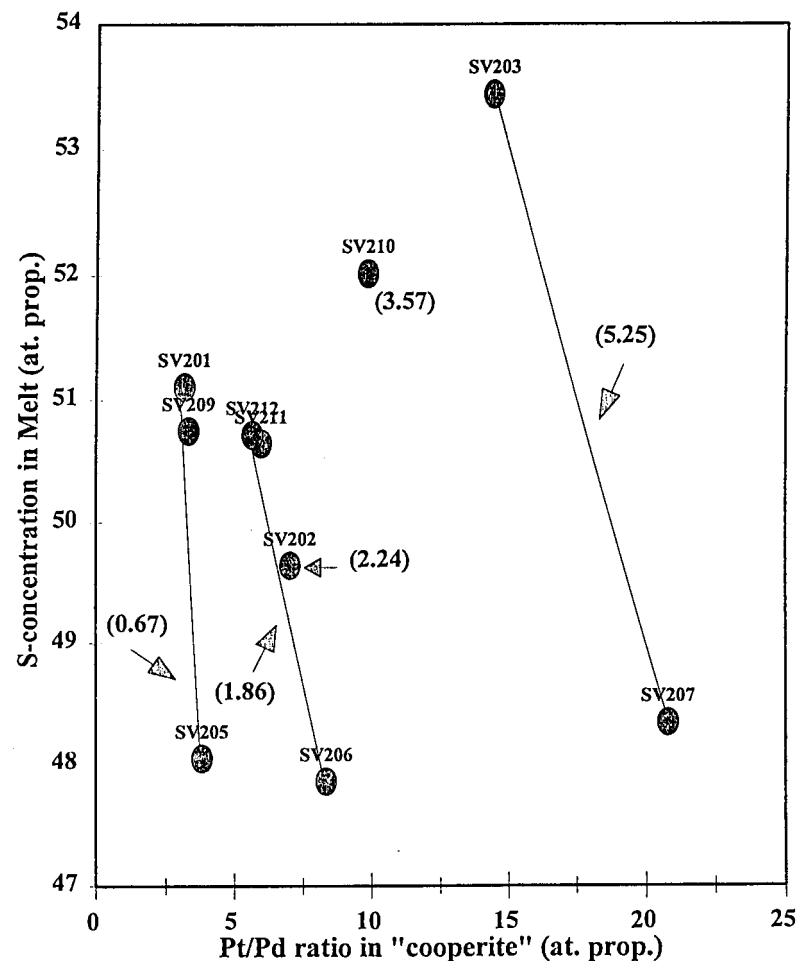


Fig. 5. Pt/Pd ratio in "cooperite" versus S-concentration in coexisting melt in atomic proportions (sample numbers are placed above symbols, Pt/Pd ratio (atomic proportions) of the initial charges in parenthesis).

with increasing sulphur fugacity (Figs. 2 and 5). Fig. 6 shows that PdS becomes stable at higher sulphur fugacities than PtS (BARIN et al. 1977), i.e., higher f_{S_2} will stabilize "cooperite" with higher Pd-content. However, the starting compositions (i.e., Pt/Pd ratio in the initial charges) do not permit the formation of braggite.

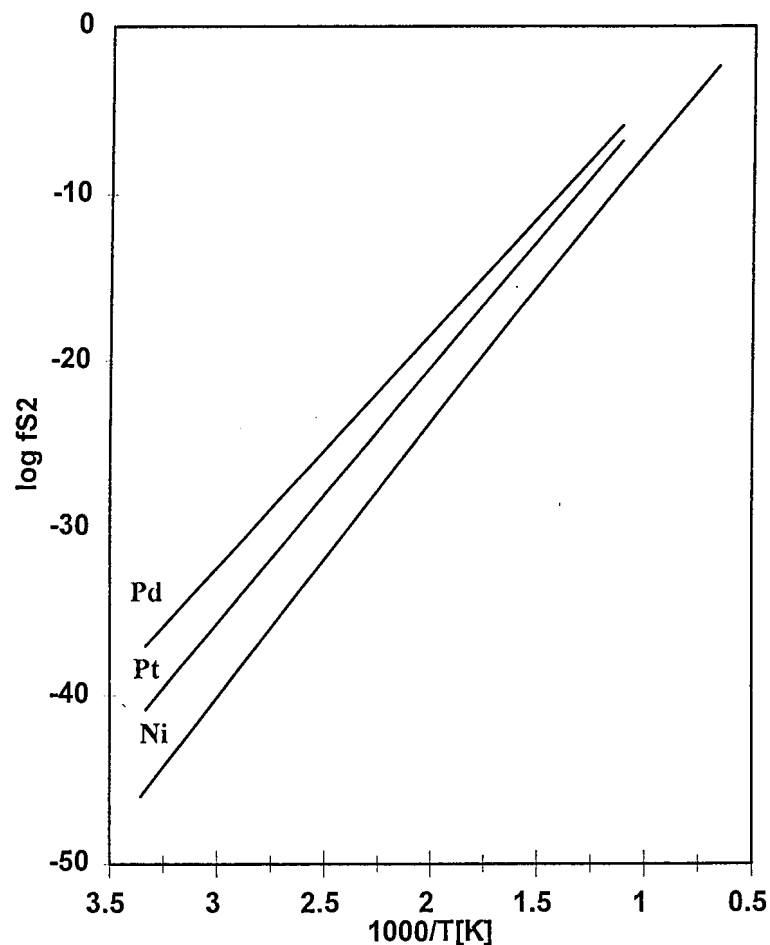


Fig. 6. Sulphur pressures versus temperature for Pd+S/PdS, Pt+S/PtS and Ni+S/NiS (data from BARIN et al. 1973).

Summary

The following observations in the system Pt–Pd–Ni–S at 1000 °C can be highlighted:

1. The maximum solubility of Pd in "cooperite" at 1000 °C is in excess of 11.4 atomic per cent in a Ni- and S-saturated environment.
2. There is a strong positive correlation between the Pt/Pd ratios of cooperite and the coexisting melt.
3. The Ni-content varies between 2.5 and 3.2 atomic per cent and increases slightly with increasing Pt/Pd ratio of the cooperite as well as with increasing sulphur pressure of formation.

4. The Pt/Pd ratio of the quenched "cooperite" decreases with increasing sulphur pressure within each group of constant initial Pt/Pd ratio.
5. "Cooperite" compositions are dependent on a more complex interplay of factors than previously assumed. More experiments at different temperatures will have to be carried out in order to establish the temperature dependence of the Ni- and Pd-solubility in cooperite, to pinpoint the maximum Pd-concentration in cooperite more precisely and to determine the possible stability of braggite at this temperature.

Acknowledgements

The authors would like to thank JULIANA BRUWER for fruitful discussions, A. V. ATANASOV for the assistance in the microprobe analyses, L. J. CABRI for synthetic standards, and Zeiss South Africa for assisting us with microscope facilities.

References

- ALAPIETI, T. & LAHTINEN, J. J. (1986): Stratigraphy, petrology, and platinum-group element mineralization of the early Proterozoic Penikat layered intrusion, northern Finland. – *Econ. Geol.* 81, 1126–1136.
- ARNOLD, R. G. (1971): Evidence for Liquid Immiscibility in the System FeS–S. – *Econ. Geol.* 66, 1121–1130.
- ARNOLD, R. G. & MALIK, O. P. (1975): The NiS–S System above 980 °C – A Revision. – *Econ. Geol.* 70, 176–182.
- BARIN, O., KNACKE, O. & KUBASCHEWSKI, O. (1977): Thermochemical properties of inorganic substances (Supplement). – Springer Verlag, Berlin, Heidelberg, New York, 861 pp.
- BARKOV, A. YU., PAKHOMOVSKII, Y. A. & MEN'SHIKOV, Y. P. (1995): Zoning in the platinum-group sulphide minerals from the Lukkulaivaara and Imandrovsky layered intrusions, Russia. – *N. Jb. Miner. Abh.* 169, 97–117.
- BRYNARD, H. J., DE VILLIERS, J. P. R. & VILJOEN, E. A. (1976): A mineralogical investigation of the Merensky Reef at the Western Platinum Mine, near Marikana, South Africa. – *Econ. Geol.* 71, 1299–1307.
- CABRI, L. J., LAFLAMME, J. H. G., STEWARD, J. M., TURNER, K. & SKINNER, B. J. (1978): On cooperite, braggite, and vysotskite. – *Amer. Miner.* 63, 832–839.
- GENKIN, A. D. & EVSTIGNEEVA, T. L. (1986): Associations of platinum-group minerals of the Noril'sk copper-nickel sulphide ores. – *Econ. Geol.* 81, 1203–1212.
- GULYANITSKAYA, Z. F., PAVLYUCHENKO, N. M., BLOKHINA, L. I. & ZVIADADZE, G. N. (1979): The Ni–NiS–PtS system. – *Izv. Akad. Nauk. SSSR, Neorg. Materialy.* 15, 1933–1938 (in Russian).
- HALKOHO, T. A. A., ALAPIETI, T. T. & LAHTINEN, J. J. (1990): The Sompujärvi PGE reef in the Penikat layered intrusion, northern Finland. – *Miner. Petrol.* 42, 39–55.
- HUHTELIN, T. A., ALAPIETI, T. T. & LAHTINEN, J. J. (1990): The Pasivaara PGE reef in the Penikat layered intrusion, northern Finland. – *Miner. Petrol.* 42, 57–70.
- KAISER, H. & SPECKER, H. (1956): Bewertung und Vergleich von Analysenverfahren. – *Z. Analyt. Chem.* 149, 46–66.
- KARUP-MØLLER, S. & MAKOVICKY, E. (1993): The system Pd–Ni–S at 900°, 725°, 550°, and 400 °C. – *Econ. Geol.* 88, 1261–1268.



- KINGSTON, G. A. & EL-DOSUKY, B. T. (1982): A contribution on the platinum-group mineralogy of the Merensky Reef at the Rustenburg Platinum Mine. – *Econ. Geol.* 71, 1299–1307.
- KINLOCH, E. D. (1982): Regional trends in the platinum-group mineralogy of the Critical Zone of the Bushveld Complex, South Africa. – *Econ. Geol.* 77, 1328–1347.
- KULLERUD, G. (1971): Experimental techniques in dry sulphide research. – In: ULMER, G. C. (ed.): *Research Techniques for High Pressure and High Temperature*. – Springer Verlag, Berlin–Heidelberg–New York, 289–315.
- McLAREN, C. H. & DE VILLIERS, J. P. R. (1982): The platinum-group chemistry and mineralogy of the UG–2 chromitite layer of the Bushveld Complex. – *Econ. Geol.* 77, 1348–1366.
- MERKLE, R. K. W. & VERRYN, S. M. C. (1991): Coexisting cooperite and braggite – new data. Papers, International Congress on Applied Mineralogy, 1991. – Pretoria, South Africa, Paper 61, 17 pp.
- MOH, G. H. & TAYLOR, L. A. (1971): Laboratory techniques in experimental sulphide petrology. – *N. Jb. Miner. Mh.* 1971, 450–459.
- MOSTERT, A. B., HOFMEYER, P. K. & POTGIETER, G. A. (1982): The platinum-group mineralogy of the Merensky Reef at the Impala Platinum Mines, Bophuthatswana. – *Econ. Geol.* 77, 1385–1394.
- NELL, J. (1987): Phase Relations in the system Nickel–Copper–Sulphur–Ruthenium at 1200 °C. – Mintek Report No. M307, 8 pp.
- PEYERL, W. (1982): The influence of the Driekop dunite pipe on the platinum-group mineralogy of the UG–2 chromitite in its vicinity. – *Econ. Geol.* 77, 1432–1438.
- SCHWELLNUS, J. S. I., HIEMSTRA, S. A. & GASPARRINI, E. (1976): The Merensky Reef at the Atok Platinum Mine and its environs. – *Econ. Geol.* 71, 249–260.
- SKINNER, B. J., LUCE, F. D., DILL, J. A., ELLIS, D. E., HAGAN, H. A., LEWIS, D. M., ODELL, D. A., SVERJENSKY, D. A. & WILLIAMS, N. (1976): Phase relations in ternary portions of the system Pt–Pd–Fe–As–S. – *Econ. Geol.* 71, 1469–1475.
- TAYLOR, J. R. (1985): Phase relationships and thermodynamic properties of the Pd–S system. – *Metallurgical Transactions B.* 16 B, 143–148.
- TODD, S. G., KEITH, D. W., LE ROY, L. W., SCHISSEL, D. J., MANN, E. L. & IRVINE, T. N. (1982): The J–M platinum–palladium reef of the Stillwater Complex, Montana: I. Stratigraphy and petrology. – *Econ. Geol.* 77, 1454–1480.
- VERRYN, S. M. C. & MERKLE, R. K. W. (1994): Compositional variation of cooperite, braggite, and vysotskite from the Bushveld Complex. – *Miner. Mag.* 58, 223–234.
- VOLBORTH, A., TARKIAN, M., STUMPFL, E. F. & HOUSLEY, R. M. (1986): A Survey of the Pd–Pt mineralization along the 35 km Strike of the J–M Reef, Stillwater Complex, Montana. – *Can. Miner.* 24, 329–346.

Received: August 13, 1996; accepted: September 24, 1996.

Authors' address:

Applied Mineralogy Group, Department of Geology, University of Pretoria, Pretoria 0002, South Africa, e-mail: SABINE@SCIENTIA.UP.AC.ZA.

Synthetic “Cooperite”, “Braggite”, and “Vysotskite” in the system PtS-PdS-NiS at 1100 °C, 1000 °C, and 900 °C

S. M. C. Verryyn and R. K. W. Merkle

Applied Mineralogy Group, Department of Earth Sciences, University of Pretoria, Pretoria,
South Africa

With 6 Figures

Received October 1, 1998;
revised version accepted September 7, 1999

Summary

Results of experimental investigations in the dry system PtS-PdS-NiS at 1100 °C, 1000 °C, and 900 °C are presented. The phases observed at 1100 °C are “cooperite” and a melt, at 1000 °C “cooperite”, “braggite”, and a melt and at 900 °C “cooperite”, “braggite”, “vysotskite”, Ni_{1-x}S, and a melt. At 1100 °C the maximum solubility of Ni in ideal, Pd-free “cooperite” is 2.7 atomic per cent and the Pd-content limit in Ni-free “cooperite” is 12.8 atomic per cent. At 1000 °C the maximum solubility of Ni in ideal, Pd-free “cooperite” is 3.3 atomic per cent and the Pd-content in Ni-free “cooperite” is 13.7 atomic per cent. The “braggite” composition ranges from Pt_{0.56}Pd_{0.38}Ni_{0.06}S and Pt_{0.59}Pd_{0.41}S in a Ni-saturated and Ni-free environment respectively to Pt_{0.18}Pd_{0.80}Ni_{0.02}S and Pt_{0.14}Pd_{0.86}S respectively. At 900 °C the maximum Ni-content in ideal Pd-free “cooperite” is 3.1 atomic per cent and the Pd-limit in Ni-free “cooperite” is 12.5 atomic per cent. The “braggite” composition ranges from Pt_{0.59}Pd_{0.29}Ni_{0.12}S and Pt_{0.60}Pd_{0.40}S for a Ni-saturated and Ni-free environment respectively, to Pd_{0.91}Ni_{0.09}S and PdS respectively. The Ni-content in “braggite” and “vysotskite” increases slightly with increasing Pt/Pd ratios and is higher at 900 °C than at 1000 °C. Comparison of experimental trends with cooperite, braggite, and vysotskite analyses from the literature implies high temperatures of formation for Pt-Pd-Ni sulphides in placers if Ni-saturation is assumed.

Zusammenfassung

Synthetischer „Cooperit”, „Braggit” und „Vysotskit” im System PtS-PdS-NiS bei 1100 °C, 1000 °C und 900 °C

Ergebnisse experimenteller Untersuchungen im trockenen System PtS-PdS-NiS bei 1100 °C, 1000 °C und 900 °C werden dargestellt. Bei 1100 °C sind die Phasen "Cooperit" und Schmelze, bei 1000 °C "Cooperit", "Braggit" und Schmelze und bei 900 °C "Cooperit", "Braggit", "Vysotskit", $Ni_{1-x}S$ und Schmelze stabil. Bei 1100 °C ist die maximale Löslichkeit von Ni in idealem, Pd-freiem "Cooperit" 2.7 Atomprozent und der Pd-Gehalt in Ni-freiem "Cooperit" liegt bei maximal 12.8 Atomprozent. Bei 1000 °C ist die maximale Löslichkeit von Ni in idealem, Pd-freiem "Cooperit" 3.3 Atomprozent und der Pd-Gehalt in Ni-freiem "Cooperit" liegt bei maximal 13.7 Atomprozent. Die Zusammensetzung des "Braggits" variiert zwischen $Pt_{0.56}Pd_{0.38}Ni_{0.06}S$ und $Pt_{0.18}Pd_{0.80}Ni_{0.02}S$ in einem Ni-gesättigtem und zwischen $Pt_{0.59}Pd_{0.41}S$ und $Pt_{0.14}Pd_{0.86}S$ in einem Ni-freien Umfeld. Bei 900 °C liegt die maximale Löslichkeit von Ni in idealem Pd-freiem "Cooperit" bei 3.1 Atomprozent und der Pd-Gehalt in Ni-freiem "Cooperit" liegt bei maximal 12.5 Atomprozent. Die Zusammensetzung des "Braggits" variiert zwischen $Pt_{0.59}Pd_{0.29}Ni_{0.12}S$ und $Pd_{0.89}Ni_{0.08}S$ in einem Ni-gesättigten und zwischen $Pt_{0.59}Pd_{0.40}S$ und PdS in einem Ni-freien Umfeld. Der Nickelgehalt in "Braggit" und "Vysotskit" nimmt mit zunehmendem Pt/Pd Verhältnis zu und ist bei 900 °C höher als bei 1000 °C. Ein Vergleich der experimentellen Trends mit Cooperit, Braggit und Vysotskit Analysen aus der Literatur weist auf eine Hochtemperaturbildung der Pt-Pd-Ni Sulfide in Seifenlagerstätten hin, wenn man von Nickelsättigung ausgeht.

Introduction

From an economic point of view, cooperite, braggite, and vysotskite are arguably the most important platinum group minerals because of their high proportions in the platinum group ores of the Bushveld Complex (e.g. *Brynard et al.*, 1976; *Schwellnus et al.*, 1976; *Kingston and El-Dosuky*, 1982; *Mostert et al.*, 1982; *Kinloch*, 1982; *McLaren and De Villiers*, 1982; *Peyerl*, 1982), of the Stillwater Complex (e.g. *Todd et al.*, 1982; *Volborth et al.*, 1986) and of Noril'sk (e.g. *Genkin and Evstigneeva*, 1986).

However, the compositional variation of these minerals (i.e. the compositional relationships between coexisting cooperite and braggite) is so poorly understood (*Verryyn and Merkle*, 1994) that it was felt necessary to investigate the system PtS-PdS-NiS experimentally. Results of experiments performed at 900 °C, 1000 °C, and 1100 °C are presented here.

Experimental procedures

Experiments were conducted under dry conditions following standard procedures in evacuated quartz-glass capsules (*Moh and Taylor*, 1971; *Kullerud*, 1971). Charges of 250–300 mg were prepared and sealed under a vacuum of $\sim 2 \times 10^{-5}$ bar. The Pt, Pd, and Ni content in the experimental charges was varied. We are aware of the effects of variable S-content (*Verryyn and Merkle*, 1996), however, here we report only on initial sulphur contents of 50 atomic per cent. All charges were pre-reacted at 800 °C for ± 3 weeks. After further tempering for 8 hours at 1200 °C to achieve quick homogenization in the melt stage, the charges were reacted at the relevant temperatures between 10 (at 1100 °C) and 36 (at 900 °C) days. The experimental charges were quenched in ice-water.

Analytical technique

Polished sections of the quenched products were studied by reflected light microscopy. The compositional variation of the products was determined by electron microprobe analysis on a JEOL 733 microprobe in wavelength-dispersive mode. The accelerating potential was 20 kV and the beam current 5×10^{-8} A. Multiple spot analyses were taken on “cooperite”, “braggite”, and “vysotskite”. Synthetic PdS (L_{α} line) was used for Pd, the K_{α} line for S on the same standard, synthetic $Pt_{0.7}Pd_{0.3}S$ (L_{α} line) for Pt and synthetic NiS (K_{α} line) for Ni. Solidified melts were analysed by a defocussed beam or scanning multiple preselected areas using the same standards as for the solid phases.

Results

The compositions of melt and coexisting “cooperite”, “braggite”, and “vysotskite are summarized in Table 1.

At $1100^{\circ}C$ (Fig. 1), the two phases observed are “cooperite” and a melt. The PdS-NiS join is occupied by a melt with a maximum solubility of 9.0 atomic per cent Pt along the PtS-NiS join as well as along PtS-PdS join. Towards the central portion of the melt field along the PdS-NiS join, the Pt content decreases to a minimum of 3.5 atomic per cent. The maximum solubility of Ni in ideal, Pd-free “cooperite” coexisting with Pd-free melt along the PtS-NiS join is 2.7 atomic per cent. The Pd-content limit in Ni-free “cooperite” coexisting with Ni-free melt lies at 12.8 atomic per cent (Fig. 4). The Ni-content in “cooperite” at $1100^{\circ}C$ decreases slightly with increasing Pd-content.

At $1000^{\circ}C$ (Fig. 2), the compositional field of the melt is reduced and a third phase corresponding to “braggite” appears. Maximum solubility of Pt in the melt along the PtS-PdS join is 1.1 atomic per cent. The Pt-concentration in melt coexisting with coexisting “cooperite” and “braggite” (i.e. all three phases coexist) decreases sharply to a minimum of 0.7 atomic per cent and rises to 4.0 atomic per cent Pt along the PtS-NiS join. A similar trend is observed at $900^{\circ}C$. The maximum solubility of Ni in ideal, Pd-free “cooperite” along the PtS-NiS join is 3.3 atomic per cent. The Pd content in Ni-free “cooperite” coexisting with “braggite” at $1000^{\circ}C$ is 13.7 atomic per cent (Fig. 4). The Ni-content in “cooperite” in a Ni-saturated environment decreases slightly with increasing Pd-content, but is slightly higher than at $1100^{\circ}C$. The “braggite” composition ranges from $Pt_{0.56}Pd_{0.38}Ni_{0.06}S$ and $Pt_{0.59}Pd_{0.41}S$ in a Ni-saturated and Ni-free environment respectively to $Pt_{0.18}Pd_{0.80}Ni_{0.02}S$ and $Pt_{0.14}Pd_{0.86}S$ respectively. The Ni-concentration in “braggite” in a Ni-saturated environment decreases with increasing Pd content (Fig. 5).

At $900^{\circ}C$ (Fig. 3), the compositional field of the melt is further reduced compared to that at $1000^{\circ}C$, especially on the Pd-rich side of the PdS-NiS join. The compositional field of “braggite” is now stretching down to the PdS-NiS join. The melt which coexists with Pt-free “vysotskite” (with a maximum Ni-content of 4.3 atomic per cent) contains 25.0 atomic per cent Pd. This is in good agreement with results at $900^{\circ}C$ by *Karup-Møller* and *Makovicky* (1993), who obtained a maximum Ni content of 3.9 atomic per cent and a maximum Pd content of 23.3

Table 1. Mean (arithmetic) experimental results of the system PtS-PdS-NiS at 1100°C, 1000°C and 900°C in weight per cent (wt%) and atomic per cent (at%). Values in parenthesis show the standard deviation at the 1 σ level. N number of analyses per experiment

Sample	Phases		Pt	Pd	Ni	S	TOTAL
1100°C							
SV337	"Cooperite"	wt%	83.43 (0.37)	1.41 (0.33)	1.04 (0.08)	13.74 (0.15)	99.62
		at%	48.20	1.49	2.00	48.31	(N=17)
	Melt	wt%	31.75 (3.08)	6.92 (1.28)	35.10 (3.09)	26.08 (1.45)	99.45
		at%	9.93	3.97	36.48	49.63	(N=10)
SV338	"Cooperite"	wt%	74.62 (0.37)	9.19 (0.53)	0.38 (0.06)	15.04 (0.26)	99.23
		at%	40.50	9.15	0.69	49.67	(N=39)
	Melt	wt%	9.79 (6.55)	61.62 (5.88)	10.51 (1.98)	17.72 (1.67)	99.64
		at%	3.69	42.55	13.15	40.61	(N=21)
SV339	"Cooperite"	wt%	78.48 (0.58)	7.10 (0.55)	0	15.23 (0.18)	100.82
		at%	42.61	7.07	0	50.32	(N=7)
SV340	"Cooperite"	wt%	70.84 (0.57)	13.43 (0.48)	0	16.02 (0.32)	100.29
		at%	36.71	12.76	0	50.52	(N=38)
	Melt	wt%	21.40 (6.94)	62.32 (1.68)	0	16.70 (0.61)	100.42
		at%	9.02	48.16	0	42.83	(N=16)
SV342	"Cooperite"	wt%	84.28 (0.91)	0	1.45 (0.03)	14.28 (0.15)	100.02
		at%	47.89	0	2.74	49.37	(N=39)
	Melt	wt%	30.56 (7.39)	0	40.53 (6.05)	28.78 (1.79)	100.21
		at%	8.98	0	39.57	51.45	(N=15)
SV1102	"Cooperite"	wt%	72.06 (0.29)	11.48 (0.41)	0.38 (0.02)	15.71 (0.36)	99.63
		at%	37.93	11.08	0.66	50.32	(N=117)
	Melt	wt%	10.99 (4.54)	61.38 (2.69)	8.80 (1.99)	18.19 (0.76)	99.36
		at%	4.17	42.72	11.10	42.01	(N=15)
SV1103	"Cooperite"	wt%	80.21 (0.21)	4.06 (0.35)	0.86 (0.03)	14.69 (0.38)	99.83
		at%	44.59	4.14	1.59	49.69	(N=96)
	Melt	wt%	18.84 (5.92)	26.75 (3.49)	28.21 (5.76)	25.44 (1.67)	98.98
		at%	5.95	15.50	29.63	48.92	(N=5)
SV1104	"Cooperite"	wt%	80.78 (0.29)	3.50 (0.28)	0.94 (0.07)	14.55 (0.28)	99.77
		at%	45.16	3.59	1.75	49.50	(N=44)
	Melt	wt%	23.59 (5.07)	17.54 (2.73)	33.88 (2.99)	24.68 (1.33)	99.69
		at%	7.41	10.10	35.35	47.15	(N=6)
SV1105	"Cooperite"	wt%	77.08(0.24)	7.11 (0.29)	0.65 (0.05)	15.16 (0.34)	99.99
		at%	41.77	7.06	1.17	49.99	(N=53)
	Melt	wt%	10.65 (7.62)	43.87 (8.41)	22.74 (9.28)	23.09 (1.29)	100.35
		at%	3.47	26.19	24.60	45.74	(N=21)
1000°C							
SV301	"Braggite"	wt%	24.15 (1.11)	54.32 (1.03)	0.50 (0.12)	21.36 (0.37)	100.34
		at%	9.46	39.00	0.65	50.89	(N=150)
	Melt	wt%	3.34 (1.86)	70.63 (1.80)	4.43 (1.07)	20.25 (0.94)	98.65
		at%	1.23	47.82	5.44	45.51	(N=9)
SV303	"Braggite"	wt%	18.45 (0.92)	60.05 (1.19)	0	21.03 (0.44)	99.59
		at%	7.19	42.92	0	49.89	(N=44)
	Melt	wt%	3.01 (0.62)	75.26 (1.75)	0	20.23 (0.23)	98.52
		at%	1.14	52.25	0	46.61	(N=3)
SV305	"Cooperite"	wt%	82.84 (0.93)	1.91 (0.52)	1.71 (0.06)	14.12 (0.15)	100.58
		at%	46.55	1.97	3.19	48.29	(N=11)
	Melt	wt%	12.59 (5.94)	12.04 (3.55)	45.76 (6.13)	29.68 (0.94)	100.08
		at%	3.43	6.01	41.40	49.16	(N=33)
SV306	"Cooperite"	wt%	78.77 (0.84)	5.25 (0.66)	1.61 (0.20)	14.56 (0.18)	100.18
		at%	43.20	5.28	2.93	48.59	(N=20)
	Melt	wt%	12.53 (2.34)	16.08 (2.51)	42.82 (2.43)	29.13 (1.17)	100.55
		at%	3.47	8.15	39.36	49.02	(N=52)

(continued)



Table 1 (continued)

Sample	Phases		Pt	Pd	Ni	S	TOTAL
SV308	"Cooperite"	wt%	71.33 (0.99)	12.01 (0.97)	1.37 (0.11)	15.47 (0.37)	100.18
		at%	37.14	11.47	2.37	49.02	(N=80)
	Melt	wt%	12.71 (3.67)	32.20 (3.46)	29.70 (4.24)	26.19 (1.51)	100.79
		at%	3.85	17.90	29.93	48.32	(N=21)
SV309	"Cooperite"	wt%	73.99 (0.90)	9.58 (0.55)	1.37 (0.35)	15.11 (0.32)	100.05
		at%	39.34	9.34	2.42	48.89	(N=150)
	Melt	wt%	10.35 (4.47)	24.22 (1.77)	37.16 (4.32)	29.21 (1.40)	100.93
		at%	2.91	12.47	34.69	49.93	(N=26)
SV310	"Cooperite"	wt%	70.35 (0.10)	11.56 (0.53)	1.05 (0.04)	15.83 (0.41)	98.79
		at%	36.76	11.08	1.82	50.34	(N=6)
	"Braggite"	wt%	59.52 (0.34)	21.78 (0.96)	1.63 (0.41)	16.70 (0.49)	99.63
		at%	28.82	19.34	2.62	49.21	(N=58)
	Melt	wt%	3.87 (2.56)	32.16 (1.36)	41.71 (1.77)	23.97 (0.24)	101.72
		at%	1.11	16.98	39.91	42.00	(N=2)
SV311	"Braggite"	wt%	59.13 (0.88)	21.97 (0.84)	1.91 (0.19)	16.53 (0.23)	99.55
		at%	28.66	19.52	3.08	48.75	(N=9)
	Melt	wt%	7.64 (3.69)	32.67 (2.50)	32.73 (4.03)	27.93 (1.19)	100.97
		at%	2.21	17.3	31.41	49.08	(N=45)
SV312	"Braggite"	wt%	41.20 (0.83)	38.38 (0.84)	1.43 (0.21)	18.82 (0.44)	99.83
		at%	17.85	30.48	2.06	49.61	(N=56)
	Melt	wt%	8.19 (2.54)	48.25 (3.12)	18.70 (3.99)	24.99 (1.34)	100.13
		at%	2.63	28.46	19.99	48.92	(N=73)
SV313	"Braggite"	wt%	23.28 (0.95)	55.63 (0.86)	0.62 (0.17)	20.69 (0.69)	100.23
		at%	9.19	40.28	0.81	49.72	(N=53)
	Melt	wt%	4.66 (2.59)	63.59 (2.12)	8.64 (2.52)	22.44 (0.77)	99.33
		at%	1.63	40.69	10.02	47.66	(N=43)
SV314	"Braggite"	wt%	32.01 (0.86)	48.02 (0.76)	1.06 (0.21)	19.43 (0.55)	100.54
		at%	13.24	36.41	1.46	48.89	(N=66)
	Melt	wt%	6.91 (2.27)	57.21 (2.02)	12.58 (2.64)	23.31 (0.68)	100.02
		at%	2.34	35.50	14.15	48.01	(N=35)
SV316	"Cooperite"	wt%	70.40 (1.10)	14.36 (0.87)	0	15.81 (0.22)	100.59
		at%	36.49	13.65	0	49.86	(N=16)
	"Braggite"	wt%	60.16 (0.87)	23.35 (0.75)	0	17.13 (0.19)	100.65
		at%	29.03	20.66	0	50.31	(N=18)
SV317	"Cooperite"	wt%	71.29 (0.99)	11.48 (0.75)	1.06 (0.09)	15.94 (0.42)	99.77
		at%	36.96	10.91	1.83	50.29	(N=22)
	"Braggite"	wt%	58.91 (1.09)	21.83 (0.88)	2.00 (0.11)	17.57 (0.48)	100.69
		at%	27.72	18.84	3.13	50.31	(N=24)
	Melt	wt%	2.31 (1.34)	31.18 (3.83)	38.86 (1.84)	27.15 (1.22)	99.44
		at%	0.65	16.16	36.5	46.69	(N=11)
SV318	"Cooperite"	wt%	76.20 (0.67)	9.51 (0.67)	0	14.74 (0.30)	100.49
		at%	41.56	9.51	0	48.92	(N=18)
SV320	"Cooperite"	wt%	84.74 (0.54)	0	1.74 (0.20)	14.05 (0.24)	100.55
		at%	48.14	0	3.29	48.57	(N=14)
	Melt	wt%	15.47 (0.71)	0	52.77 (0.70)	32.57 (0.40)	100.81
		at%	3.98	0	45.08	50.94	(N=9)
SV1001	"Braggite"	wt%	50.12 (0.53)	30.56 (0.74)	1.65 (0.12)	17.69 (0.32)	99.83
		at%	22.86	25.55	2.50	49.09	(N=13)
	Melt	wt%	9.54 (1.55)	39.05 (3.23)	26.31 (1.51)	27.04 (0.87)	100.87
		at%	2.86	21.49	26.25	49.39	(N=12)

(continued)

Table 1 (continued)

Sample	Phases		Pt	Pd	Ni	S	TOTAL
900°C							
SV321	"Cooperite"	wt%	81.89 (1.41)	2.26 (0.96)	1.72 (0.15)	14.13 (0.22)	100.00
		at%	46.07	2.33	3.22	48.38	(N=50)
	Melt	wt%	7.34 (1.80)	9.65 (2.20)	49.76 (3.35)	32.10 (0.57)	98.84
		at%	1.90	4.59	42.87	50.64	(N=23)
SV322	"Cooperite"	wt%	77.94 (0.90)	5.43 (0.65)	2.16 (0.35)	15.06 (0.49)	100.53
		at%	41.74	5.33	3.84	49.08	(N=35)
	Melt	wt%	7.97 (5.74)	12.17 (3.75)	48.58 (5.84)	31.47 (1.52)	100.18
		at%	2.08	5.82	42.13	49.97	(N=26)
SV323	"Cooperite"	wt%	72.08 (1.18)	9.23 (0.73)	2.43 (0.28)	15.75 (0.50)	99.49
		at%	37.36	8.77	4.19	49.68	(N=63)
	Melt	wt%	5.79 (1.21)	19.03 (1.91)	43.24 (1.57)	31.06 (0.96)	100.01
		at%	1.54	9.26	39.03	50.17	(N=22)
SV324	"Cooperite"	wt%	71.06 (0.41)	9.95 (0.26)	2.45 (0.06)	15.56 (0.35)	99.02
		at%	36.99	9.50	4.24	49.28	(N=7)
	"Braggite"	wt%	61.40 (1.25)	16.39 (0.71)	3.91 (0.29)	17.36 (0.37)	99.07
		at%	29.23	14.30	6.19	50.28	(N=39)
	Melt	wt%	4.65 (1.65)	17.59 (11.36)	47.98 (10.10)	30.64 (2.61)	100.87
		at%	1.21	8.43	41.66	48.70	(N=15)
SV325	"Cooperite"	wt%	70.50 (0.21)	11.16 (0.32)	2.44 (0.03)	15.44 (0.34)	99.57
		at%	36.52	10.60	4.20	48.67	(N=16)
	"Braggite"	wt%	60.95 (1.22)	17.42 (1.00)	3.82 (0.34)	17.47 (0.59)	99.66
		at%	28.76	15.07	5.99	50.17	(N=33)
	Melt	wt%	7.03 (12.32)	19.73 (3.99)	39.69 (3.34)	29.48 (1.17)	95.88
		at%	1.98	10.20	37.21	50.60	(N=16)
SV326	"Braggite"	wt%	53.75 (1.04)	23.67 (0.89)	3.90 (0.21)	18.11 (0.47)	99.42
		at%	24.40	19.70	5.88	50.02	(N=22)
	Melt	wt%	4.18 (2.82)	25.10 (3.04)	36.95 (4.90)	27.30 (1.30)	93.54
		at%	1.23	13.57	36.21	48.99	(N=50)
SV327	"Braggite"	wt%	42.98 (1.32)	32.86 (1.12)	3.88 (0.31)	19.97 (0.54)	99.70
		at%	18.09	25.35	5.43	51.14	(N=24)
	Melt	wt%	2.61 (1.31)	25.07 (4.37)	38.09 (5.57)	28.65 (1.67)	94.42
		at%	0.75	13.15	36.22	49.88	(N=83)
SV328	"Braggite"	wt%	34.66 (1.28)	40.41 (0.96)	3.71 (0.28)	21.38 (0.26)	100.17
		at%	13.8	29.49	4.90	51.80	(N=31)
	Melt	wt%	3.24 (2.40)	32.00 (5.71)	31.57 (5.41)	25.36 (1.48)	92.11
		at%	1.01	18.27	32.67	48.05	(N=15)
SV330	"Braggite"	wt%	31.12 (1.32)	43.20 (1.01)	3.66 (0.11)	21.00 (0.29)	98.98
		at%	12.43	31.65	4.86	51.06	(N=38)
	Melt	wt%	2.23 (0.77)	31.85 (1.91)	34.87 (1.91)	28.34 (0.58)	97.29
		at%	0.64	16.73	33.21	49.42	(N=26)
SV331	"Cooperite"	wt%	70.69 (1.54)	12.90 (1.09)	0	15.69 (0.13)	99.29
		at%	37.24	12.47	0	50.30	(N=20)
	"Braggite"	wt%	59.44 (1.26)	22.78 (1.02)	0	17.52 (0.29)	99.73
		at%	28.60	20.10	0	51.30	(N=14)
SV332	"Cooperite"	wt%	70.40 (0.87)	12.30 (0.68)	0.91 (0.45)	16.17 (0.30)	99.78
		at%	36.22	11.60	1.56	50.62	(N=7)
	"Braggite"	wt%	60.36 (1.79)	19.13 (1.16)	2.65 (0.20)	18.03 (0.24)	100.18
		at%	28.19	16.40	4.12	51.29	(N=51)
SV334	"Cooperite"	wt%	78.11 (1.06)	7.36 (0.85)	0	14.27 (0.19)	99.74
		at%	43.77	7.56	0	48.66	(N=67)
		SV335	"Braggite"	wt%	18.43 (0.22)	55.22 (0.12)	3.77 (0.01)
at%	6.82			37.49	4.64	51.05	(N=2)
	Melt	wt%	0.23 (0.15)	35.86 (4.67)	35.42 (3.66)	28.80 (1.76)	100.31
		at%	0.06	18.32	32.80	48.82	(N=22)
SV336	"Cooperite"	wt%	85.36 (0.65)	0	1.66 (0.46)	14.04 (0.22)	101.09
		at%	48.41	0	3.13	48.46	(N=22)
	"Ni _{1-x} S"	wt%	1.29 (0.081)	0	64.67 (0.21)	36.86 (0.13)	102.82
		at%	0.29	0	48.79	50.92	(N=9)

(continued)

Table 1 (continued)

Sample	Phases		Pt	Pd	Ni	S	TOTAL
SV917	“Vysotskite”	wt%	0	69.16 (0.37)	3.69 (0.15)	24.00 (0.49)	96.84
		at%	0	44.48	4.30	51.22	(N=15)
	Melt	wt%	0	44.22 (1.52)	25.78 (1.33)	26.00 (0.63)	97.01
		at%	0	24.95	26.37	48.69	(N=10)

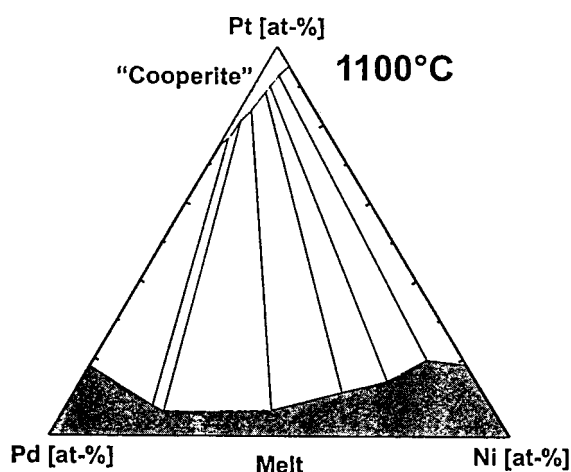


Fig. 1. Phase relations in the system PtS-PdS-NiS in cation proportions at 1100 °C

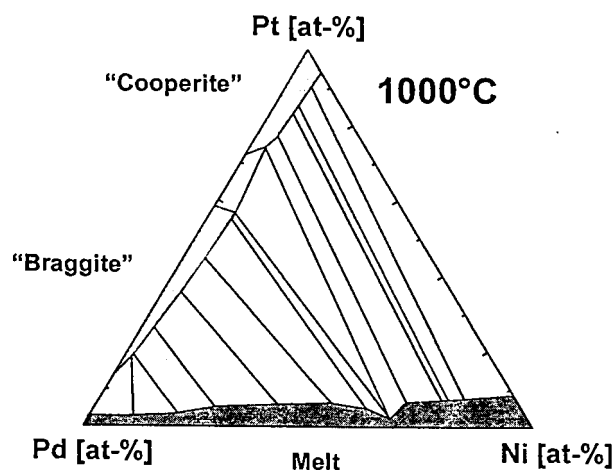


Fig. 2. Phase relations in the system PtS-PdS-NiS in cation proportions at 1000 °C

atomic per cent. At 900 °C $Ni_{1-x}S$ is stable with a maximum solubility of 0.3 atomic per cent Pt along the PtS-NiS join. Pt-free $Ni_{1-x}S$ contains 0.6 atomic per cent Pd, if coexisting with a melt containing 6.2 atomic per cent Pd (*Karup-Møller and Makovicky, 1993*). Similar to the observations at 1000 °C, the Pt-concentration in melt coexisting with coexisting “cooperite” and “braggite” (i.e. all three phases

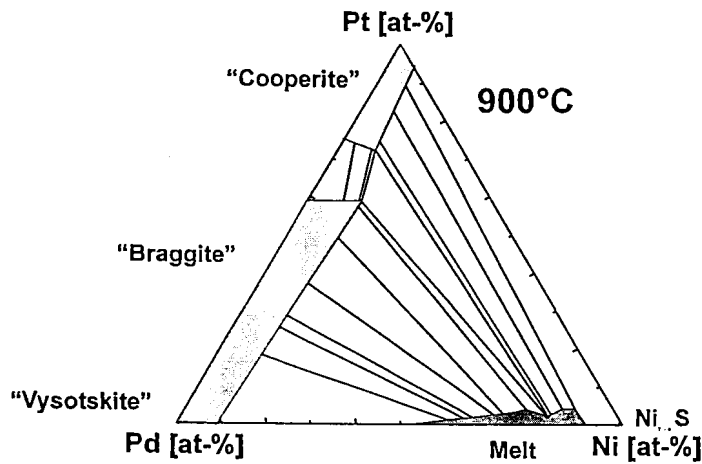


Fig. 3. Phase relations in the system PtS-PdS-NiS in cation proportions at 900 °C

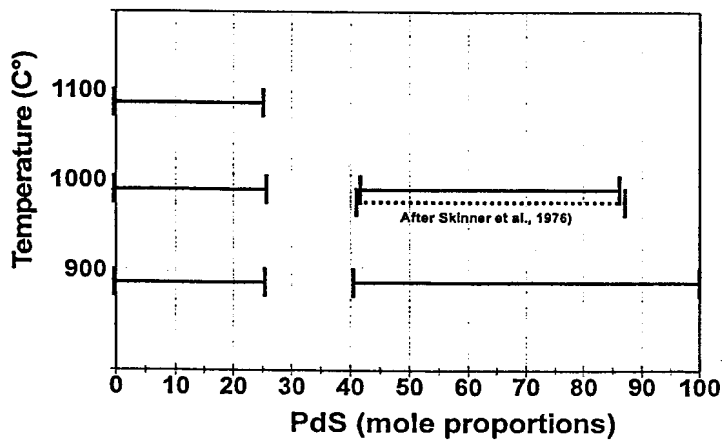


Fig. 4. Stability of Ni-free “cooperite”, “braggite”, and “vysotskite” from our experimental data, as well as data according to *Skinner et al.* (1976)

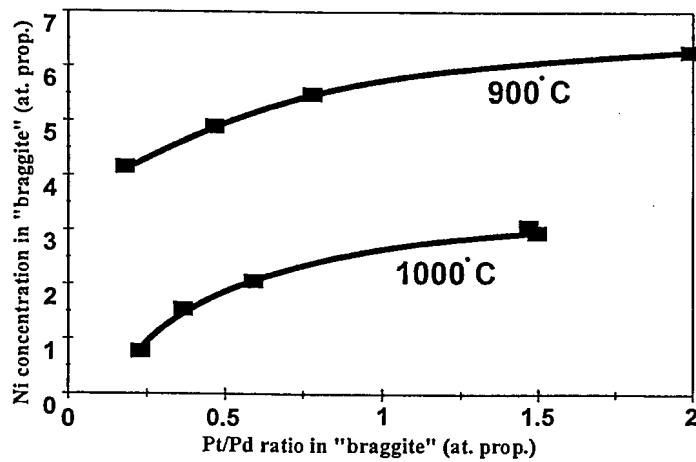


Fig. 5. Pt/Pd ratio versus Ni-concentration in “braggite” in atomic proportions at 900 °C and 1000 °C

coexist) decreases sharply to a minimum of 1.2 atomic per cent and rises again towards the PtS-NiS join.

The maximum solubility of Ni in ideal Pd-free “cooperite” along the PtS-NiS join is 3.1 atomic per cent. The Pd limit in Ni-free “cooperite” coexisting with “braggite” at 900 °C is 12.5 atomic per cent, lower than that at 1000 °C. The “braggite” composition ranges from $\text{Pt}_{0.59}\text{Pd}_{0.29}\text{Ni}_{0.12}\text{S}$ and $\text{Pt}_{0.59}\text{Pd}_{0.40}\text{S}$ for a Ni-saturated and Ni-free environment respectively to $\text{Pd}_{0.89}\text{Ni}_{0.08}\text{S}$ and PdS respectively. The Ni-concentration in “braggite” in a Ni-saturated environment decreases slightly with increasing Pd content, but is higher than at 1000 °C (Fig. 5).

Discussion

In natural magmatic systems, base metal sulphides/arsenides can take up the entire PGE contents of the sulphide melt at its crystallization temperature. *Makovicky et al. (1990)* studied solubilities of PGE in base metal sulphides/arsenides at various temperatures and chemistries and showed that the PGE dissolved at high temperature may be expelled on cooling, in that way becoming available for postmagmatic mineral forming processes. Solubilities of Ni in (Pt, Pd)S, as well as Pd solubility in cooperite and Pt solubility in braggite are sensitive to temperature and phase assemblages. The mineral compositions therefore have the potential to indicate at which stage of the development of the ore deposit these phases were exsolved or suffered overprinting by fluids. From our results it can be deduced that the Ni-content of braggite with varying Pt/Pd ratios in a NiS saturated environment is a function of temperature; a higher Ni-content indicating a lower equilibration temperature. This is in agreement with the findings in the system Pd-Ni-S by *Karup-Møller and Makovicky (1993)*. Cooperite is stable at temperatures above 1100 °C, whereas braggite is only stable at temperatures below 1100 °C and pure vysotskite is only stable below 1000 °C.

Comparison of the experimental results with data taken from the literature (Fig. 6) indicate that a large amount of data points of natural cooperite, braggite, and vysotskite fall outside the stability fields established for 1000 °C and 900 °C. All, but one, analyses of cooperite, braggite, and vysotskite from placer deposits throughout the world published by *Cabri et al. (1996)* follow the trend experimentally established in a Ni-saturated environment for 1000 °C. Data published by *Halkoaho (1989)* follow a trend similar to the one experimentally established in a Ni-saturated environment at 900 °C. These temperatures could be affected by the Ni/Fe ratio in the base-metal sulphide assemblage (*Makovicky and Karup-Møller, 1995*). However, analyses of braggite, vysotskite—and also cooperite, show that generally no Fe was detected in these minerals. The large amount of braggite and vysotskite analyses plotting on the Ni-rich side of the compositional fields established in this study are obviously due to an equilibration temperature of less than 900 °C if a Ni-saturated environment is assumed. This would be in accordance with the trends established by *Karup-Møller and Makovicky (1993)* for (Pd, Ni)S. There are, however, still compositions reported for which no experimental equivalents have been observed to date and the origin of these compositions remains an unsolved problem.

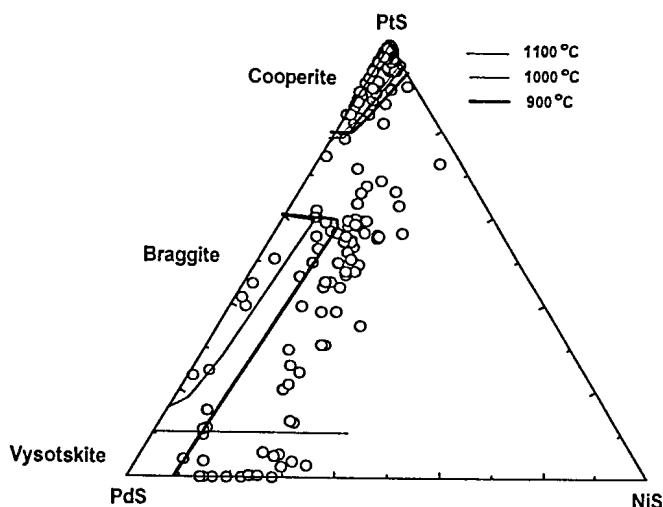


Fig. 6. Compositional variation of cooperite, braggite, and vysotskite analyses from various localities in mole proportions. Data taken from: *Bannister and Hey* (1932), *Cabri et al.* (1978, 1996), *Criddle and Stanley* (1985), *Genkin and Evstigneeva* (1986), *Halkoaho* (1989), *Kingsto and El-Dosuky* (1982), *Laputina and Genkin* (1975), *Mostert et al.* (1982), *Schwellnus et al.* (1976), *Tarkian* (1987), *Todd et al.* (1982) and *Volborth et al.* (1986) [this Figure excludes the data from *Merkle and Verryn* (1991) and *Verryn and Merkle* (1994)]

Acknowledgements

We would like to express our gratitude to *L. J. Cabri* for providing us with synthetic standards, to *Zeiss South Africa* for assisting us with microscope facilities, to *AMPLATS* for supporting the ongoing experimental work in the Pt-Pd-Ni-S system, and to *MINTEK* for support to establish the experimental sulphide laboratory. Financial support from the University of Pretoria is greatly appreciated. Likewise we would like to thank *E. Makovicky* and an anonymous referee for their constructive comments.

References

- Bannister FA, Hey MH* (1932) Determination of minerals in platinum concentrates from the Transvaal by X-ray methods. *Mineral Mag* 28: 188–206
- Brynard HJ, de Villiers JPR, Viljoen EA* (1976) A mineralogical investigation of the Merensky Reef at the Western Platinum Mine, near Marikana, South Africa. *Econ Geol* 71: 1299–307
- Cabri LJ, Laflamme JHG, Steward JM, Turner K, Skinner BJ* (1978) On cooperite, braggite, and vysotskite. *Am Mineral* 63: 832–839
- Cabri LJ, Harris DC, Weiser TW* (1996) Mineralogy and distribution of platinum-group mineral (PGM) placer deposits of the world. *Explor Mining Geol* 5: 73–167
- Criddle AJ, Stanley JS* (1985) Characteristics optical data for cooperite, braggite and vysotskite. *Can Mineral* 23: 149–169
- Genkin AD, Evstigneeva TL* (1986) Associations of platinum-group minerals of the Noril'sk copper-nickel sulfide ores. *Econ Geol* 81: 1203–12
- Halkoaho T* (1989) Ala-Penican platinametalliminerali saatiot Penikkain kerrosintruusiossa. Raportti no 2, Peräpohjan platinaprojekti, Oulun Yliopisto, 173pp

- Karup-Møller S, Makovicky E* (1993) The system Pd-Ni-S at 900, 725, 550, and 400 °C. *Econ Geol* 88: 1261–1268
- Kingston GA, El-Dosuky BT* (1982) A contribution on the platinum-group mineralogy of the Merensky Reef at the Rustenburg Platinum Mine. *Econ Geol* 71: 1299–307
- Kinloch ED* (1982) Regional trends in the platinum-group mineralogy of the Critical Zone of the Bushveld Complex, South Africa. *Econ Geol* 77: 1328–47
- Kullerud G* (1971) Experimental techniques in dry sulphide research. In: *Ulmer GC* (ed) *Research techniques for high pressure and high temperature*. Springer, Berlin Heidelberg New York Tokyo, pp 289–315
- Laputina IP, Genkin AD* (1975) Minerals of the braggite-vysotskite series. *Izomorpizm Mineraly*, Izdat. Nauka, pp 146–150 (in Russian)
- Makovicky E, Karup-Møller S* (1995) The system Pd-Fe-Ni-S at 900 and 725 °C. *Mineral Mag* 59: 685–702
- Makovicky E, Karup-Møller S, Makovicky M, Rose-Hansen J* (1990) Experimental studies on the phase systems Fe-Ni-Pd-S and Fe-Pt-Pd-As-S applied to PGE deposits. *Mineral Petrol* 42: 307–319
- McLaren CH, De Villiers JPR* (1982) The platinum-group chemistry and mineralogy of the UG-2 chromitite layer of the Bushveld Complex. *Econ Geol* 77: 1348–66
- Merkle RKW, Verryin SMC* (1991) Coexisting cooperite and braggite – new data. *Papers, International Congress on Applied Mineralogy, 1991, Pretoria, South Africa*, Paper 61, 17pp
- Moh GH, Taylor LA* (1971) Laboratory techniques in experimental sulphide petrology. *N Jb Mineral Mh* 1991: 450–459
- Mostert AB, Hofmeyr PK, Potgieter GA* (1982) The platinum-group mineralogy of the Merensky Reef at the Impala Platinum Mines, Bophuthatswana. *Econ Geol* 77: 1385–94
- Peyerl W* (1982) The influence of the Driekop dunite pipe on the platinum-group mineralogy of the UG-2 chromitite in its vicinity. *Econ Geol* 77: 1432–8
- Schwellnus JSI, Hiemstra SA, Gasparrini E* (1976) The Merensky Reef at the Atok Platinum Mine and its environs. *Econ Geol* 71: 249–60
- Skinner BJ, Luce FD, Dill JA, Ellis DE, Hagan HA, Lewis DM, dell DA, Sverjensky DA, Williams N* (1976) Phase relations in ternary portions of the systems Pt-Pd-Fe-As-S. *Econ Geol* 71: 1469–1475
- Tarkian M* (1987) Compositional variations and reflectance of the common platinum-group minerals. *Mineral Petrol* 36: 169–190
- Todd SG, Keith DW, Le Roy LW, Schissel DJ, Mann EL, Irvine TN* (1982) The J-M platinum-palladium reef of the Stillwater Complex, Montana. I. Stratigraphy and petrology. *Econ Geol* 77: 1454–80
- Verryin SMC, Merkle RKW* (1994) Compositional variation of cooperite, braggite, and vysotskite from the Bushveld Complex. *Mineral Mag* 58: 223–234
- Verryin SMC, Merkle RKW* (1996) Observations on factors affecting the compositional variation of synthetic “cooperite” in the system Pt-Pd-Ni-S at 1000 °C. *N Jb Mineral Mh* 10: 471–482
- Volborth A, Tarkian M, Stumpfl EF, Housley RM* (1986) A survey of the Pd-Pt mineralization along the 35 km strike of the J-M Reef, Stillwater Complex, Montana. *Can Mineral* 24: 329–46

Authors' address: *S. M. C. Verryin* and *R. K. W. Merkle*, Applied Mineralogy Group, Department of Earth Sciences, University of Pretoria, Pretoria, 0002, South Africa, e-mail: Sabine@scientia.up.ac.za